

University of Denver

Digital Commons @ DU

Electronic Theses and Dissertations

Graduate Studies

2023

Post-Translational Modification of Proteins via Ambient Air Pollutants and Endogenous Reactive Species

Rachel Lauren Davey
University of Denver

Follow this and additional works at: <https://digitalcommons.du.edu/etd>



Part of the [Analytical Chemistry Commons](#), and the [Biochemistry Commons](#)

Recommended Citation

Davey, Rachel Lauren, "Post-Translational Modification of Proteins via Ambient Air Pollutants and Endogenous Reactive Species" (2023). *Electronic Theses and Dissertations*. 2249.
<https://digitalcommons.du.edu/etd/2249>

This Dissertation is brought to you for free and open access by the Graduate Studies at Digital Commons @ DU. It has been accepted for inclusion in Electronic Theses and Dissertations by an authorized administrator of Digital Commons @ DU. For more information, please contact jennifer.cox@du.edu, dig-commons@du.edu.

Post-Translational Modification of Proteins via Ambient Air Pollutants and Endogenous Reactive Species

Abstract

Proteins can react with reactive oxygen species (ROS) and reactive nitrogen species (RNS) to form post-translational modifications (PTMs), which can affect protein structure and function. The formation of 3-nitrotyrosine (NTyr) and dityrosine (DiTyr) upon reaction of proteins with ROS/RNS are two common PTMs studied due to their stability and irreversibility, as well as their ability to enhance the allergenicity of pollen allergens upon formation. Many common techniques used to study the formation of these PTMs can reliably detect the PTMs but can only provide semi-quantitative information due to many assumptions and limitations. In Chapter 2 we present an analysis of the common methodologies used and provide analytical perspectives for improved quantification.

NTyr can form via the reaction of proteins and urban air pollutants and may have implications in the increase in allergic disease seen worldwide. The reaction of proteins with ozone and nitrogen dioxide has been previously studied in controlled laboratory studies, but not extensively in urban air. In Chapter 3 we develop and characterize a method for the exposure of proteins to urban air, analysis, and quantification of NTyr in samples after exposure. An extensive ambient study was further conducted (Chapter 4) and the nitration degree, or NTyr concentration, of the exposed samples was correlated with air pollutant concentrations and atmospheric conditions. The formation of DiTyr in the exposed samples was also detected in this study, representing the first time the detection of oligomerization of proteins was reported in ambient air.

The reactions of proteins with endogenous ROS/RNS upon inhalation may be a further mechanism for the increase in allergenicity seen. Peroxynitrite (ONOO⁻) is an endogenous ROS formed under oxidative stress conditions. Here we show how using ONOO⁻ *in vitro* to mimic oxidative stress *in vivo* has experimental artifacts, like an increase in pH that alters the reaction mechanism (Chapter 5), as well as how it reacts site-selectively with lactoferrin (Chapter 6). The studies shown provide information to tie together the nitration reactions occurring both in urban air and endogenously, which is imperative to determining the role each play in the increase in allergic disease.

Document Type

Dissertation

Degree Name

Ph.D.

Department

Chemistry and Biochemistry

First Advisor

John Alexander Huffman

Second Advisor

Keith Miller

Third Advisor

Michelle Knowles

Keywords

Air pollution, Nitration, Oligomerization, Oxidative stress, Ozone, Peroxynitrite

Subject Categories

Analytical Chemistry | Biochemistry | Biochemistry, Biophysics, and Structural Biology | Chemistry | Physical Sciences and Mathematics

Publication Statement

Copyright is held by the author. User is responsible for all copyright compliance.

Post-Translational Modification of Proteins via Ambient Air Pollutants and
Endogenous Reactive Species

A Dissertation

Presented to

the Faculty of the College of Natural Sciences and Mathematics

University of Denver

In Partial Fulfillment

of the Requirements for the Degree

Doctor of Philosophy

by

Rachel Lauren Davey

June 2023

Advisor: John Alexander Huffman, PhD

©Copyright by Rachel Lauren Davey 2023

All Rights Reserved

Author: Rachel Lauren Davey
Title: Post-Translational Modification of Proteins via Ambient Air Pollutants and Endogenous Reactive Species
Advisor: John Alexander Huffman, PhD
Degree Date: June 2023

Abstract

Proteins can react with reactive oxygen species (ROS) and reactive nitrogen species (RNS) to form post-translational modifications (PTMs), which can affect protein structure and function. The formation of 3-nitrotyrosine (NTyr) and dityrosine (DiTyr) upon reaction of proteins with ROS/RNS are two common PTMs studied due to their stability and irreversibility, as well as their ability to enhance the allergenicity of pollen allergens upon formation. Many common techniques used to study the formation of these PTMs can reliably detect the PTMs but can only provide semi-quantitative information due to many assumptions and limitations. In Chapter 2 we present an analysis of the common methodologies used and provide analytical perspectives for improved quantification.

NTyr can form via the reaction of proteins and urban air pollutants and may have implications in the increase in allergic disease seen worldwide. The reaction of proteins with ozone and nitrogen dioxide has been previously studied in controlled laboratory studies, but not extensively in urban air. In Chapter 3 we develop and characterize a method for the exposure of proteins to urban air, analysis, and quantification of NTyr in samples after exposure. An extensive ambient study was further conducted (Chapter 4) and the nitration degree, or NTyr concentration, of the exposed samples was correlated with air pollutant concentrations and atmospheric conditions. The formation of DiTyr in

the exposed samples was also detected in this study, representing the first time the detection of oligomerization of proteins was reported in ambient air.

The reactions of proteins with endogenous ROS/RNS upon inhalation may be a further mechanism for the increase in allergenicity seen. Peroxynitrite (ONOO^-) is an endogenous ROS formed under oxidative stress conditions. Here we show how using ONOO^- *in vitro* to mimic oxidative stress *in vivo* has experimental artifacts, like an increase in pH that alters the reaction mechanism (Chapter 5), as well as how it reacts site-selectively with lactoferrin (Chapter 6). The studies shown provide information to tie together the nitration reactions occurring both in urban air and endogenously, which is imperative to determining the role each play in the increase in allergic disease.

Acknowledgements

To my mentor and advisor Dr. J. Alex Huffman. Your guidance, helpful critiques, and analytical thinking has shaped me into the scientist I am today. Thank you for supporting me through every hurdle, pushing me to my potential, and respecting the importance of mental health.

To the Huffman Lab group members, both past and present. Thank you for shaping my graduate career and supporting me, especially Dr. Amani Alhalwani, Dr. Ben Swanson, Nicole Savage, Alex Volkova, and Maxwell Freeman. Thank you also to all the undergraduate students along the way for helping make this such a fulfilling experience.

To my graduate committee, Drs. Michelle Knowles, Keith Miller, and Rebecca Powell for the participation on my defense committee and the support throughout my entire graduate program.

To the Max Plank Institute for Chemistry, especially Drs. Katrin Reinmuth-Selzle and Ulrich Poschl, for the great collaborations and opportunities to study in Germany.

To the Department of Chemistry and Biochemistry for the opportunity to learn and grow as a scientist and the financial support via the Phillipson Grant.

To Team Davey: my parents, siblings, and friends. Thank you for picking up my midnight calls, telling me every day I can do whatever I put my mind to, and supporting me every step of the way.

To my husband, Jake Younkin. Thank you for the endless support every single day. You celebrated every up with me, as well as helped me through every down. I can't express how much your love has meant to me throughout this whole process.

Table of Contents

Chapter One: Introduction	1
1.1 Oxidative Chemical Reactions of Proteins	1
1.1.1 Heterogeneous Aerosol Chemistry	1
1.1.2 Endogenous Chemistry	3
1.2 Overview of Post-Translational Modifications.....	6
1.2.1 Importance and Relevance of PTMs.....	6
1.2.2 Effects of PTMs	7
1.3 Nitrotyrosine and Dityrosine Overview	9
1.4 Relevant Mechanisms of PTM Formation.....	12
1.4.1 PTM Formation via Reaction with ONOO ⁻	12
1.4.2 PTM Formation via Reaction with O ₃ and NO ₂	16
1.5 Motivation.....	19
1.5.1 Negative Effects on Human Health	19
1.5.2 Method Development.....	20
1.6 Research Aims	22
Chapter Two: Nitrotyrosine and Dityrosine	24
2.1 Nitration	24
2.1.1 Ntyr in Urban Air.....	24
2.1.2 Ntyr within the Human Body.....	25
2.2 Analytical Methods of Ntyr Detection and Quantification.....	26
2.2.1 Detection Methods of Ntyr	27
2.2.2 Quantification Methods of Ntyr.....	30
2.3 Dimerization and Oligomerization	32
2.4 Detection and Quantification of DiTyr	34
2.5 Limitations of Ntyr and DiTyr Detection and Quantification	35
2.6 Additional Analytical Considerations.....	38
2.6.1 Baseline Correction and Integration	38
2.6.2 Micropipette Precision.....	41
2.6.3 Amicon Centrifugal Unit Cleaning.....	43
Chapter Three: Heterogeneous Nitration Reaction of BSA Protein with Urban Air: Improvements in Experimental Methodology.....	46
3.1 Abstract	46
3.2 Introduction.....	47
3.2.1 Importance of Heterogeneous Protein Reactions in the Atmosphere	47
3.2.2 Mechanisms of Study.....	49
3.2.3 Reducing Experimental Uncertainties and Artifacts.....	52
3.3 Materials and Methods.....	53
3.3.1 Materials	53

3.3.2 Nitration of BSA by TNM	54
3.3.3 Spectroscopic Analysis	54
3.3.4 Protein Extraction	55
3.3.5 HPLC-DAD Analysis and ND Determination.....	56
3.3.6 Gas-Phase Instruments and Pollutant Data	56
3.3.7 O ₃ Loss Over PM Filters.....	57
3.3.8 Ambient Setup	57
3.4 Results and Discussion	58
3.4.1 Particulate Filters	58
3.4.2 Protein Extraction vs Filter Media Type.....	60
3.4.3 Protein Extraaction Efficiency	62
3.4.4 HPLC Calibration Curves	66
3.4.5 Ambient Application.....	68
3.5 Conclusion	71

Chapter Four: Heterogenous Reaction of BSA Protein with Urban Air: A Long-Term Ambient Study **83**

4.1 Abstract	83
4.2 Introduction.....	83
4.3 Materials and Methods.....	86
4.3.1 Materials	86
4.3.2 Exposure to Ambient Air.....	87
4.3.3 HPLC-DAD Analysis and ND Determination.....	89
4.3.4 SEC-HPLC Analysis.....	90
4.4 Results and Discussion	91
4.5 Conclusion	98

Chapter Five: Reaction of Proteins with Peroxynitrite: pH Determines Degree of Nitration and Oligomerization..... **105**

5.1 Abstract	105
5.2 Introduction.....	106
5.3 Materials and Methods.....	109
5.3.1 Materials	109
5.3.2 Nitration of BSA with ONOO ⁻	111
5.3.3 Spectroscopic Analysis	112
5.3.4 Nitration Degree Analysis.....	113
5.3.5 Dimer and Oligomerization Analysis	114
5.4 Results and Discussion	115
5.4.1 Reaction of BSA with ONOO ⁻ Results in pH Increase.....	115
5.4.2 DiTyr Formation Occurs at High ONOO ⁻ Concentrations	118
5.4.3 Reaction Mechanism is Determined by pH	120
5.4.4 Importance of Reaction Conditions	126

5.5 Conclusion	128
Chapter Six: Site-Selective Nitration of Lactoferrin Upon Peroxynitrite Exposure and Efficacy of Ergothioneine Inhibition	137
6.1 Abstract	137
6.2 Introduction.....	137
6.3 Materials and Methods.....	142
6.3.1 Materials	142
6.3.2 Treatment of LF with ONOO ⁻ and EGT	142
6.3.3 Tyryptic Digestion	143
6.3.4 QTOF-MS/MS Analysis and ND _y Determination	143
6.3.5 HPLC-DAD Anaylsis and ND Determination.....	145
6.4 Results and Discussion	146
6.4.1 Total ND of LF Reaction with ONOO ⁻	148
6.4.2 Site-Selectivity of ONOO ⁻ Nitration.....	148
6.4.3 EGT Reduces Nitration of LF.....	150
6.5 Conclusion	153
Chapter Seven: Conclusions	160
7.1 Summary of Conclusions.....	160
7.2 Ambient Air Reactions	160
7.3 Oxidative Stress Reactions	162
7.4 Analytical Considerations.....	163
7.5 Limitations	164
7.6 Perspectives and Future Directions.....	166
References.....	169
Appendix A: HPLC Integration Igor Code.....	194
Appendix B: Micropipette Precision	196
Appendix C: Chapter 3 Supplement.....	198
Appendix D: Chapter 5 Supplement.....	204
Appendix E: Ozone Filter Test Igor Code.....	208
Appendix F: Density of H₂O and PBS	210
Appendix G: Site-Selective Nitration of LF and ONOO⁻.....	214
Appendix H: Pollen Rupture	219
Appendix I: Amb a 1 and Amb a 11 Preliminary Results	224
Appendix J: Ntyr ELISA Protocol	225
Appendix K: TNM Nitration Protocol.....	227
Appendix L: Theoretical pH Calculations and Buffer Capacity	228
Appendix M: Average Ambient Data Igor Code.....	230
Appendix N: UV-Vis Calibration	231

Appendix O: A poem to my PhD 233

List of Figures

Chapter One

Figure 1.1. Nitration of Tyr residue	10
Figure 1.2. Dimerization of Tyr	11
Figure 1.3. Relevant reactions for the formation of Ntyr from ONOO ⁻	14
Figure 1.4. Relevant reactions for DiTyr formation.	15
Figure 1.5. Reaction mechanism of Tyr with O ₃ and NO ₂	18
Figure 1.6. Reaction schematic of BSA and O ₃ /NO ₂	19

Chapter Two

Figure 2.1. Absorption properties of Tyr and Ntyr.....	28
Figure 2.2. Loss of Tyr fluorescence when nitrated.	28
Figure 2.3. HPLC-DAD detection of Ntyr.....	31
Figure 2.4. HPLC-DAD baseline correction and integration scheme.	39
Figure 2.5. HPLC-DAD baseline correction and integration for ambient samples	41
Figure 2.6. Histogram of calculated volume delivered for micropipettes	43
Figure 2.7. HPLC-DAD before and after centrifugal unit cleaning	45

Chapter Three

Figure 3.1. Schematic representing steps in ambient exposure	53
Figure 3.2. O ₃ loss over PM filters	60
Figure 3.3. Protein extraction interference.	62
Figure 3.4. Protein extraction efficiency of PP syringe filter	66
Figure 3.5. Calibration of HPLC response versus protein concentration	67
Figure 3.6. Nitration degree of four samples of BSA exposed to urban air	70

Chapter Four

Figure 4.1. Details for ambient exposure set-up	89
Figure 4.2. ND response corresponded to total integrated O ₃ and NO ₂	93
Figure 4.3. ND response corresponded to ratios of O ₃ /BSA and O ₃ / Tyr	94
Figure 4.4. ND response versus NO _x , NO _y , and NO _z	95
Figure 4.5. ND response corresponded to RH, temperature, and time	96
Figure 4.6. ND response corresponded to the sum of measured ROS.....	97

Chapter Five

Figure 5.1. ND and pH response as molar ratio increases	117
Figure 5.2. ND, OD, and fluorescence response as molar ratio increases	120
Figure 5.3. ND, DD, and OD response as pH increases	123
Figure 5.4. Fluorescence response as pH increases	124
Figure 5.5. Reaction mechanism of Tyr with ONOO ⁻ to form Ntyr or DiTyr.....	126
Figure 5.6. Reaction of BSA with ONOO ⁻ at differing buffer capacities.....	127

Chapter Six

Figure 6.1. Total nitration results of LF nitrated with ONOO ⁻	147
Figure 6.2. Site-selectivity of LF nitration with ONOO ⁻	150
Figure 6.3. Total ND of LF upon treatment with EGT	151
Figure 6.4. Relative ND of NLF treated with EGT	153

Appendices

Figure C1. Exemplary absorption spectra of quartz and glass filter interference.....	198
Figure C2. Schematic representing extraction efficiency process	200
Figure C3. Density determination of 400 µg BSA in PBS	201
Figure C4. Change in density of 0-500 µg/mL BSA in PBS.....	201
Figure C5. Exemplary absorption spectra showing protein loss over Amicon filter.....	202
Figure C6. HPLC integration scheme	203
Figure D1. Excitation emission matrices of BSA and ONOO ⁻ reaction products	204
Figure D2. Variance of ND response depending on experimental conditions	205
Figure D3. Exemplary chromatograms of SEC-HPLC.....	205
Figure D4. HPLC-DAD calibration.....	206
Figure D5. SEC calibration.....	207
Figure F1. Density determination for various BSA concentrations in PBS	211
Figure F2. Density determination for purchased Gibco PBS	212
Figure F3. Density determination for purchased Gibco H ₂ O and MQ H ₂ O	213
Figure G1. Treatment of LF with ET scavenges ONOO ⁻ radicals	216
Figure H1. Absorbance spectra of nitrated pollen extract	221
Figure H2. Ntyr ELISA quantification of nitrated pollen extract.....	222
Figure I1. Preliminary results of n-AMB reacted with ONOO ⁻	224
Figure N2. UV-Vis calibration using potassium dichromate.....	232

List of Tables

Main Text

Table 3.1. Slope of calibration curve	68
Table 4.1. Preliminary results detecting oligomerization in ambient samples	98
Table 6.1. LC-MS/MS results for NLF and NLF + EGT samples	152

Appendices

Table D1. HPLC-DAD calibration metrics	206
Table G1. Tryptic peptides of NLF identified by LC-MS/MS	217
Table G2. Preferred peptides used for QTOF-MS/MS analysis	218
Table L1. Theoretical pH calculations for 0.5/1 ONOO ⁻ /Tyr.....	228
Table L2. Theoretical pH calculations for 5/1 ONOO ⁻ /Tyr	229
Table N1. UV-Vis spectrometer calibration using potassium dichromate	231

List of Abbreviations

Amb a 1	ambrosia a 1
BCA	bicinchoninic acid assay
BSA	bovine serum albumin
Cys	cysteine
DiTyr	dityrosine
EEM	excitation emission matrix
EGT	ergothioneine
ELISA	enzyme-linked immunosorbent assay
et al.	and coworkers
HPLC-DAD	high performance liquid chromatography-diode array detector
LF	lactoferrin
Met	methionine
NO ₂	nitrogen dioxide
NLF	nitrated lactoferrin
Ntyr	3-nitrotyrosine
O ₃	ozone
ONOO ⁻	peroxynitrite
PBS	phosphate-buffered saline
Phe	phenylalanine
PTM	post-translational modification
RT	room temperature

TNM..... tetranitromethane
Trp..... tryptophan
Tyr..... tyrosine
UV-Vis..... ultraviolet-visible

Chapter One: Introduction

1.1 Oxidative chemical reactions of proteins

1.1.1 Heterogeneous aerosol chemistry

Atmospheric aerosols are very small particles suspended in a gas. Aerosols derived from biogenic sources, like viruses, bacteria, mold, plants, or pollen, are referred to as biogenic aerosols and liquid and solid materials lofted as fragments of biological material are referred to as bioaerosols (Sénéchal et al., 2015). In the context of air pollution, the terms aerosol and particulate matter (PM) are often used interchangeably. However, an aerosol is a collection of suspended particles and the surrounding gases, whereas a particulate, or PM, refers just to the suspended solid or liquid matter (Donahue et al., 2009). PM with a diameter less than 2.5 μm ($\text{PM}_{2.5}$) is able to be deposited deep into the lungs of the respiratory tract, which can induce oxidative stress (Shiraiwa et al., 2017).

Proteins make up an important component of PM (between 1 and 2% of $\text{PM}_{2.5}$) (Menetrez et al., 2007). Pollen proteins that are responsible for the allergenic response are referred to as pollen allergens. Free allergens derived from bioaerosols are able to bind to fine PM, which leads to allergen-containing aerosols capable of being transported deep into respiratory airways (Knox et al., 1997). In addition, pollen proteins in ambient air can react with reactive air pollutants and be chemically modified. For example, proteins can be efficiently nitrated and cross-linked at atmospherically relevant air pollutant

concentrations (Franze et al., 2005; Liu et al., 2017; Reinmuth-Selzle et al., 2014; Shiraiwa et al., 2012). In many cases, when allergens are chemically modified their allergenic potential can be altered, which will be discussed more in Section 1.5.1 (Beck et al., 2013; Duque et al., 2014; Frank & Ernst, 2016; Ghiani et al., 2016; Gruijthuijsen et al., 2006; Hochscheid et al., 2014; Naas et al., 2016; Sénéchal et al., 2015; Zhou et al., 2021).

The current geological epoch during which human activities have impacted the environment enough to induce geological change is referred to as the Anthropocene Epoch (Reinmuth-Selzle et al., 2017; Shiraiwa et al., 2017). One characteristic of the Anthropocene is large increases in the concentrations of gaseous air pollutants, such as nitrogen dioxide (NO₂), ozone (O₃), and carbon dioxide (CO₂) (Reinmuth-Selzle et al., 2017; Shiraiwa et al., 2017). High concentrations of these air pollutants have been shown to cause adverse health effects, such as cardiovascular, respiratory, and allergenic diseases (Brunekreef & Holgate, 2002; Pöschl & Shiraiwa, 2015; Reinmuth-Selzle et al., 2017; Shiraiwa et al., 2017; West et al., 2016). Furthermore, the gaseous air pollutants are reactive and are able to react with PM in the atmosphere, producing further health concerns (Reinmuth-Selzle et al., 2017; Shiraiwa et al., 2017). Two of the most studied reactive gaseous air pollutants are O₃ and NO₂, due to their high ambient concentrations, and relevant mechanisms by which these pollutants react with proteins in PM are discussed in Section 1.4.2.

Ground-level O₃ is a subset of tropospheric O₃ and is formed through chemical reactions of volatile organic compounds (VOCs), nitrogen oxides (NO_x), and sunlight

(Fishman et al., 1979). Further discussion of O₃ reactions here refer to ground-level O₃, and will be referred to as only O₃ for the remainder of the text. O₃ is highly reactive, and evidence dating to the 1960s has shown that it can react with proteins and amino acids (Mudd et al., 1969). O₃ concentrations in Denver, CO are particularly important, as Denver was ranked 7th most polluted city in the United States for ground-level O₃ concentration in 2022 (Martinez, 2022). Another reactive atmospheric air pollutant is NO₂, which is formed from the combustion of fossil fuels and photochemical smog (Bascom et al., 2012). NO₂ is broadly reactive, and when inhaled, can damage lung epithelium. One hypothesis explaining this effect relates to the reactive modification of biomolecules on the surface of the epithelium, one important example being protein nitration (Persinger et al., 2012). This will be discussed further in Section 1.3.

Further study of the heterogeneous reactions of gaseous air pollutants on bioaerosols is extremely important, because of the health implications these reactions play with respect to public health, and because of the many questions that remain. A particular limitation of the current research is quantifying the concentration of reaction products in ambient air and using that data to elucidate potential mechanisms that occur. Additionally, the current methods for detection and quantification of the reaction products between PM and gaseous reagents have limitations, which will be discussed in Chapter 2.

1.1.2 Endogenous chemistry

Chemical reactions that occur within the human body, referred to here as endogenous chemistry, are important to human physiology. The body is a dynamic chemical environment where many reactions are always occurring. Reduction-oxidation (redox) reactions play a vital role in maintaining cellular functions and the detoxification of harmful molecules (Fraunberger et al., 2016; Harwell, 2007). Reactive oxygen species (ROS) and reactive nitrogen species (RNS) are often found in high concentrations in the human body and can originate from the metabolism of oxygen (O_2) in the mitochondria (Lin & Beal, 2006). An imbalance in the redox environment of cells and tissues, i.e. when the environment becomes more oxidative, can result in cell and tissue damage and is referred to as oxidative stress (Fraunberger et al., 2016; Pizzino et al., 2017). Accordingly, oxidative stress can be responsible for the onset of many diseases, such as cancer, cardiovascular disease, neurological disease, respiratory disease, and rheumatoid arthritis (Pizzino et al., 2017). Nitrosative stress, or an increase in the relative concentration of RNS species, has also been associated with diseases, particularly cardiovascular disease and neurodegenerative disease (F. Wang et al., 2021; Yoon et al., 2021).

Nitrosative and oxidative stress are closely related. ROS, such as the superoxide anion ($O_2^{\cdot-}$), hydroxyl radical ($\cdot OH$), hydrogen peroxide (H_2O_2), and nitric oxide ($\cdot NO$), also participate in the formation of RNS species (F. Wang et al., 2021). The peroxynitrite anion ($ONOO^-$) is also an important ROS and biological oxidant that plays roles as a mediator in signal transduction and the disruption of cellular redox homeostasis (Radi,

2013b). The conjugate acid of ONOO^- is peroxyxynitrous acid (ONOOH). The two species are in acid-base equilibrium under biologically relevant conditions, with a pK_a of 6.8 (Bartesaghi & Radi, 2018; Radi, 2013). ONOO^- is a short-lived transient species in biological systems, making it difficult to detect. However, the reaction of ONOO^- within biological systems leads to stable products, the reaction product with proteins being referred to as post-translational modifications (PTMs). These products have become biomarkers for ONOO^- and oxidative stress in cells and tissues (Ferrer-Sueta et al., 2018). Two major PTMs resulting from oxidative and nitrosative stress in the human body are nitrotyrosine (NTyr), resulting from nitration, and dityrosine (DiTyr), resulting from dimerization. These PTMs are commonly used as biomarkers for stress and disease in the body and will be more thoroughly discussed in Section 1.3 and Chapter 2. Furthermore, ONOO^- is extremely reactive and will decay in pH-neutral solution via homolysis or isomerization, making the study of ONOO^- reactions difficult (Pryor & Squadrito, 1995). In the laboratory, the addition of ONOO^- to reaction mixtures is most commonly performed via the bolus addition, or addition all at one time, which will be discussed in Chapter 5.

As discussed, high levels of oxidative stress pose a threat to human health. Antioxidants neutralize ROS and RNS species (Pérez de la Lastra et al., 2022). Therefore, endogenous antioxidants play a crucial role in regulating endogenous redox chemistry, and the removal of ROS and RNS by antioxidants has been shown to prevent oxidative damage (Ilari et al., 2020; Lauro et al., 2016). Common antioxidants in the human body are glutathione and ascorbate, both of which have been shown to reduce

relevant ONOO⁻-mediated radicals in cells (Folkes et al., 2011; Gaucher et al., 2018; Radi, 2012). Furthermore, the cytotoxic effects of ONOO⁻ have been shown to decrease when antioxidants are present (Miller et al., 1998). Due to this, further study of relevant antioxidants and their specific reactions with ONOO⁻ is important.

Research regarding the reaction of ONOO⁻ and lactoferrin (LF), a protein found in human milk and other bodily fluids, has been conducted previously in the Huffman Lab (Alhalwani et al., 2018, 2019, 2023). Mass spectrometry (MS) results show that a biologically-relevant concentration of ONOO⁻ is able to nitrate selective Tyr residues, altering protein structure and function (Alhalwani et al., 2019). Questions remain, however, regarding the site-selectivity of ONOO⁻ reactions of LF and other relevant proteins. In addition, preliminary research regarding the ability of L-ergothioneine (EGT), a naturally-derived antioxidant, to prevent the oxidative damage of ONOO⁻ on LF has been conducted (Alhalwani et al., 2023). Further research is needed to determine the extent of EGT's ability to protect from oxidative damage in ONOO⁻ reactions.

1.2 Overview of post-translational modifications

1.2.1 Importance and relevance of PTMs

PTMs occur after proteins have been translated from mRNA and are an essential mechanism by which the diversity of protein function can be expanded beyond what is dictated by DNA (Wang et al., 2013). Proteins can undergo a variety of different chemical modifications. The focus here is on PTMs that are the products of proteins reacting with ROS and/or RNS, as mentioned in Section 1.1. Upon interaction with ROS

and/or RNS various reactions may occur, including reactions with redox-sensitive amino acid side chains. These amino acids include cysteine (Cys), methionine (Met), tryptophan (Trp), tyrosine (Tyr), phenylalanine (Phe), and histidine (His) (Bachi et al., 2013; Mudd et al., 1969; Reinmuth-Selzle et al., 2017).

PTMs caused by ROS/RNS reactions change the properties of a protein and can lead to structural and functional changes. These changes can impact further responses in the human body, such as the immune response and allergies, which will be discussed further in Section 1.5 (Tikhonov et al., 2021). PTM's are often associated with certain diseases, like kidney disease, but the biological significance of most PTMs in pathogenesis remain unclear (Bandoowala & Sengupta, 2020; Landino et al., 2004; Tikhonov et al., 2021). Because of this, the study of individual PTMs and deciphering the role they play in disease is important. Laboratory reagents are commonly used to induce PTMs on proteins to study their effects *in vitro*. Common reagents that mimic RNS and ROS are tetranitromethane (TNM) and ONOO⁻, as discussed in Section 1.4.

Modification of proteins also impacts the detection and quantification of the targeted protein. For instance, the modification of Trp results in the decrease of its intrinsic fluorescence properties (Yamakura & Ikeda, 2006). In addition, Trp is often detected via chromatography coupled with UV-Vis absorbance spectroscopy or mass spectrometry. However, when oxidized or nitrated, the limit of detection and ionization efficiency of the protein is altered. For immunoassay detection, a specific antibody for the modified residue must be used. As one example, an antibody for 6-nitrotryptophan has been developed for use in detection (Ikeda et al., 2007).

1.2.2 Effects of PTMs

ROS and RNS reactions determine various PTMs, some of which are extremely stable and irreversible (Forrester & Stamler, 2012). The human body is designed to counteract a small amount of oxidative stress by removing some ROS and RNS directly. As mentioned, proteins with amino acids containing redox-active side chains can react with oxidants and undergo regulatory chemical modification, the most common being oxidation of Cys and Met, resulting in PTMs (Bachi et al., 2013). These regulatory PTMs are often reversible and are a part of a protein's normal function, such as in proteins involved in redox signaling processes. Therefore, reversible redox modifications may protect from irreversible damage to mild oxidative stress, as well as regulate protein structure and activity (Bachi et al., 2013). A common example of a reversible PTM is the formation of intra- or intermolecular disulfide bonds (Bachi et al., 2013; Lukesh et al., 2013; Ulrich & Jakob, 2019).

Irreversible PTMs occur when there is an imbalance between oxidants and antioxidants. ROS and RNS. Examples of irreversible PTMs are cross-linking of proteins due to DiTyr formation, and Tyr and Trp nitration and halogenation (Bachi et al., 2013). These PTMs may result in permanent loss of protein function, unfolding, or proteolytic degradation (Cai & Yan, 2013; Marinelli et al., 2018). For example, Cys oxidation can be induced by oxidative stress and has been shown to influence the structure and function of proteins (Landino et al., 2004; Marinelli et al., 2018).

In general, the switch from reversible to irreversible PTMs can be correlated with increasing ROS and RNS levels, as shown by *Bachi et al.* and *Selzle et al.* (Bachi et al.,

2013; Reinmuth-Selzle et al., 2017). Low levels of ROS/RNS are referred to as homeostatic or physiological levels, which result in common reversible PTMs, of Cys thiol side chains for example. Slightly elevated levels result in stress and adaptive states and lead to modifications like glutathione mixed disulfide formation. Finally, high levels of ROS/RNS lead to maladaptive and injurious states, which result in irreversible modifications of Cys, like sulfonic acid, and nitration of Tyr and Trp (Forrester & Stamler, 2012).

1.3 NTyr and DiTyr overview

It has been shown that Tyr residues in proteins typically represent, on average, 3-4 mol percent (mol %) of total residues in a protein (Bartesaghi et al., 2007). Tyr residues have a large phenolic amphipathic side-chain that can participate in hydrogen bond formation and undergo nonpolar interactions (Koide & Sidhu, 2009). Both solvent-exposed and buried Tyr residues can be present in a protein, but on average only 15% of Tyr residues are buried (Bartesaghi et al., 2007; Koide & Sidhu, 2009; Radi, 2012). The reactivity of the phenol group allows Tyr residues to undergo a variety of PTMs (Campolo et al., 2020).

NTyr (3-nitrotyrosine) is formed after the substitution of a hydrogen by a nitro (NO_2) group in the ortho position with respect to the OH group of the phenolic ring, shown in Figure 1.1 (Souza et al., 2008). The formation of NTyr is radical-mediated and the radical generated at the oxygen atom is stabilized by resonance within the aromatic ring, resulting in the addition of the NO_2 group only in the ortho position. NTyr is a

stable product and has been associated with inflammation, ageing, cancer, rheumatism, diabetes, and neurodegeneration (Bandookwala & Sengupta, 2020; Radi, 2012; Souza et al., 2008). In addition, nitration of proteins has been shown to increase the allergenic potential of allergens (Gruijthuijsen et al., 2006; Karle et al., 2012; Reinmuth-Selzle et al., 2023).

The addition of the NO₂ group on the phenolic ring of the Tyr residue alters the chemical properties of the amino acid (Radi, 2012). Nitration of Tyr changes the pKa of the hydroxyl (OH) group from 10 to 7.2, as well as impairs hydrogen bonding capability, which causes a disruption in protein structure (Radi, 2012; Souza et al., 2008; Zhan et al., 2015). Nitration also adds a hydrophobic substituent that often creates local steric restrictions and conformational changes (Radi, 2012).

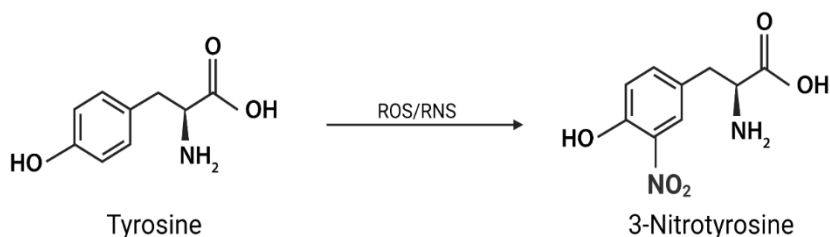


Figure 1.1. Nitration of Tyr residue via ROS/RNS. Created at BioRender.com.

DiTyr (L,L-dityrosine) can be formed via the cross-linking of Tyr residues both intramolecularly and intermolecularly, shown in Figure 1.2 (Malencik & Anderson, 2003). DiTyr is highly stable and irreversible, allowing for detection to be possible in both *in vitro* and *in vivo* experiments (Gross & Sizer, 1959; Maina et al., 2022). DiTyr

occurs naturally in some proteins, including in structural proteins where it is believed to increase stability and strength of the protein (Waykole & Heidemann, 2009). However, the formation of DiTyr in proteins is also associated with disease, specifically Alzheimer's disease, Parkinson's, cystic fibrosis, and acute myocardial infarction (heart attack) (Atwood et al., 2003; Mayer et al., 2014; Souza et al., 2000). Furthermore, DiTyr has been detected on human Alzheimer's disease tau protein oligomers (Al-Hilaly et al., 2014; Maina et al., 2022).

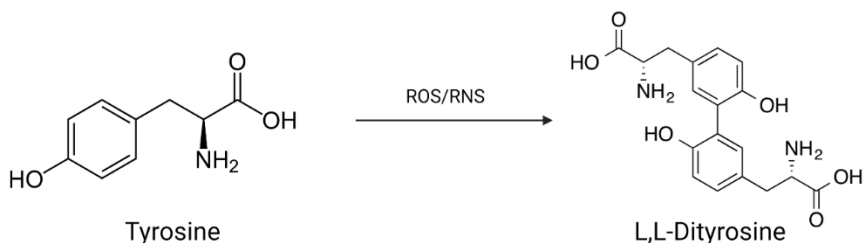


Figure 1.2. Dimerization of Tyr via ROS/RNS. Created at BioRender.com.

DiTyr and NTyr may occur simultaneously under oxidative and nitrosative stress conditions (Malencik & Anderson, 2003). The formation of NTyr and DiTyr via the reaction of ONOO^- and amino acids was shown by *Van der Vliet et al.* in 1994 and 1995 (Van der Vliet et al., 1995; van der Vliet et al., 1994). The reaction product and ratio of products formed depends on the environment, concentration, and pH (Lyman et al., 1996; Zhang et al., 2001). This will be discussed more in Chapter 5. However, because of this, it is important to consider and monitor the formation of both products when studying ONOO^- reactions.

Although other PTMs can be formed via the reactions of proteins with both ONOO^- and NO_2/O_3 , the focus of this dissertation will be NTyr and DiTyr formation, due to their prevalence and association with both endogenous reactions with ONOO^- and heterogenous aerosol chemistry with O_3 and NO_2 . There has been extensive research on both NTyr and DiTyr, however questions remain regarding the role each plays in allergenicity and respiratory disease, as well as the relative concentrations of each in ambient air. Furthermore, there are limitations to the detection and quantification of these PTMs that need to be overcome to further research. NTyr and DiTyr, as well as the detection and quantification methods used for both PTMs and the limitations, will be discussed in further detail in Chapter 2.

1.4 Relevant mechanisms of PTM formation

1.4.1 PTM formation via reaction with ONOO^-

ONOO^- can promote oxidation reactions either directly or by secondary radicals, including $\cdot\text{OH}$ and nitrogen dioxide ($\cdot\text{NO}_2$) (Ischiropoulos et al., 1992). ONOO^- can act as an oxidant via nucleophilic substitution ($\text{S}_{\text{N}}2$) and electron transfer (ET) mechanisms, and it can also act as a Lewis base and form reactive adducts. Due to this, ONOO^- can react with many different biomolecules and is known to nitrate phenolic compounds (Halfpenny & Robinson, 1952). The reactivity of ONOO^- with amino acids in proteins will be discussed here as a brief overview. For further information, *Ferrer-Sueta et al.* published a more comprehensive review of ONOO^- reactivity with biomolecules (Ferrer-Sueta et al., 2018).

ONOO⁻ can oxidize Met, including to sulfoxide in proteins, which is a PTM known to alter protein function (Berlett et al., 1998). Trp can react with ONOO⁻ directly or with free radicals derived from ONOO⁻, leading to many possible oxidized and nitrated products (Alvarez & Radi, 2003; Beatriz Alvarez et al., 1996; Padmaja et al., 2016). The most specific modification of ONOO⁻ in biological systems, however, is oxidation and nitration of Tyr. Tyr nitration, or the formation of NTyr, has been studied extensively since the early 1990's and is a PTM that can alter the function of a protein (Ferrer-Sueta et al., 2018). It has been associated with many diseases and inflammatory conditions, and has therefore become a biomarker of oxidative and nitrosative stress (Ziegler et al., 2019). It should be noted that both NTyr and nitrated Trp can be formed via other mechanisms (i.e. involving heme peroxidases), so the detection of these species in a biological system is not solely indicative of ONOO⁻ (Ferrer-Sueta et al., 2018).

One mechanism by which ONOO⁻ is produced endogenously is by the reaction of free radicals ·NO and O₂^{·-} (Figure 1.3) (Ferrer-Sueta et al., 2018; Pfeiffer et al., 1997). The formation of ONOO⁻ *in vivo* from ·NO and superoxide O₂^{·-} is kinetically favored, as indicated by its large rate constant (4-16 x 10⁹ M⁻¹) (Denicola et al., 1996; Ferrer-Sueta et al., 2018). ·NO is uncharged and nonpolar, which allows it to freely diffuse through cellular membranes, compared to O₂^{·-} that has low permeability due to its anionic character (pKa is 4.8) (Takahashi & Asada, 1983). ONOO⁻ is most likely formed *in vivo* where O₂^{·-} is, due to ·NO being able to diffuse easily across cellular membranes and having a longer half-life than O₂^{·-} (Lancaster, 1994). As mentioned, ONOO⁻ is a transient species. Once formed, there are three major possibilities of the fate of ONOO⁻. It can

isomerize to nitrate (NO_3^-), be reduced to nitrite (NO_2^-), or be reduced to $\cdot\text{NO}_2$ (Ferrer-Sueta et al., 2018). Focus here will be centered on $\cdot\text{NO}_2$, due to its role in NTyr formation. When ONOO^- is reduced to $\cdot\text{NO}_2$, $\cdot\text{OH}$ is also produced, which is an O_2 -derived reactive species (Campolo et al., 2020). Oxidation of amino acids via $\cdot\text{OH}$ also results in chemical and structural changes (Malencik & Anderson, 2003).

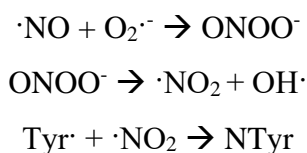


Figure 1.3. Relevant reactions for the formation of NTyr from ONOO^- .

$\cdot\text{NO}_2$ is a free radical formed *in vivo*, as well as an air pollutant, and is both a very strong oxidant ($E^\circ = \cdot\text{NO}_2/\text{NO}_2^- = 0.99 \text{ V}$) and nitrating agent (Stanbury, 1989). Because of this, $\cdot\text{NO}_2$ can react directly with many molecules in biological systems. The oxidation chemistry of $\cdot\text{NO}_2$ is described in detail by *Augusto et al.* and *Prütz et al.* (Augusto et al., 2002; Prütz et al., 1985). Briefly, it is capable of recombination with other radicals, electron transfer, and addition to unsaturated bonds (Augusto et al., 2002). All reactions except electron transfer are able to take place in both gas and liquid phase (Augusto et al., 2002; Ferrer-Sueta et al., 2018). Most crucially to the discussion here, $\cdot\text{NO}_2$ can react with biomolecule-derived radicals, including the tyrosyl radical ($\text{Tyr}\cdot$), to form NTyr (Prütz et al., 1985). $\cdot\text{NO}_2$ can also oxidize Tyr (Prütz et al., 1985). The ET

reaction of Tyr and $\cdot\text{NO}_2$ at alkaline pH ($\text{TyrO}^- + \cdot\text{NO}_2 \rightarrow \text{TyrO}\cdot + \text{NO}_2^-$) is particularly important and will be discussed more in Chapter 5 (Ferrer-Sueta et al., 2018).

The phenol side chain of Tyr is able to undergo one-electron oxidation to form $\text{Tyr}\cdot$ (Campolo et al., 2020). This can occur via three mechanisms, oxidation then deprotonation, deprotonation then oxidation, and a concerted oxidation/deprotonation (hydrogen abstraction) (Campolo et al., 2020). At physiological pH the phenolic OH group is protonated and the formation of $\text{Tyr}\cdot$ occurs mainly through hydrogen abstraction ($\text{TyrH} + \text{X} \rightarrow \text{Tyr}\cdot + \text{XH}\cdot$) (Campolo et al., 2020; Warren et al., 2012). At higher pH values, however, the mechanism involving deprotonation first followed by oxidation is more relevant (Campolo et al., 2020; Warren et al., 2012). Once the $\text{Tyr}\cdot$ is formed, a radical-radical reaction between two $\text{Tyr}\cdot$ molecules can occur, generating DiTyr (Figure 1.4). Many ONOO⁻-derived radicals can mediate the oxidation of Tyr to $\text{Tyr}\cdot$, including $\cdot\text{NO}_2$ and $\text{OH}\cdot$ (Ferrer-Sueta et al., 2018). The oxidation of Tyr by $\text{OH}\cdot$ occurs almost always through the initial addition of the $\text{OH}\cdot$ to the aromatic ring (Ferrer-Sueta et al., 2018).

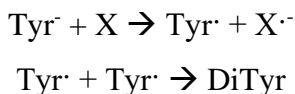


Figure 1.4. Relevant reactions for DiTyr formation.

It is important to note that ONOO⁻-mediated free radical reactions can result in the formation of NTyr and DiTyr, as shown, as well as many other secondary products,

including 3-hydroxytyrosine produced from the addition of $\cdot\text{OH}$ to Tyr \cdot (Santos et al., 2000). The biochemistry of ONOO^- is complex and only briefly discussed here. *Ferrer-Sueta et al.* published an extensive review in 2018 for more information (Ferrer-Sueta et al., 2018). The reactions of ONOO^- will often be referred to as homogeneous reactions, as they are conducted in aqueous solution, like the conditions found in the human body.

1.4.2 PTM formation via reaction with O_3 and NO_2

In the atmosphere, ROS and RNS species are generated via photochemistry and reactions involving oxidants and aerosols, and many common air pollutants can react as ROS and RNS in ambient air (Reinmuth-Selzle et al., 2017). The gaseous reactions of air pollutants and aerosols or proteins are referred to as heterogeneous reactions, due to two phases (gas and solid or gas and liquid) being involved. A substantial number of different reactions can occur due to the complexity of atmospheric chemistry, however only the reactions of O_3 and NO_2 with proteins will be discussed here. Furthermore, O_3 is able to react with proteins in the atmosphere at many residues, including Tyr, Trp, His, Cys, and Met due to the reactivity of these residues (Sharma & Graham, 2010). However, only the heterogeneous reactions of Tyr residues with O_3 and NO_2 to form NTyr and DiTyr are considered here.

The heterogeneous gaseous reaction of Tyr with O_3 and NO_2 is also radical-mediated, like the endogenous reactions previously discussed, as Tyr is a reactive species in the atmosphere (Figure 1.5). Therefore, Tyr acts as a sink for atmospheric oxidants. The reaction of O_3 that leads to cleaved unsaturated bonds is referred to as ozonolysis.

The nitration reaction of Tyr in the atmosphere is initiated by the reaction of Tyr with O₃ (ozonolysis), followed by reaction with NO₂ when present to form NTyr (Sandhiya et al., 2014). Reaction oxygen intermediates (ROIs) are formed after the first reaction, consisting of Tyr[•], which can either react with NO₂ or cross link with each other to form DiTyr (Figure 1.5) (Kampf et al., 2015; Reinmuth-Selzle et al., 2017). Also like the endogenous reactions, Tyr oxidation and nitration in the atmosphere depend on the environment where the Tyr residues are present. Ozonolysis may also result in the formation of other oxidized products (Liu et al., 2017). The mechanism for NTyr formation with O₃ and NO₂ was studied by *Sandhiya et al.* using computational methods (Sandhiya et al., 2014). In this study, the initial oxidation by O₃ was found to proceed by hydrogen abstraction, resulting in the formation of Tyr[•]. The formation of Tyr[•] was determined to be irreversible under atmospheric conditions and the subsequent nitration reaction with NO₂ was shown to occur as well, consistent with previous studies (Liu et al., 2017; Reinmuth-Selzle et al., 2014; Sandhiya et al., 2014).

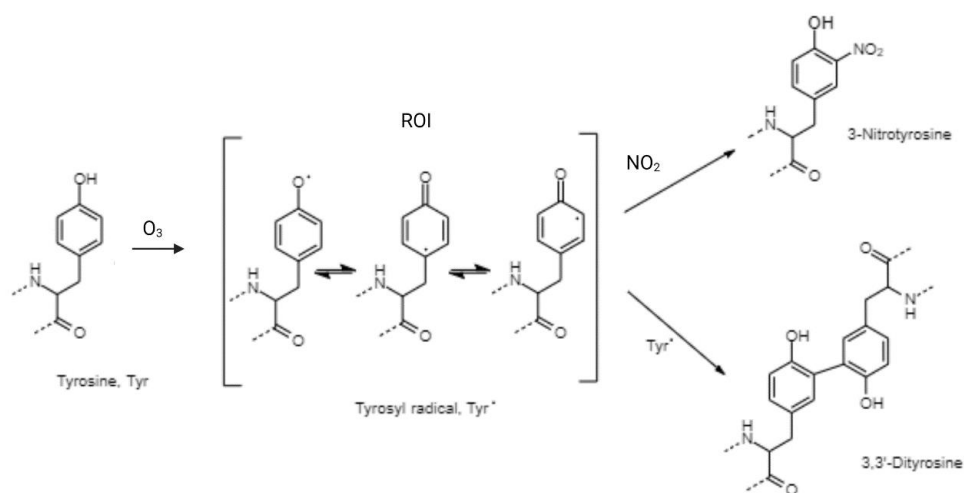


Figure 1.5. Reaction mechanism of Tyr with O_3 and NO_2 . Created at BioRender.com.

Liu et al. employed kinetic models to fit experimental data from the reactions of bovine serum albumin (BSA) protein with O_3 and NO_2 (Liu et al., 2017). BSA is a commonly used experimental protein with 21 Tyr residues. Results have shown that both NTyr formation and DiTyr cross-linking are sensitive to O_3 concentration and insensitive to NO_2 concentration. In addition, results confirmed that the reaction with O_3 to form ROI's is the rate-limiting step for NTyr formation, and that protein nitration qualitatively occurs faster than protein oligomerization, consistent with previous studies (Liu et al., 2017; Sandhiya et al., 2014; Souza et al., 2008). Figure 1.6 shows the reaction scheme of the relevant BSA nitration and oligomerization reactions from this study (Liu et al., 2017).

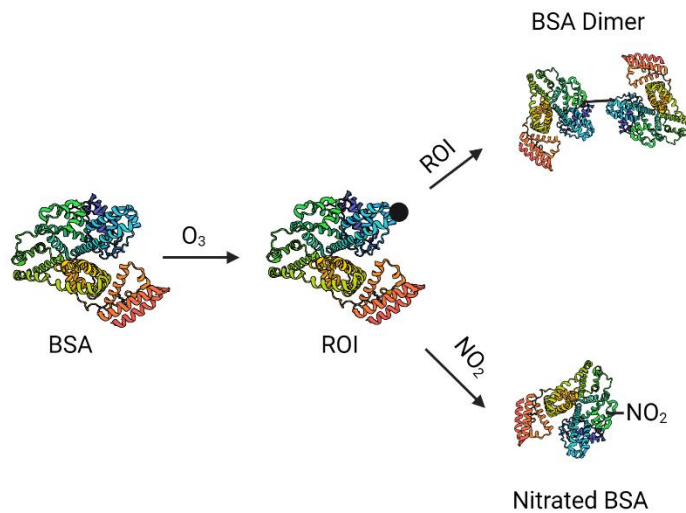


Figure 1.6. Reaction schematic of BSA and O_3/NO_2 , modified from *Liu et al.* (2017). Created at BioRender.com.

1.5 Motivation

1.5.1 Negative effects on human health

Hay fever and allergic rhinitis account for more than 13 million visits to doctor offices every year (L. Ziska et al., 2011; L. H. Ziska et al., 2019). There is substantial evidence showing that various climate change factors are causing an effect on allergies (Reinmuth-Selzle et al., 2017). Temperature rise and CO_2 concentrations are causing longer allergy seasons and higher pollen counts (L. Ziska et al., 2011). Furthermore, NO_2 and O_3 concentrations are causing an increase in the allergenic response to pollen (D'Amato, 2011; Duque et al., 2014; Gruijthuijsen et al., 2006; Reinmuth-Selzle et al., 2017). Due to this data and other observations that climate is changing rapidly at higher

latitudes, the EPA recognizes allergies as one of the most robust examples of how climate change is increasing risks to human health.

Ragweed pollen (*Ambrosia artemisiifolia*) is airborne as an aerosol in high concentrations across the US and Europe and represents a significant allergen for a considerable fraction of the population. Allergenic pollen proteins, or allergens, are responsible for the allergic response (IgE, immunoglobulin E) that occurs in some humans. Amb a 1 and Amb a 11 are the major ragweed allergens (Bouley et al., 2015; Wolf et al., 2017; Wopfner et al., 2009; Zhao et al., 2016). Allergens have been shown to react with oxidative air pollutants, resulting in an increase in relative allergenicity and the nitration reaction has been shown to increase the IgE response of proteins (Gruijthuisen et al., 2006). Reactions of other common allergens, like Bet v 1 (birch pollen) and Phl p 5 (grass pollen), with RNS and ROS have been investigated, but no studies have looked into the nitration and oligomerization reactions of Amb a 1 and Amb a 11 or the extent to which nitration occurs in ambient air (Backes et al., 2021; Reinmuth-Selzle et al., 2014; Selzle et al., 2013). In addition, PM_{2.5}, which includes proteins, can be deposited deep into the lungs of the respiratory tract, which further induces oxidative stress. Oxidative stress reactions, like ONOO⁻, cause further modification of the protein endogenously, which affects the functionality of the protein. More research is needed to determine the extent to which nitration and oligomerization of allergens occurs in the atmosphere, as well as how the PTMs further affect the respiratory tract and immune response.

1.5.2 Method development

There are a variety of scientific questions regarding the reactions of ROS and RNS with proteins that cannot be studied due to a lack of methodology or experimental design. Important analytical techniques for the study of NTyr and DiTyr will be discussed in Chapter 2. However, many of the current techniques have limitations, and there is a need for the advancement of various methodologies and analysis. Two important examples are 1) the lack of ability to detect PTMs directly in the atmosphere, and 2) the lack of understanding of experimental artifacts when reacting ONOO⁻ with proteins *in vitro*.

Studies surrounding the reactions of proteins with O₃ and NO₂ are commonly conducted using a flow reactor, where O₃ and NO₂, as well as other reactants, have been synthetically produced (Backes et al., 2021; Liu et al., 2017; Reinmuth-Selzle et al., 2014). This method is ideal for being able to vary the concentrations and mixtures of gaseous reactants, as well as reaction time, temperature, and relative humidity (RH). However, it does not represent the complex nature of the reactions occurring in ambient air. Therefore, it is important to be able to detect these reactions in ambient air and quantify the extent of which they occur.

Another example of the need for further study is regarding the reactions of ONOO⁻ and proteins to mimic oxidative stress in the human body. As discussed, ONOO⁻ is very reactive and the site-selectivity for many proteins is still not understood. However, to further study the reactions ONOO⁻ is often added in bolus amounts. This mechanism does not always directly represent what occurs *in vivo*, and experimental

artifacts may occur. It is therefore imperative these *in vitro* mechanisms are further analyzed.

1.6 Research aims

As shown throughout this chapter, a large amount of research has been conducted regarding the reactions of ROS and RNS with proteins and how these reactions interplay with the increase of allergic disease seen worldwide. However, various scientific questions remain. Further research is needed to better understand the roles of atmospheric RNS and ROS species, endogenous ROS and RNS species, and antioxidants in the increase in allergenic response.

There are many aspects of atmospheric and endogenous chemistry that overlap but have not been tied together. The main linkage to be discussed in this dissertation is between the atmospheric chemistry proteins in ambient air undergo, and the further chemistry that occurs once the proteins are inhaled through the respiratory tract inducing oxidative stress reactions. The extent of NTyr formation in urban air is, at this point, still unknown and there are no studies showing oligomerization formation in the atmosphere. Furthermore, comparison of NTyr formation in the atmosphere and endogenously has not been extensively conducted and many of the mechanistic details are still unknown. This dissertation aims to fill the gap between atmospheric and endogenous nitration and oligomerization and show that mechanistically the multiphase gaseous reactions and aqueous reactions are very similar.

In addition, there are various limitations in the current experimental methodology that prevent answering some questions regarding this linkage discussed. For instance, methodology to detect nitration occurring in ambient air in real time does not exist and previous work has only studied total PM samples. Quantification methods for PTMs involve many assumptions and the most widely available techniques, like ELISA, can only give semi-quantitative information. This dissertation aims to improve the methodology and quantification of PTMs in complex samples, as well as provide perspective on the importance of analytical method development.

This dissertation demonstrates the achievement of the following research goals:

1. To improve the experimental methodology of studying the heterogeneous reactions occurring with proteins and O_3/NO_2 in ambient air (Chapter 3).
2. To determine the relative concentrations of NTyr formation in urban ambient air and correlate NTyr formation to ambient air pollutant concentrations (Chapter 4).
3. To determine the extent of which experimental conditions, like pH, alter the reaction mechanism of proteins with $ONOO^-$ (Chapter 5).
4. To study the site-selectivity of the reaction of $ONOO^-$ and LF and efficacy of EGT to prevent the reactions (Chapter 6).

Additional work supporting the main chapters can be found in Appendices A through N.

Chapter Two: Nitrotyrosine and Dityrosine

2.1 Nitration

2.1.1 NTyr in urban air

The chemical modification of bioaerosol proteins in the atmosphere has been linked to an increase in respiratory disease and allergies (Gruijthuisen et al., 2006; Ito et al., 2018, 2019; Liu et al., 2017). The following section is not meant to be comprehensive, but to give further background into the research that has been conducted showing NTyr formation in ambient air as well as the implications nitrated pollen proteins have. Pollen grains around 20 μm can be transported up to 1,000 km, and the long-range transport of ragweed pollen has been detected (Grewling et al., 2016; Müller-Germann et al., 2017). In addition, Amb a 1 has been observed in particles $< 5 \mu\text{m}$, which can stay in the air for days or weeks (Grewling et al., 2016). Therefore, proteins can react with atmospheric pollutants for an extended period, allowing for increased modification.

NTyr has been detected in polluted urban air samples and the relationship of NTyr with PM and O₃ in the atmosphere was shown by *Ito et al.* after collecting PM samples using a high volume air sampler (Franze et al., 2005; Ito et al., 2018). *Franze et al.* collected environmental samples and detected NTyr in urban road dust, window dust, and fine air PM, and the observed rates of NTyr formation was correlated to NO₂ and O₃ concentrations (Franze et al., 2005). In addition, *Ogino et al.* detected protein in PM samples and the proteins were partially nitrated (Ogino et al., 2021).

As mentioned, it has been shown that environmental allergens trigger the immune response and chemical modification of allergens enhances the response. Bet v 1 and Phl p 1 have been studied extensively by researchers at the Max Plank Institute for Chemistry and Bet v 1 has also been investigated by researchers at the University of Salzburg (Ackaert et al., 2014; Backes et al., 2021; Reinmuth-Selzle et al., 2014). The nitration of Bet v 1 was shown to proliferate specific T-cell lines more than the unmodified allergen (Ackaert et al., 2014). Chemical modification of Phl p 5 was shown to enhance Toll-like receptor 4 (TLR4) activation (Reinmuth-Selzle et al., 2023). Immunochemical analysis also showed that the allergenicity of London plane (*Platanus x acerifolia*) pollen was enhanced after allergens were exposed to O₃ and NO₂ (Ribeiro et al., 2017). Finally, changes in the IgE response were observed of *Acer negundo*, *Platanus x acerifolia*, and *quercus robur* pollen following O₃ exposure and *Platanus* pollen allergen Pla a 3 was shown to be nitrated and oxidized in a later study (Duque et al., 2014; Zhou et al., 2021). *Frank and Ernst* review the effects of NO₂ and O₃ on pollen allergenicity in 2016 and *Senechal et al.* reviewed the effects of major atmospheric pollutants on pollen grains in 2015 (Frank & Ernst, 2016; Sénéchal et al., 2015).

2.1.2 NTyr within the human body

As mentioned, oxidative and nitrosative stress are considered driving factors in many endogenous pathological conditions. Protein Tyr nitration has become a PTM biomarker for oxidative stress, often impacting protein structure and function. It has been estimated that approximately 1-10 Tyr residues per 100,000 proteins are nitrated under

inflammatory conditions, and even early immunological studies showed that protein dinitrophenyl derivatives enhance the immune response (Parker et al., 1962; Souza et al., 2008). Presented here are some key findings from the literature outlining the role NTyr plays in the human body.

The presence of NTyr in human samples was shown by MS, both in protein samples and as a free amino acid (Pacher et al., 2007). *Sacksteder et al.* identified proteins sensitive to nitration and of the 29 proteins identified more than half are involved in Parkinson's disease, Alzheimer's disease, or other neurodegenerative disorders (Sacksteder et al., 2006). Furthermore, when mice were treated with an experimental model of Parkinson's disease an increased level of nitration was identified (Sacksteder et al., 2006). *Lee et al.* reviewed the role of NTyr in neurodegenerative disease and atherosclerosis (Lee et al., 2009). Nitrated proteins in *in vivo* disease models were investigated, and the major nitrated proteins were involved in energy metabolism (redox reactions), consistent with the current understanding of how NTyr forms. The mitochondria, therefore, is considered to be the center of nitration (Lee et al., 2009).

In addition to NTyr studies in disease states, individual proteins have been studied upon modification. The nitration of LF has been shown to alter protein structure and function, decreasing the antibacterial ability of LF (Alhalwani et al., 2019, 2023). Upon nitration, some proteins can become completely inactivated, as seen by manganese superoxide dismutase (Peluffo & Radi, 2007). Lastly, nitrated α -synuclein at different Tyr residues exhibited reduced binding affinity (Burai et al., 2015).

2.2 Analytical methods of NTyr detection and quantification

2.2.1 Detection methods of NTyr

Due to extensive research on PTMs that has been conducted, various detection methods exist, including immunoassays and spectrometry. A common hurdle in PTM research, however, is that analytical quantification is necessary to answer some of the scientific questions. However, in many cases qualitative or semi-quantitative biochemical techniques are all easily accessible. The following sections regarding the detection and quantification of NTyr and DiTyr are not meant to be comprehensive, but rather provide the necessary information for the subsequent chapters. Various PTM detection and quantification reviews have been published, some of which are referenced here (Bandookwala et al., 2019; Batthyány et al., 2016; Duncan, 2003; Hawkins & Davies, 2019; Herce-Pagliai et al., 1998; Teixeira et al., 2016; Tsikas, 2017).

UV-Vis spectroscopy enables the detection of NTyr both as a free amino acid and in proteins due to its absorbance spectrum. Tyr and NTyr both have an absorption peak at 280 nm. In addition, NTyr can be detected in pure samples qualitatively and semi-quantitatively via the absorbance around 430 nm in alkaline conditions (Crow & Beckman, 1995). The absorbance properties are pH-dependent, and in neutral and acidic conditions NTyr has an absorbance maximum around 350 nm (Yang et al., 2010). Figure 2.1 shows the absorbance properties of Tyr and NTyr. NTyr is a yellow color in solution. Because absorption properties of NTyr, high-performance liquid chromatography coupled with diode-array detection (HPLC-DAD), is often employed as a detection and quantification technique, discussed in the next section.

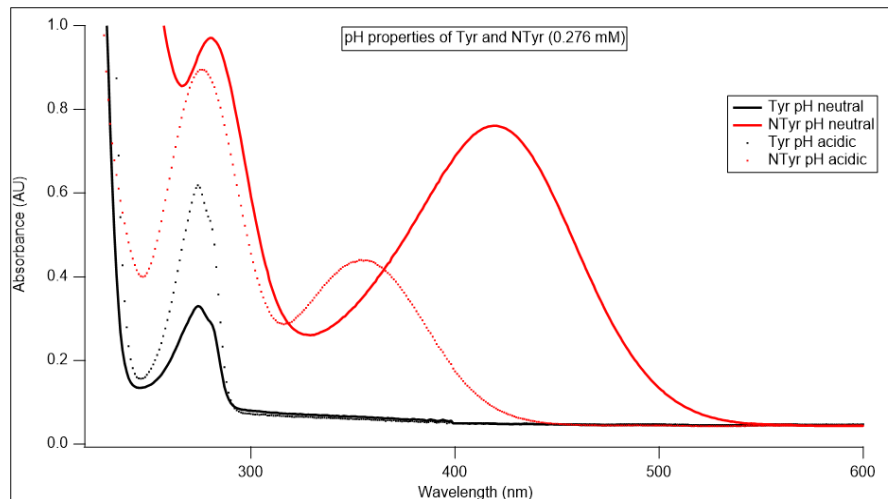


Figure 2.1. Absorption properties of Tyr and NTyr, obtained via UV-Vis measurements of standards. Red lines indicate NTyr and black lines represent Tyr. Solid lines are at neutral pH and dotted lines at acidic pH.

The loss of the intrinsic fluorescence properties of Tyr is also indicative of NTyr formation, shown in Figure 2.2.

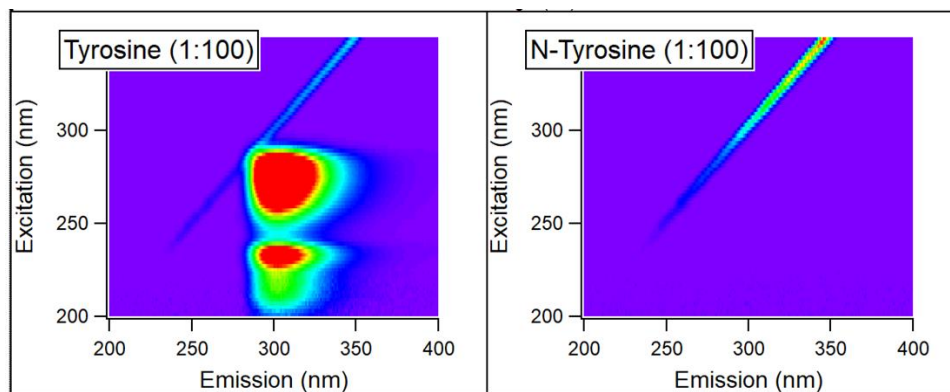


Figure 2.2. Loss of Tyr fluorescence when nitrated, obtained via fluorescence measurements of Tyr and NTyr standards. Red color represents high intensity, purple represents low intensity. 1:100 is the dilution factor from a 1.0 mg/mL standard in PBS.

Immunoassays are another common method utilized for the detection of NTyr. Enzyme-linked immunosorbent assay (ELISA) employs the use of labeled antibodies for the detection of a specific substrate. There are different types of ELISA's, two of which are direct and sandwich. Direct ELISA uses one antibody while sandwich ELISA requires a matched antibody pair, resulting in more specific detection. The detection of NTyr is commonly conducted using direct ELISA (see optimized protocol in Appendix J). Specific methodology can be optimized for the analyte of interest. For instance, *Alhalwani et al.* developed a sandwich ELISA method for the selective detection of nitrated LF (Alhalwani et al., 2018). While ELISA's can offer very specific detection of a desired analyte, common interferences can occur, and the quantification is based off a calibration curve. This poses a problem when the analyte is chemically modified to an unknown extent.

Two commonly used well plate assays, the bicinchoninic assay (BCA) and Bradford assay, are used to determine total protein concentration. While not specific to NTyr, they are important to note here, because they can detect proteins that have been chemically modified, as long as the modification does not impact the assay mechanism. Many methods used to detect protein concentration, like UV-Vis spectroscopy applying Beer's Law, are not reliable once a PTM has occurred due to the molar absorptivity changing to an unknown degree. The BCA assay relies on the formation of a Cu^{2+} -protein complex and compares the unknown sample signal to a calibration standard. The BCA, however, has many problems associated with it, including common interferences and systematic error at low analyte concentrations (bias above 15%) (Rogatsky, 2021).

Similarly, the Bradford assay is not reliable at low analyte concentrations and is not as sensitive as the BCA (Ernst & Zor, 2010).

2.2.2 Quantification methods of NTyr

While various immunoassays, like ELISA's, are considered quantification methods, limitations apply when used with chemically modified proteins, making these methods only semi-quantitative. Similarly, spectrometric properties, like absorbance maxima and extinction coefficients can be altered when chemical modification occurs, so spectroscopic quantification is also semi-quantitative. However, analytical techniques for the quantification of NTyr has been greatly improved, as reviewed by *Bandookwala et al.* in 2019 (Bandookwala et al., 2019).

Briefly mentioned in the last section, HPLC-DAD is often used to detect and quantify NTyr in protein samples. *Selze et al.* determined a metric referred to as nitration degree (ND) to quantify the nitration of intact protein samples using HPLC-DAD without the need for nitrated protein standards (Selzle et al., 2013). The ND is the concentration of NTyr divided by the sum of the concentrations of NTyr and Tyr. In HPLC measurements Tyr and NTyr are measured simultaneously, so because both Tyr and NTyr have absorption maxima at 280 nm the relative contribution of each to the absorbance is necessary to calculate ND. Scaling factors k and f are used to scale the extinction coefficients and ND is determined using Equation 1 (Selzle et al., 2013).

$$ND = \frac{A_{NTyr,357}}{A_{NTyr,357} + \frac{f}{k}(A_{all,280} - kA_{NTyr,357})} \quad (\text{Equation 1})$$

Figure 2.3 shows a schematic of the detection of nitrated proteins via HPLC-DAD, using BSA (bovine serum albumin, a commonly used test protein) as an example. The wavelength 357 nm is used as it was determined to be the absorption maxima in acidic conditions, as used by the HPLC (Selzle et al., 2013). Gas chromatography methods are also commonly used to detect and quantify NTyr but are not discussed here.

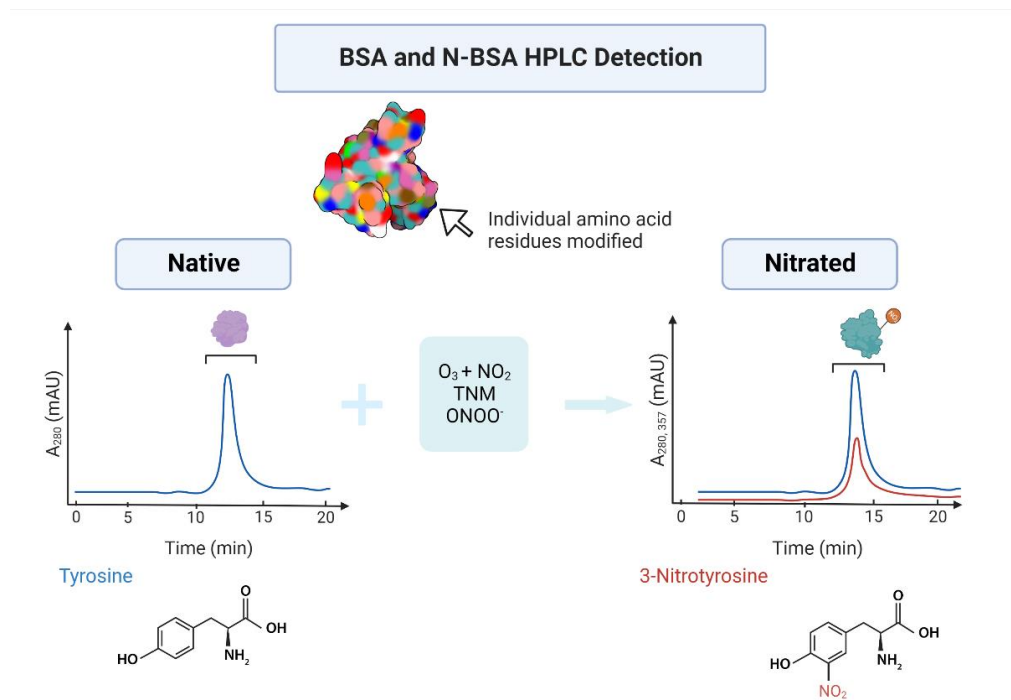


Figure 2.3. HPLC-DAD detection of NTyr schematic once individual amino acid residues are modified. Blue line represents absorbance at 280 nm and red line 357 nm. Created at BioRender.com.

As mentioned, the site-selectivity of NTyr formation is dependent on the molecular structure of the protein and reaction conditions (Reinmuth-Selzle et al., 2014). Analyzing the specific NTyr sites, therefore, requires analytical techniques. Tandem mass spectrometry (MS/MS) is often used to analyze proteins and PTMs. Briefly described, proteins are digested during sample work-up into peptides. The peptides are then analyzed via MS/MS. *Zhan et al.* wrote a review article on the MS analysis of NTyr-containing peptides (Zhan et al., 2015). In nitrated protein samples the ND is able to be determined for individual NTyr-containing peptides, as well as site-specific information for nitrated and oxidated amino acids. Electrospray ionization (ESI) allows for the detection and characterization of many PTMs since direct sequence information is obtained, as well as multiple charge peaks can be generated, which is ideal for peptide analysis. Quadrupole time-of-flight (Q-TOF) and orbitrap MS detectors are ideal for peptide analysis due to the high resolution.

2.3 Dimerization and oligomerization

As stated in Chapter 1, DiTyr can be a naturally occurring component of protein structure, or a product of oxidative stress, environmental or endogenous. DiTyr formation in proteins is usually the result of two protein molecules cross-linking. The steric hinderances involved in a single protein molecule make it less likely for DiTyr to form intramolecularly. Because of this, the terms DiTyr formation, dimerization, and oligomerization are commonly used to refer to the same PTM. However, oligomerization is mostly used to refer to the formation of higher oligomers (> dimer; i.e. trimer, etc). As

discussed in Chapter 1, the reaction mechanisms for the formation of DiTyr are related to the NTyr mechanism, and the reaction product is mostly determined by the reaction conditions and availability of reactants. Therefore, it is important to monitor the formation of both NTyr and DiTyr when reacting proteins with ROS and RNS.

As noted, there is extensive research on NTyr as a PTM. However, there is not as much literature on DiTyr formation and oligomerization and its role in allergies and disease. A simple Web of Science search (March 15th, 2023) gave 1,196 results for “dityrosine,” compared to 7,367 results for “nitrotyrosine.” Luckily, as the evidence for the strong relationship between the formation of DiTyr and NTyr grows, more research including DiTyr is being done.

DiTyr crosslinks have been identified in Alzheimer’s disease, as well as Parkinson’s disease, and cerebrospinal fluid (Maina et al., 2022; Mukherjee et al., 2017). In addition, crosslinks were formed in collagen and amyloid- β as the result of vitamin b-12 deficiency (Koseki et al., 2021). Free DiTyr has also been found in the urine of diabetic patients (Kato et al., 2009). *Malencik and Anderson* reviewed the early research on DiTyr formation in 2003 (Malencik & Anderson, 2003). The role of DiTyr formation and oligomerization in allergies and oxidative stress is also important, but has not been investigated extensively. *Kofler et al.* have shown that dimerization of Bet v 1 alters the allergenic potential of the protein (Kofler et al., 2014). Furthermore, the formation of protein dimers and oligomers through DiTyr crosslinks upon reaction with O₃ have been reported (Kampf et al., 2015). However, further research is needed to better understand

the extent of DiTyr formation that occurs under oxidative and environmental stress, as well as its role in allergies.

2.4 Detection and quantification of DiTyr

Similar to the detection of NTyr, various techniques are commonly used to detect DiTyr and oligomers. As with DiTyr, sample conditions and the need for quantitative results dictate the specific technique chosen. This section briefly summarizes some of the methods used with respect to DiTyr formation in the atmosphere and under oxidative stress. It is not discussed here, but DiTyr ELISA methods also can be used like NTyr ELISA protocols. *DiMarco and Giulivi* reviewed the early detection methods of DiTyr in 2006, but advancements have been made since (DiMarco & Giulivi, 2007).

While the formation of NTyr from Tyr results in a decrease of fluorescence, DiTyr does have fluorescence properties. The fluorescent properties of DiTyr are pH-dependent, as shown by *Malencik and Anderson* (Malencik & Anderson, 2003). In alkaline solution, excitation of DiTyr at 320 nm results in fluorescence emission at 400 nm (Malencik & Anderson, 2003). It should be noted that DiTyr is a potential energy transfer donor to NTyr, so energy transfer and quenching may occur if there is the simultaneous occurrence of DiTyr and NTyr in the same protein molecule, depending on the distance between donor and receptor (Malencik & Anderson, 2003).

SDS-PAGE with silver stain is also a common technique used to detect DiTyr and higher oligomers in protein and biological samples. When using pure protein samples, it is easy to determine the expected molecular mass of dimers, trimers, and higher

oligomers (i.e. MW x 2, 3, etc.). *Backes et al.* show the use of SDS-PAGE to detect oligomerization of Phl p 5 upon exposure to O₃, NO₂, and ONOO⁻ (Backes et al., 2021).

MS techniques are used to detect overall oligomerization and MS/MS is a useful tool for detecting free DiTyr in complex mixtures and protein samples. *Verrastro et al.* review the MS-based methods for identifying oxidized proteins in disease (Verrastro et al., 2015). However, there are limitations to using MS/MS to determine cross-linked DiTyr residues. *Mukherjee et al.* developed a method for using MS/MS to identify and characterize DiTyr peptides using the fragmentation pattern of a synthetic peptide (Mukherjee et al., 2017, 2019). Synthetic peptides with specific PTMs are costly and often require manufacturing, so this method is not possible for all cases.

Size exclusion chromatography coupled with DAD (SEC-HPLC) is a fast and reliable technique for determining the degree of oligomerization in an intact protein sample. Often times a protein mixture standard is used as a calibrant and the retention time gives information regarding the size of the protein molecules in the sample, as SEC separates based on hydrodynamic size. *Kampf et al.* show the use of this method to determine DiTyr formation upon exposure to O₃, and reported degrees of oligomerization as the sum of the respective oligomer to the sum of monomer and all oligomer peaks (Kampf et al., 2015). The simultaneous determination of ND and oligomerization is also possible via SEC-HPLC (Liu, Reinmuth-Selzle, et al., 2017). Gas chromatography methods also exist for the detection of DiTyr but are not discussed here.

2.5 Limitations of NTyr and DiTyr detection and quantification

There are various limitations of NTyr and DiTyr detection and quantification, so care is needed when choosing an analysis technique. Some examples of error were discussed in, however a few more examples are discussed here.

As mentioned, ELISA techniques are able to selectively detect NTyr and nitrated proteins. However, their use in quantification has many assumptions tied into it. For one, the signal is compared to a calibration curve made with nitrated protein standards. We have determined that this does not give accurate information regarding the extent to which a protein is nitrated. For instance, many of our nitrated protein samples are nitrated with TNM. When using this to compare the overall NTyr concentration to nitrated proteins via ONOO⁻ or O₃/NO₂, the difference in nitration mechanism, site-selectivity, and reaction conditions are not taken into account. Therefore, the NTyr concentration determined can only be compared to the nitrated standards and does not represent an absolute concentration.

The required sample work-up for MS/MS can incorporate problems when analyzing proteins with PTMs. If the protein has already been modified prior to analysis sample work-up, it must be ensured that no further modifications occur and that the sample work-up modifications do not interfere with analysis. For example, in MS/MS analysis protein samples are digested, most often via trypsin, and the resulting peptides are analyzed. During the trypsin digestion cysteine residues are alkylated, which does not allow for their pre-digested PTM analysis to occur. Other considerations in MS/MS analysis are needed, including ionization efficiency and proteasomal cleavage rates.

Trypsin is highly specific, cutting at the carboxyl side of arginine and lysine residues. However, at NTyr sites in proteins and peptides there are decreased proteasomal cleavage rates (Silvina Bartesaghi et al., 2018). Similarly, the ionization efficiency in MS/MS analysis is not the same for nitrated and native peptides. Therefore, some nitrated peptides might not be analyzed as efficiently as native, resulting in measurement bias.

As discussed, once nitrated the extinction coefficient of the protein or amino acid is altered. This makes the quantification of NTyr concentration and total protein concentration of modified proteins difficult, as the determined concentration will also only be relative to a standard that is nitrated to a different unknown extent than the samples. Spectroscopic properties are often dependent on sample conditions, so the limit of detection (LOD) and limit of quantification (LOQ) may vary as well. Furthermore, other modifications, like nitrated Trp, have similar spectroscopic properties, so other modifications may alter the signal. *Selzle et al.* compare commonly used methods for determining protein content (Reinmuth-Selzle et al., 2022).

Many of the same limitations of detection and quantification of NTyr apply to DiTyr. ELISA methods rely on calibration standards, and spectroscopic measurements are only valid for pure protein samples. Sample conditions also dictate what detection and quantification considerations apply, as well as certain sample work-up conditions must be avoided as to not form artificial DiTyr before samples are analyzed. Also, as briefly discussed in Section 2.4, use of MS/MS analysis for the quantification of DiTyr cross-linkages in digested protein samples requires further improvement. While MS and HPLC

methods can detect and quantify the extent of oligomerization that has occurred in a protein sample, they do not elucidate the location of the cross-linkage.

2.6 Additional analytical considerations

2.6.1 Baseline correction and integration

Due to the large number of uncertainties with NTyr and DiTyr detection, especially with commonly available techniques, a major part of my doctoral studies has required analytical development and method characterization. More details will be given with respect to each project in Chapters 3-6, however three common questions will be discussed here. The first is regarding the HPLC-DAD data and how it is integrated. We have found that the software the HPLC system uses to baseline subtract and integrate peak areas gives very different results depending on the sample compared to when the integration is done by hand. In many of our analyses for NTyr detection, the integrated peak area is placed into the nitration degree calculation. Because this metric is a ratio it is not concentration dependent, allowing us to compare multiple samples across experiments. It is therefore important the integration strategy used is the same across all samples and accurately depicts the peak area.

Figure 2.4 shows the integration strategy we have employed throughout the work presented here. Due to using a gradient chromatographic elution method, our samples often have a sloping baseline. Our protein samples elute later in the chromatographic run and we often use lower concentration samples, so accurate subtraction of this sloping baseline is important. Figure 2.4 represents the baseline subtraction and integration

strategy used. In this case the 280 nm wavelength is being analyzed. Integrated peak areas were cross-referenced with integration done by hand, and the integration scheme was modified until the values matched. This analysis has also been conducted with the 357 nm wavelength and a nitrated BSA standard, which allowed the LOD, LOQ, and analytical sensitivity of our HPLC method to be determined. This is shown in Chapter 3.

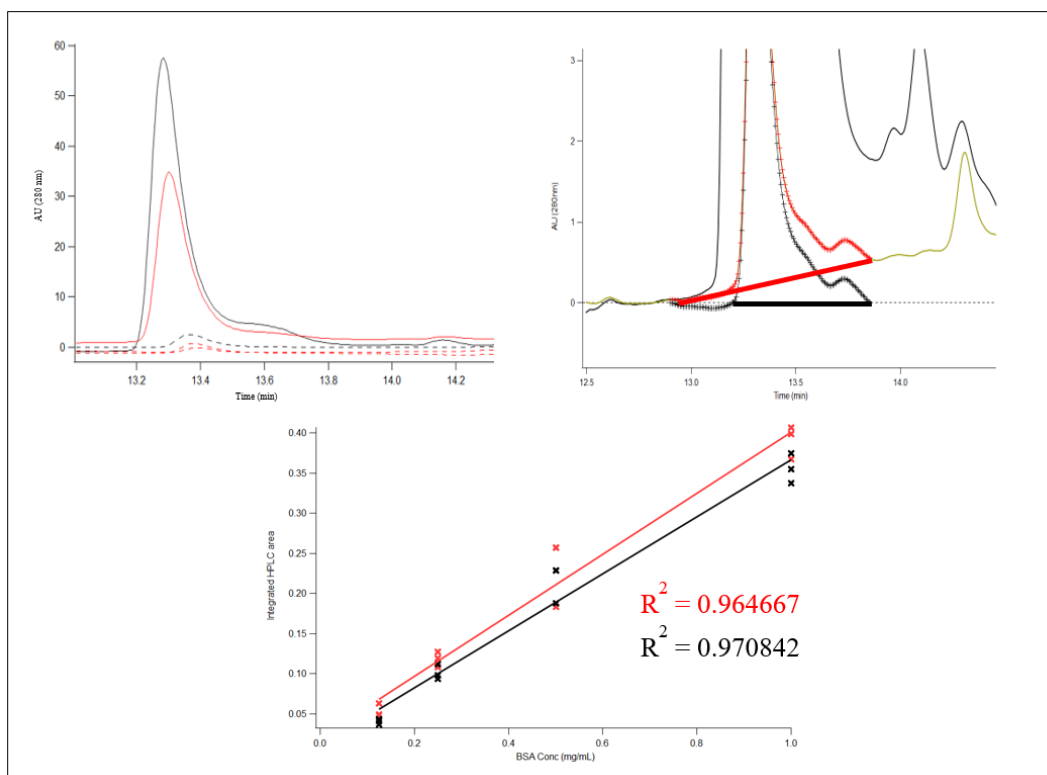


Figure 2.4. HPLC-DAD baseline correction and integration scheme. First top plot shows the raw 280 nm (blue) and 357 nm (red) chromatograms. Second top plot is baseline subtraction methods, flat baseline in black and a sloping baseline in red. Bottom plot is calibration curve with the BSA concentration on the x-axis (mg/mL) and the integrated peak area on the y-axis.

Figure 2.4 represents a standard protein sample, but we also wanted to ensure our integration strategy works on more complex and unknown samples. An example of the integration scheme used on an ambient sample is shown in Figure 2.5. The black dotted curve represents a H₂O blank, the black curve represents the raw data, the red curve represents the raw data once the baseline has been subtracted, and the blue curve represents the data that is integrated. As shown, the ambient data samples can often be low concentration and the raw data often has a baseline below zero. Our integration scheme accounts for this and allows for the correct integrated peak area to be obtained. Because this analysis is done very often, we developed Igor code to baseline subtract and integrate peaks of interest semi-automatically. The Igor code can be found in Appendix A.

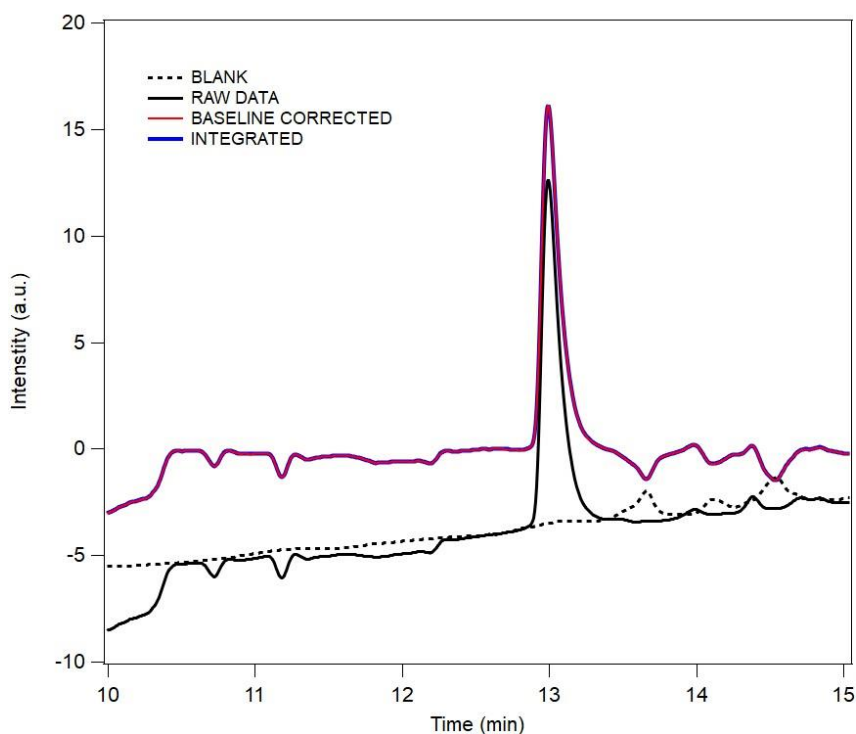


Figure 2.5. HPLC-DAD baseline correction and integration used for ambient samples. Dotted line is blank, black line is raw data, red line is baseline corrected data, and blue line is integrated data.

2.6.2 Micropipette precision

Another common question in our analytical research is the precision and accuracy of the micropipettes used. The micropipettes have been calibrated and are used appropriately depending on volume required, however there have been times in our research that the accuracy and precision of the micropipettes are very important. For instance, in many of our nitration experiments a very small volume of nitrating agent is required to be delivered ($< 1 \mu\text{L}$). In these experiments the same exact volume is needed to be delivered for the nitration response to then be compared across multiple samples,

reaction conditions, etc. However, often it is noticeable that the same volume is not accurately delivered. An example of this is discussed in Chapter 5.

The accuracy and precision of each micropipette are determined by the manufacturers and reported. However, the accuracy and precision vary depending on the volume used, and values for each volume are not reported. To test the accuracy and precision of the micropipettes used for these experiments, we developed an experiment using the absorbance of a standard at a certain concentration, delivered a volume using a micropipette of the standard into a 96-well plate to match the concentration, and back-calculated the volume delivered by the micropipette. Experimental details can be found in Appendix B. Figure 2.6 shows two histograms each using a different volume that are commonly used in our experiments. It is noticeable that the volume delivered is not the same as the intended volume. More work is being done to further analyze this, but we believe this may play a larger role in experimental uncertainty at lower volumes.

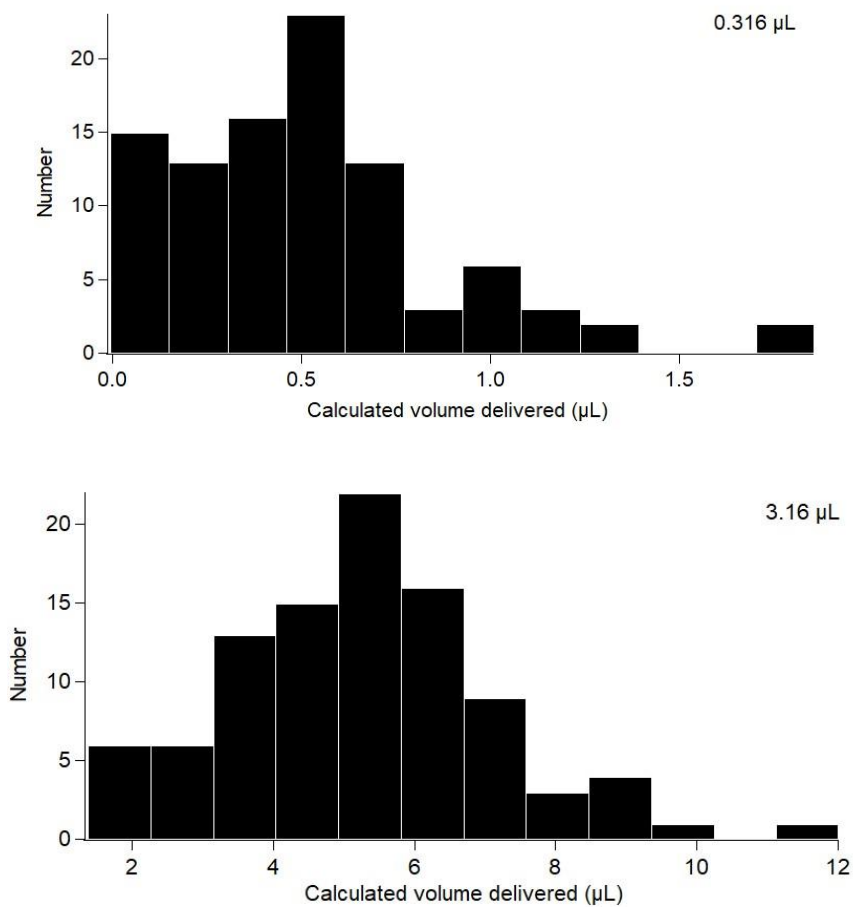


Figure 2.6. Histogram of calculated volume delivered compared to pipette volume. Top is 0.316 μL and bottom is 3.16 μL.

2.6.3 Amicon centrifugal unit cleaning

Another commonly used technique in nitration experiments is to “clean” the reaction products after the nitration reaction to remove all byproducts and remaining unreacted nitration agent. To do this, Amicon centrifugal units are utilized due to the small volume and concentrations of the samples. Minimizing sample loss is imperative,

especially when quantification of the final protein concentration of the sample is required.

As stated above, total protein concentration determination is not always trivial, and each method has its limitations. In our experimental set-ups the total protein concentration is assumed to be the same as before cleaning after the cleaned sample is diluted back to the starting volume. However, the cleaning efficiency of the Amicon filters had not been analyzed previously, due to limitations of prior methods (i.e. UV-Vis and ELISA not accurately quantifying modified proteins compared to unmodified proteins, discussed above). Using the HPLC (Figure 2.7) we were able to quantify the cleaning efficiency of the filters, which allows us to account for the sample loss in protein concentration quantification. The experimental details are discussed more in Chapter 3 and Appendix C. However, it was determined that the cleaning process through the Amicon filter has 96.18% sample retention.

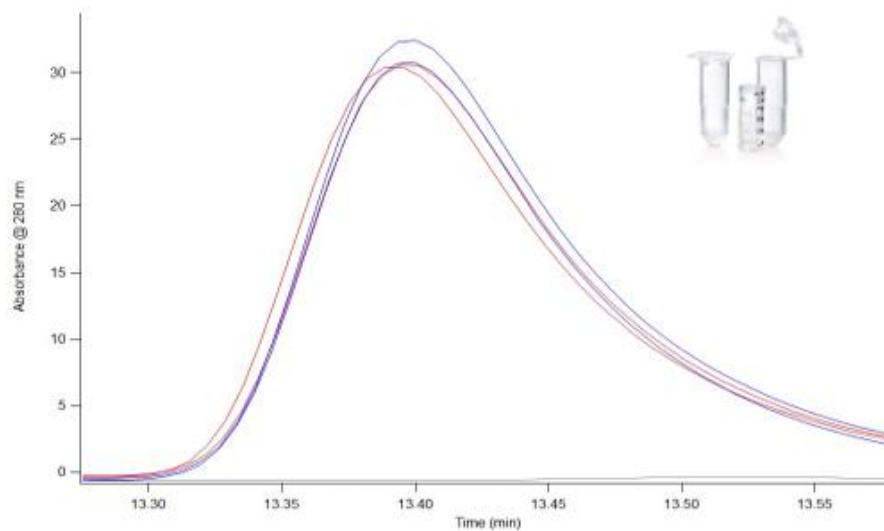


Figure 2.7. HPLC-DAD before and after centrifugal unit cleaning. Blue line is before cleaning and red, black, and purple lines are three separate samples after cleaning.

Chapter Three: Heterogeneous Nitration Reaction of BSA Protein with Urban Air: Improvements in Experimental Methodology

Peer-reviewed and published in the following form, with only minor formatting
modification:

Davey, R. L., Mattson, E. J., & Huffman, J. A. (2022). Heterogeneous nitration reaction
of BSA protein with urban air: improvements in experimental methodology.
Analytical and Bioanalytical Chemistry 2021, 1–12. <https://doi.org/10.1007/S00216-021-03820-8>

3.1 Abstract

Gas-phase ozone (O₃) and nitrogen dioxide (NO₂) can react with environmentally exposed proteins to induce chemical modifications such as the formation of nitrotyrosine (NTyr). Certain proteins with these modifications have also been shown to promote adverse health effects and can trigger an immune response. It is hypothesized that proteinaceous material suspended in the atmosphere as particulate matter, e.g. embedded in pollen, can undergo heterogeneous reactions to produce chemically modified proteins that impact human health, especially in urban areas. To investigate the protein modification process under ambient outdoor reaction conditions, bovine serum albumin

(BSA) protein samples were loaded onto filters and exposed to urban air in Denver, Colorado (USA). Losses and measurement artifacts were measured independently to calculate nitration effects on the protein via high-performance liquid chromatography and to support the experimental methodology. O₃ loss from inlet lines using three commonly used particulate filters was quantified, showing a range of ambient O₃ concentration losses from 3.2% for Kynar[®] (polyvinylidene fluoride) filters to > 60% for commonly used HEPA filters. Protein mass extraction efficiency was calculated as a function of filter material and protein mass using both native and nitrated BSA. Finally, we show examples of BSA samples nitrated by exposure to urban air as a proof-of-concept for future studies, highlighting the potential for atmospherically relevant NTyr formation. The methodology vetted here provides support for a wide variety of experimental efforts related to exposure of analytes to O₃ and more broadly to an expanding field of protein modification in ambient air.

3.2 Introduction

3.2.1 Importance of heterogeneous protein reactions in the atmosphere

The effects of polluted urban air on human and environmental health are widespread and being more fully understood (Ackaert et al., 2014; Backes et al., 2021; Frank & Ernst, 2016; Ghiani et al., 2016; Gruijthuijsen et al., 2006; Reinmuth-Selzle et al., 2017; Shiraiwa et al., 2012; Taylor et al., 2004). One broad avenue to health impact is via reactive oxygen and nitrogen species (ROS/RNS) that can be generated in the atmosphere via oxidative chemical reactions of air pollutants (Estillore et al., 2016;

Mayorga et al., 2021; Reinmuth-Selzle et al., 2017). These highly-reactive species can further interact with proteins to induce post-translational modifications (PTMs) that are, in most cases, irreversible (Backes et al., 2021; Estillore et al., 2016; Franze et al., 2005; Ito et al., 2018, 2019; Reinmuth-Selzle et al., 2014, 2017; Sandhiya et al., 2014). A common PTM implemented as a biomarker for inflammation and oxidative stress is nitrotyrosine (NTyr), which can be formed via the nitration of the aromatic amino acid tyrosine with a variety of nitrating agents (Gruijthuijsen et al., 2006; Liu, Reinmuth-Selzle, et al., 2017; Reinmuth-Selzle et al., 2014; Albert van der Vliet et al., 1995). Nitration has been reported upon nitrogen dioxide (NO₂) and ozone (O₃) exposure, e.g. to bovine serum albumin (BSA) and Bet v 1, the major allergen in birch pollen (Franze et al., 2005; Reinmuth-Selzle et al., 2014; Sandhiya et al., 2014; Selzle et al., 2013; Shiraiwa, Pö, et al., 2012; Zhou et al., 2021), requiring only relatively low gas concentrations (Liu et al., 2017). The reaction of tyrosine and O₃ involves the formation of a tyrosyl radical, which further reacts with NO₂ in a second step to form NTyr (Lai et al., 2020). Due to the reactive nature of the tyrosyl radical, other PTMs like hydroxylation, oxidation, nitrosylation, and dityrosine are possible (Lahoutifard et al., 2002; Liu et al., 2017; Mudd et al., 1969) and have been studied for other amino acids, proteins, and polycyclic aromatic hydrocarbons (PAHs) in the atmosphere (Arey et al., 1986; Backes et al., 2021; Mudd et al., 1969; Reinmuth-Selzle et al., 2014; Zhou et al., 2021).

Studies have reported the linkage of increased pollen allergenicity to exposure to urban air pollutants, like NO₂ and O₃ (Lang-Yona et al., 2016; Liu et al., 2017; Petersen

et al., 1998; Zhou et al., 2021). Additionally, the direct exposure of allergenic proteins, like Bet v 1, to polluted outdoor air has been shown to increase the allergenic potential of the protein (Ackaert et al., 2014; Gruijthuijsen et al., 2006; Karle et al., 2012). The chemical modification of proteins, like nitration, has been linked to both an increase in Immunoglobulin E (IgE) response (Baraldi et al., 2006; Cuinica et al., 2014; Gruijthuijsen et al., 2006; Parker et al., 1962) and immunogenic properties (Ackaert et al., 2014; Karle et al., 2012; Ziegler et al., 2020). Due to extensive this evidence, as well as the large increase in seasonal allergy prevalence, the study of atmospherically relevant proteins and pollen is important to better understand these effects.

3.3.2 Mechanisms of study

The most common method to study the chemical effects of air pollution on pollen or proteins has been to expose them to manufactured gases in the laboratory. In one study, BSA was exposed to varying levels of O₃, NO₂, and relative humidity (RH) by passing the gasses through solid BSA protein on syringe filters (Yang et al., 2010; Zhang et al., 2011). In separate studies, BSA solutions were loaded into glass tubes, dried with N₂ gas, and exposed to O₃ produced from synthetic air flowed through a mercury vapor lamp (Kampf et al., 2015; Liu et al., 2017). *Reinmuth-Selze et al.* placed Bet v 1 on cellulose acetate syringe filters and the protein-loaded syringe filters were exposed to pollutants in a flow reactor (Reinmuth-Selze et al., 2014). Frank and Ernst provided a broad review of other exposure studies (Frank & Ernst, 2016), including the exposure of O₃ and NO₂ (Ribeiro et al., 2017), O₃ only (Duque et al., 2014), NO₂ only (Cuinica et al.,

2014), and the combined effect of CO, SO₂, and O₃ (Cuinica et al., 2015). Finally, pollen extracts have been exposed directly to diesel exhaust (Chen et al., 2020). Here we aim to discuss a common ambient exposure system used for proteins and to identify procedural uncertainties and artifacts to better aid future studies.

Direct ambient exposure refers to experiments where pollen or proteins are exposed to ambient urban air, whereas indirect ambient exposure refers to experiments where pollen is exposed naturally, while on the plant, through growth in the urban environment, or through being grown in environments enriched in specific gas-phase pollutants. Studies using indirect ambient exposure on pollen have shown widespread effects (Beck et al., 2013; Franze et al., 2005; Ghiani et al., 2012; Suárez-Cervera et al., 2008). For instance, ragweed plants grown in elevated NO₂ conditions and pollen samples collected from trees near high traffic roads translated to an increased IgE response of the pollen (Zhao et al., 2016). It is difficult, however, to correlate the effect, e.g. enhanced allergenicity, to the specific chemical or physical modification in the plant or pollen due to an abundance of variables.

Using direct exposure in an environmental chamber allows for controlled reaction conditions and exposing pollen or proteins directly to ambient air allows for more variables to be studied, e.g. other pollutants or temperature, and for individual chemical or physical modifications in the pollen or protein to be correlated to the immunological or allergenic response. In direct exposure studies, is important to choose a particulate matter (PM) filter and experimental procedure that reduce O₃ losses due to adsorption and reactivity of O₃. Teflon tubing is typically chosen for its low reactivity with O₃. It is also

imperative the PM filter has a small enough filter size to efficiently block deposition of ambient PM. Reference methods established by the Environmental Protection Agency (EPA) for measuring ambient concentration of air pollutants use a standard Teflon PM pre-filter (47 mm, 5 μm ; 40 CFR Part 53) to reduce interference in gas-phase sampling instruments, but such filters are insufficient for experiments outlined here, because they allow a fraction of submicron particles to deposit onto protein samples. A study regarding the ambient exposure of a fungal allergen used a HEPA (high efficiency particulate air) filter to block PM deposition onto samples (Lang-Yona et al., 2016). Another similar study was performed in which glass fiber pre-filters were inserted in the gas-flow directly before protein samples and the pre-filter was shown to reduce O_3 by 80% (Franze et al., 2003). This shows how significantly the choice of pre-filter can alter reactive gaseous concentrations downstream, which is especially important when quantitative correlation with O_3 concentration is being studied.

An appropriately chosen sample filter is also important to reduce artifacts and sample losses. Properties such as pore size, minimal extraction artifacts, and low amounts of protein binding in aqueous extractions are important. Both syringe and non-syringe filters have been used in this type of ambient sampling and cellulose acetate and polypropylene (PP) filters have been compared, but PP is considered best for high performance liquid chromatography (HPLC) analysis (Keller et al., 2008; Williams, 2004). *Ito et al.* collected airborne PM on quartz filters using a high-volume air sampler (Ito et al., 2018). *Franze et al.* lyophilized an aqueous solution of BSA onto different types of syringe filters (diameter 25 mm), including glass fiber syringe filters (pore size 1

μm), cellulose (0.45 μm), cellulose acetate (1.2 μm), and aluminum oxide (0.2 μm) (Franze et al., 2005). In addition, *Franze et al.* used glass fiber syringe filters (Franze et al., 2003). Here, we show uncertainties introduced by different filter media.

3.2.3 Reducing experimental uncertainties and artifacts

While the detection of protein PTMs upon exposure to ambient air has been conducted widely, uncertainties remain in the technical approaches utilized. Here, we present experiments conducted to address these concerns (Figure 3.1). By using BSA, which is a commonly used test protein with 21 tyrosine residues (UniProt P02769), we were able to compare our results to previous studies discussed here. We determined the O_3 loss across three commonly used PM filters and the protein extraction efficiencies of common protein-loading filters. This was done to ensure accurate quantification of the protein after modification by urban air without relying on assays or using the molar absorptivity due to changes after chemical modification. Also, by using HPLC and an absorbance ratio to determine the ND, the absolute protein concentration is not required. By conducting these experiments, we address experimental uncertainties and artifacts. The reduction of these uncertainties further improves experimental procedures, which will help aid in the next generation of studies related to direct ambient exposure of proteins.

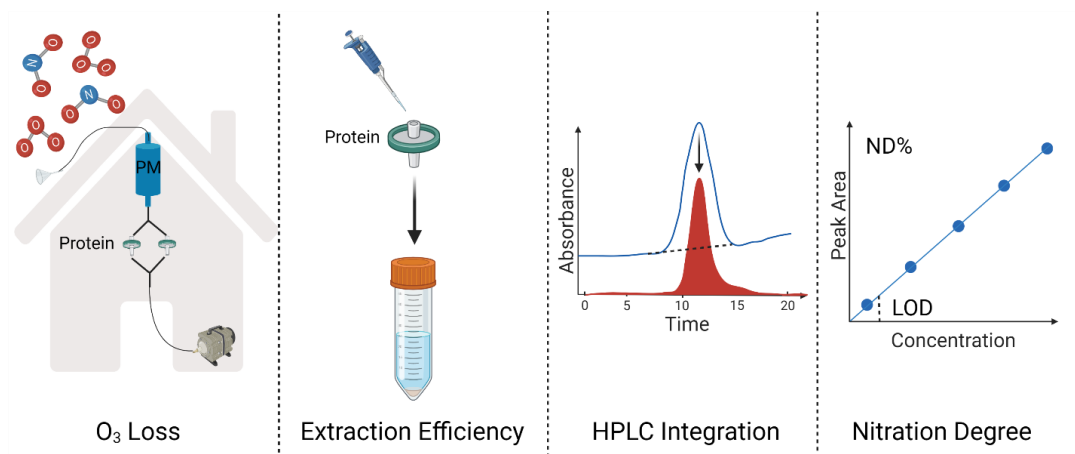


Figure 3.1. Schematic representing steps in ambient exposure and analysis experiments. Created with BioRender.com

3.3 Materials and Methods

3.3.1 Materials

Bovine serum albumin (BSA; A7030), tetranitromethane (TNM; T25003), sodium phosphate dibasic (RES20908-A702X), potassium phosphate monobasic (P5655), potassium chloride (P9333), and sodium chloride (S9625) were purchased from Sigma-Aldrich. Trifluoroacetic acid (85183) was obtained from Thermo Fisher Scientific and acetonitrile (ACN; 100030) from Millipore Sigma. Amicon Ultra-0.5 centrifugal filters (10 kDa, 0.5 mL size; UFC503008) and Amicon Ultra centrifugal filters (10 kDa, 4 mL size; UFC803024) were purchased from Calbiochem. A 1.0 mL quartz cuvette with 10 mm path length (MF-W-10-LID) was obtained from Science Outlet.

Luer-Lock PP syringe filters (0.45 μm , 25 mm; SF14691) were purchased from Tisch Scientific, glass fiber filters (47 mm; 61631) and HEPA filter capsules (12144) from Pall (12144), and Advantec quartz fiber filters (25 mm; QR20025mm) from Cole-

Parmer. Kynar[®] (polyvinylidene fluoride; PVDC) filters were purchased from Parker Balston and Teflon tubing (3/16" ID, 1/4" OD; 5239K12) from McMaster. Inlet line was constructed using Swagelock fittings. A DryCal Defender 220 Series (Mesa Labs) was used to measure airflow of ambient inlets.

The buffer used was phosphate-buffered saline (1xPBS; 8.1 mM sodium phosphate dibasic, 0.8 mM sodium phosphate monobasic, 1.3 mM potassium chloride, and 68.0 mM sodium chloride at pH 7.4). An analytical balance (Ohaus Explorer EX125D; ± 0.01 mg) was used for all mass measurements. All data analysis was done in Igor Pro (Wavemetrics). Graphics created at BioRender.com.

3.3.2 Nitration of BSA by TNM

The nitration reaction of BSA with TNM followed the procedure from *Alhalwani et al.* (Alhalwani et al., 2018). Briefly, the TNM reaction occurs in a mixture of PBS buffer and 20% ethanol, followed by addition of TNM based on the chosen TNM/Tyr molar ratio, and stirred at room temperature (RT) for 2 hours. The reaction is quenched by using an Amicon 10 kDa centrifugal unit to filter excess reagent from the reaction vessel and product. The modified protein is further referred to as nitrated BSA, or NBSA.

3.3.3 Spectroscopic analysis

The absorbance of light at 357 nm is commonly used as a general tool for the detection of NTyr, due to the addition of the NO₂ group to tyrosine. A Cary 100 Bio UV-vis spectrophotometer was calibrated using potassium dichromate and

determined to be within accepted values. Absorbance values were measured at a wavelength range of 250 - 500 nm in 2 nm increments at RT using a 10 mm quartz cuvette.

3.3.4 Protein extraction

PBS (4 mL) was placed in conical tubes with either quartz or glass filters, and the absorption of the extract was spectroscopically analyzed to give the absorbance of the blank. Extracts produced through this protocol were also flushed through a PP syringe filter before spectroscopic analysis. PBS (4 mL) was directly flushed through a PP syringe filter and the blank absorbance of the extract was taken. BSA (50 μ L of 2.0 mg/mL BSA in PBS) was loaded onto each filter and extracted with PBS using the same protocol.

Solutions of BSA in PBS (0 – 500 μ g/mL) were prepared in order to calculate solution density at varying concentrations. The 0 μ g/mL BSA sample was PBS, alone. For each concentration, volume increments (0.5 – 10 mL) of the BSA solutions were aliquoted using a BRAND[®] Transferpette[®] S pipette (BR705880, BR705874) and weighed to determine the mass (n = 3). It is important to note that because the volumes used are measured via micropipettes, the precision of this process is limited by the precision of micropipettes used (\pm 0.6 - 3%).

To determine the extraction efficiency, BSA (4.99 g/mL BSA in PBS stock; 50 - 500 μ g BSA) was placed onto PP syringe filters and extracted with 4 mL PBS (referred to as extract). The same mass of BSA was placed in a falcon tube with 4 mL PBS

(referred to as reference). The absorbance of each extract and reference sample were spectroscopically analyzed and the extracted volume was weighed.

3.3.5 HPLC-DAD analysis and ND determination

Protein solutions were analyzed using RP-HPLC-DAD (reverse-phase high performance liquid chromatography with diode-array detection) as previously described (Selzle et al., 2013). Briefly, modified or exposed samples were concentrated using Amicon centrifugal units and placed in glass HPLC vials and analyzed using a HPLC-DAD system (Agilent 1200 series) that was calibrated to detect nitration using BSA reacted with TNM at a 1/1 (TNM/Tyr) molar ratio. A C₁₈ column (Supelco Discovery BioWide Pore 25 cm x 2.1 mm, 5 μm) with eluents 0.1% (v/v) trifluoroacetic acid in water (eluent A) and ACN (eluent B) were used for chromatographic separation. Gradient elution was performed at a flow rate of 300 μL/min, and for each run the solvent gradient started at 3% B followed by a linear gradient to 90% B within 15 min. Absorbance was monitored at wavelengths of 280 and 357 nm. The sample injection volume was 25 μL, and each chromatographic run was repeated three times (measurement replicates) with a water blank in between. The nitration degree (ND) of each sample was determined, as previously described by Selzle et al. (Selzle et al., 2013), using the integrated peak areas of both 280 nm and 357 nm peaks (Selzle et al., 2013).

3.3.6 Gas-phase instruments and pollutant data

Air pollutant data was collected using instruments operating continuously at monitoring sites in Denver, CO managed by the Colorado Department of Public Health and Environment (CDPHE). The two sites used for this study were La Casa (39.779460, -105.005124) and Rocky Flats North (39.912799, -105.188587). Each site has a variety of air pollutant monitors that continuously collecting data. NO₂ data was collected via a Model T200 Chemiluminescence NO/NO₂ /NO_y Analyzer (Teledyne API) and O₃ data was collected via Model T400 UV Absorption O₃ Analyzer (Teledyne API).

3.3.7 O₃ loss over PM filters

Two collocated O₃ instruments were used over four separate experiments. Both instruments had a Teflon 1 μm pre-filter in place. The test instrument had an additional PM filter placed upstream of the final pre-filter, but not the reference instrument. To ensure instrument comparability, the instrument responses were compared for 6-16 days before and after each filter was added. A Kynar[®] filter was placed in front of the test instrument and the responses were logged and compared for 27 days, 20 days for a HEPA filter, and 28 days for a PP syringe filter.

3.3.8 Ambient set-up

A 3 m Teflon sample line (1/4" outer diameter) was led from the roof of each monitoring site into the building where the protein samples were placed. BSA (100 μL of 4.0 mg/mL BSA in PBS) was placed on 2 separate sample filters and a PM filter was

placed directly before the samples in the set-up to ensure only ambient gases passed through the samples. An air pump (Gast high-capacity vacuum pump; DOA-P704-AA) was used to continually pump air through the filters at a rate of 12 L/min total (~6 L/min to each sample). BSA samples were exposed to ambient air for 1-2 weeks each.

3.4 Results and Discussion

3.4.1 Particulate filters

To support the selection of an appropriate PM filter for ambient protein analysis, where avoiding O₃ reactivity is important, three different types of commonly used PM filters were tested using two identical O₃ monitors. To ensure instrument compatibility, the O₃ response was compared for six days before the test filters were placed, as well as 6-16 days in between each test filter. The two instruments (reference and test) showed high correlation at most O₃ concentrations (overall R² 1.00), but poor correlation at O₃ concentrations below 3 ppb O₃, points which were subsequently removed before analysis. Data was also filtered to remove electronic spikes. The two O₃ data sets were then plotted against each other (Figure. 3.2a). Baseline and slope measurements for the test instrument were adjusted (b + 0.003; m x 1.005) so the adjusted fit line passed through the origin with a slope of 1.00. The same correction was applied to test instrument data for all subsequent comparisons.

No additional filter was placed in front of the reference instrument, whereas a sequence of three different filters were used in front of the test instrument. Upon placing the Kynar[®] filter in front of the test instrument, the O₃ response immediately dropped

with respect to the reference instrument signal but returned within 2 hours. Every new PM filter will have a 'burn-in' period when it temporarily absorbs more O₃. Therefore, the immediate drop in O₃ was likely due to conditioning of receptor sites in the filter, and so the first 2 hours of data comparison were removed from analysis. Following signal response adjustment, as discussed above, the slope of the correlation between reference and Kynar[®] was 0.968 (Figure 3.2b). By subtracting the reduction from a slope of unity, the Kynar[®] filter showed an O₃ loss of 3.2%. The process was repeated for the HEPA filter (Figure 3.2c) and PP syringe filter (Figure 3.2d) resulting in losses of 63.6% and 5.9%, respectively. This suggests that the Kynar[®] filter was optimal for use as a PM filter due to its minimal effect on O₃ loss, while the PP filter could be useable if necessary and collocated O₃ concentration is adjusted appropriately. Due to the common use of HEPA filters, the observation that HEPA filters reduced O₃ concentration by 63.6% is important for many ambient studies concerned with urban gas exposure. These should be avoided whenever O₃ loss may be important. Organic material within PM deposited onto the filters provides surface area for O₃ adsorption and reaction, so O₃ loss will also increase with PM loading (Hytinen et al., 2003). For this reason, new PM filters were used here in all cases. Care should be taken to occasionally replace loaded PM filters with new filters during similar exposure experiments.

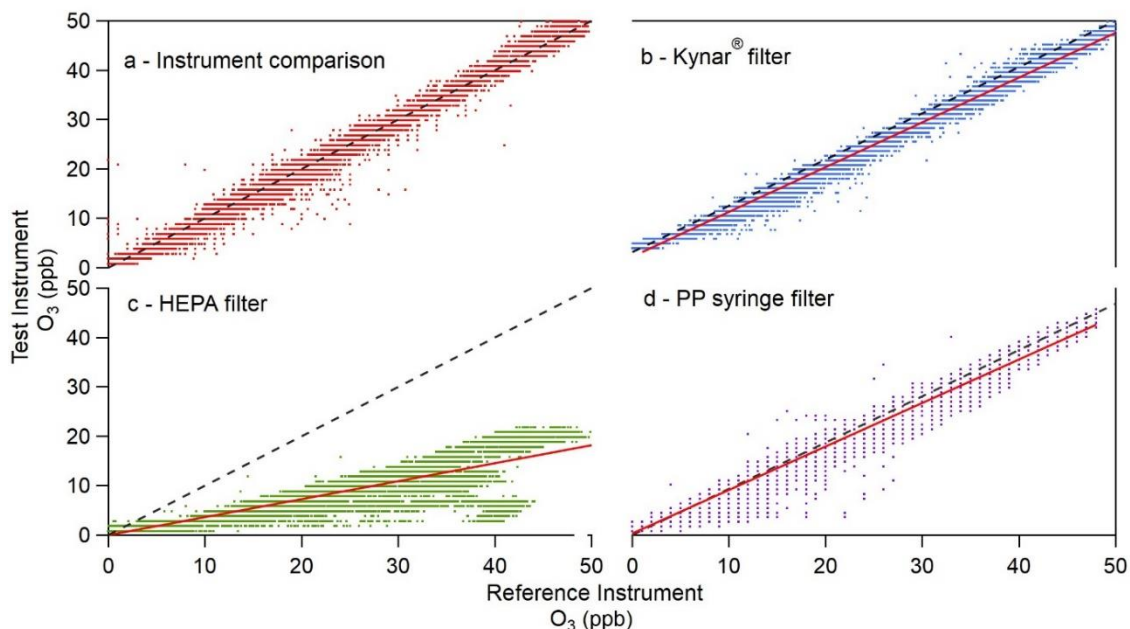


Figure 3.2. O₃ loss over PM filters. Dotted black lines represent 1:1 line and solid red lines represent linear fit of individual 1 min. data points, shown as dots. **a** Direct comparison of both O₃ instruments no additional filter ($R^2 = 1.00$), **b** Kynar[®] filter ($R^2 = 0.993$), **c** HEPA filter ($R^2 = 0.849$), **d** PP syringe filter ($R^2 = 0.992$).

3.4.2 Protein extraction vs filter media type

The nitration response, or formation of NTyr, of protein samples can be monitored in various ways. Most commonly used is a method by which ND is calculated, as explained by *Selzle et al.* (Selzle et al., 2013). Briefly, both unmodified (in this case, no NTyr) and modified proteins show a 280 nm absorbance peak. Upon formation of NTyr in the modified protein, the 280 nm peak intensity increases slightly, and an absorbance peak at 357 nm is introduced under acidic conditions (pH ~3) (Selzle et al., 2013). This 357 nm peak is not present in unmodified proteins and grows upon nitration, thus ND is a modified ratio of 357 nm to 280 nm (Selzle et al., 2013).

To be able to quantify extracted protein amount after modification, using absorption spectroscopy, it is important to avoid filters that leech light-absorbing contaminants into solution. To identify optimal filter media on which to load protein before ambient exposure, BSA in buffer was loaded onto each filter type and absorbance was measured at 280 nm. Buffer solutions washed through both quartz and glass fiber filters became visibly cloudy and exhibited high background absorbance (Appendix C Figure C1) due to large amounts of soluble and insoluble filter components washed into solution. Filter blanks for quartz and glass fiber filters produced high background values (Figure 3.3 dashed bars). In contrast, the PP syringe filter did not interfere with the absorbance at 280 nm (Figure 3.3) and produced a minimal blank signal (0.02 ± 0.01). The PP syringe filter BSA extract signal (0.04 ± 0.02) was within the uncertainty range of the matching BSA reference signal (0.06 ± 0.03). The quartz and glass extracts were also filtered in a second step using a PP syringe filter to remove suspended material washed off the primary filters. A high background absorbance remained, however, as shown by the smaller bars (filter + PP) in Figure 3.3. Given these observations, PP syringe filters alone were determined optimal to use as protein-loading filters for ambient exposure.

It is important to note these experiments were done to optimize the use of small mass amounts of protein for direct ambient exposure and NTyr detection using UV-vis. The need to avoid interference using absorption spectroscopy, as discussed here, may not be necessary for bulk PM collection or detection of other PTMs. In other applications, for example, quartz filters are used widely for PM collection, where spectroscopic analysis is

not utilized or where absorption wavelengths >400 nm are used (Ito et al., 2018). For reasons stated, quartz filters are not a viable option here.

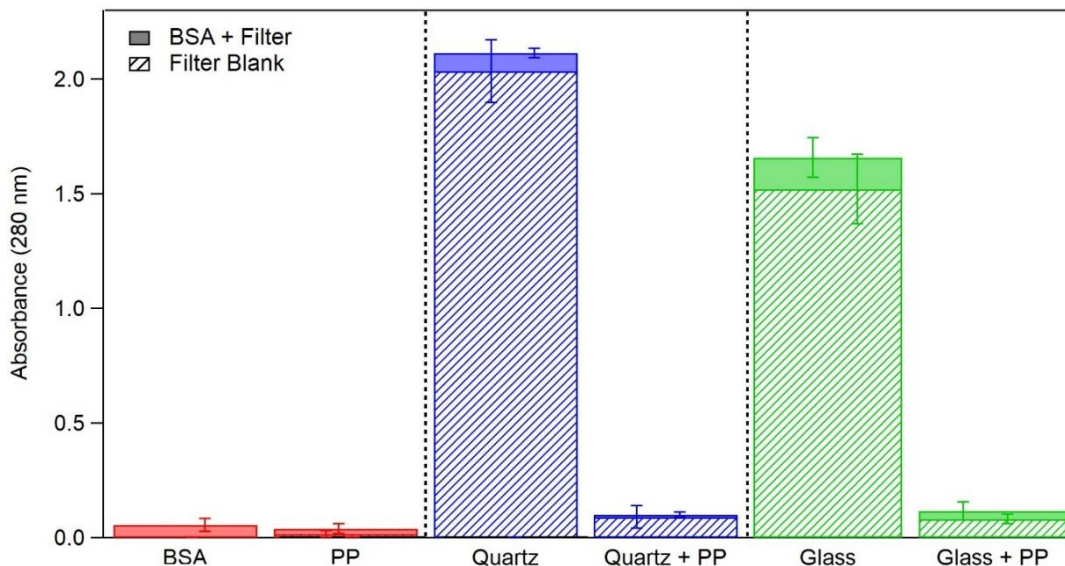


Figure 3.3. Protein extraction interference at absorbance value of 280 nm from different filter media. BSA (50 μ L of 2.0 mg/mL BSA in PBS; red bar, left) loaded onto each filter and extracted with 4 mL PBS. Striped bars represent the filter blank of each sample, which is the filter in PBS with no protein. Solid bars represent the filter with BSA, extracted with PBS. Error bars represent the standard deviation from sample replicates ($n = 2-5$).

3.4.3 Protein extraction efficiency

Due to the nature of the type of ambient sampling and analysis proposed, there are many places in the process for sample loss. To verify that exposed protein is not being lost or retained on the filter through the extraction process, the extraction efficiency of BSA (purity $\geq 98\%$) off the PP syringe filter was determined (see Appendix C Figure C2). The concentration of protein in a sample can be spectroscopically analyzed using

Beer's Law ($A = \epsilon lC$; where ϵ is molar absorptivity, l is pathlength, and C is solution concentration) if ϵ is known. The ϵ values can be measured for native BSA, but are unknown for NBSA (nitrated BSA) because even slight differences in nitration reaction conditions, i.e. when exposed to ambient reactants, can cause BSA to be nitrated to varying degrees, resulting in different ϵ values. Therefore, to determine the extraction efficiency without using ϵ values, a gravimetric analysis was performed, utilizing the density (ρ in g/mL) of BSA in PBS. The densities of varying BSA concentrations (0 – 500 $\mu\text{g/mL}$ BSA in PBS) were determined by plotting the mass (μg) of the sample as a function of volume (mL), where the slope of the fit line determined the density (see Appendix C Figure C3). Due to the dilute nature of the solutions, the density of solution was essentially that of water and thus did not significantly change (see Appendix C Figure C4; $n = 3$) as a function of BSA concentration (1.002 ± 0.001 g/mL).

To measure filter extraction efficiency, the same mass of BSA (50 - 500 μg) was measured on an analytical balance, put into solution using PBS volume measured by micropipette, and separately placed onto PP syringe filters and extracted (extract) or directly placed into falcon tubes (reference; m_{ref}). The absorbance value at 280 nm was measured for each solution. Upon extraction, an unknown volume of BSA in PBS solution remained on the filter, so the concentration of the extract is thus unknown. Assuming the spectroscopic pathlength and ϵ of solution are constant before and after extraction, a rearrangement of ratios of Beer's Law in Equation 3.1 shows that:

$$C_{extract} = \frac{A_{extract}}{A_{ref}} C_{ref} \quad (\text{Equation 3.1})$$

This assumption is reasonable, because molar absorptivity is concentration independent, even if absorbance is not. The mass of the extracted solution ($m_{solution}$) was measured on an analytical balance and recorded, as was the solution density ($\rho_{solution}$; see Appendix C Figure C4). The volume of extracted solution ($V_{solution}$) can thus be determined:

$$V_{solution} = \frac{m_{solution}}{\rho_{solution}} \quad (\text{Equation 3.2})$$

The mass of BSA in the extracted volume can thus further be calculated:

$$m_{extract} = C_{extract} V_{solution} \quad (\text{Equation 3.3})$$

By taking the ratio of mass of BSA in the extract to mass of BSA in the reference ($\frac{m_{extract}}{m_{ref}}$), the extraction efficiency was determined for each mass of BSA (50 - 500 μg).

Shown in Figure 3.4, the extraction efficiency is plotted against BSA concentration. The extraction efficiency of 400 μg BSA was determined to be the highest at $99 \pm 2\%$ ($n = 3$), so 400 μg BSA was placed on the PP syringe filters being exposed to urban air.

The nitration reaction that occurs on proteins changes various physical properties, such as acidity and size (De Filippis et al., 2006). To determine that these physical and chemical changes do not affect the extraction efficiency of the modified or exposed protein, a similar experiment was done with modified NBSA produced through reaction of BSA with TNM. Using the same method as described above, NBSA was placed on a PP syringe filter and extracted, and the absorbance values were compared to a NBSA reference. This process determined NBSA extracted with similar efficiency ($99 \pm 2\%$ for

400 μg BSA) as unmodified BSA. Similarly, because the protein samples are continuously exposed to urban air for up to 2 weeks, the process was also repeated after BSA remained on the filter for 14 days in a desiccator, and the extraction efficiency remained the same ($98 \pm 2\%$ for 400 μg BSA). Finally, this extraction experiment was conducted to determine the protein loss after filtering with an Amicon centrifugal unit, used for cleaning and concentrating before HPLC analysis. Comparing the absorbance values before and after filtering, it was determined the protein loss of BSA over the Amicon filter is $8.6 \pm 0.4\%$ ($n = 3$; exemplary spectra shown in see Appendix C Figure C5).

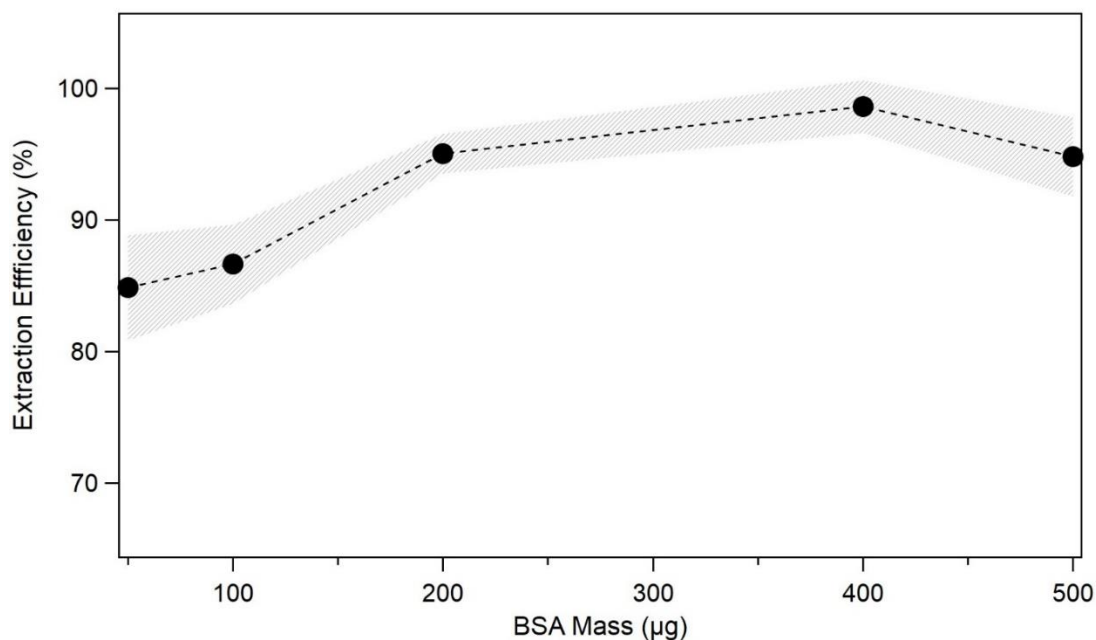


Figure 3.4. Protein extraction efficiency of PP syringe filter for a range of BSA mass loading. Line is to guide eye. Dashed area represents standard error of replicates ($n = 3$). Extraction efficiency for 400 μg BSA determined to be $98 \pm 2\%$.

3.4.4 HPLC calibration curves

As mentioned, both 280 nm and 357 nm absorbance values are used to determine the ND (Selzle et al., 2013). Samples of BSA and NBSA were injected onto the HPLC at concentrations in the range 0.1 – 1.0 mg/mL to establish calibration curves at 280 nm and 357 nm for both unmodified and modified protein. Due to a sloping baseline, each raw chromatogram data was blank-subtracted (using average chromatogram taken from three water blanks at the beginning of each day), and the integrated signal was calculated as the area under the curve and above a line drawn from the baseline before and after the protein peak at retention time 13.4 min (see Appendix C, Figure C6). Calibration curves for each HPLC-DAD absorbance wavelength were determined by plotting the integrated peak area

as a function of protein concentration (Figure 3.5). The BSA and NBSA at 280 nm, as well as NBSA at 357 nm curves show linear fits, as expected. The BSA at 357 nm plot shows a flat line near zero, which is expected because unmodified BSA does not have an absorbance peak at 357 nm.

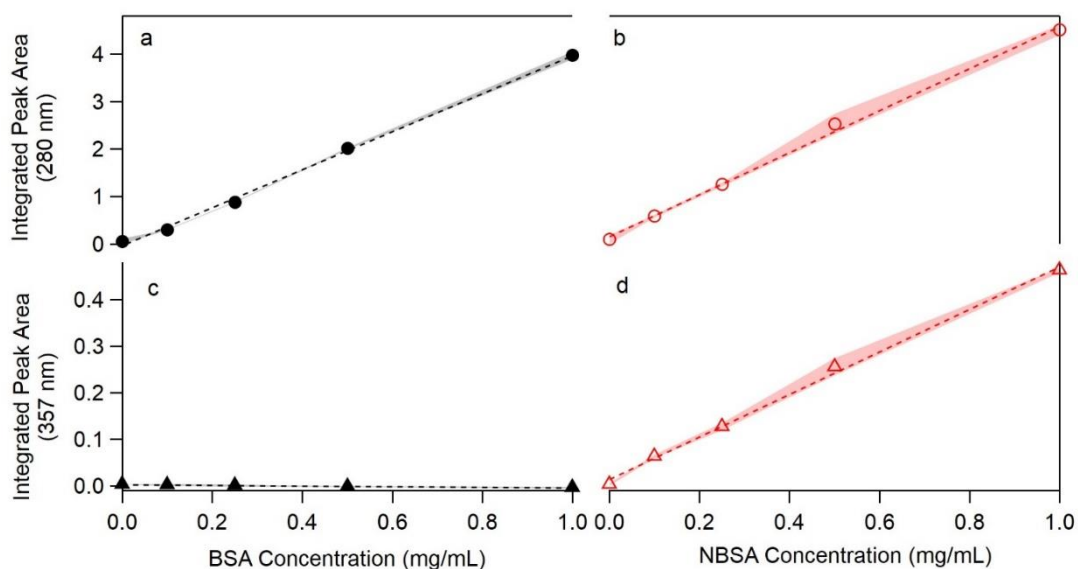


Figure 3.5. Calibration of HPLC response versus protein concentration. NBSA calibrant produced by treatment of BSA with 1/1 TNM/Tyr molar ratio. Shaded area represents standard deviation ($n = 3$). Black closed markers represent BSA and red open markers represent NBSA. Circle symbols collected at absorbance 280 nm; triangles at 357 nm. Dotted line is linear fit. **a** BSA at 280 nm ($R^2 = 0.998$); **b** NBSA at 280 nm ($R^2 = 0.997$); **c** BSA at 357 nm ($R^2 = 0.975$); **d** NBSA at 357 nm ($R^2 = 0.997$).

The calibration curves were used to determine the limit of detection (LOD), limit of quantification (LOQ), and analytical sensitivity (γ) for each of the three absorbing peaks (Table 3.1). The LOD and LOQ values were calculated using the relationships discussed, i.e. by Şengül (Şengül, 2016):

$$LOD = 3 \times \left(\frac{\sigma}{m}\right) \quad (\text{Equation 3.4})$$

$$LOQ = 10 \times \left(\frac{\sigma}{m}\right) \quad (\text{Equation 3.5})$$

where σ is the standard deviation of the y-intercept and m is the slope of the calibration curve (Şengül, 2016). The LOD of the NBSA 357 nm peak thus determines the non-detectable nitration value to be concentrations below 0.05 mg/mL NBSA.

Analytical sensitivity was calculated as follows:

$$\gamma = m/s_s \quad (\text{Equation 3.6})$$

where m is the slope of the calibration curve and s_s is the standard deviation of the signals (Skoog et al., 1992). This definition has the benefit of taking both the slope and precision of the measurement into account.

Table 3.1. Slope of calibration curve (units of peak area per mg mL⁻¹), LOD, LOQ, and analytical sensitivity, γ (units of mL mg⁻¹), calculated for each of the three absorbing peaks.

Absorbance Signal	Slope	LOD	LOQ	γ
BSA 280 nm	4.0 ± 0.1	0.04 mg/mL	0.14 mg/mL	24.6
NBSA 280 nm	4.4 ± 0.1	0.05 mg/mL	0.16 mg/mL	8.0
NBSA 357 nm	0.46 ± 0.01	0.05 mg/mL	0.15 mg/mL	7.2

3.4.5 Ambient application

The city of Denver and the northern Front Range of Colorado is one of the most polluted regions of the United States, based on annual O₃ averages. The region frequently

sees O₃ concentrations of 60 – 80 ppb, for example, as well as NO₂ concentrations in the 10 - 30 ppb range (Cooper et al., 2012). To test the discussed method of ambient exposure, extraction, and analysis, BSA samples were placed on filters at the two monitoring sites in the Denver area. Two sites were utilized because the Rocky Flats North monitoring site generally has higher O₃ concentrations, whereas the La Casa site usually has higher NO₂ concentrations due to elevation and proximity to major highways. BSA is used as a test protein for this ambient application because gas-chamber laboratory studies have been conducted with BSA previously, as mentioned, so results can be compared to the controlled results (Franze et al., 2005).

Shown in Figure 3.6 is the nitration response of BSA after exposure to urban air involving the corresponding average O₃ and NO₂ concentrations during exposure. The lowest ND detected in this proof-of-concept study was 0.17%, correlating to exposure from an average of 34.4 ppb O₃ and 5.9 ppb NO₂. The highest ND detected was 1.17% from average exposure of 40.0 ppb O₃ and 3.6 ppb NO₂. For reference, the NBSA standards prepared for HPLC calibration (reacted at a 1/1 TNM/Tyr ratio) showed a ND of 7.6%. This essentially serves as the upper limit for nitration. Thus, the range of exposures via heterogeneous reaction observed in the four preliminary samples represents a ND of 2.2 – 15.4% relative to the observed maximum ND from TNM reaction, and may therefore, be environmentally significant.

Many lab-based studies of BSA exposure, have utilized much higher O₃ and NO₂ concentrations, i.e. 100 ppb NO₂ and 200 ppb O₃, and so concentrations in almost all ambient situations will be much lower (Franze et al., 2005; Liu et al., 2017). In part, this

means that optimizing extraction efficiency and procedures is necessary to be able to detect more subtle changes in the protein as would be expected in ambient environments.

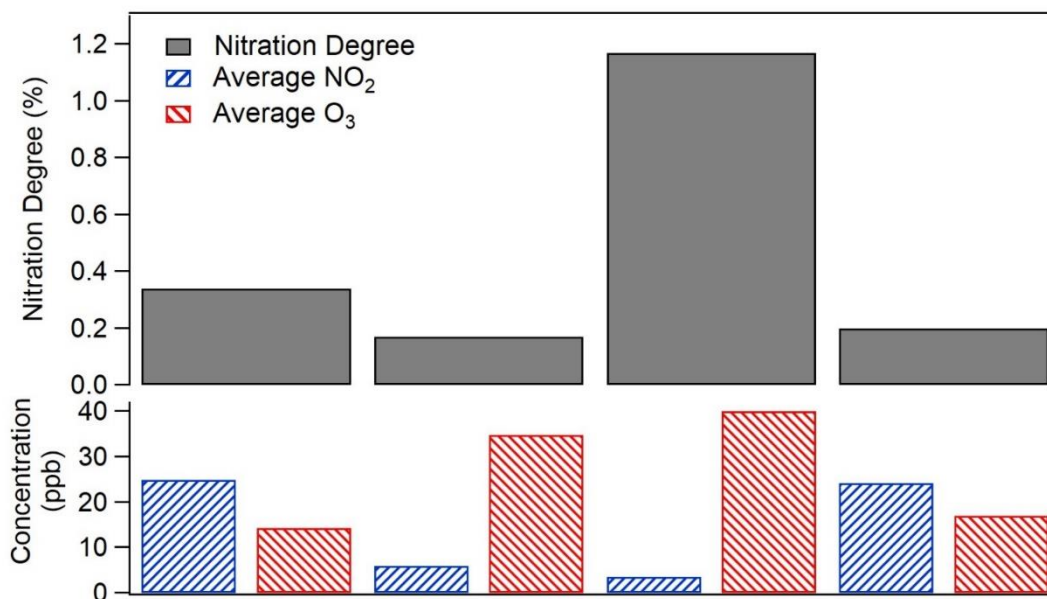


Figure 3.6. Nitration degree of four samples of BSA exposed to urban air (top, dark bars). NO₂ (blue, striped bars) and O₃ (red, striped bars) show ambient values during each protein exposure experiment (7 - 14 days). For comparison, NBSA calibration standards used (reacted at a 1/1 TNM/Tyr ratio) had a ND of 7.6%

3.5 Conclusion

Nitration, or NTyr formation, can be used as a biomarker for inflammation and can be formed in the atmosphere by the interaction of proteins and ROS and RNS, specifically O₃ and NO₂. It is thus important to study the extent of nitration occurring in the atmosphere to better understand air pollutant effects on human health. Multiple

studies have exposed proteins to direct air pollutants in gaseous flow reactors, which is helpful in determining the effects of individual air pollutants on proteins, but few studies have directly exposed proteins to urban ambient air. This type of ambient study introduces more uncertainty and opportunity for sample loss, and the experimental methodology had not previously been thoroughly examined. The work shown follows up on these other similar studies; however, through testing previous approaches we were able to quantify and reduce procedural uncertainties.

As a part of this study, we quantified O₃ loss across the PM filter in the exposure set-up, quantified protein sample loss using various filter media as a function of sample mass and determined analytical metrics of sensitivity and detection limits for both modified and unmodified BSA at the wavelengths of interest. The analyses discussed here will further aid in reducing uncertainties within future studies.

By using BSA we were able to compare our results to previous studies, which show nitration using higher gas concentrations. NTyr formation through gaseous reactions with O₃ and NO₂ is dependent on the accessibility of these reactants to the Tyr residues in the protein, so nitration results will vary depending on Tyr location and number in proteins being exposed. It is thus important to further study these reactions with other proteins to be able to quantify how much nitration is occurring in urban air. Furthermore, by determining the specific Tyr residues that are modified, links to the increase in allergenicity and immunological effects seen can be further investigated.

More work is required to correlate the nitration response to specific O₃ and NO₂ concentrations, as well as to quantify how much nitration occurs in highly polluted areas.

In addition, other variations in environmental conditions, e.g. RH and temperature, can vary nitration results and other PTMs can be formed through these gaseous reactions as well, e.g. nitrosylation or di-tyrosine formation. However, the results shown here can reduce uncertainties in further studies and aid in quantifying the extent of modification occurring in urban air.

References

- Ackaert, C., Kofler, S., Horejs-Hoeck, J., Zulehner, N., Asam, C., Von Grafenstein, S., Fuchs, J. E., Briza, P., Liedl, K. R., Bohle, B., Ferreira, F., Brandstetter, H., Oostingh, G. J., & Duschl, A. (2014). The impact of nitration on the structure and immunogenicity of the major birch pollen allergen Bet v 1.0101. *PLoS ONE*, 9(8). <https://doi.org/10.1371/journal.pone.0104520>
- Alhalwani, A. Y., Repine, J. E., Knowles, M. K., & Huffman, J. A. (2018). Development of a sandwich ELISA with potential for selective quantification of human lactoferrin protein nitrated through disease or environmental exposure. *Analytical and Bioanalytical Chemistry*, 410(4), 1389–1396. <https://doi.org/10.1007/s00216-017-0779-7>
- Arey, J., Zielinska, B., Atkinson, R., Winer, A. M., Ramdahl, T., & Pitts, J. N. (1986). The formation of nitro-PAH from the gas-phase reactions of fluoranthene and pyrene with the OH radical in the presence of NO_x. *Atmospheric Environment* (1967), 20(12), 2339–2345. [https://doi.org/10.1016/0004-6981\(86\)90064-8](https://doi.org/10.1016/0004-6981(86)90064-8)
- Backes, A. T., Reinmuth-Selzle, K., Leifke, A. L., Ziegler, K., Krevert, C. S., Tscheuschner, G., Lucas, K., Weller, M. G., Berkemeier, T., Pöschl, U., & Fröhlich-Nowoisky, J. (2021). Oligomerization and Nitration of the Grass Pollen Allergen Phl p 5 by Ozone, Nitrogen Dioxide, and Peroxynitrite: Reaction Products, Kinetics, and Health Effects. *International Journal of Molecular Sciences*, 22(14), 7616. <https://doi.org/10.3390/IJMS22147616>
- Baraldi, E., Giordano, G., Pasquale, M. F., Carraro, S., Mardegan, A., Bonetto, G.,

- Bastardo, C., Zacchello, F., & Zanconato, S. (2006). 3-Nitrotyrosine, a marker of nitrosative stress, is increased in breath condensate of allergic asthmatic children. *Allergy*, *61*(1), 90–96. <https://doi.org/10.1111/J.1398-9995.2006.00996.X>
- Beck, I., Jochner, S., Gilles, S., McIntyre, M., Buters, J. T. M., Schmidt-Weber, C., Behrendt, H., Ring, J., Menzel, A., & Traidl-Hoffmann, C. (2013). High environmental ozone levels lead to enhanced allergenicity of birch pollen. *PLoS ONE*, *8*(11). <https://doi.org/10.1371/journal.pone.0080147>
- Chen, Y., Han, L., Zhou, Y., Yang, L., & Guo, Y. S. (2020). Artemisia Pollen Extracts Exposed to Diesel Exhaust Enhance Airway Inflammation and Immunological Imbalance in Asthmatic Mice Model. *International Archives of Allergy and Immunology*, *181*(5), 342–352. <https://doi.org/10.1159/000505747>
- Cooper, O. R., Gao, R.-S., Tarasick, D., Leblanc, T., & Sweeney, C. (2012). Long-term ozone trends at rural ozone monitoring sites across the United States, 1990–2010. *Journal of Geophysical Research: Atmospheres*, *117*(D22), 22307. <https://doi.org/10.1029/2012JD018261>
- Cuinica, L. G., Abreu, I., & Esteves Da Silva, J. (2014). Effect of air pollutant NO₂ on *Betula pendula*, *Ostrya carpinifolia* and *Carpinus betulus* pollen fertility and human allergenicity. *Environmental Pollution*, *186*, 50–55. <https://doi.org/10.1016/j.envpol.2013.12.001>
- Cuinica, L. G., Cruz, A., Abreu, I., & Da Silva, J. C. G. E. (2015). Effects of atmospheric pollutants (CO, O₃, SO₂) on the allergenicity of *Betula pendula*, *Ostrya carpinifolia*, and *Carpinus betulus* pollen. *International Journal of Environmental Health*

- Research*, 25(3), 312–321. <https://doi.org/10.1080/09603123.2014.938031>
- De Filippis, V., Frasson, R., & Fontana, A. (2006). 3-Nitrotyrosine as a spectroscopic probe for investigating protein-protein interactions. *Protein Science*, 15, 967–986. <https://doi.org/10.1110/ps.051957006>
- Duque, L., Gomes, C., Abreu, I., Sousa, R., Ribeiro, H., Esteves da Silva, J., & Cruz, A. (2014). Changes in the IgE-reacting protein profiles of *Acer negundo*, *Platanus x acerifolia* and *Quercus robur* pollen in response to ozone treatment. *International Journal of Environmental Health Research*, 24(6), 515–527. <https://doi.org/10.1080/09603123.2013.865716>
- Estillore, A. D., Trueblood, J. V., & Grassian, V. H. (2016). Atmospheric chemistry of bioaerosols: heterogeneous and multiphase reactions with atmospheric oxidants and other trace gases. *Chemical Science*, 7(11), 6604–6616. <https://doi.org/10.1039/C6SC02353C>
- Frank, U., & Ernst, D. (2016). Effects of NO₂ and Ozone on Pollen Allergenicity. *Frontiers in Plant Science*, 7(2), 2–5. <https://doi.org/10.3389/fpls.2016.00091>
- Franze, T., Weller, M. G., Niessner, R., & Pöschl, U. (2003). Enzyme immunoassays for the investigation of protein nitration by air pollutants. *Analyst*, 128(7), 824–831. <https://doi.org/10.1039/b303132b>
- Franze, T., Weller, M. G., Niessner, R., & Pöschl, U. (2005). Protein nitration by polluted air. *Environmental Science and Technology*, 39(6), 1673–1678. <https://doi.org/10.1021/es0488737>
- Ghiani, A, Aina, R., Asero, R., Bellotto, E., & Citterio, S. (2012). Ragweed pollen

collected along high-traffic roads shows a higher allergenicity than pollen sampled in vegetated areas. *Allergy*, 67(4), 887–894. <https://doi.org/10.1111/j.1398-9995.2012.02846.x>

Ghiani, Alessandra, Bruschi, M., Citterio, S., Bolzacchini, E., Ferrero, L., Sangiorgi, G., Asero, R., & Perrone, M. G. (2016). Nitration of pollen aeroallergens by nitrate ion in conditions simulating the liquid water phase of atmospheric particles. *Science of the Total Environment*, 573, 1589–1597.

<https://doi.org/10.1016/j.scitotenv.2016.09.041>

Gruijthuijsen, Y. K., Grieshuber, I., Stöcklinger, A., Tischler, U., Fehrenbach, T., Weller, M. G., Vogel, L., Vieths, S., Pöschl, U., & Duschl, A. (2006). Nitration Enhances the Allergenic Potential of Proteins. *International Archives of Allergy and Immunology*, 141(3), 265–275. <https://doi.org/10.1159/000095296>

Hyttinen, M., Pasanen, P., Salo, J., Bjö, M., Vartiainen, M., & Kalliokoski, P. (2003).

Reactions of Ozone on Ventilation Filters. *Indoor and Built Environment*.

<https://doi.org/10.1177/142032603033362>

Ito, T., Ogino, K., Nagaoka, K., & Takemoto, K. (2018). Relationship of particulate matter and ozone with 3-nitrotyrosine in the atmosphere. *Environmental Pollution*, 236, 948–952. <https://doi.org/10.1016/j.envpol.2017.10.069>

Ito, T., Ogino, K., Nagaoka, K., Takemoto, K., Nishiyama, R., & Shimizu, Y. (2019).

Detection of 3-nitrotyrosine in atmospheric environments via a highperformance liquid chromatography-electrochemical detector system. *Journal of Visualized Experiments*, 2019(143), 3–9. <https://doi.org/10.3791/58371>

- Kampf, C. J., Liu, F., Reinmuth-Selzle, K., Berkemeier, T., Meusel, H., Shiraiwa, M., & Pöschl, U. (2015). Protein Cross-Linking and Oligomerization through Dityrosine Formation upon Exposure to Ozone. *Environmental Science and Technology*, 49(18), 10859–10866. <https://doi.org/10.1021/acs.est.5b02902>
- Karle, A. C., Oostingh, G. J., Mutschlechner, S., Ferreira, F., Lackner, P., Bohle, B., Fischer, G. F., Vogt, A. B., & Duschl, A. (2012). Nitration of the pollen allergen bet v 1.0101 enhances the presentation of bet v 1-derived peptides by HLA-DR on human dendritic cells. *PLoS ONE*, 7(2). <https://doi.org/10.1371/journal.pone.0031483>
- Keller, B. O., Sui, J., Young, A. B., & Whittall, R. M. (2008). Interferences and contaminants encountered in modern mass spectrometry. *Analytica Chimica Acta*, 627(1), 71–81. <https://doi.org/10.1016/J.ACA.2008.04.043>
- Lahoutifard, N., Ammann, M., Gutzwiller, L., Ervens, B., & George, C. (2002). The impact of multiphase reactions of NO₂ with aromatics: a modelling approach. *Atmos. Chem. Phys*, 2(3), 215–226. <https://doi.org/https://doi.org/10.5194/acp-2-215-2002>
- Lai, C. K., Tang, W. K., Siu, C., & Chu, I. K. (2020). Evidence for the Prerequisite Formation of Phenoxy Radicals in Radical-Mediated Peptide Tyrosine Nitration In Vacuo. *Chemistry – A European Journal*, 26(1), 331–335. <https://doi.org/10.1002/chem.201904484>
- Lang-Yona, N., Shuster-Meiseles, T., Mazar, Y., Yarden, O., & Rudich, Y. (2016). Impact of urban air pollution on the allergenicity of *Aspergillus fumigatus* conidia:

Outdoor exposure study supported by laboratory experiments. *Science of the Total Environment*, 541(December 2018), 365–371.

<https://doi.org/10.1016/j.scitotenv.2015.09.058>

Liu, F., Lakey, P. S. J., Berkemeier, T., Tong, H., Kunert, A. T., Meusel, H., Cheng, Y., Su, H., Fröhlich-Nowoisky, J., Lai, S., Weller, M. G., Shiraiwa, M., Pöschl, U., & Kampf, C. J. (2017). Atmospheric protein chemistry influenced by anthropogenic air pollutants: nitration and oligomerization upon exposure to ozone and nitrogen dioxide. *Faraday Discussions*, 200, 413–427. <https://doi.org/10.1039/c7fd00005g>

Liu, F., Reinmuth-Selzle, K., Lai, S., Weller, M. G., Pöschl, U., & Kampf, C. J. (2017). Simultaneous determination of nitrated and oligomerized proteins by size exclusion high-performance liquid chromatography coupled to photodiode array detection. *Journal of Chromatography A*, 1495(2), 76–82.

<https://doi.org/10.1016/j.chroma.2017.03.015>

Mayorga, R. J., Zhao, Z., & Zhang, H. (2021). Formation of secondary organic aerosol from nitrate radical oxidation of phenolic VOCs: Implications for nitration mechanisms and brown carbon formation. *Atmospheric Environment*, 244, 117910. <https://doi.org/10.1016/j.atmosenv.2020.117910>

Mudd, J. B., Leavitt, R., Ongun, A., & McManus, T. T. (1969). Reaction of ozone with amino acids and proteins. *Atmospheric Environment (1967)*, 3(6), 669–681. [https://doi.org/10.1016/0004-6981\(69\)90024-9](https://doi.org/10.1016/0004-6981(69)90024-9)

Parker, C. W., Kern, M., & Eisen, H. N. (1962). Polyfunctional dinitrophenyl haptens as reagents for elicitation of immediate type allergic skin responses. *The Journal of*

Experimental Medicine, 115(4), 789–801. <https://doi.org/10.1084/jem.115.4.789>

Petersen, A., Schramm, G., Schlaak, M., & Becker, W. M. (1998). Post-translational modifications influence IgE reactivity to the major allergen Phl p 1 of timothy grass pollen. *Clinical and Experimental Allergy : Journal of the British Society for Allergy and Clinical Immunology*, 28(3), 315–321. <https://doi.org/10.1046/j.1365-2222.1998.00221.x>

Reinmuth-Selzle, K., Kampf, C. J., Lucas, K., Lang-Yona, N., Fröhlich-Nowoisky, J., Shiraiwa, M., Lakey, P. S. J., Lai, S., Liu, F., Kunert, A. T., Ziegler, K., Shen, F., Sgarbanti, R., Weber, B., Bellinghausen, I., Saloga, J., Weller, M. G., Duschl, A., Schuppan, D., & Pöschl, U. (2017). Air Pollution and Climate Change Effects on Allergies in the Anthropocene: Abundance, Interaction, and Modification of Allergens and Adjuvants. *Environmental Science and Technology*, 51(8), 4119–4141. <https://doi.org/10.1021/acs.est.6b04908>

Reinmuth-Selzle, K., Kampf, C. J., Samonig, M., Shiraiwa, M., Yang, H., Gadermaier, G., Brandstetter, H., Huber, C. G., Duschl, A., & Oostingh, G. J. (2014). Nitration of the Birch Pollen Allergen Bet v 1.0101: Efficiency and Site-Selectivity of Liquid and Gaseous Nitrating Agents. *Journal of Proteome Research*, 13, 1570–1577. <https://doi.org/10.1021/pr401078h>

Ribeiro, H., Costa, C., Abreu, I., & Esteves da Silva, J. C. G. (2017). Effect of O₃ and NO₂ atmospheric pollutants on *Platanus x acerifolia* pollen: Immunochemical and spectroscopic analysis. *Science of the Total Environment*, 599–600, 291–297. <https://doi.org/10.1016/j.scitotenv.2017.04.206>

- Sandhiya, L., Kolandaivel, P., & Senthilkumar, K. (2014). Oxidation and nitration of tyrosine by ozone and nitrogen dioxide: Reaction mechanisms and biological and atmospheric implications. *Journal of Physical Chemistry B*, *118*(13), 3479–3490. <https://doi.org/10.1021/jp4106037>
- Selzle, K., Ackaert, C., Kampf, C. J., Kunert, A. T., Duschl, A., Oostingh, G. J., & Pöschl, U. (2013). Determination of nitration degrees for the birch pollen allergen Bet v 1. *Analytical and Bioanalytical Chemistry*, *405*(27), 8945–8949. <https://doi.org/10.1007/s00216-013-7324-0>
- Şengül, Ü. (2016). Comparing determination methods of detection and quantification limits for aflatoxin analysis in hazelnut. *Journal of Food and Drug Analysis*, *24*(1), 56–62. <https://doi.org/10.1016/J.JFDA.2015.04.009>
- Shiraiwa, M., Pö, U., & Knopf, D. A. (2012). *Multiphase Chemical Kinetics of NO₃ Radicals Reacting with Organic Aerosol Components from Biomass Burning*. <https://doi.org/10.1021/es300677a>
- Shiraiwa, M., Selzle, K., Yang, H., Sosedova, Y., Ammann, M., & Pöschl, U. (2012). Multiphase chemical kinetics of the nitration of aerosolized protein by ozone and nitrogen dioxide. *Environmental Science and Technology*, *46*(12), 6672–6680. <https://doi.org/10.1021/es300871b>
- Skoog, D. A., Holler, J. F., & Crouch, S. R. (1992). *Principles of instrumental analysis*. Saunders College Pub.
- Suárez-Cervera, M., Castells, T., Vega-Maray, A., Civantos, E., Del Pozo, V., Fernández-González, D., Moreno-Grau, S., Moral, A., López-Iglesias, C., Lahoz, C., & Seoane-

- Camba, J. A. (2008). Effects of air pollution on Cup a 3 allergen in Cupressus arizonica pollen grains. *Annals of Allergy, Asthma and Immunology*, 101(1), 57–66. [https://doi.org/10.1016/S1081-1206\(10\)60836-8](https://doi.org/10.1016/S1081-1206(10)60836-8)
- Taylor, P. E., Flagan, R. C., Miguel, A. G., Valenta, R., & Glovsky, M. M. (2004). Birch pollen rupture and the release of aerosols of respirable allergens. *Clinical and Experimental Allergy*, 34(10), 1591–1596. <https://doi.org/10.1111/j.1365-2222.2004.02078.x>
- van der Vliet, A., Eiserich, J. P., O’Neill, C. A., Halliwell, B., & Cross, C. E. (1995). Tyrosine modification by reactive nitrogen species: A closer look. *Archives of Biochemistry and Biophysics*, 319(2), 341–349. <https://doi.org/10.1006/abbi.1995.1303>
- Williams, S. (2004). Ghost peaks in reversed-phase gradient HPLC: a review and update. *Journal of Chromatography A*, 1052(1–2), 1–11. <https://doi.org/10.1016/J.CHROMA.2004.07.110>
- Yang, H., Zhang, Y., & Pöschl, U. (2010). Quantification of nitrotyrosine in nitrated proteins. *Analytical and Bioanalytical Chemistry*, 397(2), 879–886. <https://doi.org/10.1007/s00216-010-3557-3>
- Zhang, Y., Yang, H., & Pöschl, U. (2011). Analysis of nitrated proteins and tryptic peptides by HPLC-chip-MS/MS: site-specific quantification, nitration degree, and reactivity of tyrosine residues. *Analytical and Bioanalytical Chemistry*, 399, 459–471. <https://doi.org/10.1007/s00216-010-4280-9>
- Zhao, F., Elkelish, A., Durner, J., Lindermayr, C., Winkler, J. B., Ru, F., Behrendt, H.,

- Traidl-hoffmann, C., Holzinger, A., Ko, W., Braun, P., Toerne, C. Von, & Hauck, S. M. (2016). Common ragweed (*Ambrosia artemisiifolia* L .): allergenicity and molecular characterization of pollen after plant exposure to elevated NO₂. *Plant, Cell, and Environment*, *39*, 147–164. <https://doi.org/10.1111/pce.12601>
- Zhou, S., Wang, X., Lu, S., Yao, C., Zhang, L., Rao, L., Liu, X., Zhang, W., Li, S., Wang, W., & Wang, Q. (2021). Characterization of allergenicity of *Platanus* pollen allergen a 3 (Pla a 3) after exposure to NO₂ and O₃. *Environmental Pollution*, *278*, 116913. <https://doi.org/10.1016/J.ENVPOL.2021.116913>
- Ziegler, K., Kunert, A. T., Reinmuth-Selzle, K., Leifke, A. L., Widera, D., Weller, M. G., Schuppan, D., Fröhlich-Nowoisky, J., Lucas, K., & Pöschl, U. (2020). Chemical modification of pro-inflammatory proteins by peroxynitrite increases activation of TLR4 and NF- κ B: Implications for the health effects of air pollution and oxidative stress. *Redox Biology*, *37*, 101581. <https://doi.org/10.1016/j.redox.2020.101581>

Chapter Four: Heterogeneous Reaction of BSA Protein with Urban Air: A Long-Term Ambient Study

In preparation for submission for peer-review.

4.1 Abstract

Ambient air pollutants like ozone (O_3) and nitrogen dioxide (NO_2) can act as reactive oxygen species (ROS) and reactive nitrogen species (RNS) and chemically react with proteins in the atmosphere, forming post-translational modifications (PTMs). The prevalence of allergic disease, including allergic rhinitis and asthma, has been increasing globally and one hypothesis as to a component of this increase is the reaction of allergens with ROS/RNS in the atmosphere is causing an increase in the allergenicity of the proteins. Nitration (NTyr) is a PTM that forms via the reaction with O_3 and NO_2 and it has been shown that the allergenic potential of NTyr-containing proteins is enhanced. NTyr formation competes with oligomerization (DiTyr cross-linking), which has also been shown to form in the presence of O_3 . We have previously shown preliminary results showing the nitration of bovine serum albumin (BSA) in ambient air via O_3 and NO_2 . Here we present a more extensive study correlating NTyr formation in the Front Range of Colorado, a highly polluted region, to O_3 concentrations. Additionally, we present a

proof-of-concept study showing the formation of DiTyr upon reaction to high ROS concentrations in ambient air.

4.2 Introduction

Air pollutants in ambient air can act as reactive oxygen and nitrogen species (ROS/RNS) and chemically react with particulate matter (PM) in the atmosphere. Proteins can make up a significant portion of atmospheric PM and can react with ROS/RNS in ambient air to form post-translational modifications (PTMs). When airborne allergenic proteins, like pollen allergens, are chemically modified the allergenic potential of the proteins may be enhanced (Ackaert et al., 2014; Duque et al., 2014; Frank & Ernst, 2016; Ghiani et al., 2016; Hochscheid et al., 2014). Allergic disease has been increasing globally over the past few decades and the reaction of air pollutants with allergenic proteins is one hypothesized mechanism for the rise (Asher et al., 2006; Liu et al., 2017; Pawankar et al., n.d.; Reinmuth-Selzle et al., 2017).

Ozone (O₃) and nitrogen dioxide (NO₂) have been shown to react directly with proteins and allergen carriers, like pollen grains and fungal spores, causing PTMs to form (Frank & Ernst, 2016). One significant PTM is nitration, or the formation of 3-nitrotyrosine (NTyr). NTyr can form via the reaction of tyrosine (Tyr) residues in proteins and O₃/NO₂ and is an extremely stable modification product, allowing for its detection in ambient air samples (Reinmuth-Selzle et al., 2017). *Franze et al.* showed that proteins can be nitrated by polluted ambient air almost 20 years ago in 2005 (Franze et al., 2005). Since then, many studies have been conducted to elucidate more information

regarding protein nitration in the atmosphere and the role nitration has played on the increase in allergies (Backes et al., 2021; Davey et al., 2022; Ito et al., 2019; Lang-Yona et al., 2016; Liu et al., 2017; Reinmuth-Selzle et al., 2014). However, many questions remain including the extent to which nitration occurs in ambient air, the relationships between individual air pollutants and nitration, and what other PTMs could be playing a role.

Protein cross-linking, also referred to as oligomerization or dityrosine (DiTyr) formation, is another PTM that can form via the reaction of Tyr residues and O₃ (Backes et al., 2021; Kampf et al., 2015; Liu et al., 2017). The nitration and oligomerization reactions are both 2-step mechanisms, involving the formation of a tyrosyl radical followed by a secondary reaction to form either product (Bartesaghi & Radi, 2018; Sandhiya et al., 2014). The mechanistic considerations are lengthy, but briefly, Tyr reacts with an ROS/RNS, like O₃, to form the tyrosyl radical. This reaction is followed by either the reaction with NO₂ radical to form NTyr or the reaction with another Tyr radical to form DiTyr. It is becoming clearer that NTyr and DiTyr are competing processes and the kinetics and concentrations of ROS/RNS present dictate which PTM forms (Backes et al., 2021; Kampf et al., 2015; Liu et al., 2017). Because of this, both reaction products should be considered. It should be noted that due to its reactive nature, the tyrosyl radical can react with many of the radicals present, as is the case in ambient air, to form a variety of reaction products, as shown by *Bartesaghi and Radi* (Bartesaghi & Radi, 2018). Nitration and oligomerization are focused on here.

It has previously been shown that NTyr formation in collected airborne PM corresponds to O₃, humidity, and PM in the atmosphere by *Ito et al.* (Ito et al., 2018). *Lang-Yona et al.* showed that exposing allergenic mold *Aspergillus fumigatus* to polluted ambient air increased the allergenicity via nitration (Lang-Yona et al., 2016). Furthermore, the nitration reaction of the pollutants with *Aspergillus fumigatus* showed to occur within the first 12 hours of exposure, followed by deamidation (Lang-Yona et al., 2016). In laboratory gas-chamber experiments, protein nitration and oligomerization have been shown to occur upon exposure to atmospherically relevant O₃ and NO₂ concentrations (Backes et al., 2021; Kampf et al., 2015; Liu et al., 2017; Reinmuth-Selzle et al., 2014). We have previously shown in a proof-of-concept study that nitration occurs in ambient air in Denver, CO, as the region often sees high concentrations of O₃ (60 – 80 ppb) and NO₂ (10 – 30 ppb) (Abeleira & Farmer, 2017; Cooper et al., 2012; Davey et al., 2022). There is little information known, however, regarding the extent of nitration that occurs, and at what ambient air pollutant concentrations the reaction proceeds. Here, we show a more comprehensive study to elucidate the nitration reaction in urban ambient air, as well as to better understand the extent of nitration occurring. This study is, to our knowledge, the first extensive study to detect nitration in protein samples reacting in urban ambient air directly. We also present preliminary results supporting the hypothesis that protein oligomerization occurs in ambient air upon exposure to high ROS concentrations.

4.3 Materials and Methods

4.3.1 Materials

Bovine serum albumin (BSA; A7030), sodium phosphate dibasic (RES20908-A702X), potassium phosphate monobasic (P5655), potassium chloride (P9333), sodium chloride (S9625), acetonitrile (ACN; 100030), and Amicon Ultra-0.5 centrifugal filters (10 kDa, 0.5 mL size; UFC503008) were purchased from Millipore Sigma (St. Louis, MO, USA). Trifluoroacetic acid (TFA; 85183) was obtained from Thermo Fisher Scientific (Waltham, MA, USA). Milli-Q H₂O (MQW) was obtained using a Millipore Milli-Q lab water system. Microcentrifuge tubes (500 μ L; LT8507 and 1.5 mL; LT8509) were purchased from Life Science Products (Frederick, CO, USA). 0.01 M phosphate-buffered saline (1xPBS; 10 mM sodium phosphate dibasic, 1.8 mM potassium phosphate monobasic, 2.7 mM potassium chloride, and 137 mM sodium chloride) was prepared in MQW and was adjusted to the desired pH of 7.4 NaOH (0.1 M).

Luer-Lock PP syringe filters (0.45 μ m, 25 mm; SF14691) were purchased from Tisch Scientific (Cleveland, OH, USA). Kynar[®] (polyvinylidene fluoride; PVDC) filters were purchased from Parker Balston (Cleveland, OH, USA) and Teflon tubing (3/16" ID, 1/4" OD; 5239K12) from McMaster (Elmhurst, IL, USA). Transferpette (BrandTech Scientific; Essex, CT, USA) automated pipettes were used to deliver volumes unless otherwise noted. An analytical balance (Ohaus Explorer EX125D; \pm 0.01 mg) was used for all mass measurements and a DryCal Definer 220 (Mesa Laboratories Inc, NJ, USA) was used to measure the flow rate. All data analysis was done in Igor Pro (Wavemetrics). Graphics were created at BioRender.com.

4.3.2 Exposure to ambient air

Ambient exposure of BSA samples was conducted for ~2.5 years, from the spring of 2020 to the fall of 2022. Samples were prepared, exposed to ambient air, and analyzed as previously described, unless otherwise noted (Davey et al., 2022). Briefly, 400 μg of BSA (4.0 mg/mL in PBS) was placed onto a PP syringe filter and placed in a desiccator overnight. Samples were placed in a sample line set up at one of two Colorado Department of Public Health and Environment (CDPHE) monitoring sites, La Casa or Rocky Flats, each having collocated pollutant and ambient instruments collecting monitoring data. Details for the sample line set up can be found in *Davey et al* and shown in Figure 4.1 (Davey et al., 2022). Two samples were placed at each site. Samples were exposed to ambient air from 14-27 days from and the flow rate (kept between 8-12 L/min) was measured using a DryCal. Blanks (PP syringe filters with no BSA) were placed on sample lines every third sample to ensure no ambient PM was depositing onto samples and unmodified samples (BSA on PP syringe filter) remained in the desiccator in the laboratory throughout each monitoring sample period to serve as a control for no exposure to ambient air. Any ambient sample where the sample line was disturbed was discarded to ensure accurate flow rate information. Air pollutant monitoring data was collected using instruments operating continuously at the monitoring sites operated by the CDPHE.

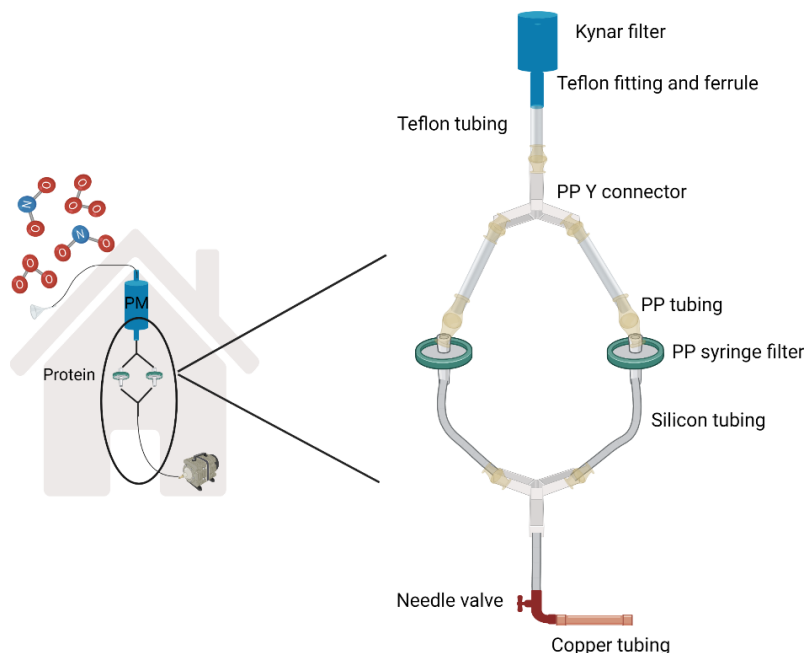


Figure. 4.1 Schematic diagram of ambient experimental set-up connections. Created with BioRender.com.

4.3.3 HPLC-DAD analysis and ND determination

After ambient exposure the BSA samples were extracted from the PP syringe filters using 4 mL PBS. Each sample was analyzed via RP-HPLC-DAD (reverse-phase high performance liquid chromatography with diode-array detection), as previously described (Davey et al., 2022; Selzle et al., 2013). Briefly, samples were concentrated using Amicon centrifugal units and placed in glass HPLC vials and analyzed using a HPLC-DAD system (Agilent 1200 series). A C₁₈ column (Supelco Discovery BioWide Pore 25 cm x 2.1 mm, 5 μm) with eluents 0.1% (v/v) trifluoroacetic acid in water (eluent A) and ACN (eluent B) were used for chromatographic separation. Gradient elution was performed at a flow rate of 300 μL/min, and for each run the solvent gradient started at

3% B followed by a linear gradient to 90% B within 15 min. Absorbance was monitored at wavelengths of 280 and 357 nm. The sample injection volume was 25 μL , and each chromatographic run was repeated three times (measurement replicates) with a water blank in between. Using the integrated peak areas of both 280 nm and 357 nm the nitration degree (ND) for each injection was calculated as previously described by *Selzle et al* (Selzle et al., 2013). Native BSA samples gave a ND value of 0.58 ± 0.09 , so all ambient samples have been adjusted for this background.

4.3.4 SEC-HPLC analysis

A subset of the ambient samples were separately analyzed using SEC-HPLC-DAD (size exclusion chromatography HPLC-DAD) as previously studies have described (Backes et al., 2021; Kampf et al., 2015; Liu, Reinmuth-Selzle, et al., 2017). Briefly, a Bio SEC column (Agilent, 300 Å, 4.6 x 150 mm, 3 μm particle size) was used with isocratic separation at a flow rate of 0.35 mL min^{-1} . The mobile phase was 150 mM NaH_2PO_4 buffer (pH 7.4), and the injection volume was 20 μL . DAD spectra were recorded at wavelengths of 220, 280, and 357 nm, and each chromatographic run was performed in triplicate. A protein standard mix 15 – 600 kDa (69385, Sigma-Aldrich) was used to calibrate a Bio SEC column and the baseline-corrected chromatographic data at 220 nm was integrated according to the calibration retention times. The retention times and peak shape of the higher oligomers varied, as well as some peaks co-eluted, so here we report oligomer degree (OD) as the integrated monomer area subtracted from the total integrated area divided by the total integrated area. It should be noted that the purchased

unmodified BSA contained a small fraction of oligomer variants, so OD values reported here have been corrected for this.

4.4 Results and Discussion

As noted, there is little information known regarding the extent of nitration occurring in ambient air. Furthermore, more information is needed to better understand the air pollutant concentrations needed to drive the reaction forward. Through exposing BSA samples to ambient air directly we have been able to elucidate more information regarding the time and exposure conditions needed to drive the nitration reaction, as well as relevant O₃ and NO₂ concentrations. By using BSA we were able to compare our results to previous laboratory studies, which show nitration using higher gas concentrations.

Liu et al. showed that both Tyr nitration and cross-linking within proteins are sensitive towards increases in O₃ concentration, but relatively insensitive to changes in NO₂ concentrations (Liu et al., 2017). Using a laboratory flow reactor BSA was exposed to constant O₃ and NO₂ (5-200 ppb) for 12 hours and results showed that NTyr formation correlates with O₃ and does not correlate with NO₂ (Liu et al., 2017). Furthermore, it was shown that nitration is kinetically favored compared to cross-linking, nitration is favored in high humidity, and ND values up to 8% were seen (Liu et al., 2017). Through our long-term ambient study, we were able to study the similar nitration and oligomerization reaction of BSA with O₃ and NO₂, as well as consider the presence of other ROS and RNS species, RH, and temperature to better study to extent of nitration in ambient air.

RP-HPLC was used to analyze all ambient samples and the ND was calculated as described by *Selzle et al.* (Selzle et al., 2013). ND is used as a quantitative metric for determining the NTyr concentration in a particular sample. ND values from 0.72 - 5.6% were seen in ambient samples, after being corrected for the background ND of unmodified BSA. Figure 4.2 shows the ND response of the ambient-exposed BSA samples versus the total integrated O₃, NO₂, and O₃ + NO₂. There is a forming relationship of ND with O₃, shown in Figure 4.2 (green circles), but not with NO₂, or O₃ + NO₂, similar to previous reports (Ito et al., 2018; Liu et al., 2017). As the O₃ concentration increases, ND also increases, which is consistent with the proposed mechanism that O₃ reacts first to form the tyrosyl radical, followed by the addition of NO₂.

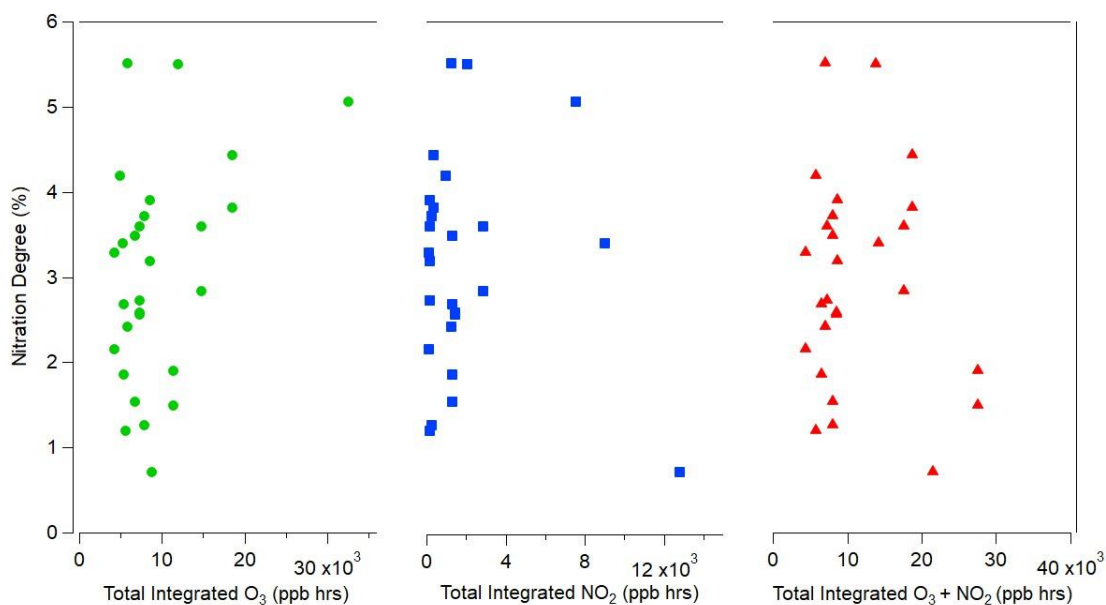


Figure 4.2 ND (%) response corresponded to total integrated O₃ and NO₂ concentrations (ppb hrs). Green circles represent O₃, blue squares represent NO₂, and red triangles represent O₃ + NO₂.

To further study to relationship of ND and O₃, the ratios of O₃ to BSA (μg) and O₃ to Tyr (moles) were calculated and correlated to ND, shown in Figure 4.3.

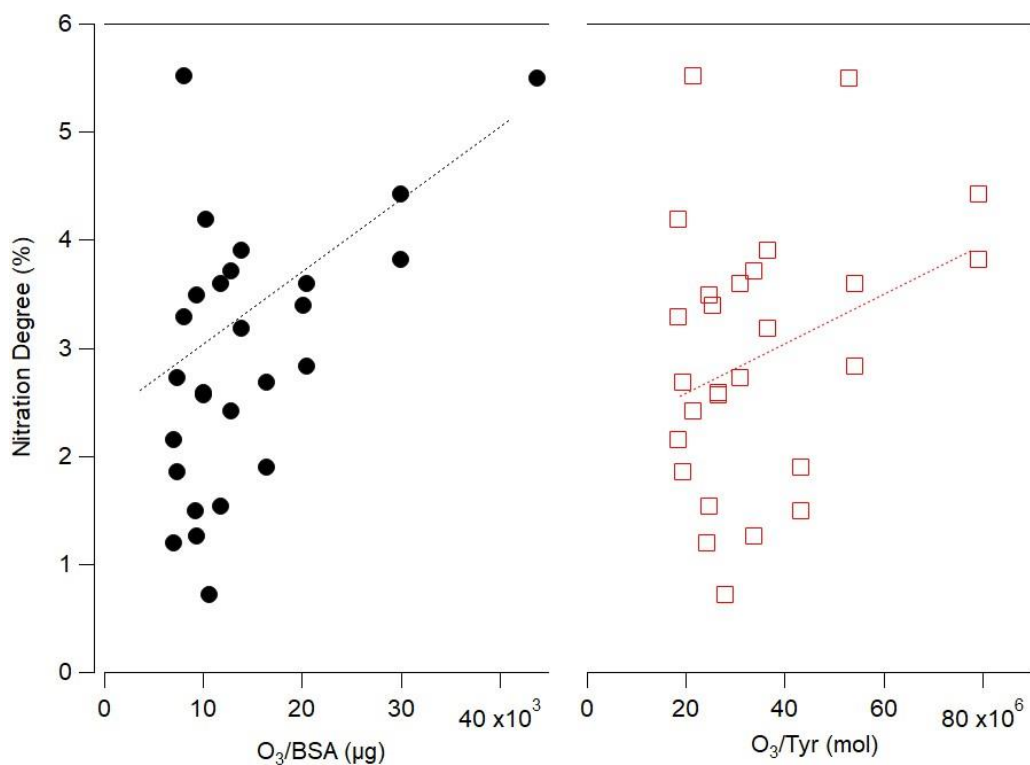


Figure. 4.3 ND (%) response corresponded to ratios of mol O₃/mol BSA (black circles) and O₃/mol Tyr (red squares). The slope of the line of ND vs O₃/BSA (µg) is 1.9 ± 0.4 and the slope of the line of ND vs O₃/Tyr (mol) is 2.2 ± 0.5 .

As noted, there is no clear correlation of ND with NO₂ (Figure 4.2), consistent with previous laboratory studies (Liu et al., 2017). However, the ND response was also analyzed versus NO_x, NO_y, NO_z (Figure 4.4). NO_x is defined as the sum of NO and NO₂ and NO_y is the sum of NO_x and NO_z. No correlations were seen.

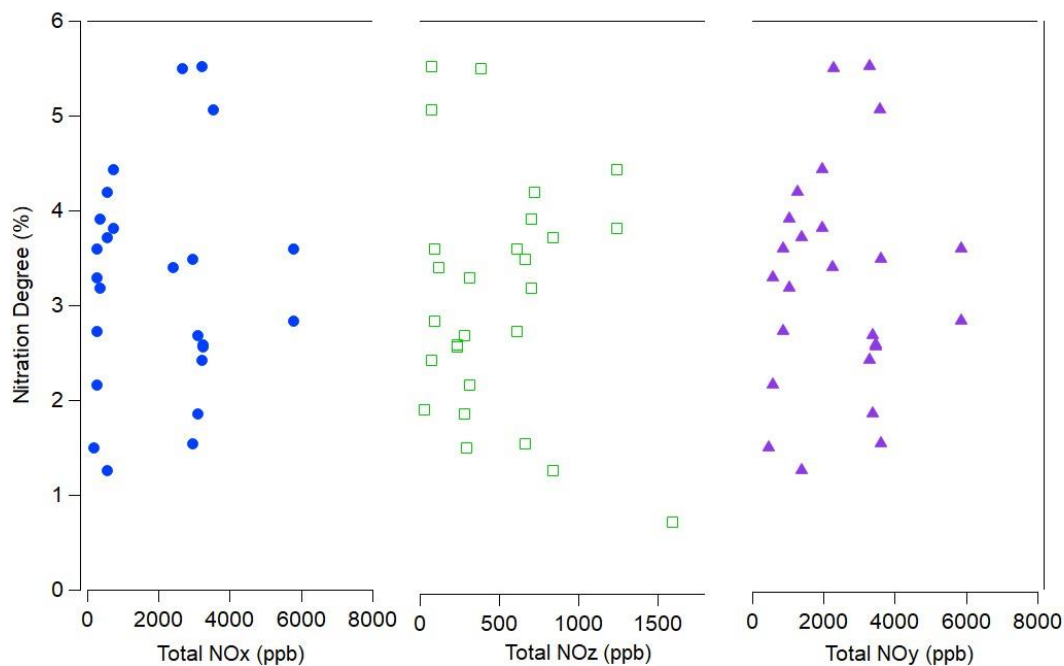


Figure 4.4 ND (%) response versus NO_x (blue circles), NO_y (green squares), NO_z (purple triangles).

In addition, our results do not clearly show a correlation between ND and RH (Figure 4.5), which is inconsistent with previous reports (Ito et al., 2018; Liu et al., 2017). However, this can be explained due to the dry climate of Denver. The average RH of the ambient samples did not exceed 55%. Figure 4.5 also shows the relationship of ND and temperature. Sandhiya et al. has shown through *ab initio* calculations that temperature can increase the formation of tyrosyl radicals via ozonolysis, so as temperature increases the ND response is expected to increase (Sandhiya et al., 2014). Our results show a relationship between ND and temperature up to ND values of ~4% (Figure 4.5), but interestingly the highest ND values seen (up to 5.6%) do not follow the trend. It is important to note here that ND is not a 0-100% scale, but rather a 0 to a max of what is

available to be nitrated scale, which is dependent on sterics, solvent access, folding, etc.

The upper limit of nitration is difficult to determine, but BSA samples nitrated via laboratory reagents TNM and ONOO⁻ result in ND values of 8-12%.

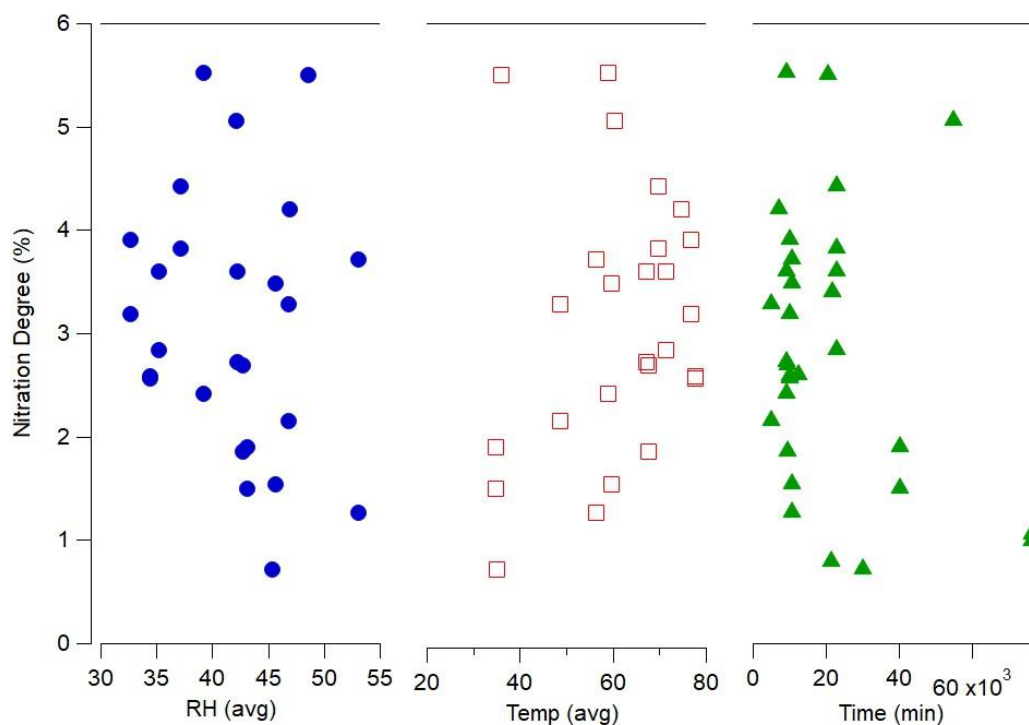


Figure 4.5 ND (%) response versus RH (blue circles), temperature (F; red squares), and time (min; green triangles).

As noted above, the formation of many PTM products is possible due to the complexity of atmospheric ROS and RNS chemistry. Many oxidants can perform the one-electron oxidation of Tyr to form the tyrosyl radical, including O₃, NO₂, and CO₃, as shown by *Bartasaghi and Radi* (Bartasaghi & Radi, 2018). Due to this, the relationship of ND and total ROS was compared, and Spearman coefficients were used to analyze the

relationship formed. Total ROS in this case is represented as the total directly measured ROS, which includes CO, NO, NO₂, NO_y, O₃, and SO₂. Figure 4.6 shows the relationship of ND and total measured ROS. The ND increases linearly as total ROS increases (Spearman coefficient 0.8), but then starts to decrease as the total ROS reaches 3×10^4 ppb. We propose this is a result of either increased exposure time associated with high ROS, or the formation of other PTM products due to the abundance of ROS.

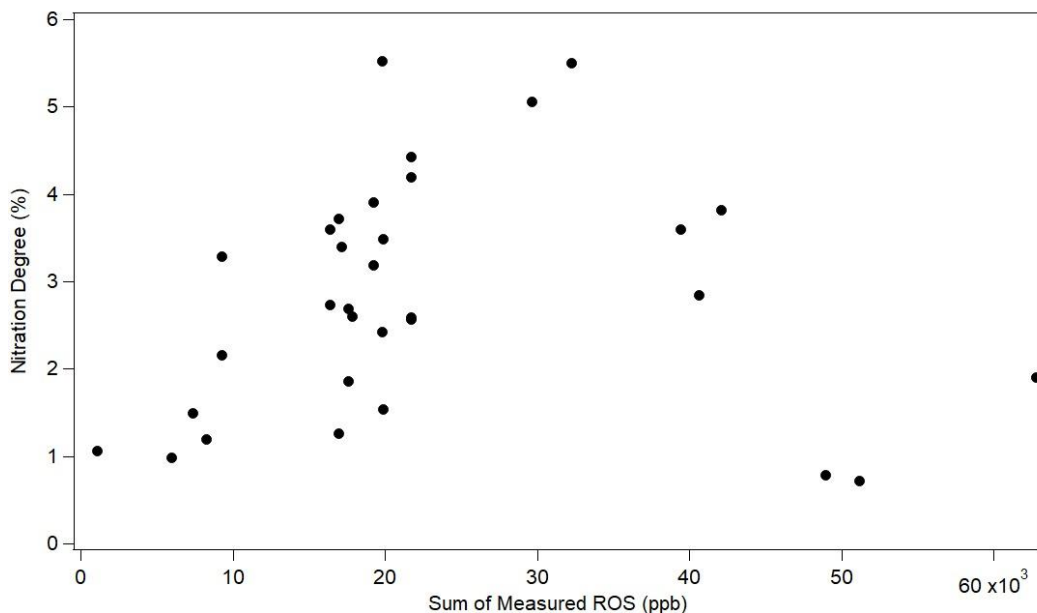


Figure 4.6 ND (%) response correlated to the sum of the measure ROS.

A subset of the samples with low ND values and high ROS exposure were analyzed as a proof-of-concept study using SEC-HPLC. The OD was calculated as a metric to quantify the amount of oligomerization formed in each sample, after being corrected for the background OD of unmodified BSA. Table 1 shows results for

oligomerization formation in the high ROS samples with low ND values. OD values of 0.99 - 56.1% were detected. This is the first study, to our knowledge, to show direct oligomerization upon ambient exposure of a protein. Future studies are needed to better elucidate the extent of oligomerization in ambient air. It is important to note that due to the complexity of atmospheric ROS and RNS present in ambient air a wide variety of other PTM products could form, including 3-nitrosotyrosine from the reaction of Tyr and NO (Bartesaghi & Radi, 2018). In our study the ambient concentrations of NO₂ were higher than NO by about 2 orders of magnitude. However, in future studies it may be important to monitor the formation of more PTM products.

Table 4.1. Preliminary results detecting oligomerization in high ROS ambient samples. Unmodified BSA has a degree of nitration and oligomerization, so ND and OD values shown have been subtracted to account for this baseline.

Sample	Total ROS (ppb)	ND (%)	OD (%)
Unmodified BSA	0	0	0
1	30 x 10 ³	5.5 ± 0.1	0.99 ± 0.03
2	42 x 10 ³	3.82 ± 0.02	1.2 ± 0.2
3	41 x 10 ³	2.84 ± 0.03	15.0 ± 0.1
4	63 x 10 ³	1.9 ± 0.1	29.05 ± 0.05
5	49 x 10 ³	0.79 ± 0.08	39.6 ± 0.2
6	51 x 10 ³	0.72 ± 0.09	56.1 ± 0.3

4.5 Conclusion

The worldwide increase in allergic disease may be associated with air pollution and chemical reactions in the atmosphere. O₃ and NO₂ react with proteins in ambient air to form nitration and oligomerization products. Little is known regarding the extent to which these reactions occur in ambient air. Here we report an extensive study of the nitration reaction of BSA in ambient air to compare ambient results to previously reported laboratory studies. Our ambient results show a correlation between nitration and O₃ concentrations, consistent with previous studies. In addition, we provide preliminary results supporting the hypothesis that oligomerization competes with nitration in ambient air, especially at high ROS concentrations. Future studies to elucidate other PTMs occurring in ambient air may be important to better understand the complexity of the increased allergenicity of proteins upon exposure to air pollutants.

References

- Abeleira, A. J., & Farmer, D. K. (2017). Summer ozone in the northern Front Range metropolitan area: Weekend-weekday effects, temperature dependences, and the impact of drought. *Atmospheric Chemistry and Physics*, *17*(11), 6517–6529.
<https://doi.org/10.5194/ACP-17-6517-2017>
- Ackaert, C., Kofler, S., Horejs-Hoeck, J., Zulehner, N., Asam, C., Von Grafenstein, S., Fuchs, J. E., Briza, P., Liedl, K. R., Bohle, B., Ferreira, F., Brandstetter, H., Oostingh, G. J., & Duschl, A. (2014). The impact of nitration on the structure and immunogenicity of the major birch pollen allergen Bet v 1.0101. *PLoS ONE*, *9*(8).
<https://doi.org/10.1371/journal.pone.0104520>
- Asher, M. I., Montefort, S., Björkstén, B., Lai, C. K., Strachan, D. P., Weiland, S. K., & Williams, H. (2006). Worldwide time trends in the prevalence of symptoms of asthma, allergic rhinoconjunctivitis, and eczema in childhood: ISAAC Phases One and Three repeat multicountry cross-sectional surveys. *Lancet*, *368*(9537), 733–743.
[https://doi.org/10.1016/S0140-6736\(06\)69283-0](https://doi.org/10.1016/S0140-6736(06)69283-0)
- Backes, A. T., Reinmuth-Selzle, K., Leifke, A. L., Ziegler, K., Krevert, C. S., Tscheuschner, G., Lucas, K., Weller, M. G., Berkemeier, T., Pöschl, U., & Fröhlich-Nowoisky, J. (2021). Oligomerization and Nitration of the Grass Pollen Allergen Phl p 5 by Ozone, Nitrogen Dioxide, and Peroxynitrite: Reaction Products, Kinetics, and Health Effects. *International Journal of Molecular Sciences*, *22*(14), 7616.
<https://doi.org/10.3390/IJMS22147616>
- Bartesaghi, S., & Radi, R. (2018). Fundamentals on the biochemistry of peroxynitrite and

protein tyrosine nitration. *Redox Biology*, 14(September 2017), 618–625.

<https://doi.org/10.1016/j.redox.2017.09.009>

Cooper, O. R., Gao, R.-S., Tarasick, D., Leblanc, T., & Sweeney, C. (2012). Long-term ozone trends at rural ozone monitoring sites across the United States, 1990–2010. *Journal of Geophysical Research: Atmospheres*, 117(D22), 22307.

<https://doi.org/10.1029/2012JD018261>

Davey, R. L., Mattson, E. J., & Huffman, J. A. (2022). Heterogeneous nitration reaction of BSA protein with urban air: improvements in experimental methodology. *Analytical and Bioanalytical Chemistry* 2021, 1–12. <https://doi.org/10.1007/S00216-021-03820-8>

Duque, L., Gomes, C., Abreu, I., Sousa, R., Ribeiro, H., Esteves da Silva, J., & Cruz, A. (2014). Changes in the IgE-reacting protein profiles of *Acer negundo*, *Platanus x acerifolia* and *Quercus robur* pollen in response to ozone treatment. *International Journal of Environmental Health Research*, 24(6), 515–527.

<https://doi.org/10.1080/09603123.2013.865716>

Frank, U., & Ernst, D. (2016). Effects of NO₂ and Ozone on Pollen Allergenicity. *Frontiers in Plant Science*, 7(2), 2–5. <https://doi.org/10.3389/fpls.2016.00091>

Franze, T., Weller, M. G., Niessner, R., & Pöschl, U. (2005). Protein nitration by polluted air. *Environmental Science and Technology*, 39(6), 1673–1678.

<https://doi.org/10.1021/es0488737>

Ghiani, A., Bruschi, M., Citterio, S., Bolzacchini, E., Ferrero, L., Sangiorgi, G., Asero, R., & Perrone, M. G. (2016). Nitration of pollen aeroallergens by nitrate ion in

- conditions simulating the liquid water phase of atmospheric particles. *Science of the Total Environment*, 573, 1589–1597. <https://doi.org/10.1016/j.scitotenv.2016.09.041>
- Hochscheid, R., Schreiber, N., Kotte, E., Weber, P., Cassel, W., Yang, H., Zhang, Y., Pöschl, U., & Müller, B. (2014). Nitration of Protein Without Allergenic Potential Triggers Modulation of Antioxidant Response in Type II Pneumocytes. *Journal of Toxicology and Environmental Health, Part A*, 77(12), 679–695. <https://doi.org/10.1080/15287394.2014.888023>
- Ito, T., Ogino, K., Nagaoka, K., & Takemoto, K. (2018). Relationship of particulate matter and ozone with 3-nitrotyrosine in the atmosphere. *Environmental Pollution*, 236, 948–952. <https://doi.org/10.1016/j.envpol.2017.10.069>
- Ito, T., Ogino, K., Nagaoka, K., Takemoto, K., Nishiyama, R., & Shimizu, Y. (2019). Detection of 3-Nitrotyrosine in Atmospheric Environments via a High-performance Liquid Chromatography-electrochemical Detector System. *JoVE (Journal of Visualized Experiments)*, 2019(143), e58371. <https://doi.org/10.3791/58371>
- Kampf, C. J., Liu, F., Reinmuth-Selzle, K., Berkemeier, T., Meusel, H., Shiraiwa, M., & Pöschl, U. (2015). Protein Cross-Linking and Oligomerization through Dityrosine Formation upon Exposure to Ozone. *Environmental Science and Technology*, 49(18), 10859–10866. <https://doi.org/10.1021/acs.est.5b02902>
- Lang-Yona, N., Shuster-Meiseles, T., Mazar, Y., Yarden, O., & Rudich, Y. (2016). Impact of urban air pollution on the allergenicity of *Aspergillus fumigatus* conidia: Outdoor exposure study supported by laboratory experiments. *Science of the Total Environment*, 541, 365–371. <https://doi.org/10.1016/j.scitotenv.2015.09.058>

- Liu, F., Lakey, P. S. J., Berkemeier, T., Tong, H., Kunert, A. T., Meusel, H., Cheng, Y., Su, H., Fröhlich-Nowoisky, J., Lai, S., Weller, M. G., Shiraiwa, M., Pöschl, U., & Kampf, C. J. (2017). Atmospheric protein chemistry influenced by anthropogenic air pollutants: nitration and oligomerization upon exposure to ozone and nitrogen dioxide. *Faraday Discussions*, *200*, 413–427. <https://doi.org/10.1039/c7fd00005g>
- Liu, F., Reinmuth-Selzle, K., Lai, S., Weller, M. G., Pöschl, U., & Kampf, C. J. (2017). Simultaneous determination of nitrated and oligomerized proteins by size exclusion high-performance liquid chromatography coupled to photodiode array detection. *Journal of Chromatography A*, *1495*(2), 76–82. <https://doi.org/10.1016/j.chroma.2017.03.015>
- Pawankar, R., Baena-Cagnani, C. E., Bousquet, J., Canonica, G. W., Cruz, A. A., Kaliner, M. A., & Lanierl, B. Q. (n.d.). *State of World Allergy Report 2008: Allergy and Chronic Respiratory Diseases*.
- Reinmuth-Selzle, K., Kampf, C. J., Lucas, K., Lang-Yona, N., Fröhlich-Nowoisky, J., Shiraiwa, M., Lakey, P. S. J., Lai, S., Liu, F., Kunert, A. T., Ziegler, K., Shen, F., Sgarbanti, R., Weber, B., Bellinghausen, I., Saloga, J., Weller, M. G., Duschl, A., Schuppan, D., & Pöschl, U. (2017). Air Pollution and Climate Change Effects on Allergies in the Anthropocene: Abundance, Interaction, and Modification of Allergens and Adjuvants. *Environmental Science and Technology*, *51*(8), 4119–4141. <https://doi.org/10.1021/acs.est.6b04908>
- Reinmuth-Selzle, K., Kampf, C. J., Samonig, M., Shiraiwa, M., Yang, H., Gadermaier, G., Brandstetter, H., Huber, C. G., Duschl, A., & Oostingh, G. J. (2014). Nitration of

the Birch Pollen Allergen Bet v 1.0101: Efficiency and Site-Selectivity of Liquid and Gaseous Nitrating Agents. *Journal of Proteome Research*, 13, 1570–1577.

<https://doi.org/10.1021/pr401078h>

Sandhiya, L., Kolandaivel, P., & Senthilkumar, K. (2014). Oxidation and nitration of tyrosine by ozone and nitrogen dioxide: Reaction mechanisms and biological and atmospheric implications. *Journal of Physical Chemistry B*, 118(13), 3479–3490.

<https://doi.org/10.1021/jp4106037>

Selzle, K., Ackaert, C., Kampf, C. J., Kunert, A. T., Duschl, A., Oostingh, G. J., & Pöschl, U. (2013). Determination of nitration degrees for the birch pollen allergen Bet v 1. *Analytical and Bioanalytical Chemistry*, 405(27), 8945–8949.

<https://doi.org/10.1007/s00216-013-7324-0>

Chapter Five: Reaction of Proteins with Peroxynitrite: pH Determines Degree of Nitration and Oligomerization

In preparation for submission for peer-review.

5.1 Abstract

Oxidative and nitrosative stress are produced by high levels of reactive oxygen species (ROS) and reactive nitrogen species (RNS). Peroxynitrite (ONOO^-) is a highly reactive species that causes post-translational modification (PTM) of proteins and oxidation of lipids and DNA and is therefore associated with various diseases. Two PTM's associated with the reaction of ONOO^- with proteins are nitrotyrosine (NTyr) and dityrosine (DiTyr). The commonly used method of studying ONOO^- reactions to examine the effects of these PTM's *in vitro* contains high concentrations of sodium hydroxide, due to the stability of ONOO^- in alkaline solution. The aim of this study was to determine if the addition of high concentrations of ONOO^- are therefore associated with high pH values in commonly used and biologically relevant buffer systems, and if the high pH of the reactions was associated with a mechanistic change. It was determined that in experiments using phosphate-buffered saline, a buffer most used to mimic biologically relevant conditions, the reaction quickly exceeded the buffer capacity. Furthermore, the reaction of ONOO^- with tyrosine (Tyr) residues on bovine serum albumin was

determined to be pH-dependent, where at lower pH values NTyr formation was favored and at higher pH values the formation of DiTyr was favored. As the molar ratio of ONOO⁻ to Tyr passed a value of 5/1 the nitration degree began to decrease, at which point the dimer degree began to rise. These results are consistent with mechanistic studies of Tyr and ONOO⁻ but are the first to show the pH of the aqueous reaction of ONOO⁻ and protein increasing under commonly used ONOO⁻ concentrations and are the first to detect DiTyr formation at high ONOO⁻ concentrations.

5.2 Introduction

Reactive oxygen and reactive nitrogen species (ROS/RNS) can chemically react with proteins to form post-translational modifications (PTM's), resulting in oxidized or nitrated proteins, as well as oligomers. (Backes et al., 2021; Reinmuth-Selzle et al., 2014). In particular, the formation of 3-nitrotyrosine (NTyr) is frequently used as a biomarker for oxidative and nitrosative stress (Ahsan, 2013; Campolo et al., 2020; Radi, 2013). NTyr and other PTM's can be formed via the reaction of peroxynitrite (ONOO⁻) and amino acids, like tyrosine (Tyr), in proteins *in vivo*, and are usually associated with loss of protein function and modified structure (Bartesaghi & Radi, 2018; Roy et al., 2019). Cross-linking of Tyr to 3,3'-dityrosine (DiTyr) can also occur via the reaction of proteins and ONOO⁻, and recent studies have focused on the importance of DiTyr formation as an oxidative stress biomarker in addition to NTyr (Backes et al., 2021; Bruno et al., 2020; Maina et al., 2022; Pfeiffer et al., 2000; Reinmuth-Selzle et al., 2023; Ziegler et al., 2020).

ONOO⁻ can be generated *in vivo* via the rapid reaction of superoxide (O₂⁻) and nitric oxide (NO) (van der Vliet et al., 1995). In a 2-step mechanism, a tyrosyl radical is formed via the reaction of tyrosine with a single electron oxidant, which further reacts with NO₂ radical to form the stable NTyr product (Lai et al., 2020). Therefore, ONOO⁻ does not react with Tyr directly, rather via the formation of free radicals that further react with the Tyr radical (Radi et al., 2001). Separately, dimerization of Tyr to DiTyr can occur via the same first step, but with reaction of two tyrosyl radicals in the second step. The presence of DiTyr has also been associated with certain diseases, including Alzheimers (Bartesaghi et al., 2006; Hensley et al., 1998; Ischiropoulos & Al-Mehdi, 1995; Maina et al., 2022). Studies have indicated that DiTyr and therefore oligomerization yields upon reaction with ONOO⁻ can be comparable to NTyr, depending on the experimental conditions (Pfeiffer et al., 2000). This is due to the ability of the NO₂ radical to react with both the tyrosyl radical and native Tyr residues (Ferrer-Sueta et al., 2018). The first mechanistic step in the reaction is the formation of the tyrosyl radical. With low ONOO⁻ concentrations, and therefore low generated radical concentrations, the oxidation of Tyr to tyrosyl radical is needed to occur first, followed by the remaining NO₂ radical reacting to form NTyr. If there are high amounts of Tyr, however, more of the NO₂ radical reacts directly with native Tyr residues to produce the tyrosyl radical. This consumes more of the NO₂ radical, resulting in less NTyr formation and more DiTyr formation (Bartesaghi et al., 2006; Ferrer-Sueta et al., 2018).

The detection of NTyr using UV-Vis is pH-dependent, where at neutral pH the absorbance maxima are centered at 280 nm and 357 nm, and at alkaline pH values a new

maximum appears at 430 nm (De Filippis et al., 2006). DiTyr absorbance and fluorescence properties are pH-dependent as well (D. A. Malencik & Anderson, 2003). The nitration reaction of Tyr with ONOO⁻ is also pH-sensitive and changes in pH will influence ONOO⁻-dependent nitration yields. Various studies have been conducted to determine the nitration pH profiles of protein reactions (Alvarez & Radi, 2003; Bartesaghi et al., 2006; Bartesaghi & Radi, 2018; Lemercier et al., 1997; Pfeiffer et al., 2000; Pfeiffer & Mayer, 1998; Roy et al., 2019). For example, *van der Vliet et al.* showed nitration of 4-hydroxyphenylacetic acid was maximal at pH 7.5 and fell sharply with increasing pH (van der Vliet et al., 1995). *Roy et al.* investigated the effects of ONOO⁻ at pH 7.4 and 6.0 on RNase A and saw a higher degree of nitration at pH 7.4 (Roy et al., 2019). *Bartesaghi et al.* propose acidic conditions will favor nitrite-dependent nitration pathways, whereas basic conditions favor dimerization, however experimental results have not been shown (Bartesaghi et al., 2006; Bartesaghi & Radi, 2018).

When pH increases, DiTyr formation increases due to an increase of Tyr being in its phenolate form (Bartesaghi et al., 2006). The pK_a of the phenolic hydroxyl on Tyr is 10 (Bartesaghi & Radi, 2018). The phenolate is more readily oxidized to the tyrosyl radical by the NO₂ radical. This results in a higher fraction of NO₂ radical oxidizing native Tyr rather than combining with previously-formed tyrosyl radical to yield NTyr. In a 2006 study, *Bartesaghi et al.* use computer-assisted simulations using the rate constants from literature to show the pH profiles and yields for Tyr hydroxylation, nitration, and dimerization (Bartesaghi et al., 2006). No laboratory studies have been conducted to support these results. The oxidation of Tyr to tyrosyl radical via OH radical was shown to

be pH-dependent, with yields increasing with pH. NO_2 radical can react with the tyrosyl radicals to yield NTyr or react with deprotonated Tyr to form tyrosyl radical. As mentioned, the pK_a of Tyr is 10 (Bartlesaghi et al., 2006), so the process of NO_2 radical reacting with deprotonated Tyr is much faster at alkaline pH values. This increases the steady state concentration of tyrosyl radicals. Due to this, hydroxylation has higher yields at acidic pH values, nitration yields are bell-shaped with the maximum yields being at neutral pH, and dimerization yields are higher at alkaline pH values (Bartlesaghi et al., 2006).

The vast majority of ONOO^- studies use commercial suppliers that dissolve ONOO^- in NaOH (i.e. in 4.7% NaOH). When ONOO^- is added to a reaction, the NaOH can increase the pH of the reaction well past the buffer capacity. Here we show the effects of varying ONOO^- reaction conditions and how nitration and oligomerization results differ. To our knowledge, this study is the first to show the effect of adding ONOO^- in aqueous reactions on not only pH, but to product yields. It is thus important to consider pH when extrapolating results from reactions *in vitro* to effects in the human body *in vivo*. It is important to note that many other oxidation products are possible in this reaction. There are several oxidants that can react to form the one-electron oxidation of tyrosine, such as OH radical, NO_2 radical, and CO_3^- radical. Furthermore, once the tyrosyl radical is formed many reactions can occur to form NTyr, DiTyr, 3-hydroxytyrosine, 3-nitrosotyrosine, and so on (Bartlesaghi & Radi, 2018). This study solely focuses on the pH-effects of the ONOO^- reaction and NTyr and DiTyr yields.

5.3 Materials and Methods

5.3.1 Materials

Bovine serum albumin (BSA; A7030), tetranitromethane (TNM; T25003), peroxyxynitrite (ONOO⁻; 516620) supplied in 4.7% NaOH (w/v) at 160-200 mM, sodium phosphate dibasic (RES20908-A702X), potassium phosphate monobasic (P5655), potassium chloride (P9333), sodium chloride (S9625), hydrochloric acid (HCl; 258148), sodium hydroxide (NaOH; 79724), acetonitrile (ACN; 100030), and Amicon Ultra-0.5 centrifugal filters (10 kDa, 0.5 mL size; UFC503008) were purchased from Millipore Sigma (St. Louis, MO, USA). Trifluoroacetic acid (TFA; 85183) was obtained from Thermo Fisher Scientific (Waltham, MA, USA). Milli-Q water (MQW) was obtained using a Millipore Milli-Q lab water system (18.2 mΩ. 0.01 M phosphate-buffered saline (1xPBS; pH 7.4; 10 mM sodium phosphate dibasic, 1.8 mM potassium phosphate monobasic, 2.7 mM potassium chloride, and 137 mM sodium chloride) and 0.1 M phosphate-buffered saline (10xPBS; 100 mM sodium phosphate dibasic, 18 mM potassium phosphate monobasic, 27 mM potassium chloride, and 1.37 M sodium chloride) were prepared in MQW. Phosphate buffer (PB) pH 7 (PB 7; 100 mM sodium phosphate dibasic and 18 mM potassium phosphate monobasic), phosphate buffer pH 12 (PB 12; 100 mM sodium phosphate dibasic), and ammonium bicarbonate buffer (AHC, 2M) were prepared in MQW. Each buffer was adjusted to the desired pH using HCl (0.1 M) or NaOH (0.1 M).

An analytical balance (Ohaus Explorer EX125D; ± 0.01 mg) was used for all mass measurements. A 1.0 mL quartz cuvette with 10 mm path length (MF-W-10-LID)

was obtained from Science Outlet (Lewiston, MI, USA). An InLab micro pH electrode (Mettler-Toledo; Columbus, OH, USA) was used for all pH readings. Microcentrifuge tubes (500 μ L; LT8507 and 1.5 mL; LT8509) were purchased from Life Science Products (Frederick, CO, USA). Transferpette (BrandTech Scientific; Essex, CT, USA) automated pipettes were used to deliver volumes unless otherwise noted. All data analysis was done in Igor Pro (Wavemetrics). Graphics were created at BioRender.com.

5.3.2 Nitration of BSA with ONOO⁻

The nitration reaction of BSA with ONOO⁻ followed the procedure from *Alhalwani et al.* (Alhalwani et al., 2019). Briefly, the reaction of BSA (1.0 mg mL⁻¹) with ONOO⁻ occurred in either 1xPBS buffer, 10xPBS buffer, or PB, followed by the addition of ONOO⁻ based on the chosen ONOO⁻/Tyr molar ratio. The reaction was left to sit on ice in the dark for 90 minutes. Initial pH readings were taken before the addition of ONOO⁻ and final readings were taken both immediately following the addition, upon vortexing, and after the 90 minutes. In all cases the final pH did not change after the 90-minute reaction. The reaction was quenched using an Amicon 10 kDa centrifugal unit to filter excess reagent and by-products from the reaction vessel and product, and the concentrated reaction product was diluted in the respective buffer back to the original concentration (1.0 mg mL⁻¹).

Reaction experiments were conducted across increasing molar ratios. ONOO⁻ was added to BSA in 1xPBS (pH 7.4) in volumes corresponding to molar ratios of 0.1, 0.5, 0.75, 1, 1.5, 2, 5, 10, and 20 (ONOO⁻/Tyr) and the final pH values of the reaction

mixtures were taken. A separate nitration experiment was conducted using molar ratios of 0.1, 1, 5, and 10. Unmodified BSA (not reacted with ONOO^-) and 1xPBS were used as controls. A further experiment was conducted to determine the effects of buffer capacity on the reaction. ONOO^- was added to BSA (1.0 mg mL^{-1}) in both 1xPBS (pH 7.4) and 10xPBS (pH 7.4) in volumes corresponding to the molar ratios mentioned above and the final pH of the reaction mixtures were taken. For simplicity, modified BSA samples (reacted with ONOO^-) are referred to as NBSA (nitrated BSA).

To minimize the effects of extending buffer capacity, the ONOO^- reaction was further tested in PB (100 mM) at varying pH starting values using both PB 7 and PB 12. BSA (1.0 mg mL^{-1}) was placed in PB which had been pH-adjusted to corresponding starting pH values across 6-12. ONOO^- was added corresponding to two different ONOO^- /Tyr molar ratios (0.5/1 and 5/1, $0.316 \mu\text{L}$ and $3.16 \mu\text{L}$ respectively). The reaction proceeded as outlined above and the final pH values were measured.

5.3.3 Spectroscopic analysis

The absorbance of light at 357 nm is used as a tool for the detection of NTyr in acidic and neutral solutions, as is the reduction of fluorescence intensity at excitation 280 nm upon nitration (Espey et al., 2002; Yang et al., 2010). Fluorescence in alkaline solutions at excitation wavelength 320 nm and emission wavelength 400 nm is indicative of DiTyr formation (D. A. Malencik & Anderson, 2003; Dean A. Malencik et al., 1996). Samples were diluted in PB to 0.1 mg mL^{-1} and adjusted pH until with addition of 0.1 M NaOH until pH measured 9.7, as described by *Kampf et al* (Kampf et al., 2015).

Fluorescence measurements were performed at RT on a Cary Eclipse Fluorescence Spectrometer. Excitation wavelengths were 200-400 nm (2 nm increments), and emission was recorded from 250-600 nm. Excitation and emission slit widths were both set to 5 nm and a scan rate of 600 nm/min was used.

5.3.4 Nitration degree analysis

Protein solutions were analyzed using RP-HPLC-DAD (reversed-phase high performance liquid chromatography with diode-array detection) as previously described by *Selzle et al.* (Selzle et al., 2013). Briefly, modified samples were placed in glass HPLC vials and analyzed using a HPLC-DAD system (Agilent 1200 series). A C₁₈ column (Supelco Discovery BioWide Pore 25 cm x 2.1 mm, 5 μm) with eluents 0.1% (v/v) trifluoroacetic acid in water (eluent A) and ACN (eluent B) were used for chromatographic separation. Gradient elution was performed at a flow rate of 300 μL min⁻¹, and for each run the solvent gradient started at 3% B followed by a linear gradient to 90% B over 15 min. Absorbance was monitored at wavelengths of 280 and 357 nm. The sample injection volume was 20 μL and each chromatographic run was repeated 2-3 times (measurement replicates) with 1-2 MQW blanks in between each.

The instrument was calibrated to detect nitration using unmodified BSA, BSA reacted with TNM at a 1/1 (TNM/Tyr) molar ratio, and BSA reacted with ONOO⁻ at a 1/1 (ONOO⁻/Tyr) molar ratio, as described previously (Davey et al., 2022). The limit of detection (LOD) and limit of quantification (LOQ) for both 280 nm and 357 nm were determined for each calibrant and are shown in Appendix D Table D1.

The nitration degree (ND) of each sample was determined using the integrated peak areas of both 280 nm and 357 nm peaks, as previously described by *Selzle et al* (Selzle et al., 2013). Briefly, the chromatographic data was baseline-subtracted and the area under the curve was integrated at a retention time of 13.0 min for both 280 nm and 357 nm. The integrated peak area was then inputted into the ND calculation, which accounts for the simultaneous absorption properties of NTyr at 280 nm and 357 nm (Selzle et al., 2013). It should be noted that the absorption properties of NTyr are strongly pH-dependent due to its ability to form an internal hydrogen bond between the nitro and phenolic hydroxyl group (De Filippis et al., 2006). At acidic pH, which is the case for RP-HPLC, NTyr has an absorption maximum at 357 nm (Crow & Ischiropoulos, 1996; Jiao et al., 2001; Souza et al., 1999).

5.3.5 Dimerization and oligomerization analysis

To determine oligomerization of the protein samples size exclusion chromatography (SEC) was utilized. The protein solutions were separately analyzed using SEC-HPLC-DAD as previously described (Backes et al., 2021; Kampf et al., 2015; Liu et al., 2017). Briefly, a protein standard mix 15 – 600 kDa (69385, Sigma-Aldrich) was used to calibrate a Bio SEC column (Agilent, 300 Å, 4.6 x 150 mm, 3 µm particle size), which was used with isocratic separation at a flow rate of 0.35 mL min⁻¹ (Figure D5 in Appendix D). The mobile phase was 150 mM NaH₂PO₄ buffer (adjusted to pH 7.4 by adding 0.1 M HCl), and the injection volume was 20 µL. DAD spectra were recorded at wavelengths of 220, 280, and 357 nm, and each chromatographic run was performed in

triplicate. It is important to note that molecules are separated by hydrodynamic size via SEC, so only approximate molecular weights can be determined via this calibration method (Kampf et al., 2015).

The BSA oligomer fractions were determined similarly to previously described (Backes et al., 2021; Kampf et al., 2015; Liu et al., 2017). The baseline-corrected chromatographic data at 220 nm was integrated according to the calibration retention times. The retention times and peak shape of the higher oligomers varied, as well as some peaks co-eluted, so here we report dimer degree (DD) as the ratio of the integrated dimer peak area to the total integrated area and oligomer degree (OG) as the integrated monomer area subtracted from the total integrated area divided by the total integrated area. It should be noted that the purchased unmodified BSA contained a small fraction of dimer and oligomer variants. Exemplary chromatograms are shown in Figure D3 in Appendix D.

5.4 Results and Discussion

5.4.1 Reaction of BSA with ONOO⁻ results in pH increase

BSA was reacted with ONOO⁻ at varying molar ratios (ONOO⁻/Tyr) and both native and modified BSA samples were analyzed by RP-HPLC. The ND was determined as a metric for quantifying the NTyr formation in each sample (Selzle et al., 2013). Figure 5.1 shows the ND response as molar ratio of ONOO⁻ increases, as well as the corresponding final ONOO⁻ concentration. In a previous study, *Pfeiffer et al.* showed that as the steady state of ONOO⁻ increased the nitrating efficiency of Tyr-containing

solutions increased, but leveled off at higher concentrations, consistent with results we have seen previously (Pfeiffer et al., 2000). In this study, we see similar results with the BSA reactions. ND increases upon increasing addition of ONOO⁻ to a molar ratio of 1/1, slightly increases to 5/1, and then slightly decreases with molar ratios of 10/1 and 20/1. The higher molar ratios and ONOO⁻ concentrations used here are not biologically relevant, however they are often used in reactions with proteins in *in vitro* experiments to mimic endogenous oxidative stress. The goal of this research was to determine if the increase in ND followed by a decrease was experimental artifact from adding ONOO⁻. It should be noted that ONOO⁻ is extremely reactive and is unstable at room temperature. In addition, the actual concentration of each purchased vial of ONOO⁻ varies and is given as a range (160-200 mM) and is synthesized from isoamyl nitrite and hydrogen peroxide (Uppu & Pryor, 1996). Due to this, the absolute ND value of the reaction is relative and varies with each ONOO⁻ batch, as well as if the ONOO⁻ has been thawed previously. Therefore, the data shown here is from a single experiment. However, the experiment has been repeated 6 times and the relative trend is the same (shown in Figure D2 in Appendix D).

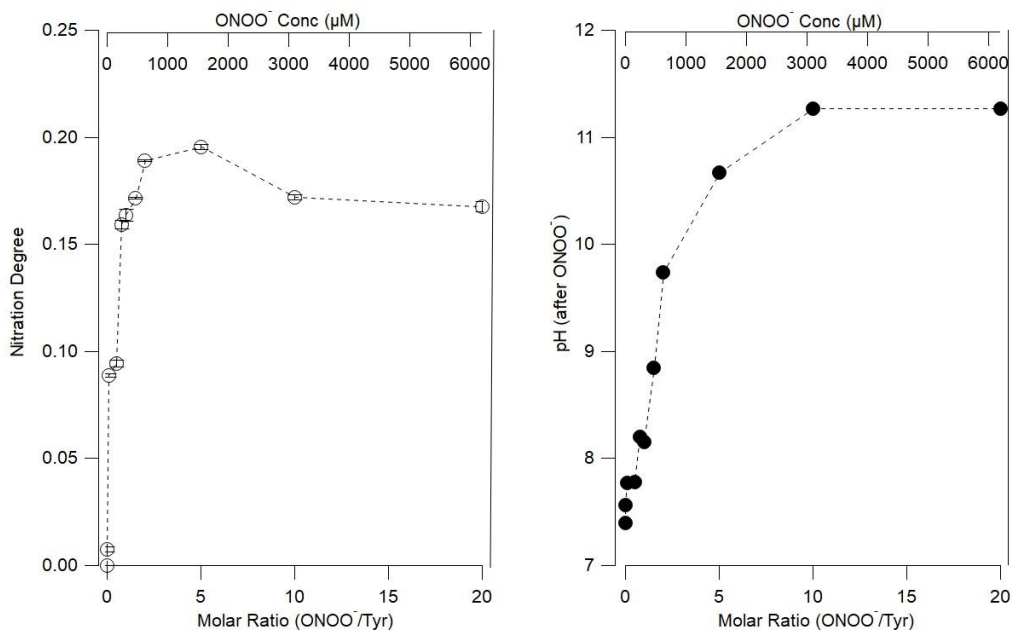


Figure 5.1 ND and pH response as molar ratio and ONOO⁻ increases in 1xPBS. Open circles represent ND and closed circles represent pH. Lines are to guide the eye.

Due to its reactivity, ONOO⁻ is commonly supplied in a strong base, therefore the bolus addition of ONOO⁻ to reaction mixtures may affect the pH of the reactions, depending on the strength of the buffer used. Furthermore, the reaction of proteins with ONOO⁻ is most conducted using 1xPBS, which corresponds to 0.01 M phosphate buffer. Figure 5.1 shows the pH values after the addition of ONOO⁻ to the BSA reaction mixtures. The addition of the ONOO⁻ in NaOH quickly exceeds the buffer capacity of the 1xPBS and the pH increases with the corresponding molar ratio, and ONOO⁻ concentration, increase. *Pfeiffer et al.* showed that DiTyr formation was predominant at low ONOO⁻ concentrations (Pfeiffer et al., 2000). However, as discussed in the

introduction and shown by *Bartesaghi et al*, at high pH DiTyr formation may outcompete NTyr formation in ONOO⁻ reactions with Tyr (Bartesaghi et al., 2006). We hypothesized, therefore, that due to the large increase in pH at increasing ONOO⁻ concentrations, DiTyr formation was outcompeting NTyr formation.

5.4.2 DiTyr formation occurs at high ONOO⁻ concentrations

To determine if DiTyr formation was occurring at high concentrations of ONOO⁻, and thus high molar ratios, in another set of experiments BSA was reacted with ONOO⁻ at increasing molar ratios. The NDs of the reaction products were determined using RP-HPLC and oligomer degree (OD) was determined using size-exclusion chromatography (SEC-HPLC). Figure 5.2 (circles) shows the ND slightly increasing from unmodified BSA to 0.1/1 NBSA, followed by a large increase to 1/1 NBSA and 5/1 NBSA. The ND, indicative of NTyr formation, slightly decreases from 5/1 to 10/1 NBSA, consistent with the previous experiment. Figure 5.2 (squares) shows the OD, indicative of DiTyr formation, increasing linearly from unmodified BSA to 5/1 NBSA, followed by only a slight increase at 10/1 NBSA. This supports the idea that DiTyr formation outcompetes NTyr formation at higher molar ratio values. Figure 5.2 is colored by the pH after the addition of ONOO⁻, confirming that the pH increased across the increasing molar ratio, consistent with observations from Figure 5.1. The formation of DiTyr species was further confirmed by fluorescence spectrometry. DiTyr has fluorescence properties in alkaline solutions, so the reaction mixtures were pH-adjusted to 9.7 with NaOH (0.1 M) and fluorescence measurements at excitation (320 nm) and emission (400 nm) wavelengths,

corresponding to DiTyr, were taken (Kampf et al., 2015; Dean A. Malencik et al., 1996). Figure 5.2 (triangles) shows the fluorescence intensity (ex 320 nm, em 400 nm) of the reaction mixtures, showing a similar trend to the DD with a linear increase to molar ratio 5/1 and a slight increase to molar ratio of 10/1. These results further support the hypothesis that DiTyr formation may outcompete NTyr formation at high ONOO⁻ concentrations but does not separate ONOO⁻ concentration from the corresponding pH increase.

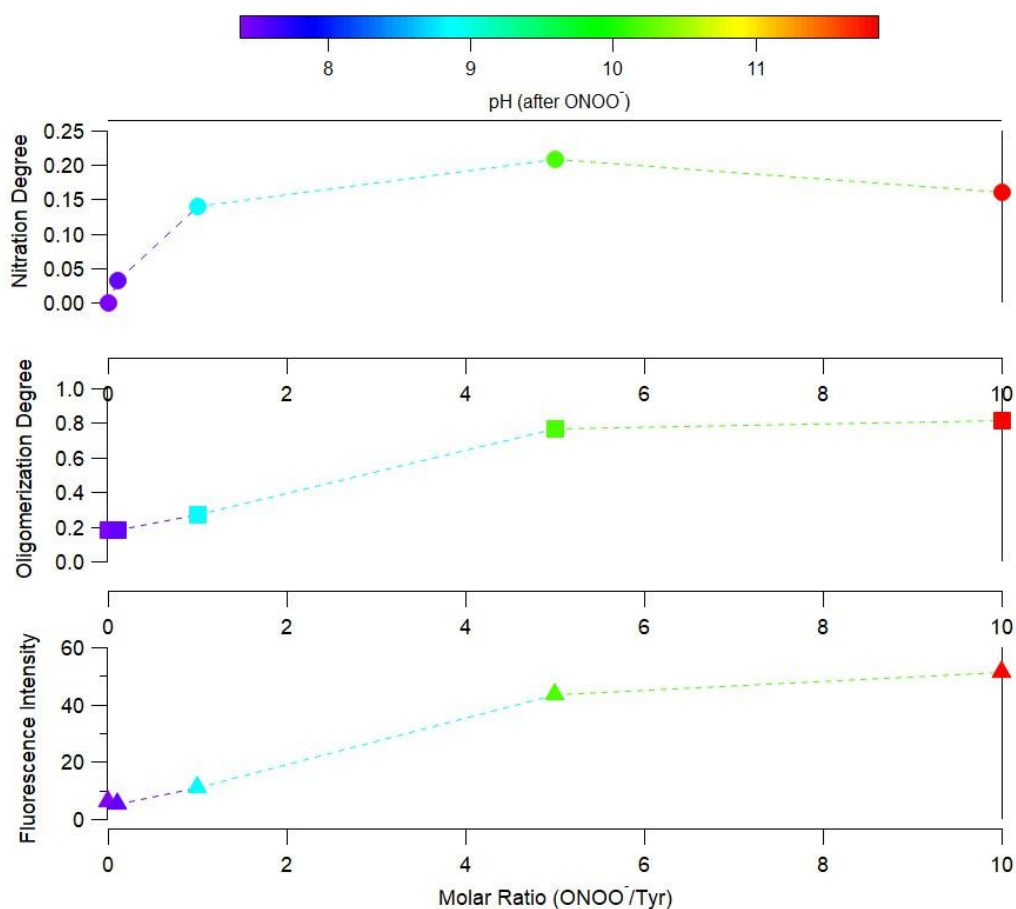


Figure 5.2. ND, OD, and fluorescence response of the reaction of BSA and ONOO⁻ as molar ratio increases. Circles represent ND, squares represent OD, and triangles represent fluorescence.

5.4.3 Reaction mechanism is determined by pH

To separate the ONOO⁻ concentration from the change in pH that corresponds to increasing the ONOO⁻ concentration, thus correlating with a pH increase from NaOH in the ONOO⁻ solution, a separate set of experiments were conducted. Two molar ratios were selected. The lower relative ratio of 0.5/1 was designed with ONOO⁻ as a limiting reagent (non-excess), and the higher relative ratio of 5/1 with ONOO⁻ is in a large excess.

At each molar ratio, ONOO⁻ was allowed to react with BSA in PB (100 mM). PB was used to buffer the reaction more than 1xPBS, and to minimize any ionic strength effects from the salts in the 1xPBS solution. Both PB 7 and PB 12 were used to further buffer each respective reaction as closely to the buffer range as possible. BSA samples were allowed to react at various pH starting values (~6-12) to obtain a similar range of final pH values after the ONOO⁻ reaction occurred. Unmodified BSA samples in each of the respective PB buffers were used as control samples. The reaction samples were analyzed via RP-HPLC and SEC-HPLC to determine the extent of formation of both nitration and oligomerization.

Figure 5.3 shows an increase of ND as the pH is increased from 6-10, then a decrease from pH 10-12. The 0.5/1 results (Figure 5.3 blue triangles) are not as clear. This may be due to the very small volume of ONOO⁻ delivered (0.316 μ L) to achieve the 0.5/1 molar ratio. Secondly, because the ONOO⁻ is below equimolar concentrations to the Tyr residues in the samples the reaction will not proceed to completion in all cases, whereas the ONOO⁻ concentration is in excess in the 5/1 molar ratio samples which allows the nitration reaction to react completely.

Figure 5.3 also shows the dimerization and oligomerization results. As the pH increases the DD increases, especially as the pH approaches 10. This is consistent with what we expect due to the pK_a of the phenolic hydroxyl of Tyr being 10, as seen in the mechanistic studies by *Bartesaghi et al.* (Bartesaghi et al., 2006; Bartesaghi & Radi, 2018). Separately, the oligomerization degree (OD) was calculated as a metric representing all higher oligomers ($MW > MW_{\text{monomer}}$) formed in the reaction. The 0.5/1

and 5/1 NBSA samples show similar results, indicating dimerization and oligomerization formation is not dependent on the ONOO⁻ concentration, but rather only the pH. This SEC data and methodology are consistent with previous studies of DiTyr formation (Kampf et al., 2015). It should be noted that the unmodified BSA samples have a small degree of both dimers and oligomers (open black squares Figure 5.3). Therefore, the DD and OD discussed refers to the concentration above this baseline. Furthermore, SEC-HPLC separates molecular masses by their hydrodynamic size and our method resulted in some peaks not being fully resolved, so only approximate molecular weights were obtained.

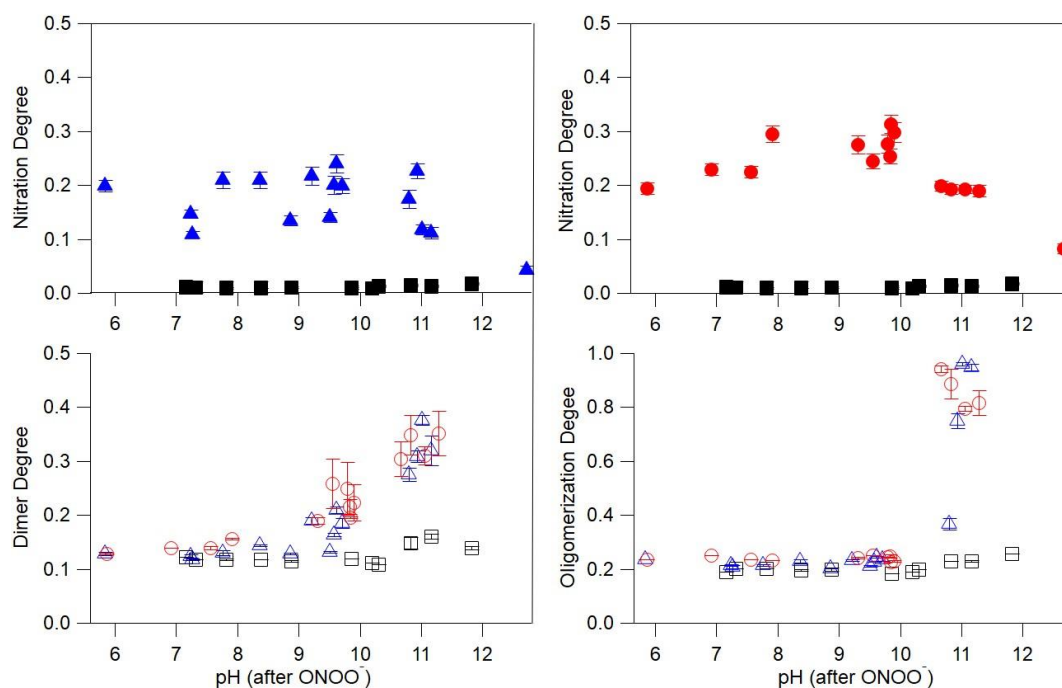


Figure 5.3. ND, DD, and OD response of the reaction of BSA and ONOO^- as pH increases. Blue represents limited (0.5/1 NBSA) ONOO^- and red represents excess (5/1 NBSA). Black represents unmodified BSA. Closed symbols are ND and open symbols are DD and OD.

DiTyr formation was further verified via fluorescence measurements (Figure 5.4). As noted, Tyr nitration results in the loss of fluorescence at excitation 220 nm and 280 nm (emission 350 nm) and DiTyr formation results in the gain of fluorescence at excitation 320 nm (emission 400 nm; in alkaline solution). Excitation emission matrices (EEMs) were taken of the unmodified BSA samples and 0.5/1 and 5/1 NBSA samples from excitation wavelength range 200-400 nm (Figure D1 in Appendix D). The fluorescence intensity of the unmodified BSA shows two fluorescence peaks at excitation 220-230 nm and 280 nm, corresponding to the excitation of Tyr and tryptophan

(Bortolotti et al., 2016). The loss of fluorescence by nitration and the gain of fluorescence due the addition of DiTyr across the samples are shown in Figure 5.4. The first 2 panels show the loss of Tyr fluorescence (ex 280 nm) as the samples are nitrated at pH 7 and pH 9.7. The second 2 panels show the gain of DiTyr fluorescence (ex 320 nm) as the samples are dimerized at pH 9.7 and pH 11. This data is consistent with previous studies of DiTyr formation (Kampf et al., 2015). Excitation emission matrices (EEMs) are shown in Figure D1 in Appendix D.

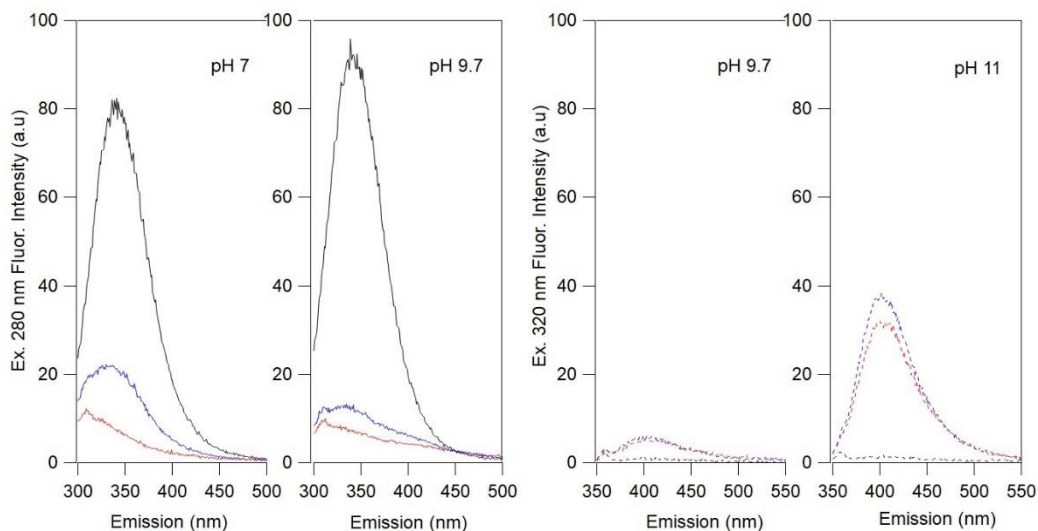


Figure 5.4. Fluorescence response of the reaction of BSA and ONOO^- as pH increases. The black lines represent the unmodified BSA, blue lines correspond to 0.5/1 NBSA, and red lines correspond to 5/1 NBSA.

Collectively, these results confirm that the switch from NTyr formation to DiTyr formation and oligomerization is pH-mediated and not due to the increase in ONOO^- concentration. When the pH was kept lower than 9, the dimerization reaction did not

occur, and the ND continued to rise or remained constant. When the pH rose above 9 when ONOO^- was in excess, the ND began to decrease, and the oligomerization reaction began increasing. Both nitration and oligomerization are two-step processes. Tyr reacts with the OH radical from ONOO^- to form a tyrosyl radical. However, NTyr formation requires a NO_2 radical to be present, whereas DiTyr formation requires another tyrosyl radical to be present (reaction mechanism shown in Figure 5.5). However, as stated in the introduction, the NO_2 radical can react with both the tyrosyl radical and native Tyr residues, which may consume the NO_2 radical resulting in less NTyr formation (Bartesaghi et al., 2006; Ferrer-Sueta et al., 2018). At higher pH values, Tyr is in its phenolate form, which is more readily oxidized to the tyrosyl radical by the NO_2 radical, resulting in a higher fraction of tyrosyl radicals to form DiTyr. It is important to note that the results shown here are from one detailed experiment, due to differences in ONOO^- reactivity making quantitative results difficult to compare, discussed below. However, experiments were conducted multiple times resulting in similar reaction trends, shown in Appendix D.

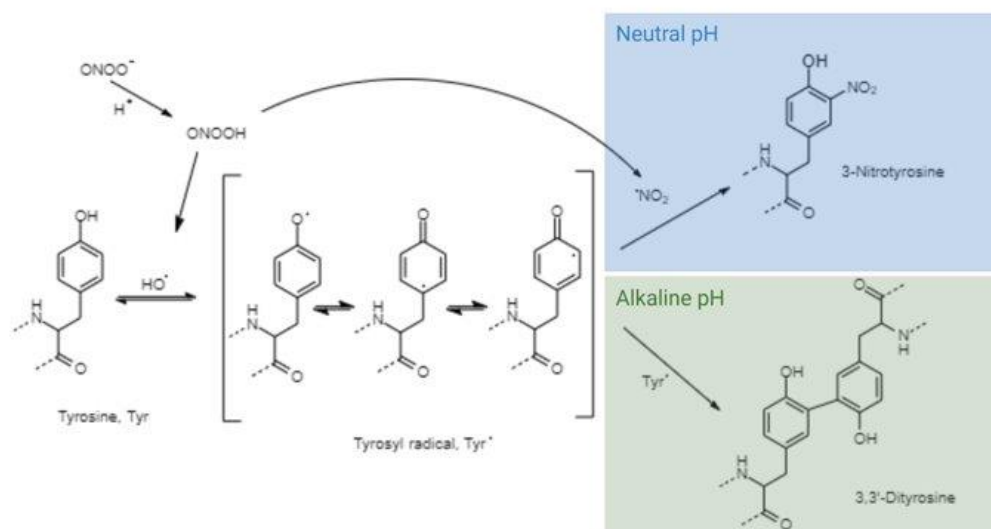


Figure 5.5. Reaction mechanism of Tyr with ONOO⁻ to form NTyr or DiTyr. Created at BioRender.com.

5.4.4 Importance of reaction conditions

To further verify pH causes the observed decrease in nitration seen e.g. in Figure 5.1, the specific reaction was carried out in higher buffer capacity to resist the change in pH. The ONOO⁻ reaction was carried out in both 1xPBS and 10xPBS at the same ONOO⁻/Tyr molar ratios (0.1/1 – 20/1) and the respective pH change was measured. Figure 5.6 shows the ND response vs the final pH (after ONOO⁻ addition). The 10xPBS (open circles) buffered the reaction to a narrower range of pH values, as expected, than the 1xPBS (closed circles). Furthermore, the 10xPBS samples do not show a decrease in ND, whereas the 1xPBS do. Similarly, the reaction of BSA with ONOO⁻ was conducted with additional ammonium bicarbonate buffer (AHC) added, as done by *Backes et al.*, to buffer the ONOO⁻ reactant (Backes et al., 2021). The results (Figure D2 in Appendix D)

show that additional buffer resists some change to pH, but also bring up the starting pH from pH 7.4. This further verifies the bolus amounts of ONOO^- in NaOH added exceed the buffer capacity of PBS, and the large increase in pH alters the reaction mechanism. This is especially important because the reaction of ONOO^- with proteins can also result in side-products, and the shift in retention time and HPLC peak broadening are indicative of hydrophobicity changes and partial unfolding, as discussed previously (Reinmuth-Selzle et al., 2023).

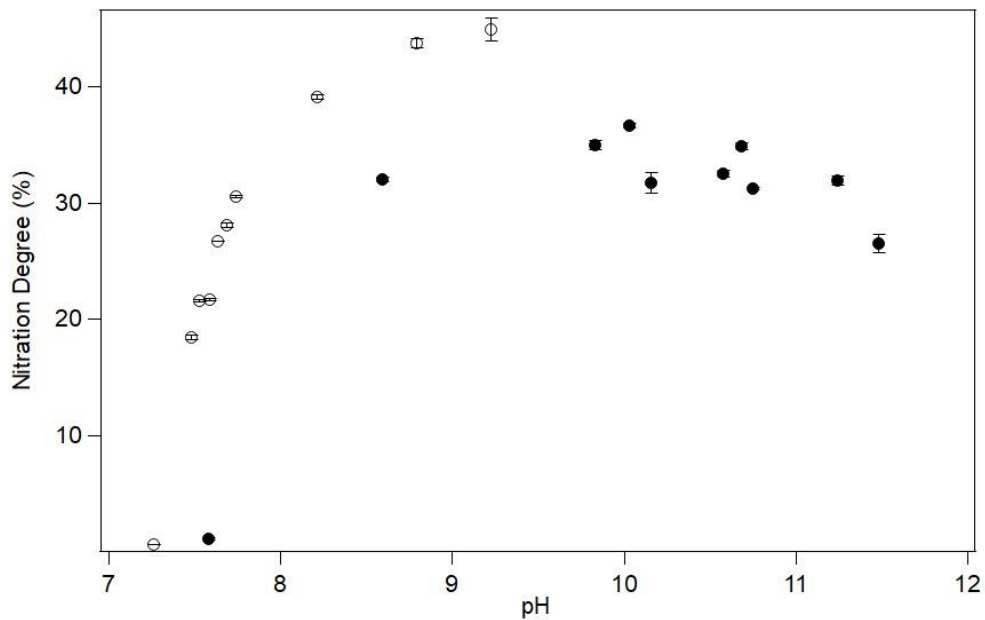


Figure 5.6. Reaction of BSA with ONOO^- at differing buffer capacities. Open circles represent 10xPBS and closed circles represent 1xPBS.

As stated previously, the concentration of purchased ONOO^- can vary and is given as a range from 160-200 mM. ONOO^- is unstable and the activity decreases about 2% a day at $-20\text{ }^\circ\text{C}$, as well as freeze-thaw cycles should be avoided (Uppu & Pryor,

1996). Therefore, experimental results using purchased ONOO⁻ vary depending on the age and preparation of the ONOO⁻. Figure D2 shows how the relative ND value is affected over the course of multiple experiments depending on if the ONOO⁻ had previously been opened or not.

ONOO⁻ nitration of Tyr is often studied *in vitro* by the bolus addition of alkaline ONOO⁻ solutions to Tyr-containing samples. However, as noted by *Pfeiffer and Mayer*, this experimental approach does not reflect what occurs *in vivo*, where ONOO⁻ is formed by the reaction of NO with O₂ at physiological pH (Pfeiffer & Mayer, 1998). The studies shown here further show that the molar ratios and ONOO⁻ concentrations used in *in vitro* experiments are no longer biologically relevant to the pH of 7.4 and extra care should be taken accordingly when planning physiological-relevant experiments with ONOO⁻.

5.5 Conclusion

The reaction of proteins with ONOO⁻ is commonly used to mimic oxidative stress in *in vitro* experiments. Many studies report the effects of ONOO⁻-mediated NTyr formation, which is vital to the understanding of the effects that may occur. However, bolus additions of ONOO⁻ to reactions in 1x or 10x buffers have a large effect on the pH of the reaction, which can lead to different chemical mechanisms to occur. Our results show the importance of using adequate buffers to keep the pH in a biologically relevant range, as well as a need to monitor the formation of other PTMs. This information is vital to accurately attributing alterations in protein function studied to specific PTMs.

References

- Ahsan, H. (2013). 3-Nitrotyrosine: A biomarker of nitrogen free radical species modified proteins in systemic autoimmunogenic conditions. *Human Immunology*, *74*(10), 1392–1399. <https://doi.org/10.1016/J.HUMIMM.2013.06.009>
- Alhalwani, A. Y., Davey, R. L., Kaul, N., Barbee, S. A., & Huffman, J. A. (2019). Modification of lactoferrin by peroxynitrite reduces its antibacterial activity and changes protein structure. *Proteins: Structure, Function, and Bioinformatics*, 1–9. <https://doi.org/10.1002/prot.25782>
- Alvarez, B., & Radi, R. (2003). Peroxynitrite reactivity with amino acids and proteins. *Amino Acids*, *25*, 295–311. <https://doi.org/10.1007/s00726-003-0018-8>
- Backes, A. T., Reinmuth-Selzle, K., Leifke, A. L., Ziegler, K., Krevert, C. S., Tscheuschner, G., Lucas, K., Weller, M. G., Berkemeier, T., Pöschl, U., & Fröhlich-Nowoisky, J. (2021). Oligomerization and Nitration of the Grass Pollen Allergen Phl p 5 by Ozone, Nitrogen Dioxide, and Peroxynitrite: Reaction Products, Kinetics, and Health Effects. *International Journal of Molecular Sciences*, *22*(14), 7616. <https://doi.org/10.3390/IJMS22147616>
- Bartesaghi, S., & Radi, R. (2018). Fundamentals on the biochemistry of peroxynitrite and protein tyrosine nitration. *Redox Biology*, *14*(August 2017), 618–625. <https://doi.org/10.1016/j.redox.2017.09.009>
- Bartesaghi, S., Valez, V., Trujillo, M., Peluffo, G., Romero, N., Zhang, H., Kalyanaraman, B., & Radi, R. (2006). Mechanistic studies of peroxynitrite-mediated tyrosine nitration in membranes using the hydrophobic probe N-t-BOC-L-tyrosine

tert-butyl ester. *Biochemistry*, 45(22), 6813–6825.

<https://doi.org/10.1021/bi060363x>

Bortolotti, A., Wong, Y. H., Korsholm, S. S., Bahring, N. H. B., Bobone, S., Tayyab, S., Van De Weert, M., & Stella, L. (2016). On the purported “backbone fluorescence” in protein three-dimensional fluorescence spectra. *RSC Advances*, 6(114), 112870–112876. <https://doi.org/10.1039/C6RA23426G>

Bruno, G., Wenske, S., Lackmann, J. W., Lalk, M., Woedtke, T. von, & Wende, K. (2020). On the liquid chemistry of the reactive nitrogen species peroxyxynitrite and nitrogen dioxide generated by physical plasmas. *Biomolecules*, 10(12), 1–25. <https://doi.org/10.3390/biom10121687>

Campolo, N., Issoglio, F. M., Estrin, D. A., Bartesaghi, S., & Radi, R. (2020). 3-Nitrotyrosine and related derivatives in proteins: precursors, radical intermediates and impact in function. *Essays in Biochemistry*, 64(1), 111–133. <https://doi.org/10.1042/ebc20190052>

Crow, J. P., & Ischiropoulos, H. (1996). Detection and quantitation of nitrotyrosine residues in proteins: In vivo marker of peroxyxynitrite. *Methods in Enzymology*, 269, 185–194. [https://doi.org/10.1016/S0076-6879\(96\)69020-X](https://doi.org/10.1016/S0076-6879(96)69020-X)

Davey, R. L., Mattson, E. J., & Huffman, J. A. (2022). Heterogeneous nitration reaction of BSA protein with urban air: improvements in experimental methodology. *Analytical and Bioanalytical Chemistry* 2021, 1–12. <https://doi.org/10.1007/S00216-021-03820-8>

De Filippis, V., Frasson, R., & Fontana, A. (2006). 3-Nitrotyrosine as a spectroscopic

- probe for investigating protein-protein interactions. *Protein Science*, *15*, 967–986.
<https://doi.org/10.1110/ps.051957006>
- Espey, M. G., Xavier, S., Thomas, D. D., Miranda, K. M., & Wink, D. A. (2002). Direct real-time evaluation of nitration with green fluorescent protein in solution and within human cells reveals the impact of nitrogen dioxide vs. peroxynitrite mechanisms. *Proceedings of the National Academy of Sciences*, *99*(6), 3481–3486.
<https://doi.org/10.1073/PNAS.062604199>
- Ferrer-Sueta, G., Campolo, N., Trujillo, M., Bartesaghi, S., Carballal, S., Romero, N., Alvarez, B., & Radi, R. (2018). Biochemistry of Peroxynitrite and Protein Tyrosine Nitration. *Chemical Reviews*, *118*(3), 1338–1408.
<https://doi.org/10.1021/ACS.CHEMREV.7B00568>
- Hensley, K., Maidt, M. L., Yu, Z., Sang, H., Markesbery, W. R., & Floyd, R. A. (1998). Electrochemical analysis of protein nitrotyrosine and dityrosine in the Alzheimer brain indicates region-specific accumulation. *Journal of Neuroscience*, *18*(20), 8126–8132. <https://doi.org/10.1523/JNEUROSCI.18-20-08126.1998>
- Ischiropoulos, H., & Al-Mehdi, A. B. (1995). Peroxynitrite-mediated oxidative protein modifications. *FEBS Letters*, *364*(3), 279–282. [https://doi.org/10.1016/0014-5793\(95\)00307-U](https://doi.org/10.1016/0014-5793(95)00307-U)
- Jiao, K., Mandapati, S., Skipper, P. L., Tannenbaum, S. R., & Wishnok, J. S. (2001). Site-Selective Nitration of Tyrosine in Human Serum Albumin by Peroxynitrite. *Analytical Biochemistry*, *293*(1), 43–52. <https://doi.org/10.1006/ABIO.2001.5118>
- Kampf, C. J., Liu, F., Reinmuth-Selzle, K., Berkemeier, T., Meusel, H., Shiraiwa, M., &

- Pöschl, U. (2015). Protein Cross-Linking and Oligomerization through Dityrosine Formation upon Exposure to Ozone. *Environmental Science and Technology*, 49(18), 10859–10866. <https://doi.org/10.1021/acs.est.5b02902>
- Lai, C. K., Tang, W. K., Siu, C., & Chu, I. K. (2020). Evidence for the Prerequisite Formation of Phenoxy Radicals in Radical-Mediated Peptide Tyrosine Nitration In Vacuo. *Chemistry – A European Journal*, 26(1), 331–335. <https://doi.org/10.1002/chem.201904484>
- Lemercier, J. N., Padmaja, S., Cueto, R., Squadrito, G. L., Uppu, R. M., & Pryor, W. A. (1997). Carbon Dioxide Modulation of Hydroxylation and Nitration of Phenol by Peroxynitrite. *Archives of Biochemistry and Biophysics*, 345(1), 160–170. <https://doi.org/10.1006/ABBI.1997.0240>
- Liu, F., Reinmuth-Selzle, K., Lai, S., Weller, M. G., Pöschl, U., & Kampf, C. J. (2017). Simultaneous determination of nitrated and oligomerized proteins by size exclusion high-performance liquid chromatography coupled to photodiode array detection. *Journal of Chromatography A*, 1495(2), 76–82. <https://doi.org/10.1016/j.chroma.2017.03.015>
- Maina, M. B., Al-Hilaly, Y. K., Oakley, S., Burra, G., Khanom, T., Biasetti, L., Mengham, K., Marshall, K., Harrington, C. R., Wischik, C. M., & Serpell, L. C. (2022). Dityrosine Cross-links are Present in Alzheimer’s Disease-derived Tau Oligomers and Paired Helical Filaments (PHF) which Promotes the Stability of the PHF-core Tau (297-391) In Vitro. *Journal of Molecular Biology*, 434(19). <https://doi.org/10.1016/J.JMB.2022.167785>

- Malencik, D. A., & Anderson, S. R. (2003). Dityrosine as a product of oxidative stress and fluorescent probe. *Amino Acids*, 25(3–4), 233–247.
<https://doi.org/10.1007/S00726-003-0014-Z/METRICS>
- Malencik, Dean A., Sprouse, J. F., Swanson, C. A., & Anderson, S. R. (1996). Dityrosine: preparation, isolation, and analysis. *Analytical Biochemistry*, 242(2), 202–213. <https://doi.org/10.1006/ABIO.1996.0454>
- Pfeiffer, S., & Mayer, B. (1998). Lack of Tyrosine Nitration by Peroxynitrite Generated at Physiological pH. *Journal of Biological Chemistry*, 273(42), 27280–27285.
<https://doi.org/10.1074/JBC.273.42.27280>
- Pfeiffer, S., Schmidt, K., & Mayer, B. (2000). Dityrosine formation outcompetes tyrosine nitration at low steady-state concentrations of peroxynitrite: Implications for tyrosine modification by nitric oxide/superoxide in vivo. *Journal of Biological Chemistry*, 275(9), 6346–6352. <https://doi.org/10.1074/JBC.275.9.6346>
- Radi, R. (2013). Protein tyrosine nitration: Biochemical mechanisms and structural basis of functional effects. *Accounts of Chemical Research*.
<https://doi.org/10.1021/ar300234c>
- Radi, R., Peluffo, G., Alvarez, M. N., Naviliat, M., & Cayota, A. (2001). Unraveling peroxynitrite formation in biological systems. *Free Radical Biology and Medicine*, 30(5), 463–488. [https://doi.org/10.1016/S0891-5849\(00\)00373-7](https://doi.org/10.1016/S0891-5849(00)00373-7)
- Reinmuth-Selzle, K., Bellinghausen, I., Leifke, A. L., Backes, A. T., Bothen, N., Ziegler, K., Weller, M. G., Saloga, J., Schuppan, D., Lucas, K., Pöschl, U., & Fröhlich-Nowoisky, J. (2023). Chemical modification by peroxynitrite enhances TLR4

activation of the grass pollen allergen Phl p 5. *Frontiers in Allergy*, 4, 5.

<https://doi.org/10.3389/FALGY.2023.1066392>

Reinmuth-Selzle, K., Kampf, C. J., Samonig, M., Shiraiwa, M., Yang, H., Gadermaier, G., Brandstetter, H., Huber, C. G., Duschl, A., & Oostingh, G. J. (2014). Nitration of the Birch Pollen Allergen Bet v 1.0101: Efficiency and Site-Selectivity of Liquid and Gaseous Nitrating Agents. *Journal of Proteome Research*, 13, 1570–1577.

<https://doi.org/10.1021/pr401078h>

Roy, P., Panda, A., Hati, S., & Dasgupta, S. (2019). pH-Dependent Nitrotyrosine Formation in Ribonuclease A is Enhanced in the Presence of Polyethylene Glycol (PEG). *Chemistry - An Asian Journal*, 14(24), 4780–4792.

<https://doi.org/10.1002/asia.201901225>

Selzle, K., Ackaert, C., Kampf, C. J., Kunert, A. T., Duschl, A., Oostingh, G. J., & Pöschl, U. (2013). Determination of nitration degrees for the birch pollen allergen Bet v 1. *Analytical and Bioanalytical Chemistry*, 405(27), 8945–8949.

<https://doi.org/10.1007/s00216-013-7324-0>

Souza, J. M., Daikhin, E., Yudkoff, M., Raman, C. S., & Ischiropoulos, H. (1999). Factors determining the selectivity of protein tyrosine nitration. *Archives of Biochemistry and Biophysics*, 371(2), 169–178.

<https://doi.org/10.1006/abbi.1999.1480>

Uppu, R. M., & Pryor, W. A. (1996). Biphasic synthesis of high concentrations of peroxynitrite using water-insoluble alkyl nitrite and hydrogen peroxide. *Methods in Enzymology*, 269, 322–329. [https://doi.org/10.1016/S0076-6879\(96\)69033-8](https://doi.org/10.1016/S0076-6879(96)69033-8)

- van der Vliet, A., Eiserich, J. P., O'Neill, C. A., Halliwell, B., & Cross, C. E. (1995). Tyrosine modification by reactive nitrogen species: A closer look. *Archives of Biochemistry and Biophysics*, 319(2), 341–349.
<https://doi.org/10.1006/abbi.1995.1303>
- Yang, H., Zhang, Y., & Pöschl, U. (2010). Quantification of nitrotyrosine in nitrated proteins. *Analytical and Bioanalytical Chemistry*, 397(2), 879–886.
<https://doi.org/10.1007/s00216-010-3557-3>
- Ziegler, K., Kunert, A. T., Reinmuth-Selzle, K., Leifke, A. L., Widera, D., Weller, M. G., Schuppan, D., Fröhlich-Nowoisky, J., Lucas, K., & Pöschl, U. (2020). Chemical modification of pro-inflammatory proteins by peroxynitrite increases activation of TLR4 and NF- κ B: Implications for the health effects of air pollution and oxidative stress. *Redox Biology*, 101581. <https://doi.org/10.1016/j.redox.2020.101581>

Chapter Six: Site-Selective Nitration of Lactoferrin Upon Peroxynitrite Exposure and Efficacy of Ergothioneine Inhibition

In preparation for submission for peer-review.

6.1 Abstract

The formation of post-translational modifications (PTM's) in proteins is associated with changes in protein structure and potential loss of function. Nitrotyrosine (NTyr) formation, or nitration, has been linked to oxidative stress, specifically via the reaction of Tyr residues with peroxynitrite (ONOO^-), a reactive species produced in the body. Lactoferrin (LF) is a multifunctional protein found in the many fluids and tissues within the human body and at sites of inflammation. Understanding the effects ONOO^- has on specific proteins is important in determining its link to inflammation and disease, as well as studying therapeutics to prevent oxidative damage. In the study presented here, the site-selectivity of ONOO^- reacted with LF is determined. The specific nitration sites are linked to the functionality of LF. Further, we study the effects ergothioneine (EGT), a L-histidine derivative with high antioxidant potential, has on preventing the nitration reaction from occurring. A concentration of 5.0 mM EGT prevented all nitration from occurring, and 0.5 mM and 1.0 mM EGT concentrations prevented nitration at physiologically relevant ONOO^- concentrations.

6.2 Introduction

Nitrotyrosine (NTyr) is a common biomarker used to represent signs of oxidative stress and damage. The formation of NTyr has been associated with many diseases, including neurodegeneration and cardiovascular injury, and is formed via the reactions of reactive oxygen species (ROS) and reactive nitrogen species (RNS) with tyrosine (Tyr) residues in proteins (Griendling & FitzGerald, 2003; Ischiropoulos & Beckman, 2003). Common ROS and RNS include hydrogen peroxide, hydroxyl radical, and peroxynitrite. Peroxynitrite (ONOO^-) is a highly reactive species produced by the human body under stress. The reaction of ONOO^- with proteins can cause a variety of post-translational modifications (PTM's), such as nitration (NTyr), oxidation, dityrosine (DiTyr), and hydroxylation of aromatic residues and NTyr residues specifically have been used as a footprint for ONOO^- (Zhang et al., 2001).

ONOO^- is formed *in vivo* via the reaction of superoxide anion (O_2^-) and nitric oxide (NO^-) and can react with different biomolecules by one or two-electron oxidations (Radi et al., 2001). It can also decompose by homolysis of peroxynitrous acid to NO_2 and OH radicals, which further participate in nitration and oxidation reactions (Alvarez & Radi, 2003; Radi et al., 2001). The mitochondria is a major source of intracellular superoxide formation, so it is also a major source of ONOO^- formation (Masubuchi et al., 2005). The mechanism behind NTyr formation via ONOO^- was elucidated at the molecular level by *Lai et al.* in 2020 (Lai et al., 2020). In this study, evidence for the prerequisite formation of phenoxy radicals and a two-step mechanism of the radical-mediated peptide tyrosine nitration was found (Lai et al., 2020).

Lactoferrin (LF, Lactotransferrin) is a protein found in human bodily fluids and tissues. It is found in high concentrations in human breast milk due to its antibacterial properties (Alhalwani et al., 2019). One of the well-studied properties of LF is its ability to bind lipopolysaccharide (LPS), a potent endotoxin that causes inflammation (Drago-Serrano et al., 2012). By binding LPS, LF inhibits its interaction with Toll-like receptor 4 (TLR4) activating complexes. Thus, LPS binding is one of the anti-inflammatory properties of LF. LF also has iron-binding properties and is able to bind one or two ferric iron molecules (Niaz et al., 2019). We have previously shown that modification of LF by ONOO⁻ changes its structure and reduces its antibacterial activity (Alhalwani et al., 2019).

Many disease states, like heart disease and hypertension, are characterized by an imbalance of ROS and antioxidant activity (Franzoni et al., 2006). Antioxidants stop the accumulation of free radicals and inhibit oxidative stress. L-ergothioneine (EGT; 2-mercaptohistidine trimethylbetaine) is a well-studied naturally occurring L-histidine derivative synthesized by fungi, mycobacteria, and cyanobacteria that has high antioxidant activity (Asahi et al., 2016). When ingested in a food source, EGT is metabolized slowly and retained in various tissues and fluids in varying concentrations. EGT is found in high concentrations in edible mushrooms (0.4 to 2 mg/g dry weight) and is conserved by mammals in the kidney, liver, seminal fluid, and erythrocytes (Franzoni et al., 2006; Nakamichi et al., 2016; Tanaka et al., 2019). It is a stable compound and upon uptake accumulates in high concentrations (100 μ M to 2 mM) via an organic cation

transporter (OCTN1; gene symbol SLC22A4) expressed in humans (Cheah & Halliwell, 2012; Tanaka et al., 2019).

Numerous studies have demonstrated the antioxidant and cytoprotective abilities of EGT and its ability to accumulate in high oxidative stress organs. *Nakamichi et al.* showed the ability of ergothioneine to cross the blood-brain barrier and show antidepressant-like effects (Nakamichi et al., 2016). *Kerley et al.* reviewed the therapeutic potential of EGT to inhibit mitochondrial dysfunction in pre-eclampsia (Kerley et al., 2018). *Asahi et al.* showed the ability of an edible mushroom containing high amounts of EGT, *Coprinus comatus*, to inhibit the UV-B-induced inflammatory responses and DNA halogenation (Asahi et al., 2016). EGT is known to scavenge radicals. It is primarily present as a thione under physiological pH, which allows it to resist oxidation (Cumming et al., 2018). *Franzoni et al.* measured the free radical scavenging capacity of EGT. Compared to other well-known antioxidants, i.e. glutathione, EGT showed the highest antioxidant activity against ONOO⁻ (5.2 ± 1.0 units), hydroxyl radicals (0.34 ± 0.09 units) and peroxy radicals (5.53 ± 1.27 units) (Franzoni et al., 2006). While the scavenging abilities of EGT have been extensively studied, the mechanistic reaction steps between EGT and strong oxidants are still unknown. Lespade studied the first steps of the reactions of EGT and hydroxyl radical and ONOO⁻ using ab initio molecular dynamics (Lespade, 2019). In the simulation, EGT reacts with the hydroxyl radical, giving it an electron. Depending on the proximity of the hydroxyl radical to EGT, the transfer is either rapid or a strong adduct is formed with EGT. No reaction or charge sharing was observed for the reaction of either peroxyxynitrous acid (the conjugate acid of ONOO⁻) or

ONOO⁻ and EGT, although they formed complexes with hydrogen bonds that remained stable for 6 ps. We have previously shown the ability of EGT to reduce the nitration of LF upon ONOO⁻ exposure, as well as its ability to protect the loss of antibacterial activity upon nitration (Alhalwani et al., 2023). However, questions remain regarding the relative concentration of EGT required, and what Tyr sites EGT can protect from nitration.

Due to the reactivity of ONOO⁻ under oxidative stress conditions, biological relevance of LF at sites of inflammation, and antioxidant properties of EGT, we have aimed to further characterize the nitration reaction of LF with ONOO⁻ and the ability of EGT to stop the reaction from occurring. In this study we employ site-selective nitration results. It is important to study site-selective nitration of ONOO⁻ with proteins because the results can indicate important biological relevance, as discussed by *Campolo et al.* (Campolo et al., 2020). It is not possible to reliably predict which Tyr residues will be nitrated in protein models. Therefore, site-selectivity results allow for further chemical properties to be analyzed, such as the solvent accessibility or the buried nature of individual Tyr residues. For instance, loop or turn structures more solvent exposed, and glycine and proline residues are often located at loops and turns. In addition, steric hinderance, the stabilization of tyrosyl radicals, and nearby residues play a role in determining the nitration of individual Tyr residues. It is important to note that cysteine or methionine residues can also react via one-electron oxidants, as discussed in Chapter 1, so other reactions can also occur. This is the first study to quantify LF nitration at different ONOO⁻ concentrations, as well as determine the site-selectivity of ONOO⁻ upon reaction with LF.

6.3 Materials and Methods

6.3.1 Materials

Lactoferrin from human milk (L0520, Lot #SLBW5976), L-Ergothioneine (EGT; E7521), trifluoroethanol (T63002), dithiothreitol (400 mM, D5545), iodoacetamide (400 mM, I6125), trypsin stock solution (1 $\mu\text{g } \mu\text{L}^{-1}$ sequencing grade trypsin, T6567, acetic acid (50 mM, 34254), and ammonium bicarbonate (NH_4HCO_3 , pH 7.8, A6141) were obtained from Sigma Aldrich. Sodium peroxyxynitrite (160-200 mM) was purchased from Merck Chemicals (now Millipore Sigma). Formic acid (28905) was purchased from Perbio Science. Formic acid in H_2O (0.1% v/v, 85170) was obtained from Thermo Fisher Scientific. Acetonitrile (ACN; Rotisolv AE70.1) and phosphate buffered saline (1X PBS-, pH 7.4 without Ca or Mg) were purchased from Carl Roth.

Reaction vials and thermomixer (Thermomixer Comfort) were purchased from Eppendorf. Amicon centrifugal units were purchased from Sigma Aldrich. C18 spin tubes (Pep Clean C18 Spin Columns) were obtained from Pierce Fisher Scientific.

6.3.2 Treatment of LF with ONOO^- and EGT

Native LF was buffered in 1X PBS(-) (pH 7.4, without Ca or Mg) to a final concentration of 1 mg mL^{-1} . NH_4HCO_3 (pH 7.8) was added to a final concentration of 50 mM to buffer the radical formation. ONOO^- was added after being thawed on ice to yield ONOO^-/Y molar ratios of 0.1, 0.5, 1, 2, 5, and 10 and the reactions were incubated on ice for 110 minutes in brown reaction vials. The reactions were stopped via centrifugation with Amicon centrifugal units with 10 kDa cutoff membranes. Samples reacted with

ONOO⁻ are referred to as nitrated LF (NLF). For the EGT-treated samples, 5 mg EGT was suspended in 250 μ L nanopure H₂O and added to the samples at a final concentration of 5.0 mM, 1.0 mM, and 0.5 mM prior to the addition of ONOO⁻.

6.3.3 Tryptic digestion

The ONOO⁻ and EGT-treated samples were tryptically digested using the protocol previously described (Reinmuth-Selzle et al., 2014). Briefly, 100 μ g protein was mixed with 5 μ L NH₄HCO₃ (100 mM), 5 μ L trifluoroethanol, and 0.4 μ L dithiothreitol (DTT) for 1 hr at 60 °C in a thermomixer. Iodoacetamide (2 μ L; 400 mM; IAM) was added and the protein mixture sat in the dark for 1 hr. DTT (0.4 μ L) was added to destroy the excess IAM and the mixture sat in the dark again for 1 hr. 60 μ L nanopure water and 20 μ L NH₄HCO₃ was added to raise the pH of the solution to around 7.5-8. Following, 2 μ L trypsin stock solution (1 μ g μ L⁻¹ in 50 mM acetic acid) was added. The protein mixture was incubated for 18 hr at 37 °C. The reaction was stopped by the addition of 0.4 μ L formic acid and the mixture was desalted using C18 spin tubes before HPLC-MS/MS analysis.

6.3.4 QTOF-MS/MS analysis and ND_y determination

An Agilent HPLC-QTOF-MS/MS system (Agilent 1200 series coupled to Agilent 6520 Accurate-Mass QTOF) was used to analyze the tryptically digested peptides as previously described by *Selzle et al* (Reinmuth-Selzle et al., 2014; Selzle et al., 2013). All modules were controlled via the Mass Hunter software (B.06.00, Agilent). A C₁₈

Advancebio peptide column (4.6 x 250 mm, 5 μ M particle size, Agilent) was used to separate the peptides at a temperature of 40 °C. Each HPLC-MS/MS run was repeated three times with injection volumes of 14, 12, and 10 μ L for better resolution of coeluting peptides. The eluents used were 3% (v/v) ACN in H₂O/formic acid (0.1% v/v; Eluent A), and 3% water/formic acid (0.1% v/v) in ACN (Eluent B). Gradient elution was used at a flow rate of 0.3 mL min⁻¹ starting from 97% A to 40% A over 30 minutes, then decreasing from 20% A over 0.1 min and continuing for 5 minutes before returning to initial conditions at 35.10 and equilibrating for 4.90 min before the next run. The eluting peptides were monitored using DAD signals of 210 nm (ref 360 nm), 280 nm (ref 450 nm), and 357 nm (ref 450 nm) for nitrated peptides. Chromatographic spectra were acquired using the Mass Hunter Qualitative Analysis software (B.06.00, Agilent).

The Dual AJS ESI ionization source was operated in positive ion mode with capillary voltage of 3,500 V, gas temperature of 325 °C, and 5 L min⁻¹ drying gas flow rate. Fragmentation of protonated ions was conducted using the auto MS/MS mode with preferred ions included, see Table G2 in Appendix G. MS spectra were recorded at an acquisition rate of 4 spectra/s for MS mode and 3 spectra/s for MS/MS mode. Protein and post-translational modification identification were performed via database searches using the Spectrum Mill software (Rev B.04.00.127, Agilent) against the database Swiss-Prot. Variable modifications searchers included nitrated tyrosine, oxidized methionine, and nitrated tryptophan. The search criteria were as follows: database: SwissProt.fasta; digest: trypsin; species: all; maximum # missed cleavages: 2; precursor-ion mass tolerance: \pm 20 ppm; fragment-ion mass tolerance: \pm 50 ppm; masses: monoisotopic; minimum detected

peaks: 4; minimum matched peak intensity: 50%, and minimum S/N: 25. Filtering criteria were: Protein score > 13; peptide score >10 and % SPI > 70. Search parameters were 50% min matched peak intensity, sequence tag length 3, min detected peaks 4, variable modifications of oxidized methionine, nitration Tyr, Nitration tryptophan. The SpectrumMill was also searched for detection of oxidized methionine, oxidized tyrosine, nitrated Tyr, nitrated tryptophan, nitrated histidine, hydroxylated Tyr, hydroxylated phenylalanine, hydroxylated tryptophan, and nitrosylated Tyr.

The individual nitration degree (ND_y) of a specific Tyr residue (Y) were determined as previously described (Reinmuth-Selzle et al., 2014). Briefly, ND_y is defined as the ratio of the spectral intensity of a modified peptide to the sum of spectral intensities for the modified and unmodified peptide (Reinmuth-Selzle et al., 2014).

6.3.5 HPLC-DAD analysis and ND determination

The treated protein solutions were analyzed using a HPLC-DAD system (Agilent 1200 series), as described previously (Selzle et al., 2013). Briefly, a C_{18} column (Vydac 238TP, 250 mmx2.1 mm inner diameter, 5 μ m particle size; Grace Vydac, Alltech) was used for separation. Eluents were 0.1 % trifluoroacetic acid in H_2O (Eluent A) and ACN (Eluent B). Gradient elution at a flow rate of 200 μ L/min was performed starting at 3% B followed by a linear gradient to 90% B within 15 min, flushing back to 3% B within 0.2 min, and 3% B for 2.8 min. A column re-equilibration time of 5 min was used before the next run and absorbance was monitored at 280 nm and 357 nm. Sample injection volume was 20 μ L and each run was repeated three times.

The total nitration degree (ND) of each sample was determined as previously described (Selzle et al., 2013). Briefly, the peak areas of the 280 nm and 357 nm peaks were used, in addition to f and k scaling factors, to determine the total ND of each sample.

6.4 Results and Discussion

6.4.1 Total ND of LF reaction with ONOO⁻

LF was successfully nitrated under varying ONOO⁻ concentrations. The nitration reaction of ONOO⁻ and LF was analyzed via HPLC-DAD and QTOF-MS/MS. The HPLC-DAD determines total nitration of the entire protein sample, whereas the QTOF-MS/MS is able to determine nitration at individual Tyr residue sites.

Figure 6.1 shows the total ND of NLF upon reaction with ONOO⁻ at increasing molar ratios (ONOO⁻/Tyr). The ND increases with increasing ONOO⁻ concentration, peaks around 1:1 molar ratio, and then begins to decrease. As shown in Chapter 5, the decrease is most likely pH-related, where the addition of ONOO⁻ in NaOH increases the pH of the reaction above 10, causing a switch from nitration to oligomerization. ONOO⁻ is stable under alkaline conditions, but decomposes at lower pH, so laboratory ONOO⁻ reagents are stored in NaOH. The concentration of ONOO⁻ in NaOH delivered to *in vitro* samples mimicking oxidative stress *in vivo* is important for biologically relevant results, because if the pH is increasing the results are no longer relevant biologically.

The nitration of tyrosine via ONOO⁻ is pH-dependent, as shown in Chapter 5. Due to chemical properties of the reactive species (OH and NO₂ radicals), the nitration

reaction occurs alongside other reactions, like oligomerization and hydroxylation.

Discussed in Chapter 5, physiological pH has higher nitration yields than dimerization and hydroxylation., and NTyr yields maximize around pH 7.4 (Ischiropoulos et al., 1992). DiTyr formation also occurs upon reaction with ONOO⁻ (Bartesaghi et al., 2007).

DiTyr yields minimal at low pH and increase towards alkaline pH (Santos et al., 2000;

van der Vliet et al., 1995). Tyr deprotonation facilitates the oxidation to Tyr radical

(Heineckes et al., 1993; Marquez & Dunford, 1995; Pfeiffer et al., 2000). The increase in

DiTyr yields with a higher Tyr/oxidant ratio is due to the decrease in the overall rate of

radical recombination (Campolo et al., 2020).

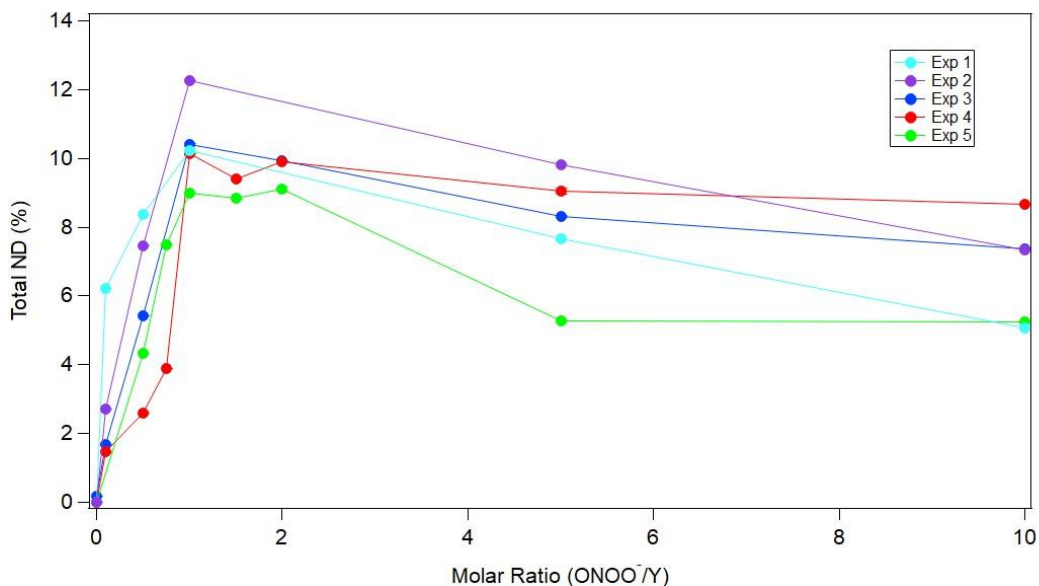


Figure 6.1. Total nitration results of LF nitrated with ONOO⁻ at increasing molar ratios. Different colors represent different experiments. Lines are to guide eye.

The reaction of ONOO⁻ and LF can vary depending on the ONOO⁻ used. Changes in reactivity can be caused from the age of the ONOO⁻ and if the ONOO⁻ reaction vial had been previously thawed before use. For this study, each line in Figure 6.1 represents a separate nitration reaction using a new ONOO⁻ vial. The absolute ND value varies, most likely due to small changes in the amount of thaw time of each reaction vial. However, each experiment shows the same trend. This coupled with the pH results shown in Chapter 5 show us the nitration of LF with ONOO⁻ is also pH-dependent and the relative ND will be determined by the final pH of the reaction mixture. Therefore, the decrease in ND as molar ratio increases (Figure 6.1) can be attributed to DiTyr formation or oligomerization occurring in competition with nitration.

6.4.2 Site-selectivity of ONOO⁻ nitration

The nitration of specific amino acids can be determined using MS/MS. In this study the focus is on nitration, but other PTM's can also be studied using this method, with the exception of cysteine oxidation due to the cysteine residues being alkylated during the trypsin digestion. The LF samples reacted with ONOO⁻ at increasing molar ratios were analyzed via MS/MS and Spectrum Mill searches were conducted for all PTM's (nitration, hydroxylation, oxidation, etc.). The detection of one nitrated Trp and multiple nitrated Tyr residues was seen. Figure 6.2 shows the ND_y results, representing the ND of each individual nitrated Tyr residue. ND_y was shown to increase with increasing ONOO⁻ concentration, similar to the total ND. The ND_y of all detected nitration sites also peak around a 1:1 molar ratio, then drops. This is also consistent with

the pH-dependency and formation of DiTyr. As noted, ND_y was calculated based on the assumption that the ionization efficiencies of unmodified and nitrated peptides are similar, as shown previously (Reinmuth-Selzle et al., 2014).

The site-selective results can give information about the accessibility of the sites to $ONOO^-$, as well as the reactivity, polarity, and steric hinderances involved in the reaction. LF has 21 Tyr residues, 20 of which were detected using this method. Of the 21, 8 Tyr residues were nitrated across all samples, to varying ND values. These residues include Tyr 84, 91, 111, 338, 343, 434, 545, and 686 (Figure 6.2). Some Tyr residues are more easily nitrated than others. For example, upon reaction of LF with $ONOO^-$, Tyr residue 686 (light blue) is nitrated to the highest degree compared to the other nitrated Tyr residues. Comparatively, Tyr residue 545 (red) is nitrated the least. It is interesting that the ND_y values of some Tyr residues, i.e. Y84 and Y91, drop more quickly than others. This could be an indication that these residues are more likely to form DiTyr than NTyr.

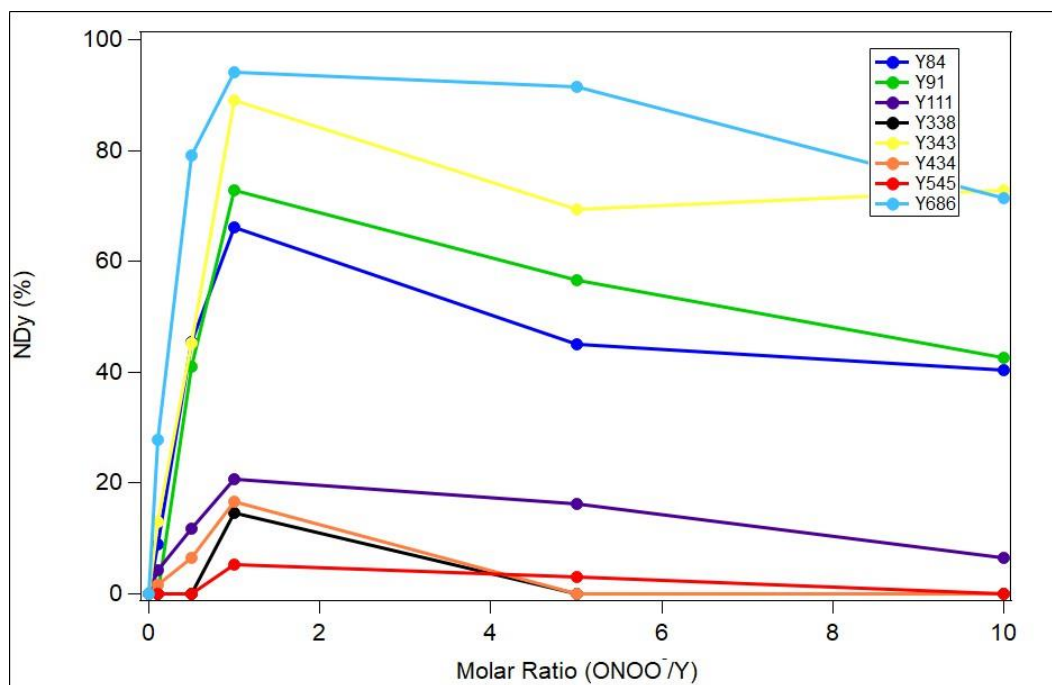


Figure 6.2. Site-selectivity of LF nitration with ONOO⁻ at increasing molar ratios. Different colors represent different Tyr sites. Y represents a Tyr residue site. Lines are to guide eye.

6.4.3 EGT reduces nitration of LF

As discussed above, EGT has been shown to inhibit NTyr formation (Alhalwani et al., 2023; Bruno et al., 2020). The ability of EGT to protect LF from nitration of ONOO⁻ was experimentally analyzed at 5 mM, 1 mM, and 0.5 mM EGT concentrations. Figure 6.3 shows the total ND of LF upon reaction with ONOO⁻ and with pre-treatment with each EGT concentration. The total ND of LF decreases completely with 5.0 mM EGT treatment and significantly with 0.5 mM and 1.0 mM, which are biologically relevant concentrations. An EGT concentration of 1.0 mM (squares) stopped nitration from occurring up to a molar ratio of 1/1, which may be too high to be physiologically

relevant. Similarly, an EGT concentration of 0.5 mM (triangles) stopped the nitration reaction up to a molar ratio of 0.5/1. EGT must be added prior to ONOO^- to be effective, shown in Appendix G. This suggests EGT scavenges ONOO^- and radicals, preventing them from interacting with amino acid residues.

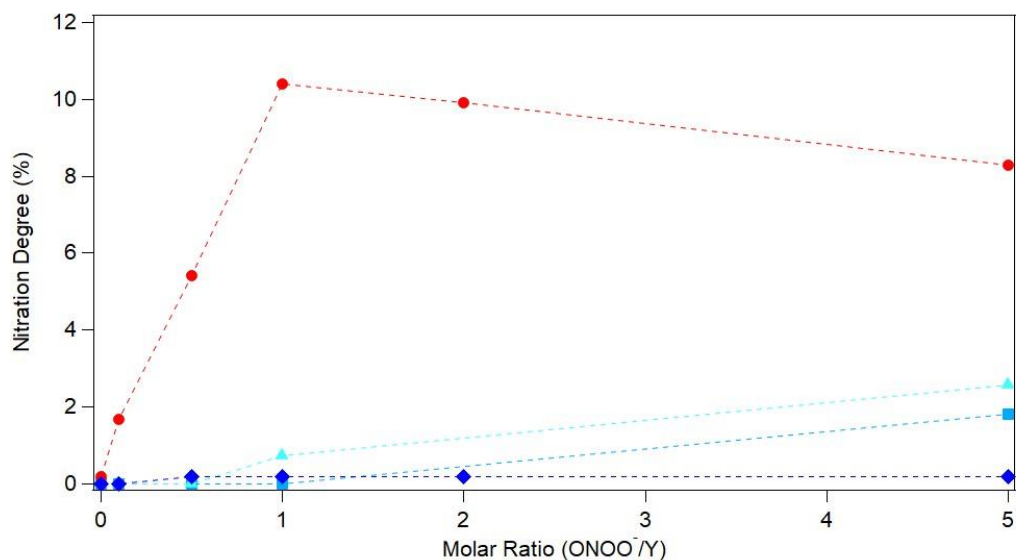


Figure 6.3. Total ND of LF upon treatment with EGT and nitration by ONOO^- . Circles represent total nitration degree of NLF with no EGT, triangles are 0.5 mM EGT, squares are 1.0 mM EGT, and diamonds are 5 mM EGT. Lines are to guide eye.

The site-selectivity of the reaction of LF with ONOO^- with and without pre-treatment of EGT at 5.0 mM was also determined. Results are shown in Table 6.1. No nitrated or hydroxylated residues were found in any of the EGT samples (samples 1 through 6), compared to multiple NTyr and one nitrated Trp residue being detected in NLF samples (samples 7 through 12). It should be noted that each sample was detected

with relatively high peptide coverage (total AA coverage) and intensities. In addition, nearly all Tyr residues were detected in all samples (19-20/21).

Table 6.1. LC-MS/MS results for NLF and NLF + 5 mM EGT samples.

Sample	Description	Total LF Spectral Intensity	Total AA Coverage	Total Tyr Coverage	N-Tyr?	N-Tyr Residues	N-W287?
1	NLF 0.1/1 + EGT	1.35E+08	67.4	20/21	no	none	no
2	NLF 0.5/1 + EGT	1.43E+08	70.9	20/21	no	none	no
3	NLF 1/1 + EGT	1.67E+08	70.9	20/21	no	none	no
4	NLF 2/1 + EGT	1.49E+08	65	19/21	no	none	no
5	NLF 5/1 + EGT	1.67E+08	70.1	20/21	no	none	no
6	NLF 10/1 + EGT	1.21E+08	69.2	20/21	no	none	no
7	NLF 0.1/1	1.49E+08	62.2	19/21	yes	Y84, Y343, Y686	yes
8	NLF 0.5/1	1.79E+08	66.4	20/21	yes	Y84, Y91, Y111, Y343, Y507, Y686	yes
9	NLF 1/1	1.57E+08	70.4	20/21	yes	Y84, Y84+91, Y111, Y343, Y434, Y454, Y507, Y686	yes
10	NLF 2/1	1.50E+08	71.9	20/21	yes	Y84, Y91, Y84+91, Y111, Y343, Y507, Y686	yes
11	NLF 5/1	1.45E+08	70.2	20/21	yes	Y84, Y91, Y84+91, Y111, Y507, Y686	yes
12	NLF 10/1	1.47E+08	69.7	20/21	yes	Y84, Y91, Y84+91, Y111, Y343, Y507, Y686	yes

The relative ratios of the ND values of the NLF samples with and without EGT samples for the 1.0 mM and 0.5 mM EGT samples were determined and analyzed, as shown in Figure 6.4. The left y axes represents the total ND of the NLF samples, and the right y axes represents the relative ND determined by the ratio of the ND values of NLF-EGT samples to the NLF samples. The line crosses the x-axis at a EGT/ONOO⁻ ratio of 2.27 mM. This shows preliminary results for the amount of EGT needed to entirely stop the reactivity of ONOO⁻.

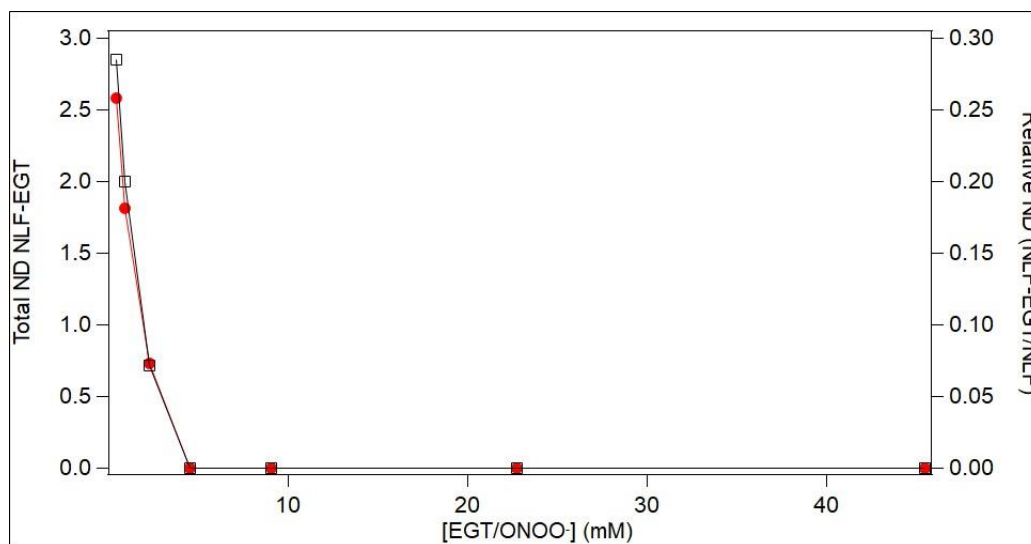


Figure 6.4. Relative ND vs EGT to ONOO⁻ Ratio. Black squares represent NLF-EGT to NLF ND ratio. Red circles represent the total ND of NLF-EGT samples.

6.5 Conclusion

The nitration reaction of ONOO⁻ and human LF was quantified, and the site-selectivity of the reaction was determined. This is the first study, to our knowledge, to quantify LF nitration with ONOO⁻.

The NLF ND increases as a function of molar ratio around 1/1, then decreases when the molar ratio is greater, consistent with Chapter 5. Furthermore, this is one of two studies (along with Selzle *et al.* 2014) that looks at site-selective nitration degree on any protein with any nitrating agent, which helps lead toward functional implications (Reinmuth-Selzle *et al.*, 2014).

EGT stops the nitration of LF, and this study is the first to quantify this using HPLC, which has benefits beyond the use of ELISA, discussed in Chapter 2. This study

is also the first to show ND ratios upon biologically relevant EGT concentrations (0.5 mM and 1.0 mM), and preliminary evidence for the relevant ONOO⁻ to EGT concentration ratio needed to stop all nitration from occurring.

References

- Alhalwani, A. Y., Davey, R. L., Kaul, N., Barbee, S. A., & Huffman, J. A. (2019). Modification of lactoferrin by peroxynitrite reduces its antibacterial activity and changes protein structure. *Proteins: Structure, Function, and Bioinformatics*, 1–9. <https://doi.org/10.1002/prot.25782>
- Alhalwani, A. Y., Davey, R. L., Repine, J. E., & Huffman, J. A. (2023). L-ergothioneine reduces nitration of lactoferrin and loss of antibacterial activity associated with nitrosative stress. *Biochemistry and Biophysics Reports*, 34, 101447. <https://doi.org/10.1016/J.BBREP.2023.101447>
- Alvarez, B., & Radi, R. (2003). Peroxynitrite reactivity with amino acids and proteins. *Amino Acids*, 25, 295–311. <https://doi.org/10.1007/s00726-003-0018-8>
- Asahi, T., Wu, X., Shimoda, H., Hisaka, S., Harada, E., Kanno, T., Nakamura, Y., Kato, Y., & Osawa, T. (2016). A mushroom-derived amino acid, ergothioneine, is a potential inhibitor of inflammation-related DNA halogenation. *Bioscience, Biotechnology, and Biochemistry*, 80(2), 313–317. <https://doi.org/10.1080/09168451.2015.1083396>
- Bartesaghi, S., Ferrer-Sueta, G., Peluffo, G., Valez, V., Zhang, H., Kalyanaraman, B., & Radi, R. (2007). Protein tyrosine nitration in hydrophilic and hydrophobic environments Review Article. *Amino Acids*, 32, 501–515. <https://doi.org/10.1007/s00726-006-0425-8>
- Bruno, G., Wenske, S., Lackmann, J. W., Lalk, M., Woedtke, T. von, & Wende, K. (2020). On the liquid chemistry of the reactive nitrogen species peroxynitrite and

nitrogen dioxide generated by physical plasmas. *Biomolecules*, *10*(12), 1–25.

<https://doi.org/10.3390/biom10121687>

Campolo, N., Issoglio, F. M., Estrin, D. A., Bartesaghi, S., & Radi, R. (2020). 3-Nitrotyrosine and related derivatives in proteins: precursors, radical intermediates and impact in function. *Essays in Biochemistry*, *64*(1), 111–133.

<https://doi.org/10.1042/ebc20190052>

Cheah, I. K., & Halliwell, B. (2012). Ergothioneine ; antioxidant potential , physiological function and role in disease ☆. *Biochimica et Biophysica Acta*, *1822*(5), 784–793.

<https://doi.org/10.1016/j.bbadis.2011.09.017>

Cumming, B., Chinta, K., Reddy, V., & Steyn, A. (2018). Role of Ergothioneine in Microbial Physiology and Pathogenesis. *Antioxidants & Redox Signaling*, *28*(6), 431–444. <https://doi.org/10.1089/ARS.2017.7300>

Drago-Serrano, M. E., De La Garza-Amaya, M., Luna, J. S., & Campos-Rodríguez, R. (2012). Lactoferrin-lipopolysaccharide (LPS) binding as key to antibacterial and antiendotoxic effects. *International Immunopharmacology*, *12*(1), 1–9.

<https://doi.org/10.1016/j.intimp.2011.11.002>

Franzoni, F., Colognato, R., Galetta, F., Laurenza, I., Barsotti, M., Stefano, R. Di, & Bocchetti, R. (2006). An in vitro study on the free radical scavenging capacity of ergothioneine : comparison with reduced glutathione , uric acid and trolox.

Biomedicine and Pharmacotherapy, *60*, 453–457.

<https://doi.org/10.1016/j.biopha.2006.07.015>

Griendling, K. K., & FitzGerald, G. A. (2003). Oxidative Stress and Cardiovascular

Injury Part I: Basic Mechanisms and In Vivo Monitoring of ROS. In *Circulation* (Vol. 108, Issue 16, pp. 1912–1916). Lippincott Williams & Wilkins.

<https://doi.org/10.1161/01.CIR.0000093660.86242.BB>

Heineckes, J. W., Li, W., Daehnke, H. L., & Goldstein, J. A. (1993). Dityrosine, a Specific Marker of Oxidation, Is Synthesized by the Myeloperoxidase-Hydrogen Peroxide System of Human Neutrophils and Macrophages*. *Journal of Biological Chemistry*, 268(6), 4069–4077.

Ischiropoulos, H., & Beckman, J. S. (2003). Oxidative stress and nitration in neurodegeneration: Cause, effect, or association? *Journal of Clinical Investigation*, 111(2), 163–169. <https://doi.org/10.1172/jci17638>

Ischiropoulos, H., Zhu, L., Chen, J., Tsai, M., Martin, J. C., Smith, C. D., & Beckman, J. S. (1992). Peroxynitrite-mediated tyrosine nitration catalyzed by superoxide dismutase. *Archives of Biochemistry and Biophysics*, 298(2), 431–437. [https://doi.org/10.1016/0003-9861\(92\)90431-U](https://doi.org/10.1016/0003-9861(92)90431-U)

Kerley, R. N., McCarthy, C., Kell, D. B., & Kenny, L. C. (2018). The potential therapeutic effects of ergothioneine in pre-eclampsia. *Free Radical Biology and Medicine*, 117, 145–157. <https://doi.org/10.1016/j.freeradbiomed.2017.12.030>

Lai, C. K., Tang, W. K., Siu, C., & Chu, I. K. (2020). Evidence for the Prerequisite Formation of Phenoxy Radicals in Radical-Mediated Peptide Tyrosine Nitration In Vacuo. *Chemistry – A European Journal*, 26(1), 331–335. <https://doi.org/10.1002/chem.201904484>

Lespade, L. (2019). Ab initio molecular dynamics of free radical-induced oxidation of

ergothioneine. *Journal of Molecular Modeling*, 25(11).

<https://doi.org/10.1007/s00894-019-4220-3>

Marquez, L. A., & Dunford, H. B. (1995). *Kinetics of Oxidation of Tyrosine and Dityrosine by Myeloperoxidase Compounds I and II IMPLICATIONS FOR LIPOPROTEIN PEROXIDATION STUDIES**. <http://www.jbc.org/>

Masubuchi, Y., Suda, C., & Horie, T. (2005). Involvement of mitochondrial permeability transition in acetaminophen-induced liver injury in mice. *Journal of Hepatology*, 42(1), 110–116. <https://doi.org/10.1016/J.JHEP.2004.09.015>

Nakamichi, N., Nakayama, K., Ishimoto, T., Masuo, Y., Wakayama, T., Sekiguchi, H., Sutoh, K., Usumi, K., Iseki, S., & Kato, Y. (2016). Food-derived hydrophilic antioxidant ergothioneine is distributed to the brain and exerts antidepressant effect in mice. *Brain and Behavior*, 6(6). <https://doi.org/10.1002/brb3.477>

Niaz, B., Saeed, F., Ahmed, A., Imran, M., Maan, A. A., Khan, M. K. I., Tufail, T., Anjum, F. M., Hussain, S., & Suleria, H. A. R. (2019). Lactoferrin (LF): a natural antimicrobial protein. <https://doi.org/10.1080/10942912.2019.1666137>, 22(1), 1626–1641. <https://doi.org/10.1080/10942912.2019.1666137>

Pfeiffer, S., Schmidt, K., & Mayer, B. (2000). Dityrosine formation outcompetes tyrosine nitration at low steady-state concentrations of peroxynitrite: Implications for tyrosine modification by nitric oxide/superoxide in vivo. *Journal of Biological Chemistry*, 275(9), 6346–6352. <https://doi.org/10.1074/JBC.275.9.6346>

Radi, R., Peluffo, G., Alvarez, M. N., Naviliat, M., & Cayota, A. (2001). Unraveling peroxynitrite formation in biological systems. *Free Radical Biology and Medicine*,

30(5), 463–488. [https://doi.org/10.1016/S0891-5849\(00\)00373-7](https://doi.org/10.1016/S0891-5849(00)00373-7)

Reinmuth-Selzle, K., Kampf, C. J., Samonig, M., Shiraiwa, M., Yang, H., Gadermaier, G., Brandstetter, H., Huber, C. G., Duschl, A., & Oostingh, G. J. (2014). Nitration of the Birch Pollen Allergen Bet v 1.0101: Efficiency and Site-Selectivity of Liquid and Gaseous Nitrating Agents. *Journal of Proteome Research*, *13*, 1570–1577.

<https://doi.org/10.1021/pr401078h>

Roy, P., Panda, A., Hati, S., & Dasgupta, S. (2019). pH-Dependent Nitrotyrosine Formation in Ribonuclease A is Enhanced in the Presence of Polyethylene Glycol (PEG). *Chemistry - An Asian Journal*, *14*(24), 4780–4792.

<https://doi.org/10.1002/asia.201901225>

Santos, C. X. C., Bonini, M. G., & Augusto, O. (2000). Role of the carbonate radical anion in tyrosine nitration and hydroxylation by peroxynitrite. *Archives of Biochemistry and Biophysics*, *377*(1), 146–152.

<https://doi.org/10.1006/abbi.2000.1751>

Selzle, K., Ackaert, C., Kampf, C. J., Kunert, A. T., Duschl, A., Oostingh, G. J., & Pöschl, U. (2013). Determination of nitration degrees for the birch pollen allergen Bet v 1. *Analytical and Bioanalytical Chemistry*, *405*(27), 8945–8949.

<https://doi.org/10.1007/s00216-013-7324-0>

Tanaka, N., Kawano, Y., Satoh, Y., Dairi, T., & Ohtsu, I. (2019). Gram-scale fermentative production of ergothioneine driven by overproduction of cysteine in *Escherichia coli*. *Scientific Reports*, *9*(1), 1895. <https://doi.org/10.1038/s41598-018-38382-w>

van der Vliet, A., Eiserich, J. P., O'Neill, C. A., Halliwell, B., & Cross, C. E. (1995).

Tyrosine modification by reactive nitrogen species: A closer look. *Archives of Biochemistry and Biophysics*, 319(2), 341–349.

<https://doi.org/10.1006/abbi.1995.1303>

Zhang, H., Joseph, J., Feix, J., Hogg, N., & Kalyanaraman, B. (2001). Nitration and

Oxidation of a Hydrophobic Tyrosine Probe by Peroxynitrite in Membranes:

Comparison with Nitration and Oxidation of Tyrosine by Peroxynitrite in Aqueous

Solution†. *Biochemistry*, 40(25), 7675–7686. <https://doi.org/10.1021/BI002958C>

Chapter Seven: Conclusions

7.1 Summary of conclusions

There has been an increase in allergic disease worldwide and many hypotheses as to what is causing the increase. One mechanism is the reaction of allergenic proteins with ROS and RNS in the atmosphere, resulting in chemical modification that enhances the allergenic potential, or IgE response, of the protein. Allergenic proteins embedded in atmospheric PM are small, $< 2 \mu\text{m}$ in size, allowing them to be suspended in the atmosphere for an extended period, as well as being transported long distances. In addition, due to their size they can deposit into the lungs upon inhalation, further reacting with endogenous ROS and RNS species. The overall goal of this dissertation was to explore the ROS and RNS chemistry associated with the increase in allergic disease further, as well as to develop and characterize analytical methodology required to quantify the reactions.

The reactions of proteins with ROS and RNS are complex and often require quantification beyond the capacity of commonly used biochemical methods. Discussed in Chapter 2, many biochemical techniques, like ELISA or BCA, can only offer semi-quantitative results due to the assumptions and pitfalls associated with the methodology. Throughout this dissertation the detection and quantification of Ntyr and DiTyr are analyzed, and the methods used to study the reactions producing these products are improved upon.

7.2 Ambient air reactions

Due to the complexities of atmospheric chemistry, there is a wide range of reactions always occurring. Proteins derived from biological sources can react with ROS and RNS species, like O₃ and NO₂ in the atmosphere and be chemically modified, resulting in PTMs. The formation of Ntyr and DiTyr via these reactions has been explored in controlled gaseous reaction chambers experiments by Liu *et al.*, which was able to provide information regarding reaction mechanisms and relevant atmospheric conditions, like temperature and RH (Liu et al., 2017). However, the extent to which these reactions occur in ambient air has yet to be explored. In Chapters 3 and 4 the methodology for studying these ambient reactions was developed and characterized, and a 2.5-year ambient study was conducted.

It is important to accurately characterize each aspect of ambient sampling methodology, especially due to the low concentration often detected. In Chapter 3 we quantified interferences, e.g. protein filter media, and chances for loss, e.g. O₃ reactivity from PM filters and lack of protein extraction, to aid in decreasing uncertainties in future studies of this kind. In Chapter 4, ND values up to 5.6% were detected, the first results showing the extent of nitration occurring in ambient air. The nitration reaction was further correlated to relevant air pollutant and atmospheric conditions, and the detection of DiTyr was shown in ambient air for the first time.

Throughout these studies it was determined that the nitration reaction of proteins with urban air pollutants can occur and be detected in ambient air, and that it is possible to occur at relatively high degrees of nitration. Our results indicate that the further study

of the nitration reaction occurring in ambient air is important in determining the role Ntyr formation plays in the increase in allergic disease. Our results tie together previously conducted laboratory studies, as well as provide a mechanism for studying this reaction in other urban centers. As mentioned, oligomerization and other PTMs also can form in ambient air and need to be explored, as well as the role of these other PTMs in the increase of IgE response.

7.3 Oxidative stress reactions

The reactions of endogenous proteins with oxidative stress reactants are complex. Furthermore, the use of *in vitro* experimental set-ups to study *in vivo* reactions and mechanisms is important but comes with pitfalls and the necessary considerations need to be explored. The reaction of proteins with ONOO⁻ in aqueous solutions has been used for decades to mimic oxidative and nitrosative stress in the human body and the only laboratory reactant widely available for purchase is ONOO⁻ supplied in NaOH. The experimental artifacts of this reaction, however, had not been taken into consideration. In Chapter 5 we show that the reaction of ONOO⁻ at increased concentrations also significantly increases the pH of the reaction, well beyond the buffer capacity of commonly used buffer systems (1xPBS), and the increase in pH alters the reaction mechanism from Ntyr formation to DiTyr formation and oligomerization. These results have implications in future studies of these reactions and represent the importance of secondary pH measurements and choosing the correct buffer system for experimental set ups. If these considerations are not taken into account reaction results may not be

indicative of actual *in vivo* conditions and therefore no longer accurately mimic endogenous oxidative stress conditions.

Determining the site-selectivity of the reaction of ONOO^- with proteins gives important information regarding the structural and functional information of the protein. For instance, we have previously shown that the nitration reaction of LF with ONOO^- affects the iron-binding capacity of LF as well as alters its structure. However, site-selective results shown in Chapter 6 give information regarding which individual Tyr residues are more easily nitrated than others and at what ONOO^- concentration each residue is nitrated at. One residue is shown to be nitrated very easily at low ONOO^- concentrations and is in the iron-binding site of LF, indicative of why nitration lowers the functionality of LF. This is only the second study to determine the site-selectivity of the nitration reaction of ONOO^- and a protein at varying ONOO^- concentrations, and various analytical considerations were required to quantify the results beyond detection, discussed below. The methodology and results shown will improve future studies in determining site-specific reaction products in individual protein reactions.

7.4 Analytical considerations

Many times throughout this dissertation the line between biochemistry and analytical chemistry was crossed in order to accurately quantify the nitration reactions occurring. Many bioanalytical techniques used for detection do not accurately or reliably quantify, which complicates analysis. In this dissertation we were able to push against methodology limitations, like the accuracy and precision of pipettes, sample loss across

filters, and low concentration samples, to improve quantification. In the site-selectivity experiments discussed in Chapter 6, various methodological considerations were required to be able to quantify the nitration reaction beyond just detection. The cleavage rates of trypsin at modified versus unmodified sites, as well as the ionization efficiencies of native versus unmodified peptides are two examples of metrics that do not matter when simply detecting Ntyr, however are very important when wanting to quantify Ntyr and compare across samples. Selzle *et al.* provided the equation and protocol for determining the ND of a protein, both the total ND of a sample and the individual ND values of each nitrated Tyr residue (Selzle et al., 2013). This metric is concentration independent, allowing for the comparison between many samples. By using this quantification tool and improving upon the methodology used in each study, this dissertation represents innovative and creative tools for the future study of the nitration reaction of proteins with both air pollutants and endogenous reactants.

7.5 Limitations

While the work presented in this dissertation benefits the specific scientific areas discussed, there are various limitations and future work required. As discussed in Chapter 2 and throughout this dissertation, the line between quantitative and qualitative results requires analysis of the methodology and assumptions being made. In many cases semi-quantitative results are the only results possible, especially when instrumentation and methodology are limited. In regards to the results presented here, there are limitations in the analysis of nitration products, as well as sources of error, both in the reactions and in

the analysis. For example, the error associated with the micropipettes used in many cases may be negligible, but in some experiments, like the pH experiments in Chapter 4, is noticeable. Furthermore, a QTOF-MS was not available for many of the experiments presented, which limited the analysis capabilities.

Sources of error and unavailable instrumentation were not the only limitations of the studies throughout this dissertation, as each chapter also had boundaries. For instance, the long-term ambient study presented in Chapter 4 was conducted using only BSA. Further studies need to be done with more atmospherically-relevant proteins, like pollen allergens. In addition, mechanistic studies regarding the interactions of proteins with O_3/NO_2 are needed to determine the effect that nitration and oligomerization have on future interactions. For example, as proteins oligomerize the surface area for the reactions may decrease, altering future chemical reactions. Future work is also needed to separate high ROS and time regarding the oligomerization reaction, as the only mechanism for increasing ROS in our sample set-up was increasing the amount of time the proteins were exposed.

The pH experiments presented in Chapter 5 serve as an important component of *in vitro* ONOO⁻ experiments used to mimic oxidative stress *in vivo*, however they were also conducted using BSA and not biologically-relevant proteins. While the pH change of the reactions is still applicable to other protein reactions, the degree of dimerization and oligomerization is dependent on the individual protein. Similarly, the site-selective nitration of LF results in Chapter 6 indicate how nitration impacts the iron-binding capabilities of LF, but oligomerization and other reaction products were not explored and

using tryptic digestion impairs the ability to study other reaction products, like oligomerization. In addition, the study of high ONOO⁻ concentration are not applicable to what would naturally occur endogenously.

7.6 Perspectives and future directions

The goal of this dissertation is to address some of the many questions that remain regarding how proteins are chemically reacted with ROS/RNS both atmospherically and endogenously. While there have been many studies conducted, as discussed throughout this dissertation, the linkages between nitration of proteins in the atmosphere and via oxidative stress in the human body are still unclear. Atmospherically, this dissertation concludes three major findings. First, O₃ and NO₂ are able to nitrate proteins in the atmosphere to a high extent relative to endogenous reactions. Second, the nitration reaction occurs in areas with high O₃ concentration, like Denver, representing a need to reduce ground-level O₃ pollution. Lastly, other reaction products, like oligomerization, are able to form and be detected in the atmosphere. Further work is thus needed to separate the role each individual reaction product plays in the increase in IgE response. This work has further implications beyond IgE, however, including the mechanisms of study for other oxidative products that form in the atmosphere, like oxidized polycyclic aromatic hydrocarbons.

Endogenously, this dissertation concludes that ONOO⁻ is able to nitrate biologically-relevant proteins site-selectively, inducing changes in protein structure and function. Even though the study of ONOO⁻ reactions with proteins is relatively well-

understood, this dissertation demonstrates that experimental artifacts, like alterations in reaction pH, are important to consider. This work has future implications beyond oxidative stress reactions, including how we mimic *in vivo* reactions to study them *in vitro*. This dissertation closes the gap between the atmospheric and endogenous reactions, however more work is still needed to fully understand the linkage. For instance, questions remain regarding how proteins already nitrated atmospherically then are nitrated further in the body.

With climate change and air pollution levels worsening the reactions of proteins in the atmosphere are likely to be enhanced. Climate change is causing an increase in the concentration of allergenic proteins released, as well as increasing the length of the pollen season. Air pollution levels, specifically O₃, are also increasing, enhancing the number of reactions with the allergenic proteins in the atmosphere, especially in urban centers. These reactions are complex and only a small subset of them have been studied. The formation of NTyr and DiTyr in the atmosphere is discussed here, but future studies of PTMs forming in urban air will be important to characterize the extent of reactions occurring and the role they play in the increase in respiratory disease, as well as how the endogenous oxidative stress reactions enhance the reactions. The increase of the relevant reactions occurring only enhances the need for analytical quantification techniques to study biochemical questions. In many cases detection is not enough, especially when comparing results across samples, reaction mechanisms, and experimental set ups. Future work to quantify reaction products more reliably will be important, as well as the

constant analytical analysis of methodology to ensure all assumptions and limitations are considered.

References

- Ackaert, C., Kofler, S., Horejs-Hoeck, J., Zulehner, N., Asam, C., von Grafenstein, S., Fuchs, J. E., Briza, P., Liedl, K. R., Bohle, B., Ferreira, F., Brandstetter, H., Oostingh, G. J., & Duschl, A. (2014). The Impact of Nitration on the Structure and Immunogenicity of the Major Birch Pollen Allergen Bet v 1.0101. *PLoS ONE*, 9(8), e104520. <https://doi.org/10.1371/journal.pone.0104520>
- Al-Hilaly, Y. K., Williams, T. L., Stewart-Parker, M., Ford, L., Skaria, E., Cole, M., Bucher, W. G., Morris, K. L., Sada, A. A., Thorpe, J. R., & Serpell, L. C. (2014). A central role for dityrosine crosslinking of Amyloid- β in Alzheimer's disease. *Acta Neuropathologica Communications*, 2(1). <https://doi.org/10.1186/2051-5960-1-83>
- Alhalwani, A. Y., Davey, R. L., Kaul, N., Barbee, S. A., & Huffman, J. A. (2019). Modification of lactoferrin by peroxynitrite reduces its antibacterial activity and changes protein structure. *Proteins: Structure, Function, and Bioinformatics*, 1–9. <https://doi.org/10.1002/prot.25782>
- Alhalwani, A. Y., Davey, R. L., Repine, J. E., & Huffman, J. A. (2023). L-ergothioneine reduces nitration of lactoferrin and loss of antibacterial activity associated with nitrosative stress. *Biochemistry and Biophysics Reports*, 34, 101447. <https://doi.org/10.1016/J.BBREP.2023.101447>
- Alhalwani, A. Y., Repine, J. E., Knowles, M. K., & Huffman, J. A. (2018). Development of a sandwich ELISA with potential for selective quantification of human lactoferrin protein nitrated through disease or environmental exposure. *Analytical and Bioanalytical Chemistry*, 410(4), 1389–1396. <https://doi.org/10.1007/s00216-017->

0779-7

Alvarez, B., & Radi, R. (2003). Peroxynitrite reactivity with amino acids and proteins.

Amino Acids, 25, 295–311. <https://doi.org/10.1007/s00726-003-0018-8>

Alvarez, Beatriz, Rubbo, H., Kirk, M., Barnes, S., Freeman, B. A., & Radi, R. (1996).

Peroxynitrite-Dependent Tryptophan Nitration. *Chemical Research in Toxicology*,

9(2), 390–396. <https://doi.org/10.1021/TX950133B>

Atwood, C. S., Perry, G., Zeng, H., Kato, Y., Jones, W. D., Ling, K. Q., Huang, X., Moir,

R. D., Wang, D., Sayre, L. M., Smith, M. A., Chen, S. G., & Bush, A. I. (2003).

Copper Mediates Dityrosine Cross-Linking of Alzheimer's Amyloid- β .

Biochemistry, 43(2), 560–568. <https://doi.org/10.1021/BI0358824>

Augusto, O., Bonini, M. G., Amanso, A. M., Linares, E., Santos, C. C. X., & De

Menezes, S. L. (2002). Nitrogen dioxide and carbonate radical anion: two emerging

radicals in biology. *Free Radical Biology and Medicine*, 32(9), 841–859.

[https://doi.org/10.1016/S0891-5849\(02\)00786-4](https://doi.org/10.1016/S0891-5849(02)00786-4)

Bachi, A., Dalle-Donne, I., & Scaloni, A. (2013). Redox proteomics: Chemical

principles, methodological approaches and biological/biomedical promises.

Chemical Reviews, 113(1), 596–698.

[https://doi.org/10.1021/CR300073P/ASSET/IMAGES/CR300073P.SOCIAL.JPEG_](https://doi.org/10.1021/CR300073P/ASSET/IMAGES/CR300073P.SOCIAL.JPEG_V03)

V03

Backes, A. T., Reinmuth-Selzle, K., Leifke, A. L., Ziegler, K., Krevert, C. S.,

Tscheuschner, G., Lucas, K., Weller, M. G., Berkemeier, T., Pöschl, U., & Fröhlich-

Nowoisky, J. (2021). Oligomerization and Nitration of the Grass Pollen Allergen Phl

p 5 by Ozone, Nitrogen Dioxide, and Peroxynitrite: Reaction Products, Kinetics, and Health Effects. *International Journal of Molecular Sciences*, 22(14), 7616.
<https://doi.org/10.3390/IJMS22147616>

Bandookwala, M., & Sengupta, P. (2020). 3-Nitrotyrosine: a versatile oxidative stress biomarker for major neurodegenerative diseases.
https://Doi.Org/10.1080/00207454.2020.1713776, 130(10), 1047–1062.
<https://doi.org/10.1080/00207454.2020.1713776>

Bandookwala, M., Thakkar, D., Sengupta, P., & Bandookwala, M. (2019). Advancements in the Analytical Quantification of Nitroxidative Stress Biomarker 3-Nitrotyrosine in Biological Matrices Advancements in the Analytical Quantification of Nitroxidative Stress Biomarker 3-Nitrotyrosine. *Critical Reviews in Analytical Chemistry*, 0(0), 1–25. <https://doi.org/10.1080/10408347.2019.1623010>

Bartesaghi, S, Ferrer-Sueta, G., Peluffo, G., Valez, V., Zhang, H., Kalyanaraman, B., & Radi, R. (2007). Protein tyrosine nitration in hydrophilic and hydrophobic environments Review Article. *Amino Acids*, 32, 501–515.
<https://doi.org/10.1007/s00726-006-0425-8>

Bartesaghi, Silvina, Ott, C., Tomasina, F., Meinl, W., Batthyany, C., Campolo, N., Bluhm, M., Hoffmann, R., Grune, T., & Radi, R. (2018). Decreased proteasome cleavage rates at nitrotyrosine sites in proteins and peptides. *Free Radical Biology and Medicine*, 128, S48. <https://doi.org/10.1016/j.freeradbiomed.2018.10.079>

Bartesaghi, Silvina, & Radi, R. (2018). Fundamentals on the biochemistry of peroxynitrite and protein tyrosine nitration. *Redox Biology*, 14(September 2017),

618–625. <https://doi.org/10.1016/j.redox.2017.09.009>

Bascom, R., Bromberg, P. A., Costa, D. A., Devlin, R., Dockery, D. W., Frampton, M. W., Lambert, W., Samet, J. M., Speizer, F. E., & Utell, M. (2012). Health effects of outdoor air pollution. Committee of the Environmental and Occupational Health Assembly of the American Thoracic Society.

https://doi.org/10.1164/Ajrccm.153.1.8542133, 153(1), 3–50.

<https://doi.org/10.1164/AJRCCM.153.1.8542133>

Batthyány, C., Bartesaghi, S., Mastrogiovanni, M., Lima, A., Demicheli, V., & Radi, R. (2016). Tyrosine-Nitrated Proteins: Proteomic and Bioanalytical Aspects.

Antioxidants & Redox Signaling, 26(7), 313–328.

<https://doi.org/10.1089/ars.2016.6787>

Beck, I., Jochner, S., Gilles, S., McIntyre, M., Buters, J. T. M., Schmidt-Weber, C., Behrendt, H., Ring, J., Menzel, A., & Traidl-Hoffmann, C. (2013). High environmental ozone levels lead to enhanced allergenicity of birch pollen. *PLoS ONE*, 8(11). <https://doi.org/10.1371/journal.pone.0080147>

Berlett, B. S., Levine, R. L., & Stadtman, E. R. (1998). Carbon dioxide stimulates peroxynitrite-mediated nitration of tyrosine residues and inhibits oxidation of methionine residues of glutamine synthetase: Both modifications mimic effects of adenylation. *Proceedings of the National Academy of Sciences of the United States of America*, 95(6), 2784–2789. <https://doi.org/doi.org/10.1073/pnas.95.6.2784>

Bouley, J., Groeme, R., Mignon, M. Le, Jain, K., & Chabre, H. (2015). Identification of the cysteine protease Amb a 11 as a novel major allergen from short ragweed. *J*

- Allergy Clin Immunol*, 1055–1064. <https://doi.org/10.1016/j.jaci.2015.03.001>
- Brunekreef, B., & Holgate, S. T. (2002). Air pollution and health. *The Lancet*, 360(9341), 1233–1242. [https://doi.org/10.1016/S0140-6736\(02\)11274-8](https://doi.org/10.1016/S0140-6736(02)11274-8)
- Burai, R., Ait-Bouziad, N., Chiki, A., & Lashuel, H. A. (2015). Elucidating the role of site-specific nitration of α -synuclein in the pathogenesis of Parkinson's disease via protein semisynthesis and mutagenesis. *Journal of the American Chemical Society*, 137(15), 5041–5052. https://doi.org/10.1021/JA5131726/SUPPL_FILE/JA5131726_SI_001.PDF
- Cai, Z., & Yan, L.-J. (2013). Protein Oxidative Modifications: Beneficial Roles in Disease and Health. *Journal of Biochemical and Pharmacological Research*, 1(1), 15. [/pmc/articles/PMC3646577/](https://pubmed.ncbi.nlm.nih.gov/24111111/)
- Campolo, N., Issoglio, F. M., Estrin, D. A., Bartesaghi, S., & Radi, R. (2020). 3-Nitrotyrosine and related derivatives in proteins: precursors, radical intermediates and impact in function. *Essays in Biochemistry*, 64(1), 111–133. <https://doi.org/10.1042/ebc20190052>
- Crow, J. P., & Beckman, J. S. (1995). Quantitation of Protein Tyrosine, 3-Nitrotyrosine, and 3-Aminotyrosine Utilizing HPLC and Intrinsic Ultraviolet Absorbance. *Methods*, 7(1), 116–120. <https://doi.org/10.1006/meth.1995.1017>
- D'Amato, G. (2011). Effects of climatic changes and urban air pollution on the rising trends of respiratory allergy and asthma. *Multidisciplinary Respiratory Medicine*, 6(1), 28. <https://doi.org/10.1186/2049-6958-6-1-28>
- Denicola, A., Freeman, B. A., Trujillo, M., & Radi, R. (1996). Peroxynitrite reaction with

- carbon dioxide/bicarbonate: Kinetics and influence on peroxyxynitrite-mediated oxidations. *Archives of Biochemistry and Biophysics*, 333(1), 49–58.
<https://doi.org/10.1006/abbi.1996.0363>
- DiMarco, T., & Giulivi, C. (2007). Current analytical methods for the detection of dityrosine, a biomarker of oxidative stress, in biological samples. *Mass Spectrometry Reviews*, 26(1), 108–120. <https://doi.org/10.1002/MAS.20109>
- Donahue, N. M., Robinson, A. L., & Pandis, S. N. (2009). Atmospheric organic particulate matter: From smoke to secondary organic aerosol. *Atmospheric Environment*, 43(1), 94–106. <https://doi.org/10.1016/J.ATMOSENV.2008.09.055>
- Duncan, M. W. (2003). A review of approaches to the analysis of 3-nitrotyrosine. *Amino Acids*, 25(3–4), 351–361. <https://doi.org/10.1007/S00726-003-0022-Z>
- Duque, L., Gomes, C., Abreu, I., Sousa, R., Ribeiro, H., Esteves da Silva, J., & Cruz, A. (2014). Changes in the IgE-reacting protein profiles of *Acer negundo*, *Platanus x acerifolia* and *Quercus robur* pollen in response to ozone treatment. *International Journal of Environmental Health Research*, 24(6), 515–527.
<https://doi.org/10.1080/09603123.2013.865716>
- Ernst, O., & Zor, T. (2010). Linearization of the Bradford protein assay. *Journal of Visualized Experiments*, 38. <https://doi.org/10.3791/1918>
- Ferrer-Sueta, G., Campolo, N., Trujillo, M., Bartsaghi, S., Carballal, S., Romero, N., Alvarez, B., & Radi, R. (2018). Biochemistry of Peroxynitrite and Protein Tyrosine Nitration. *Chemical Reviews*, 118(3), 1338–1408.
<https://doi.org/10.1021/ACS.CHEMREV.7B00568>

- Fishman, J., Ramanathan, V., Crutzen, P. J., & Liu, S. C. (1979). Tropospheric ozone and climate. *Nature*, 282(5741), 818–820. <https://doi.org/10.1038/282818A0>
- Folkes, L. K., Trujillo, M., Bartesaghi, S., Radi, R., & Wardman, P. (2011). Kinetics of reduction of tyrosine phenoxyl radicals by glutathione. *Archives of Biochemistry and Biophysics*, 506(2), 242–249. <https://doi.org/10.1016/J.ABB.2010.12.006>
- Forrester, M. T., & Stamler, J. S. (2012). A Classification Scheme for Redox-Based Modifications of Proteins. *Https://Doi.Org/10.1165/Rcmb.2006-001ED*, 36(2), 136–137. <https://doi.org/10.1165/RCMB.2006-001ED>
- Frank, U., & Ernst, D. (2016). Effects of NO₂ and Ozone on Pollen Allergenicity. *Frontiers in Plant Science*, 7(2), 2–5. <https://doi.org/10.3389/fpls.2016.00091>
- Franze, T., Weller, M. G., Niessner, R., & Pöschl, U. (2005). Protein nitration by polluted air. *Environmental Science and Technology*, 39(6), 1673–1678. <https://doi.org/10.1021/es0488737>
- Fraunberger, E. A., Scola, G., Laliberté, V. L. M., Duong, A., & Andreazza, A. C. (2016). Redox Modulations, Antioxidants, and Neuropsychiatric Disorders. *Oxidative Medicine and Cellular Longevity*, 2016. <https://doi.org/10.1155/2016/4729192>
- Gaucher, C., Boudier, A., Bonetti, J., Clarot, I., Leroy, P., & Parent, M. (2018). Glutathione: Antioxidant Properties Dedicated to Nanotechnologies. *Antioxidants* 2018, Vol. 7, Page 62, 7(5), 62. <https://doi.org/10.3390/ANTIOX7050062>
- Ghiani, A., Bruschi, M., Citterio, S., Bolzacchini, E., Ferrero, L., Sangiorgi, G., Asero, R., & Perrone, M. G. (2016). Nitration of pollen aeroallergens by nitrate ion in

- conditions simulating the liquid water phase of atmospheric particles. *Science of the Total Environment*, 573, 1589–1597. <https://doi.org/10.1016/j.scitotenv.2016.09.041>
- Grewling, Bogawski, P., Jenerowicz, D., Czarnecka-Operacz, M., Šikoparija, B., Skjøth, C. A., & Smith, M. (2016). Mesoscale atmospheric transport of ragweed pollen allergens from infected to uninfected areas. *International Journal of Biometeorology*, 60(10), 1493–1500. <https://doi.org/10.1007/S00484-016-1139-6/FIGURES/2>
- Gross, A. J., & Sizer, I. W. (1959). The Oxidation of Tyramine, Tyrosine, and Related Compounds by Peroxidase. *Journal of Biological Chemistry*, 234(6), 1611–1614. [https://doi.org/10.1016/S0021-9258\(18\)70059-8](https://doi.org/10.1016/S0021-9258(18)70059-8)
- Gruijthuisen, Y. K., Grieshuber, I., Stöcklinger, A., Tischler, U., Fehrenbach, T., Weller, M. G., Vogel, L., Vieths, S., Pöschl, U., & Duschl, A. (2006). Nitration Enhances the Allergenic Potential of Proteins. *International Archives of Allergy and Immunology*, 141(3), 265–275. <https://doi.org/10.1159/000095296>
- Halfpenny, E., & Robinson, P. L. (1952). The nitration and hydroxylation of aromatic compounds by pernitrous acid. *Journal of the Chemical Society (Resumed)*, 0, 939–946. <https://doi.org/10.1039/JR9520000939>
- Harwell, B. (2007). Biochemistry of oxidative stress. *Biochemical Society Transactions*, 35(5), 1147–1150. <https://doi.org/10.1042/BST0351147>
- Hawkins, C. L., & Davies, M. J. (2019). Detection, identification, and quantification of oxidative protein modifications. *Journal of Biological Chemistry*, 294(51), 19683–19708. <https://doi.org/10.1074/jbc.REV119.006217>

- Herce-Pagliai, C., Kotecha, S., & Shuker, D. E. G. (1998). Analytical Methods for 3-Nitrotyrosine as a Marker of Exposure to Reactive Nitrogen Species: A Review. *Nitric Oxide*, 2(5), 324–336. <https://doi.org/10.1006/NIOX.1998.0192>
- Hochscheid, R., Schreiber, N., Kotte, E., Weber, P., Cassel, W., Yang, H., Zhang, Y., Pöschl, U., & Müller, B. (2014). Nitration of Protein Without Allergenic Potential Triggers Modulation of Antioxidant Response in Type II Pneumocytes. *Journal of Toxicology and Environmental Health, Part A*, 77(12), 679–695. <https://doi.org/10.1080/15287394.2014.888023>
- Ikeda, K., Yukihiro Hiraoka, B., Iwai, H., Matsumoto, T., Mineki, R., Taka, H., Takamori, K., Ogawa, H., & Yamakura, F. (2007). Detection of 6-nitrotryptophan in proteins by Western blot analysis and its application for peroxynitrite-treated PC12 cells. *Nitric Oxide*, 16(1), 18–28. <https://doi.org/10.1016/J.NIOX.2006.04.263>
- Ilari, S., Dagostino, C., Malafoglia, V., Lauro, F., Giacotti, L. A., Spila, A., Proietti, S., Ventrice, D., Rizzo, M., Gliozzi, M., Palma, E., Guadagni, F., Salvemini, D., Mollace, V., & Muscoli, C. (2020). Protective effect of antioxidants in nitric oxide/cox-2 interaction during inflammatory pain: The role of nitration. *Antioxidants*, 9(12), 1–15. <https://doi.org/10.3390/antiox9121284>
- Ischiropoulos, H., Zhu, L., Chen, J., Tsai, M., Martin, J. C., Smith, C. D., & Beckman, J. S. (1992). Peroxynitrite-mediated tyrosine nitration catalyzed by superoxide dismutase. *Archives of Biochemistry and Biophysics*, 298(2), 431–437. [https://doi.org/10.1016/0003-9861\(92\)90431-U](https://doi.org/10.1016/0003-9861(92)90431-U)
- Ito, T., Ogino, K., Nagaoka, K., & Takemoto, K. (2018). Relationship of particulate

- matter and ozone with 3-nitrotyrosine in the atmosphere. *Environmental Pollution*, 236, 948–952. <https://doi.org/10.1016/j.envpol.2017.10.069>
- Ito, T., Ogino, K., Nagaoka, K., Takemoto, K., Nishiyama, R., & Shimizu, Y. (2019). Detection of 3-nitrotyrosine in atmospheric environments via a highperformance liquid chromatography-electrochemical detector system. *Journal of Visualized Experiments*, 2019(143), 3–9. <https://doi.org/10.3791/58371>
- Kampf, C. J., Liu, F., Reinmuth-Selzle, K., Berkemeier, T., Meusel, H., Shiraiwa, M., & Pöschl, U. (2015). Protein Cross-Linking and Oligomerization through Dityrosine Formation upon Exposure to Ozone. *Environmental Science and Technology*, 49(18), 10859–10866. <https://doi.org/10.1021/acs.est.5b02902>
- Karle, A. C., Oostingh, G. J., Mutschlechner, S., Ferreira, F., Lackner, P., Bohle, B., Fischer, G. F., Vogt, A. B., & Duschl, A. (2012). Nitration of the pollen allergen bet v 1.0101 enhances the presentation of bet v 1-derived peptides by HLA-DR on human dendritic cells. *PLoS ONE*, 7(2). <https://doi.org/10.1371/journal.pone.0031483>
- Kato, Y., Dozaki, N., Nakamura, T., Kitamoto, N., Yoshida, A., Naito, M., Kitamura, M., & Osawa, T. (2009). Quantification of modified tyrosines in healthy and diabetic human urine using liquid chromatography/tandem mass spectrometry. *Journal of Clinical Biochemistry and Nutrition*, 44(1), 67–78. <https://doi.org/10.3164/JCBN.08-185>
- Knox, R. B., Suphioglu, C., Taylor, P., Desai, R., Watson, H. C., Peng, J. L., & Bursill, L. A. (1997). Major grass pollen allergen Lol p 1 binds to diesel exhaust particles:

- Implications for asthma and air pollution. *Clinical and Experimental Allergy*, 27(3), 246–251. <https://doi.org/10.1111/J.1365-2222.1997.TB00702.X>
- Kofler, S., Ackaert, C., Samonig, M., Asam, C., Briza, P., Horejs-Hoeck, J., Cabrele, C., Ferreira, F., Duschl, A., Huber, C., & Brandstetter, H. (2014). Stabilization of the dimeric birch pollen allergen Bet v 1 impacts its immunological properties. *Journal of Biological Chemistry*, 289(1), 540–551. <https://doi.org/10.1074/JBC.M113.518795>
- Koide, S., & Sidhu, S. S. (2009). The importance of being tyrosine: Lessons in molecular recognition from minimalist synthetic binding proteins. *ACS Chemical Biology*, 4(5), 325–334. <https://doi.org/10.1021/CB800314V/>
- Koseki, K., Yamamoto, A., Tanimoto, K., Okamoto, N., Teng, F., Bito, T., Yabuta, Y., Kawano, T., & Watanabe, F. (2021). Dityrosine Crosslinking of Collagen and Amyloid- β ; Peptides Is Formed by Vitamin B12 Deficiency-Generated Oxidative Stress in *Caenorhabditis elegans*. *International Journal of Molecular Sciences* 2021, Vol. 22, Page 12959, 22(23), 12959. <https://doi.org/10.3390/IJMS222312959>
- Lancaster, J. R. (1994). Simulation of the diffusion and reaction of endogenously produced nitric oxide. *Proceedings of the National Academy of Sciences*, 91(17), 8137–8141. <https://doi.org/10.1073/PNAS.91.17.8137>
- Landino, L. M., Skreslet, T. E., & Alston, J. A. (2004). Cysteine Oxidation of Tau and Microtubule-associated Protein-2 by Peroxynitrite: MODULATION OF MICROTUBULE ASSEMBLY KINETICS BY THE THIOREDOXIN

REDUCTASE SYSTEM. *Journal of Biological Chemistry*, 279(33), 35101–35105.

<https://doi.org/10.1074/JBC.M405471200>

Lauro, F., Giacotti, L. A., Ilari, S., Dagostino, C., Gliozzi, M., Morabito, C., Malafoglia, V., Raffaelli, W., Muraca, M., Goffredo, B. M., Mollace, V., & Muscoli, C. (2016).

Inhibition of Spinal Oxidative Stress by Bergamot Polyphenolic Fraction Attenuates the Development of Morphine Induced Tolerance and Hyperalgesia in Mice.

<https://doi.org/10.1371/journal.pone.0156039>

Lee, J. R., Kim, J. K., Lee, S. J., & Kim, K. P. (2009). Role of protein tyrosine nitration in neurodegenerative diseases and atherosclerosis. *Archives of Pharmacal Research*, 32(8), 1109–1118. <https://doi.org/10.1007/S12272-009-1802-0>

Lin, M. T., & Beal, M. F. (2006). Mitochondrial dysfunction and oxidative stress in neurodegenerative diseases. *Nature 2006 443:7113*, 443(7113), 787–795.

<https://doi.org/10.1038/nature05292>

Liu, F., Lakey, P. S. J., Berkemeier, T., Tong, H., Kunert, A. T., Meusel, H., Cheng, Y., Su, H., Fröhlich-Nowoisky, J., Lai, S., Weller, M. G., Shiraiwa, M., Pöschl, U., & Kampf, C. J. (2017). Atmospheric protein chemistry influenced by anthropogenic air pollutants: nitration and oligomerization upon exposure to ozone and nitrogen dioxide. *Faraday Discussions*, 200, 413–427. <https://doi.org/10.1039/c7fd00005g>

Liu, F., Reinmuth-Selzle, K., Lai, S., Weller, M. G., Pöschl, U., & Kampf, C. J. (2017). Simultaneous determination of nitrated and oligomerized proteins by size exclusion high-performance liquid chromatography coupled to photodiode array detection. *Journal of Chromatography A*, 1495(2), 76–82.

<https://doi.org/10.1016/j.chroma.2017.03.015>

Lukesh, J. C., VanVeller, B., & Raines, R. T. (2013). Thiols and Selenols as Electron-Relay Catalysts for Disulfide-Bond Reduction. *Angewandte Chemie International Edition*, 52(49), 12901–12904. <https://doi.org/10.1002/ANIE.201307481>

Lymar, S. V., Jiang, Q., & Hurst, J. K. (1996). Mechanism of Carbon Dioxide-Catalyzed Oxidation of Tyrosine by Peroxynitrite†. *Biochemistry*, 35(24), 7855–7861. <https://doi.org/10.1021/BI960331H>

Maina, M. B., Al-Hilaly, Y. K., Oakley, S., Burra, G., Khanom, T., Biasetti, L., Mengham, K., Marshall, K., Harrington, C. R., Wischik, C. M., & Serpell, L. C. (2022). Dityrosine Cross-links are Present in Alzheimer’s Disease-derived Tau Oligomers and Paired Helical Filaments (PHF) which Promotes the Stability of the PHF-core Tau (297-391) In Vitro. *Journal of Molecular Biology*, 434(19). <https://doi.org/10.1016/J.JMB.2022.167785>

Malencik, D. A., & Anderson, S. R. (2003). Dityrosine as a product of oxidative stress and fluorescent probe. *Amino Acids*, 25(3–4), 233–247. <https://doi.org/10.1007/S00726-003-0014-Z/METRICS>

Marinelli, P., Navarro, S., Graña-Montes, R., Bañó-Polo, M., Fernández, M. R., Papaleo, E., & Ventura, S. (2018). A single cysteine post-translational oxidation suffices to compromise globular proteins kinetic stability and promote amyloid formation. *Redox Biology*, 14, 566–575. <https://doi.org/10.1016/j.redox.2017.10.022>

Martinez, J. (2022). *New Report: Denver, Fort Collins Named Among the Most Polluted Cities*. American Lung Association. <https://www.lung.org/media/press-releases/sota->

co-fy22

- Mayer, F., Pröpper, S., & Ritz-Timme, S. (2014). Dityrosine, a protein product of oxidative stress, as a possible marker of acute myocardial infarctions. *International Journal of Legal Medicine*, 128(5), 787–794. <https://doi.org/10.1007/S00414-014-1015-Z/FIGURES/2>
- Menetrez, M. Y., Foarde, K. K., Dean, T. R., Betancourt, D. A., & Moore, S. A. (2007). An evaluation of the protein mass of particulate matter. *Atmospheric Environment*, 41(37), 8264–8274. <https://doi.org/10.1016/J.ATMOSENV.2007.06.021>
- Miller, M. J., Liu, X., Clark, D. A., & Sandoval, M. (1998). The Effects of Antioxidants on the Degradation of Nitric Oxide and Peroxynitrite † 591. *Pediatric Research* 1998 43:4, 43(4), 103–103. <https://doi.org/10.1203/00006450-199804001-00612>
- Mudd, J. B., Leavitt, R., Ongun, A., & McManus, T. T. (1969). Reaction of ozone with amino acids and proteins. *Atmospheric Environment (1967)*, 3(6), 669–681. [https://doi.org/10.1016/0004-6981\(69\)90024-9](https://doi.org/10.1016/0004-6981(69)90024-9)
- Mukherjee, S., Fang, M., Mei Kok, W., Kapp, E. A., Thombare, V. J., Huguet, R., Hutton, C. A., Reid, G. E., & Roberts, B. R. (2019). *Establishing Signature Fragments for Identification and Sequencing of Dityrosine Cross-Linked Peptides Using Ultraviolet Photodissociation Mass Spectrometry*. <https://doi.org/10.1021/acs.analchem.9b02986>
- Mukherjee, S., Kapp, E. A., Lothian, A., Roberts, A. M., Vasil'Ev, Y. V., Boughton, B. A., Barnham, K. J., Kok, W. M., Hutton, C. A., Masters, C. L., Bush, A. I., Beckman, J. S., Dey, S. G., & Roberts, B. R. (2017). Characterization and

Identification of Dityrosine Cross-Linked Peptides Using Tandem Mass

Spectrometry. *Analytical Chemistry*, 89(11), 6136–6145.

https://doi.org/10.1021/ACS.ANALCHEM.7B00941/SUPPL_FILE/AC7B00941_SI_001.PDF

Müller-Germann, I., Pickersgill, D. A., Paulsen, H., Alberternst, B., Pöschl, U., Fröhlich-

Nowoisky, J., & Després, V. R. (2017). Allergenic Asteraceae in air particulate matter: quantitative DNA analysis of mugwort and ragweed. *Aerobiologia*, 33(4), 493–506. <https://doi.org/10.1007/S10453-017-9485-3/FIGURES/4>

Naas, O., Mendez, M., Quijada, M., Gosselin, S., Farah, J., Choukri, A., & Visez, N.

(2016). Chemical modification of coating of *Pinus halepensis* pollen by ozone exposure. *Environmental Pollution*, 214, 816–821.

<https://doi.org/10.1016/J.ENVPOL.2016.04.076>

Ogino, N., Ogino, K., Eitoku, M., Suganuma, N., Nagaoka, K., & Kuramitsu, Y. (2021).

The identification of tyrosine-nitrated human serum albumin in airborne particulate matter from Japan. *Atmospheric Pollution Research*, 12(5), 101050.

<https://doi.org/10.1016/J.APR.2021.03.013>

Pacher, L., Beckman, J. S., & Liaudet, L. (2007). Nitric Oxide and Peroxynitrite in

Health and Disease. *Physiol Rev*, 87, 315–424.

<https://doi.org/10.1152/physrev.00029.2006>.

Padmaja, S., Ramazenian, M. S., Bounds, P. L., & Koppenol, W. H. (2016). Reaction of peroxynitrite with L-tryptophan.

<Http://Dx.Doi.Org/10.1080/13510002.1996.11747045>, 2(3), 173–177.

<https://doi.org/10.1080/13510002.1996.11747045>

Parker, C. W., Kern, M., & Eisen, H. N. (1962). Polyfunctional dinitrophenyl haptens as reagents for elicitation of immediate type allergic skin responses. *The Journal of Experimental Medicine*, 115(4), 789–801. <https://doi.org/10.1084/jem.115.4.789>

Peluffo, G., & Radi, R. (2007). Biochemistry of protein tyrosine nitration in cardiovascular pathology. *Cardiovascular Research*, 75(2), 291–302. <https://doi.org/10.1016/J.CARDIORES.2007.04.024/2/75-2-291-FIG2.GIF>

Pérez de la Lastra, J. M., Juan, C. A., Plou, F. J., & Pérez-Lebeña, E. (2022). Nitration of Flavonoids and Tocopherols as Potential Modulators of Nitrosative Stress—A Study Based on Their Conformational Structures and Energy Content. *Stresses*, 2(2), 213–230. <https://doi.org/10.3390/STRESSES2020015>

Persinger, R. L., Blay, W. M., Heintz, N. H., Hemenway, D. R., & Janssen-Heininger, Y. M. W. (2012). Nitrogen Dioxide Induces Death in Lung Epithelial Cells in a Density-Dependent Manner. <https://doi.org/10.1165/Ajrcmb.24.5.4340>, 24(5), 583–590. <https://doi.org/10.1165/AJRCMB.24.5.4340>

Pfeiffer, S., Gorren, A. C. F., Schmidt, K., Werner, E. R., Hansert, B., Scott Bohle, D., & Mayer, B. (1997). *Metabolic Fate of Peroxynitrite in Aqueous Solution REACTION WITH NITRIC OXIDE AND pH-DEPENDENT DECOMPOSITION TO NITRITE AND OXYGEN IN A 2:1 STOICHIOMETRY**. <http://www-jbc.stanford.edu/jbc/>

Pizzino, G., Irrera, N., Cucinotta, M., Pallio, G., Mannino, F., Arcoraci, V., Squadrito, F., Altavilla, D., & Bitto, A. (2017). Oxidative Stress: Harms and Benefits for Human Health. *Oxidative Medicine and Cellular Longevity*, 2017.

<https://doi.org/10.1155/2017/8416763>

Pöschl, U., & Shiraiwa, M. (2015). Multiphase Chemistry at the Atmosphere-Biosphere Interface Influencing Climate and Public Health in the Anthropocene. *Chemical Reviews*, 115(10), 4440–4475. <https://doi.org/10.1021/CR500487S>

Prütz, W. A., Mönig, H., Butler, J., & Land, E. J. (1985). Reactions of nitrogen dioxide in aqueous model systems: Oxidation of tyrosine units in peptides and proteins. *Archives of Biochemistry and Biophysics*, 243(1), 125–134.

[https://doi.org/10.1016/0003-9861\(85\)90780-5](https://doi.org/10.1016/0003-9861(85)90780-5)

Pryor, W. A., & Squadrito, G. L. (1995). The chemistry of peroxyxynitrite: a product from the reaction of nitric oxide with superoxide.

Https://Doi.Org/10.1152/Ajplung.1995.268.5.L699, 268(5 12-5).

<https://doi.org/10.1152/AJPLUNG.1995.268.5.L699>

Radi, R. (2012). Protein Tyrosine Nitration: Biochemical Mechanisms and Structural Basis of Functional Effects. *Accounts of Chemical Research*, 46(2), 550–559.

<https://doi.org/10.1021/AR300234C>

Radi, R. (2013a). Protein tyrosine nitration: Biochemical mechanisms and structural basis of functional effects. *Accounts of Chemical Research*.

<https://doi.org/10.1021/ar300234c>

Radi, R. (2013b). Peroxyxynitrite, a Stealthy Biological Oxidant *. *Journal of Biological Chemistry*, 288(37), 26464–26472. <https://doi.org/10.1074/JBC.R113.472936>

Reinmuth-Selzle, K., Bellinghausen, I., Leifke, A. L., Backes, A. T., Bothen, N., Ziegler, K., Weller, M. G., Saloga, J., Schuppan, D., Lucas, K., Pöschl, U., & Fröhlich-

Nowoisky, J. (2023). Chemical modification by peroxyne nite enhances TLR4 activation of the grass pollen allergen Phl p 5. *Frontiers in Allergy*, 4, 5. <https://doi.org/10.3389/FALGY.2023.1066392>

Reinmuth-Selzle, K., Kampf, C. J., Lucas, K., Lang-Yona, N., Fröhlich-Nowoisky, J., Shiraiwa, M., Lakey, P. S. J., Lai, S., Liu, F., Kunert, A. T., Ziegler, K., Shen, F., Sgarbanti, R., Weber, B., Bellinghausen, I., Saloga, J., Weller, M. G., Duschl, A., Schuppan, D., & Pöschl, U. (2017). Air Pollution and Climate Change Effects on Allergies in the Anthropocene: Abundance, Interaction, and Modification of Allergens and Adjuvants. *Environmental Science and Technology*, 51(8), 4119–4141. <https://doi.org/10.1021/acs.est.6b04908>

Reinmuth-Selzle, K., Kampf, C. J., Samonig, M., Shiraiwa, M., Yang, H., Gadermaier, G., Brandstetter, H., Huber, C. G., Duschl, A., & Oostingh, G. J. (2014). Nitration of the Birch Pollen Allergen Bet v 1.0101: Efficiency and Site-Selectivity of Liquid and Gaseous Nitrating Agents. *Journal of Proteome Research*, 13, 1570–1577. <https://doi.org/10.1021/pr401078h>

Reinmuth-Selzle, K., Tchpilov, · Teodor, Backes, A. T., Tscheuschner, G., Tang, · Kai, Ziegler, K., Lucas, K., Ulrich, ·, Oschl, P. ·, Fröhlich, J., Fröhlich-Nowoisky, F., & Weller, M. G. (2022). Determination of the protein content of complex samples by aromatic amino acid analysis, liquid chromatography-UV absorbance, and colorimetry. *Analytical and Bioanalytical Chemistry* 2022, 1–14. <https://doi.org/10.1007/S00216-022-03910-1>

Ribeiro, H., Costa, C., Abreu, I., & Esteves da Silva, J. C. G. (2017). Effect of O₃ and

- NO₂ atmospheric pollutants on *Platanus x acerifolia* pollen: Immunochemical and spectroscopic analysis. *Science of the Total Environment*, 599–600, 291–297.
<https://doi.org/10.1016/j.scitotenv.2017.04.206>
- Rogatsky, E. (2021). Pandora box of BCA assay. Investigation of the accuracy and linearity of the microplate bicinchoninic protein assay: Analytical challenges and method modifications to minimize systematic errors. *Analytical Biochemistry*, 631, 114321. <https://doi.org/10.1016/J.AB.2021.114321>
- Sacksteder, C. A., Qian, W.-J., Knyushko, T. V., Wang, H., Chin, M. H., Lacan, G., Melega, W. P., Camp, D. G., Smith, R. D., Smith, D. J., Squier, T. C., & Bigelow, D. J. (2006). *Endogenously Nitrated Proteins in Mouse Brain: Links to Neurodegenerative Disease*. <https://doi.org/10.1021/BI060474W>
- Sandhiya, L., Kolandaivel, P., & Senthilkumar, K. (2014). Oxidation and nitration of tyrosine by ozone and nitrogen dioxide: Reaction mechanisms and biological and atmospheric implications. *Journal of Physical Chemistry B*, 118(13), 3479–3490.
<https://doi.org/10.1021/jp4106037>
- Santos, C. X. C., Bonini, M. G., & Augusto, O. (2000). Role of the carbonate radical anion in tyrosine nitration and hydroxylation by peroxynitrite. *Archives of Biochemistry and Biophysics*, 377(1), 146–152.
<https://doi.org/10.1006/abbi.2000.1751>
- Selzle, K., Ackaert, C., Kampf, C. J., Kunert, A. T., Duschl, A., Oostingh, G. J., & Pöschl, U. (2013). Determination of nitration degrees for the birch pollen allergen Bet v 1. *Analytical and Bioanalytical Chemistry*, 405(27), 8945–8949.

<https://doi.org/10.1007/s00216-013-7324-0>

Sénéchal, H., Visez, N., Charpin, D., Shahali, Y., Peltre, G., Biolley, J.-P., Lhuissier, F., Couderc, R., Yamada, O., Malrat-Domenge, A., Pham-Thi, N., Poncet, P., Sutra, J.-P., & Jean-, ; (2015). *A Review of the Effects of Major Atmospheric Pollutants on Pollen Grains, Pollen Content, and Allergenicity.*

<https://doi.org/10.1155/2015/940243>

Sharma, V. K., & Graham, N. J. D. (2010). Oxidation of Amino Acids, Peptides and Proteins by Ozone: A Review. *Ozone: Science and Engineering*, 32(2), 81–90.

<https://doi.org/10.1080/01919510903510507>

Shiraiwa, M., Selzle, K., Yang, H., Sosedova, Y., Ammann, M., & Pöschl, U. (2012). Multiphase chemical kinetics of the nitration of aerosolized protein by ozone and nitrogen dioxide. *Environmental Science and Technology*, 46(12), 6672–6680.

<https://doi.org/10.1021/es300871b>

Shiraiwa, M., Ueda, K., Pozzer, A., Lammel, G., Kampf, C. J., Fushimi, A., Enami, S., Arangio, A. M., Fröhlich-Nowoisky, J., Fujitani, Y., Furuyama, A., Lakey, P. S. J., Lelieveld, J., Lucas, K., Morino, Y., Pöschl, U., Takahama, S., Takami, A., Tong, H., ... Sato, K. (2017). Aerosol Health Effects from Molecular to Global Scales. *Environmental Science and Technology*, 51(23), 13545–13567.

<https://doi.org/10.1021/ACS.EST.7B04417>

Souza, J. M., Giasson, B. I., Chen, Q., Lee, V. M.-Y., & Ischiropoulos, H. (2000). Dityrosine Cross-linking Promotes Formation of Stable α -Synuclein Polymers. *Journal of Biological Chemistry*, 275(24), 18344–18349.

<https://doi.org/10.1074/jbc.m000206200>

Souza, J. M., Peluffo, G., & Radi, R. (2008). Protein tyrosine nitration—Functional alteration or just a biomarker? *Free Radical Biology and Medicine*, *45*(4), 357–366.

<https://doi.org/10.1016/j.freeradbiomed.2008.04.010>

Stanbury, D. M. (1989). Reduction Potentials Involving Inorganic Free Radicals in Aqueous Solution. *Advances in Inorganic Chemistry*, *33*(C), 69–138.

[https://doi.org/10.1016/S0898-8838\(08\)60194-4](https://doi.org/10.1016/S0898-8838(08)60194-4)

Takahashi, M. A., & Asada, K. (1983). Superoxide anion permeability of phospholipid membranes and chloroplast thylakoids. *Archives of Biochemistry and Biophysics*, *226*(2), 558–566. [https://doi.org/10.1016/0003-9861\(83\)90325-9](https://doi.org/10.1016/0003-9861(83)90325-9)

Teixeira, D., Fernandes, R., Prudêncio, C., & Vieira, M. (2016). 3-Nitrotyrosine quantification methods: Current concepts and future challenges. *Biochimie*, *125*, 1–11. <https://doi.org/10.1016/J.BIOCHI.2016.02.011>

Tikhonov, D., Kulikova, L., Rudnev, V., Kopylov, A. T., Taldaev, A., Stepanov, A., Malsagova, K., Izotov, A., Enikeev, D., Potoldykova, N., & Kaysheva, A. (2021). Changes in protein structural motifs upon post-translational modification in kidney cancer. *Diagnostics*, *11*(10), 1836.

<https://doi.org/10.3390/DIAGNOSTICS11101836/S1>

Tsikias, D. (2017). What we—authors, reviewers and editors of scientific work—can learn from the analytical history of biological 3-nitrotyrosine. *Journal of Chromatography B: Analytical Technologies in the Biomedical and Life Sciences*, *1058*(May), 68–72. <https://doi.org/10.1016/j.jchromb.2017.05.012>

- Ulrich, K., & Jakob, U. (2019). The role of thiols in antioxidant systems. *Free Radical Biology and Medicine*, *140*, 14–27.
<https://doi.org/10.1016/J.FREERADBIO.2019.05.035>
- Van der Vliet, A., Eiserich, J. P., Halliwell, B., & Cross, C. E. (1995). Modification of aromatic amino acids by reactive nitrogen species. *Biochemical Society Transactions*, *23*(2), 237S–237S. <https://doi.org/10.1042/BST023237S>
- van der Vliet, Albert, O'Neill, C. A., Halliwell, B., Cross, C. E., & Kaur, H. (1994). Aromatic hydroxylation and nitration of phenylalanine and tyrosine by peroxynitrite. *FEBS Letters*, *339*(1–2), 89–92. [https://doi.org/10.1016/0014-5793\(94\)80391-9](https://doi.org/10.1016/0014-5793(94)80391-9)
- Verrastro, I., Pasha, S., Jensen, K. T., Pitt, A. R., & Spickett, C. M. (2015). Mass spectrometry-based methods for identifying oxidized proteins in disease: Advances and challenges. *Biomolecules*, *5*(2), 378–411.
<https://doi.org/10.3390/BIOM5020378>
- Wang, F., Yuan, Q., Chen, F., Pang, J., Pan, C., Xu, F., & Chen, Y. (2021). Fundamental Mechanisms of the Cell Death Caused by Nitrosative Stress. *Frontiers in Cell and Developmental Biology*, *9*, 2506.
<https://doi.org/10.3389/FCELL.2021.742483/BIBTEX>
- Wang, Y. C., Peterson, S. E., & Loring, J. F. (2013). Protein post-translational modifications and regulation of pluripotency in human stem cells. *Cell Research* *2014* *24*:2, *24*(2), 143–160. <https://doi.org/10.1038/cr.2013.151>
- Warren, J. J., Winkler, J. R., & Gray, H. B. (2012). Redox properties of tyrosine and related molecules. *FEBS Letters*, *586*(5), 596–602.

<https://doi.org/10.1016/J.FEBSLET.2011.12.014>

Waykole, P., & Heidemann, E. (2009). Dityrosine in Collagen. *Connective Tissue Research*, 4(4), 219–222. <https://doi.org/10.3109/03008207609152224>

West, J. J., Cohen, A., Dentener, F., Brunekreef, B., Zhu, T., Armstrong, B., Bell, M. L., Brauer, M., Carmichael, G., Costa, D. L., Dockery, D. W., Kleeman, M., Krzyzanowski, M., Künzli, N., Liousse, C., Lung, S. C. C., Martin, R. V., Pöschl, U., Pope, C. A., ... Wiedinmyer, C. (2016). “what We Breathe Impacts Our Health: Improving Understanding of the Link between Air Pollution and Health.” *Environmental Science and Technology*, 50(10), 4895–4904. <https://doi.org/10.1021/ACS.EST.5B03827>

Wolf, M., Huber, T. E. T. S., Steiner, M. R. M., Aglas, L., Aloisi, M. H. I., Hofer, C. A. H., Ebner, M. A. P. C., & Jahn-schmid, P. B. A. N. F. S. B. (2017). Amb a 1 isoforms : Unequal siblings with distinct immunological features. *Experimental Allergy and Immunology*, April, 1874–1882. <https://doi.org/10.1111/all.13196>

Wopfner, N., Jahn-schmid, B., Schmidt, G., Christ, T., Hubinger, G., Briza, P., Radauer, C., Bohle, B., Vogel, L., Ebner, C., Asero, R., Ferreira, F., & Schwarzenbacher, R. (2009). The alpha and beta subchain of Amb a 1 , the major ragweed-pollen allergen show divergent reactivity at the IgE and T-cell level. *Mollecular Immunology*, 46, 2090–2097. <https://doi.org/10.1016/j.molimm.2009.02.005>

Yamakura, F., & Ikeda, K. (2006). Modification of tryptophan and tryptophan residues in proteins by reactive nitrogen species. *Nitric Oxide - Biology and Chemistry*, 14(2 SPEC. ISS.), 152–161. <https://doi.org/10.1016/j.niox.2005.07.009>

- Yang, H., Zhang, Y., & Pöschl, U. (2010). Quantification of nitrotyrosine in nitrated proteins. *Analytical and Bioanalytical Chemistry*, 397(2), 879–886.
<https://doi.org/10.1007/s00216-010-3557-3>
- Yoon, S., Eom, G. H., & Kang, G. (2021). Nitrosative Stress and Human Disease: Therapeutic Potential of Denitrosylation. *International Journal of Molecular Sciences 2021*, Vol. 22, Page 9794, 22(18), 9794.
<https://doi.org/10.3390/IJMS22189794>
- Zhan, X., Wang, X., & Desiderio, D. M. (2015). Mass spectrometry analysis of nitrotyrosine-containing proteins. *Mass Spectrometry Reviews*, 34(4), 423–448.
<https://doi.org/10.1002/MAS.21413>
- Zhang, H., Joseph, J., Feix, J., Hogg, N., & Kalyanaraman, B. (2001). Nitration and Oxidation of a Hydrophobic Tyrosine Probe by Peroxynitrite in Membranes: Comparison with Nitration and Oxidation of Tyrosine by Peroxynitrite in Aqueous Solution†. *Biochemistry*, 40(25), 7675–7686. <https://doi.org/10.1021/BI002958C>
- Zhao, F., Elkelish, A., Durner, J., Lindermayr, C., Winkler, J. B., Ru, F., Behrendt, H., Traidl-hoffmann, C., Holzinger, A., Ko, W., Braun, P., Toerne, C. Von, & Hauck, S. M. (2016). Common ragweed (*Ambrosia artemisiifolia* L .): allergenicity and molecular characterization of pollen after plant exposure to elevated NO₂. *Plant, Cell, and Environment*, 39, 147–164. <https://doi.org/10.1111/pce.12601>
- Zhou, S., Wang, X., Lu, S., Yao, C., Zhang, L., Rao, L., Liu, X., Zhang, W., Li, S., Wang, W., & Wang, Q. (2021). Characterization of allergenicity of *Platanus* pollen allergen a 3 (Pla a 3) after exposure to NO₂ and O₃. *Environmental Pollution*, 278,

116913. <https://doi.org/10.1016/J.ENVPOL.2021.116913>

- Ziegler, K., Neumann, J., Liu, F., Fröhlich-Nowoisky, J., Cremer, C., Saloga, J., Reinmuth-Selzle, K., Pöschl, U., Schuppan, D., Bellinghausen, I., & Lucas, K. (2019). Nitration of wheat amylase trypsin inhibitors increases their innate and adaptive immunostimulatory potential in vitro. *Frontiers in Immunology*, *10*(JAN), 1–10. <https://doi.org/10.3389/fimmu.2018.03174>
- Ziska, L. H., Makra, L., Harry, S. K., Bruffaerts, N., Hendrickx, M., Coates, F., Saarto, A., Thibaudon, M., Oliver, G., Damialis, A., Charalampopoulos, A., Vokou, D., Heidmarsson, S., Guðjohnsen, E., Bonini, M., Oh, J. W., Sullivan, K., Ford, L., Brooks, G. D., ... Crimmins, A. R. (2019). Temperature-related changes in airborne allergenic pollen abundance and seasonality across the northern hemisphere: a retrospective data analysis. *The Lancet Planetary Health*, *3*(3), e124–e131. [https://doi.org/10.1016/S2542-5196\(19\)30015-4](https://doi.org/10.1016/S2542-5196(19)30015-4)
- Ziska, L., Knowlton, K., Rogers, C., Dalan, D., Tierney, N., Elder, M. A., Filley, W., Shropshire, J., Ford, L. B., Hedberg, C., Fleetwood, P., Hovanky, K. T., Kavanaugh, T., Fulford, G., Vrtis, R. F., Patz, J. A., Portnoy, J., Coates, F., Bielory, L., & Frenz, D. (2011). Recent warming by latitude associated with increased length of ragweed pollen season in central North America. *Proceedings of the National Academy of Sciences of the United States of America*, *108*(10), 4248–4251. https://doi.org/10.1073/PNAS.1014107108/SUPPL_FILE/SD01.XLS

Appendix A: HPLC integration Igor code

This Igor code is to import and rename HPLC-DAD data from Excel to waves.

```
Function/S DoLoadMultipleFiles()
  Variable refNum
  String message = "Select one or more files"
  String outputPaths
  String fileFilters = "Data Files (*.txt,*.dat,*.csv):.txt,.dat,.csv;"
  fileFilters += "All Files:.*;"

  Open /D /R /MULT=1 /F=fileFilters /M=message refNum
  outputPaths = S_fileName

  if (strlen(outputPaths) == 0)
    Print "Cancelled"
  else
    Variable numFilesSelected = ItemsInList(outputPaths, "\r")
    Variable i
    for(i=0; i<numFilesSelected; i+=1)
      String path = StringFromList(I, outputPaths, "\r")
      LoadWave/A/D/J/W/K=0/L={0,0,0,0,0}
    endfor
  endif

  return outputPaths
End
```

This Igor code is used for HPLC-DAD integration, specifically designed to integrate a peak for both 280 nm and 357 nm wavelengths for input into nitration degree calculation.

```
Function BaselineCorrect(InputSampleWv, InputTimeWv, StartBaselineSubPt,
EndBaselineSubPt, EndIntegrationWindowVar)

Wave/t InputSampleWv
```

```

Wave InputTimeWv
Variable StartBaselineSubPt, EndBaselineSubPt
Variable EndIntegrationWindowVar
Variable iCount, jCount
Variable m, b

Make/o/n=(numpts(InputSampleWv)) IntegratedValWvA, IntegratedValWvB
  Make/o/n=(numpts(InputSampleWv)) SlopeWv
IntegratedValWvA = nan
IntegratedValWvB = nan
  SlopeWv = nan
For (iCount = 0 ; iCount < numpts(InputSampleWv) ; iCount += 1)
  Wave TempWv = $InputSampleWv[iCount]

  Wavestats/q/r=[StartBaselineSubPt, EndBaselineSubPt] TempWv
  TempWv -= v_avg

  Duplicate/o TempWv TempIntWv, TempIntSlopeCorrWv

  TempIntWv[0,(EndBaselineSubPt)] = nan
  TempIntWv[EndIntegrationWindowVar, numpts(TempIntWv)-1] = nan

  IntegratedValWvA[iCount] = areaxy(InputTimeWv, TempIntWv)

  m = (TempIntWv[EndIntegrationWindowVar-1] -
TempIntWv[EndBaselineSubPt+1]) / (InputTimeWv[EndIntegrationWindowVar-1] -
InputTimeWv[EndBaselineSubPt+1])
  b = TempIntWv[EndBaselineSubPt+1]
  SlopeWv[iCount] = m

  TempIntSlopeCorrWv = nan
  For (jCount = EndBaselineSubPt+1 ; jCount <= EndIntegrationWindowVar -1 ;
jCount += 1)

    TempIntSlopeCorrWv[jCount] = TempIntWv[jCount] - (m*(InputTimeWv[jCount]-
InputTimeWv[EndBaselineSubPt+1]) + b)
  Endfor

  IntegratedValWvB[iCount] = areaxy(InputTimeWv, TempIntSlopeCorrWv)

Endfor

End Function

```

Appendix B: Micropipette precision

To determine the accuracy and precision of the micropipettes an absorbance experiment was conducted. 10.0 mg/mL tryptophan (Trp) was prepared in MQ H₂O using volumetric pipettes and flasks. Two pipette volumes were tested (0.316 μ L and 3.16 μ L) due to their common use in nitration experiments. A desired final concentration was calculated to be 0.0158 mg/mL (0.316 μ L concentrated Trp (10.0 mg/mL) placed into 200 μ L MQ H₂O). A standard solution of Trp in H₂O of this concentration (0.0158 mg/mL) was made using volumetric flasks and pipettes, and the absorbance at 280 nm was taken using a UV-Vis spectrometer. Using the absorbance value and known concentration, the molar absorptivity of this solution was calculated using Beer's Law.

The same concentration was placed in each well of a 96-well UV-Vis plate (0.316 μ L concentrated Trp (10.0 mg/mL) placed into 200 μ L MQ H₂O). A plate reader was used to measure the absorbance at 280 nm for each well, along with a H₂O blank, three times each. The same experiment was done using 197 μ L H₂O and 3.16 μ L diluted Trp solution (1.0 mg/mL) to ensure the same final concentration. The blank measurements were done using the same plate and a new pipette tip was used each time to deliver the Trp into the well. Plates were placed on a plate shaker to ensure homogeneity.

Using Beer's Law and the fact that the same Trp solution is used in each experiment, it was determined that absorbance divided by pathlength (A/l) is the known value calculated (molar absorptivity and concentration are the same). The pathlength of the UV-Vis cuvette used is 10 mm. The pathlength of the plate reader varies depending on the volume being used. At a 200 μ L volume the pathlength of the plate reader was

assumed to be 5.8 mm, after verifying with sources. These values were used to back-calculate the delivered volume by the pipette from the absorbance values, along with the molar absorptivity and concentration both in M, shown below.

$$A/l = \epsilon \cdot c$$

$$A_{\text{expected}}/C_{\text{expected}} = A_{\text{experimental}}/C_{\text{experimental}}$$

$$C_{\text{experimental}} = A_{\text{experimental}}/A_{\text{expected}} (C_{\text{expected}})$$

$$C_1 V_1 = C_2 V_2$$

$$C_1 = 10.0 \text{ mg/mL Trp}$$

C_2 = calculated from absorbance value

V_2 = total volume (assume 200 + X)

V_1 = unknown (delivered volume) = X

$$C_1 X = C_2 (200 + X)$$

rearrange

$$X (C_1 - C_2) = 200 C_2$$

$$X = 200 C_2 / C_1 - C_2$$

$$\text{Delivered volume} = 200 \mu\text{L} (C_{\text{experimental}}) / (C_{\text{Trpstock}} - C_{\text{experimental}})$$

Appendix C: Chapter 3 supplement

Appendix C was included as the online supplement in the peer-reviewed and published version of the following publication, which was reformatted here as Chapter 3.

Davey, R. L., Mattson, E. J., & Huffman, J. A. (2022). Heterogeneous nitration reaction of BSA protein with urban air: improvements in experimental methodology. *Analytical and Bioanalytical Chemistry* 2021, 1–12. <https://doi.org/10.1007/S00216-021-03820-8>

Supplement to:

Heterogeneous nitration reaction of BSA protein with urban air: improvements in experimental methodology

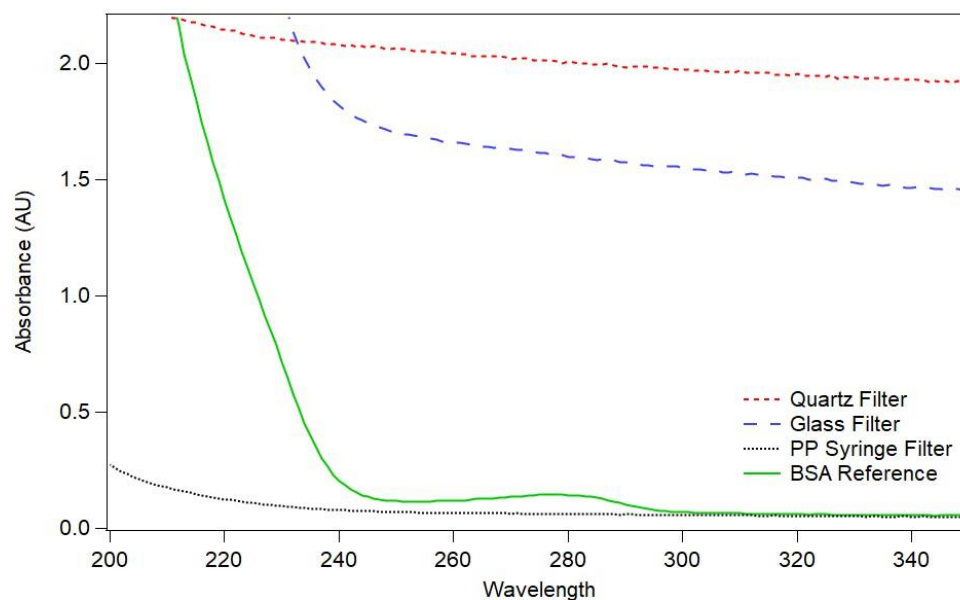


Figure C1. Exemplary absorption spectra showing quartz and glass filter interference. Solid green line is BSA in PBS (50 μ L of 2.0 mg/mL BSA in PBS), dotted black line is PP syringe filter extract in PBS, blue dashed line is glass filter extract in PBS, and red dashed line is quartz filter extract in PBS.

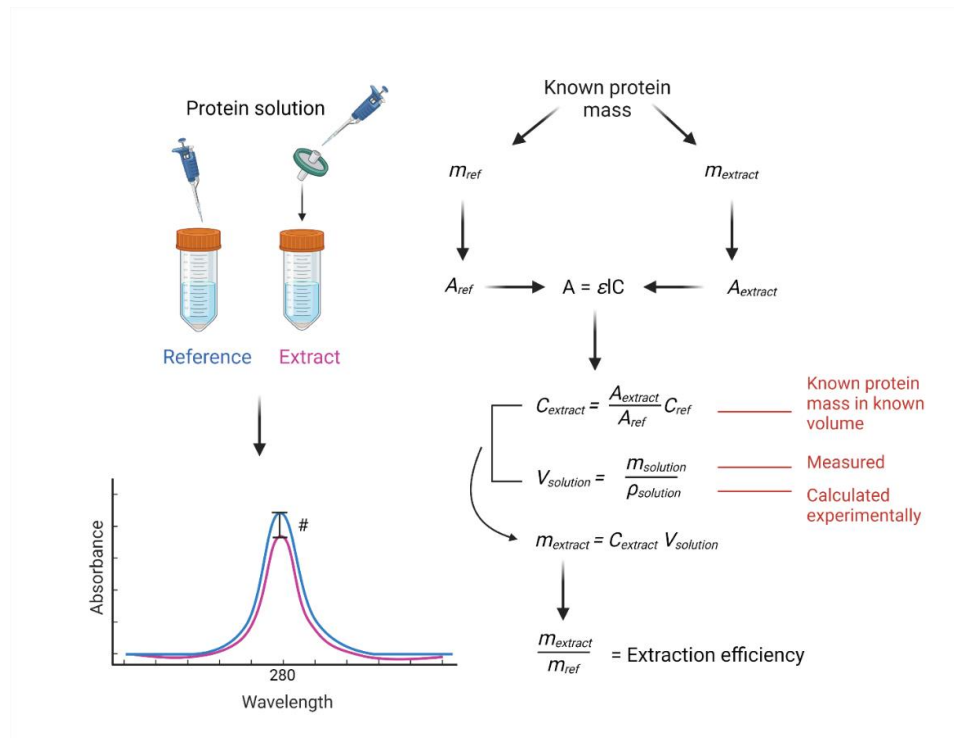


Figure C2. Schematic representing extraction efficiency process. Created with BioRender.com.

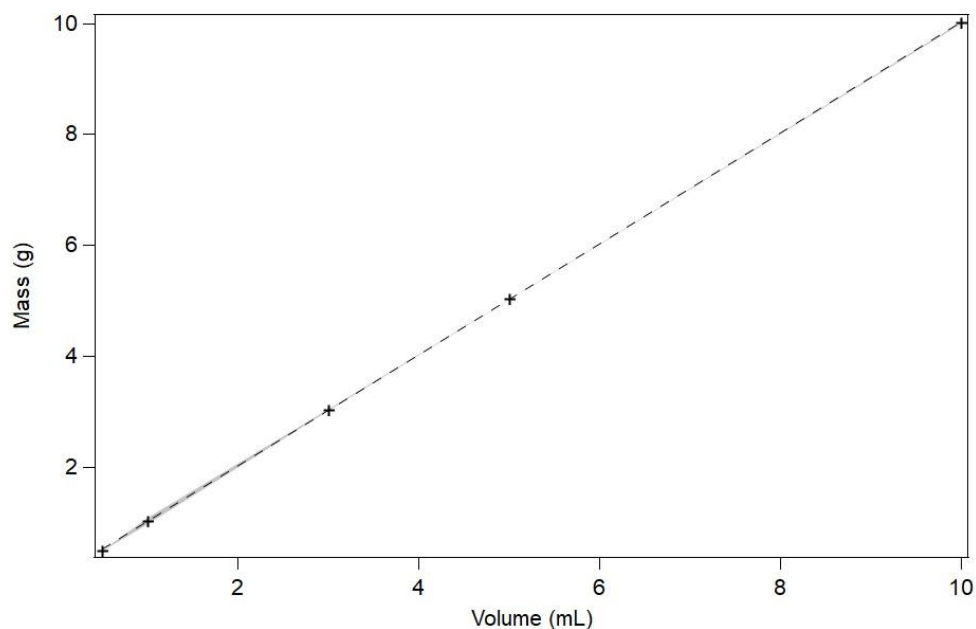


Figure C3. Density determination of 400 μg BSA in PBS. Dashed line is linear fit and shaded error represents standard deviation ($R^2 = 0.9999$; $m = 1.000 \pm 0.002$, $n = 3$).

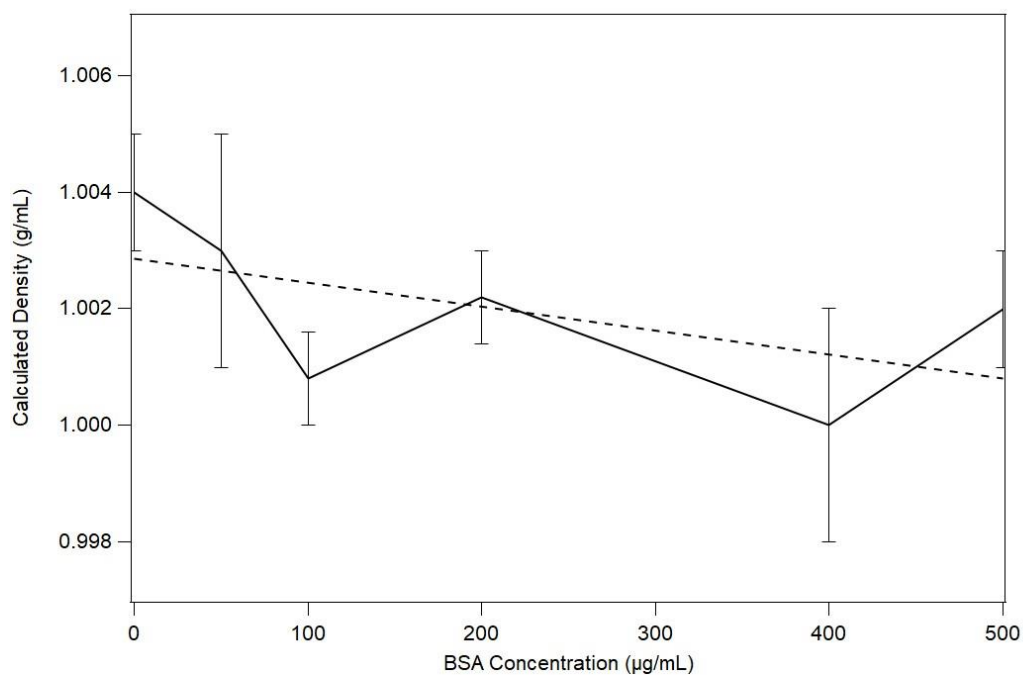


Figure C4. Change in density of 0 – 500 $\mu\text{g}/\text{mL}$ BSA in PBS. Dashed line is linear fit. Due to small deviations in density, the average density (1.002 ± 0.001 g/mL) was used.

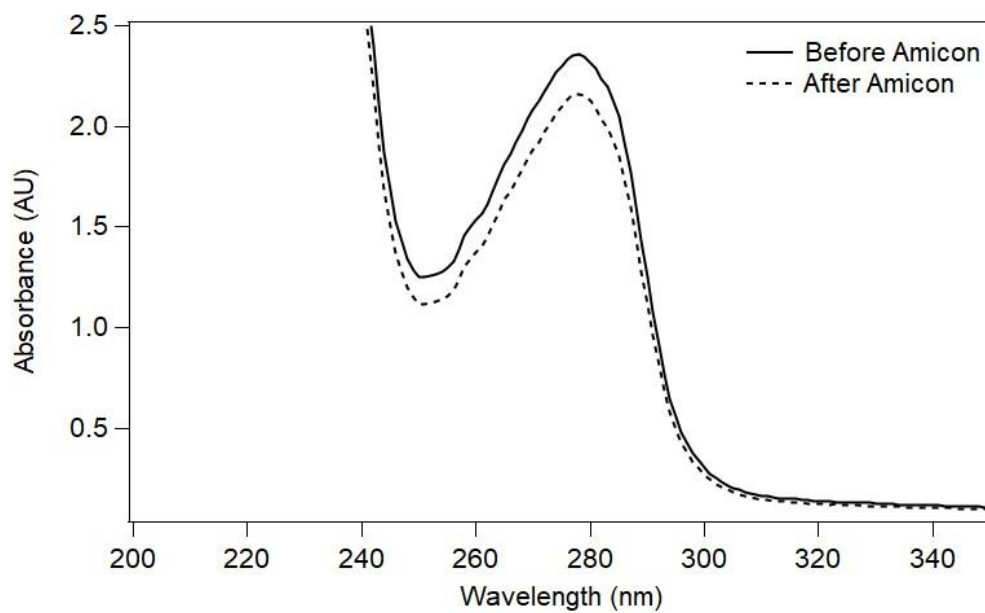


Figure C5. Exemplary absorption spectra showing protein loss of 1.0 mg/mL BSA over Amicon filter. Solid line represents absorbance at 280 nm before Amicon filter and dotted line represents absorbance at 280 nm after Amicon filter. Loss of BSA determined to be $8.6 \pm 0.4\%$ ($n = 3$) after Amicon filter.

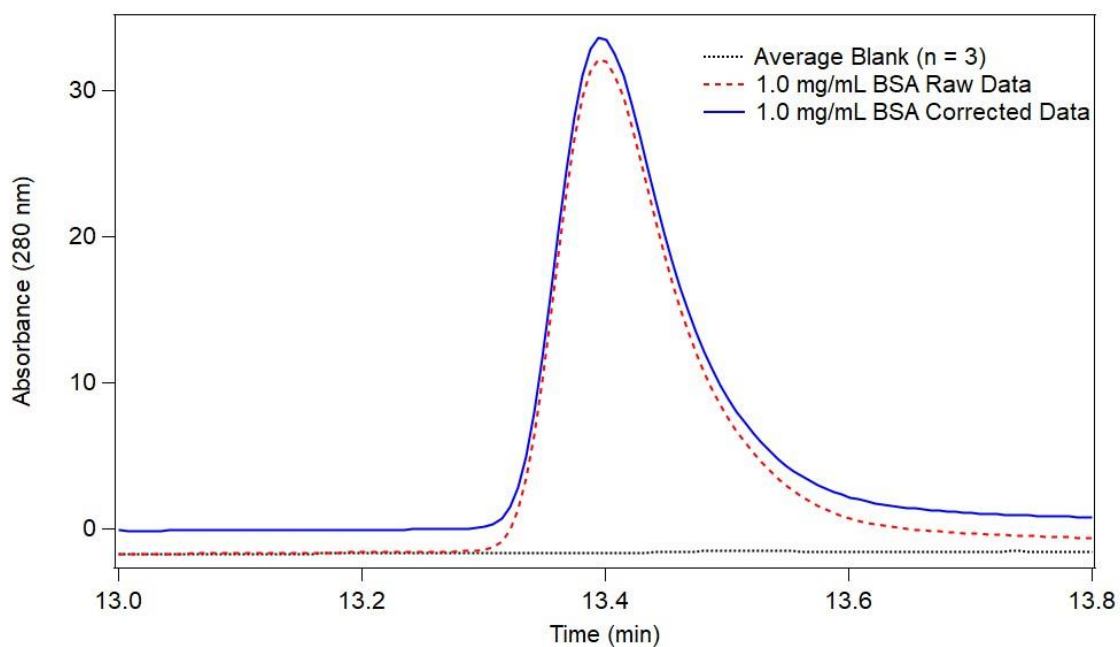


Figure C6. HPLC integration scheme. Red dashed line represents exemplary raw chromatogram of 1.0 mg/mL BSA, black dotted line represents an average chromatogram taken from three water blanks, and blue solid line represents the blank-corrected data which was further integrated.

Appendix D: Chapter 5 supplement

Appendix D serves as the supplemental information for Chapter 5.

Supplement to:

Reaction of proteins with peroxynitrite: pH determines degree of nitration and oligomerization

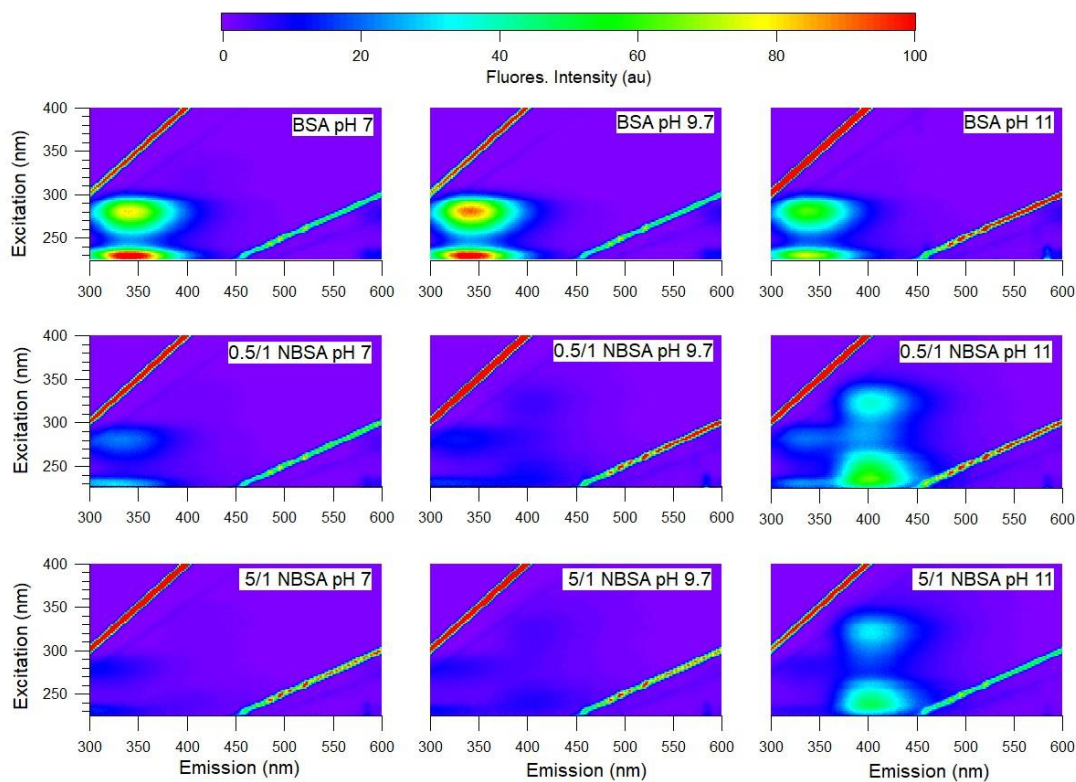


Figure D1. Excitation emission matrices of BSA and ONOO⁻ reaction products.

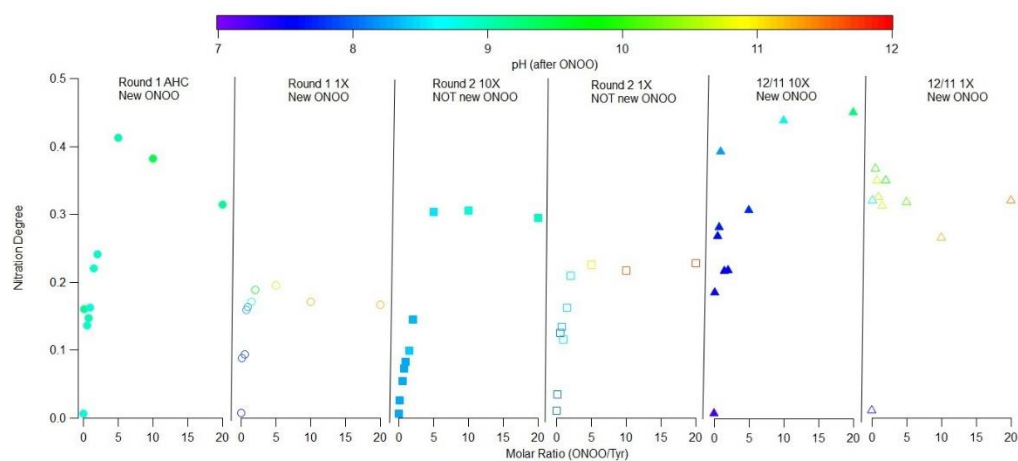


Figure D2. Variance of ND response depending on experimental conditions.

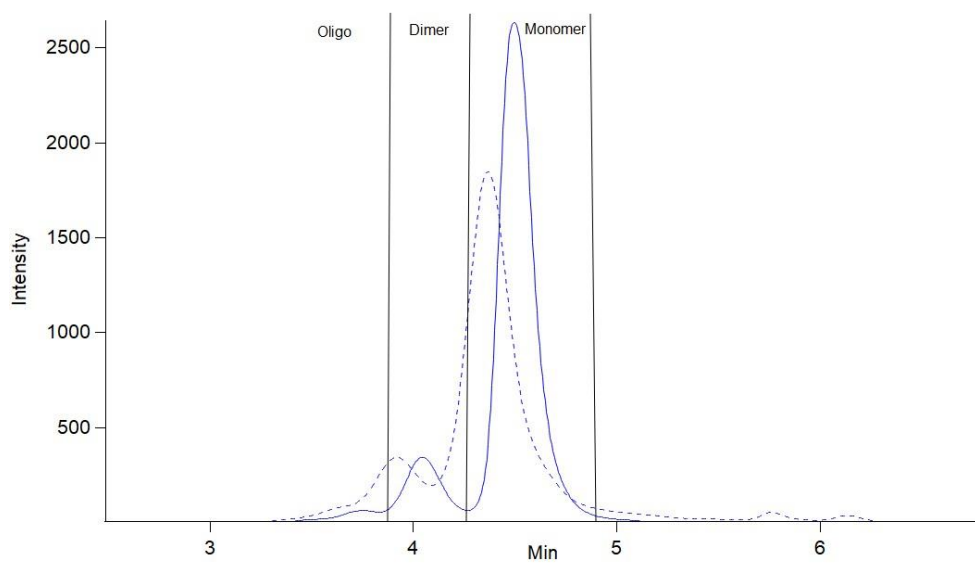


Figure D3. Exemplary chromatograms of SEC-HPLC. Solid line represents native BSA and dotted line represents BSA reacted with ONOO^- .

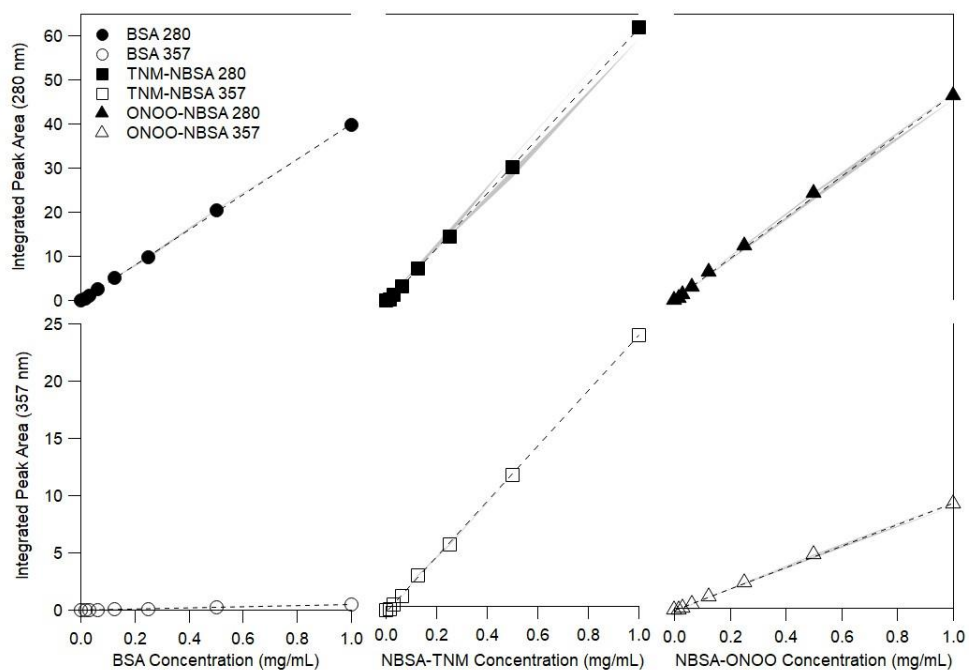


Figure D4. HPLC-DAD calibration.

Table D1. Slope of HPLC calibration curves (units of peak area per mg mL⁻¹), R² values, LOD (mg mL⁻¹), and LOQ (mg mL⁻¹) calculated for each absorbing peak and each calibrant.

	Unmodified BSA		1/1 TNM/Tyr BSA		1/1 ONOO/Tyr BSA	
	BSA 280 nm	BSA 357 nm	NBSA-TNM 280 nm	NBSA-TNM 357 nm	NBSA-ONOO 280 nm	NBSA-ONOO 357 nm
R ²	0.9996	0.9943	0.9998	0.9997	0.9990	0.9991
m	40.0 ± 0.3	0.49 ± 0.02	62.4 ± 0.4	24.2 ± 0.2	46.8 ± 0.6	9.4 ± 0.1
LOD	0.009	0.04	0.008	0.008	0.02	0.01
LOQ	0.03	0.1	0.03	0.03	0.05	0.05

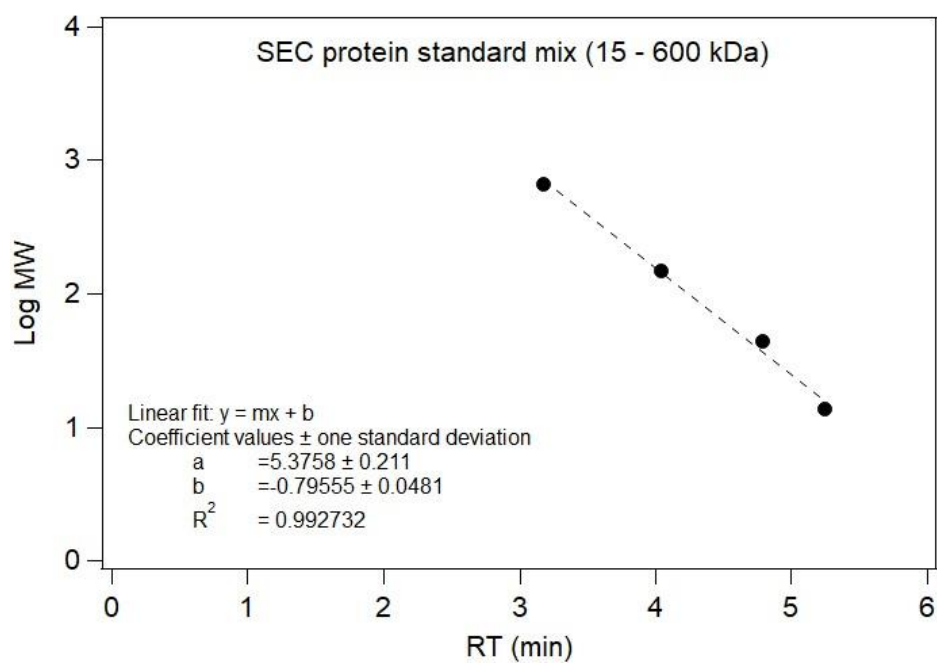


Figure D5. SEC calibration obtained using protein standard mixture.

Appendix E: Ozone filter test Igor code

This Igor code was used for the ozone filter tests in Chapter 3.

```
Function SimpleFilter(InputWv, Threshold)
    Wave InputWv
    Variable Threshold
    Variable n

    Duplicate/o InputWv FilteredWv
    For (n = 0 ; n < numpnts(InputWv) ; n += 1)
        If (InputWv[n] <= Threshold)
            FilteredWv[n] = nan
        Endif
    Endfor
End Function
```

This Igor code is used to look at the slope every 8 hours between two instruments and set the number of points threshold.

```
Function SlopeValuesNumpnts(EPAWv, CoWv, DateWv, FloatBVar,
    NumPntsFilterVar)

    Wave EPAWv, CoWv, DateWv
    Variable FloatBVar
    Variable NumPntsFilterVar
    Variable StartPt, StopPt, n

    Wave StartPtWv, StopPtWv

    Make/o/n=(numpnts(StartPtWv)) NewSlopeWv, NewR2Wv, NewNumPntsWv
    NewSlopeWv = nan
    NewR2Wv = nan
    NewNumPntsWv = nan
    Duplicate/o DateWv NewDateWv
    Deletepoints 0,1e9, NewDateWv
    Insertpoints 0,numpnts(StartPtWv), NewDateWv
```

```

For (n = 0 ; n < numpnts(StartPtWv) ; n += 1)
    StartPt = StartPtWv[n]
    StopPt = StopPtWv[n]
    If (FloatBVar == 1)
        CurveFit/q/M=2/W=0 line,
CoWv[StartPt,StopPt]/X=EPAWv[StartPt,StopPt]/D
    Elseif (FloatBVar == 0)
        K0 = 0
        CurveFit/q/H="10" line,
CoWv[StartPt,StopPt]/X=EPAWv[StartPt,StopPt]/D
    Endif
    wave w_coef
        NewSlopeWv[n] = W_coef[1]
        NewR2Wv[n] = v_r2

        Wavestats/q/r=[StartPt,StopPt] CoWv
        NewNumPntsWv[n] = v_npnts
        If (v_npnts < NumPntsFilterVar)
            NewSlopeWv[n] = nan
            NewR2Wv[n] = nan
        Endif

        NewDateWv[n] = DateWv[StartPt]

Endfor

End Function

```

Appendix F: Density of H₂O and PBS

To determine the extraction efficiency of various filters for use in ambient sampling (discussed in Chapter 3 and Appendix C) the density and mass of the liquid that is extracted are needed to determine the volume, because the filter soaks up some of the liquid and it remains on the filter. The density of BSA in PBS (1x; made in laboratory) was analyzed to determine if as the concentration of BSA in PBS increases the density raises above one. The change in density and the density curve for 400 μg are shown in Appendix C, however the other individual density curves with linear regression information are shown in Figure F1 for use in experiments requiring volumes other than 400 μg . The density values were determined to be 1.004 ± 0.001 g/mL for PBS, 1.003 ± 0.002 g/mL for 50 $\mu\text{g/mL}$ BSA in PBS, 1.0008 ± 0.0008 g/mL for 100 $\mu\text{g/mL}$ BSA in PBS, 1.0022 ± 0.0008 g/mL for 200 $\mu\text{g/mL}$ BSA in PBS, and 1.002 ± 0.001 g/mL for 500 $\mu\text{g/mL}$ BSA in PBS.

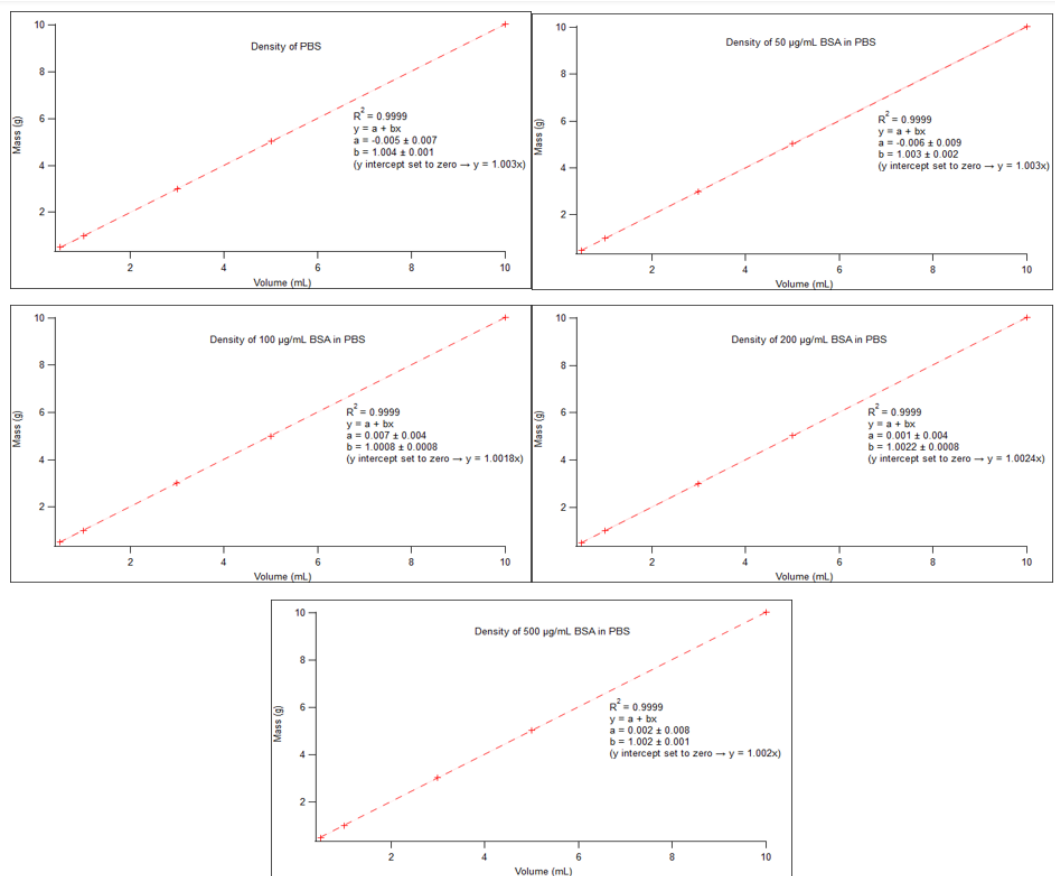


Figure F1. Density determination for various BSA concentrations in PBS.

The density values of two H₂O sources and a purchased PBS (1x) source were also determined for use in extraction experiments. The two H₂O sources tested were the MQ H₂O from the MQ system and purchased H₂O from Gibco. Purchased PBS was acquired from Gibco. The density determination curves are shown in Figures F2 and F3. The density value for Gibco PBS was calculated to be 1.000 ± 0.004 g/mL. The density value for Gibco H₂O was calculated to be 0.99 ± 0.01 g/mL and the density value for MQ H₂O was calculated to be 1.00 ± 0.06 g/mL.

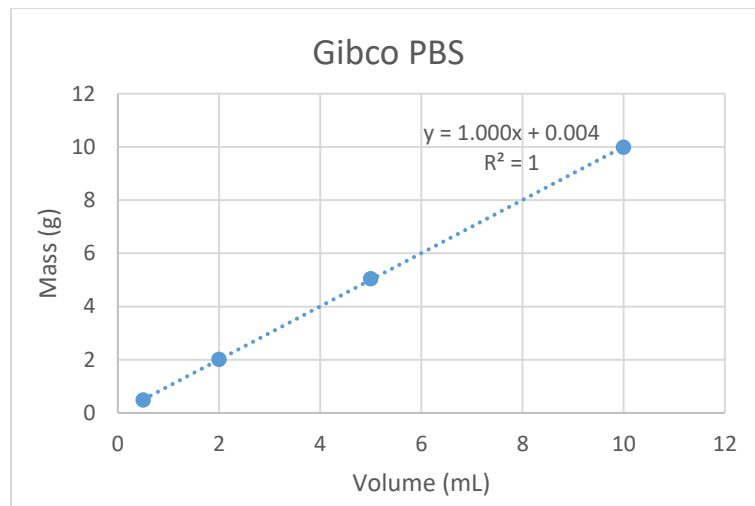


Figure F2. Density determination for purchased Gibco PBS.

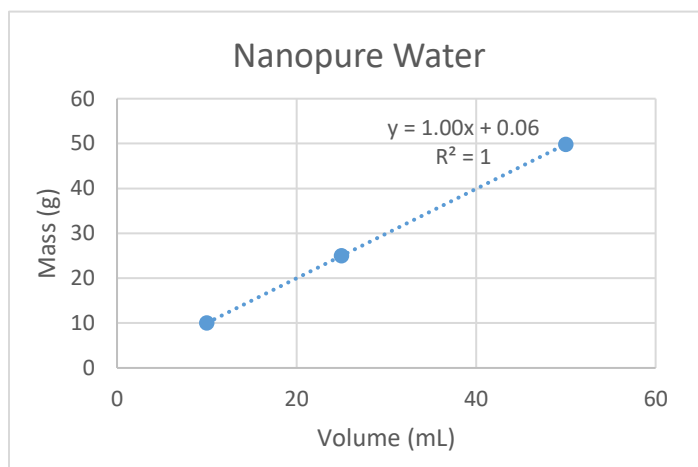
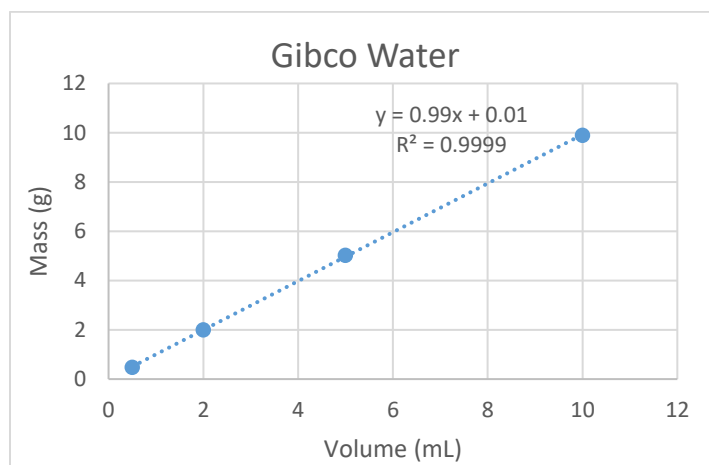


Figure F3. Density determination for purchased Gibco H₂O and MQ H₂O.

Appendix G: Site-selective nitration of LF and ONOO⁻

The following results were peer-reviewed and published as part of the following:

Alhalwani, A. Y., Davey, R. L., Kaul, N., Barbee, S. A., & Huffman, J. A. (2019).

Modification of lactoferrin by peroxynitrite reduces its antibacterial activity and changes protein structure. *Proteins: Structure, Function, and Bioinformatics*, 1–9.
<https://doi.org/10.1002/prot.25782>

To investigate the post-translational effects ONOO⁻ has on lactoferrin, both the native protein and ONOO⁻-treated protein were tryptically digested and analyzed via LC-MS/MS. A software tool called Scaffold was used to validate and interpret the MS data. Scaffold uses a Label Free Quantification (LFQ) method to quantify the peptides. Using a peptide threshold of 95%, the tryptic peptides of NLF show nitration of both tyrosine (Y) and tryptophan (W) residues, including one tyrosine in the iron binding site (Y92) and six nitrated residues in total. It is important to note that in the tryptic digestion cysteine residues are alkylated and reduced. Cysteine oxidation products are thus not able to be identified via this analysis. No methionine oxidation was observed at this peptide threshold.

The LC-MS/MS results (Table G1) show relatively high peptide coverage, which provides a clear representation of the modifications present in the ONOO⁻-treated sample

(native showed 86% and ONOO⁻- treated sample showed 80% amino acid coverage). Nitration of six residues, including 4 of 21 tyrosine and 2 of 10 tryptophan, in the treated sample were observed, including: Y85, Y92, Y112, W288, Y344, and W367. One nitrated tyrosine, Y92, is located in the iron-binding site of lactoferrin, which could explain why the iron-binding ability of the ONOO⁻-treated sample was lowered (Table G1). It is hypothesized that the nitration of residues observed, as well as possible cysteine oxidation, contributed to the loss of protein structure and function seen.

Table G1. LC-MS/MS data. Tryptic peptides of NLF identified by LC-MS/MS. Lowercase letters represent modified residues.

Modified			
State	Residue	Tryptic Peptide	LFQ¹
Native		ADAVTLDGGFIYEAGLAPYK	4.46 x 10 ⁷
Treated	Y85 and Y92	ADAVTLDGGFIyEAGLAPyK	8.09 x 10 ⁵
Native		THYYAVAVVK	7.32 x 10 ⁶
Treated	Y112	THyYAVAVVK	1.27 x 10 ⁵
Native		EDAIWNLLR	8.6 x 10 ⁷
Treated	W288	EDAIwNLLR	7.0 x 10 ⁵
			5.46 x 10 ⁶
Native		VPPRIDSGLYLGSGYFTAIQNLR	6.38 x 10 ⁵
Treated	Y344	VPPRIDSGLYLGSGyFTAIQNLR	3.33 x 10 ⁵
Native		VVWCAVGEQELR	7.49 x 10 ⁷
Treated	W367	VVwCAVGEQELR	2.56 x 10 ⁵

¹LFQ = label free quantification

The following serves as the supplemental information for Chapter 6.

Supplement to

Site-Selective Nitration of Lactoferrin Upon Peroxynitrite Exposure and Efficacy of Ergothioneine Inhibition

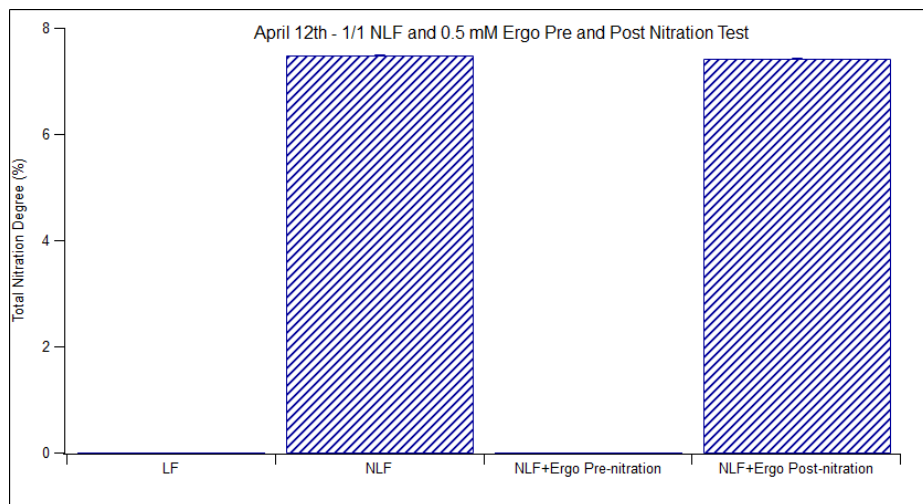


Figure G1. Treatment of LF with ET scavenges ONOO⁻ radicals

Table G2. Preferred peptides used for QTOF-MS/MS analysis.

Prec. m/z	Delta m/z (ppm)	Z	Prec. Type	Ret. Time (min)	Peptide
922	100	1	Exclude	0	contaminant (from old method)
622.02	100	1	Exclude	0	contaminant (from old method)
1221.99	100	1	Exclude	0	contaminant (from old method)
1521.97	100	1	Exclude	0	contaminant (from old method)
2071.04	100	1	Preferred	17.8	(R)ADAVTLDGGFIYEAGLAPY(L)
2116.04	100	1	Preferred	18.82	Y84 OR Y91
2161.04	100	1	Preferred	20	Y84Y91
1975.85	100	1	Preferred	15.6	(K)CAFSSQEPYFSYSGAFK(C)
1362.71	100	1	Preferred	15.1	(K)CGLVPVLAENYK(S)
1407.71	100	1	Preferred	16.4	Y434
1524.66	100	1	Preferred	13.2	(R)DEYELLCPDNTR(K)
1862.77	100	1	Preferred	12.1	(K)FDEYFSQSCAPGSDPR(S)
1907.77	100	1	Preferred	12.9	Y507
1804.81	100	1	Preferred	11.5	(K)GEADAMSLDGGYVYTAGK(C)
1849.81	100	1	Preferred	14.15	Y417 OR Y419
2088.01	100	1	Preferred	19.18	(R)IDSGLYLGSGYFTAIQNLR(K)
2133.01	100	1	Preferred	20.1	Y343 OR Y338
2858.37	100	1	Preferred	15.1	(K)SQQSSDPDPCVDRPVEGYLAVAVVR(R)
1150.63	100	1	Preferred	1.6	(R)THYYAVAVVK(K)
1195.63	100	1	Preferred	11.2	Y111 OR Y112
1240.63	100	1	Preferred	12.4	Y111Y112
1536.84	100	1	Preferred	15.5	(K)YLG PQYVAGITNLK(K)
1581.84	100	1	Preferred	16.6	Y686
1097.51	100	1	Preferred	12	(R)YYGYTGAFR(C)
1142.51	100	1	Preferred	14	Y545
1664.94	100	1	Preferred	13.27	(K)YLG PQYVAGITNLKK(C)
1709.94	100	1	Preferred	14.43	Y686
3132.36	100	1	Preferred	19.5	(R)ESTVFEDLSDEAERDEYELLCPDNTR(K)
3177.36	100	1	Preferred	20.3	Y246
1129.6	100	1	Preferred	18.2	(K)EDAIWNLLR(Q)
1174.6	100	1	Preferred	18.3	W287

Appendix H: Pollen rupture

The following protocol was developed for use in rupturing pollen, following by nitration.

1. Weigh out 1 mg BSA/pollen using analytical balance
2. Place BSA/pollen in 1 mL ultrapure water (or 1xPBS)
3. Load 300 μ L BSA/pollen solution onto filter and place in large Falcon sterile conical tube
4. Let sit overnight
5. Add 4 mL 1xPBS to conical tube with filter
6. Place vial on platform shaker at medium (about 80 RPM) for 15 minutes
7. Sonicate for 10 minutes with no heat
8. Place back on platform shaker at medium for another 15 minutes
9. Bring filter to rim of conical tube using clean tweezers and rinse both sides with 2 mL 1xPBS, collecting runoff into same tube to remove as much visual pollen as possible
10. Add a small stir bar and place tube onto stir plate for 15 minutes on the highest RPM to break apart as much pollen as possible
11. Reduce RPM to medium-high and let stir for another 30 minutes
12. Remove conical tube from stir plate
13. Using a 25 mm syringe filter with 0.45 μ m polypropylene membrane filter the entire mixture into the top part of a 10k centrifuge tube

- *Note:* centrifuge tube only holds about 4mL, so must perform step 14 with the first 4mL and step 17 with any remaining volume
14. Centrifuge for 15 minutes at 7,500g using fixed-angle rotor
 15. After centrifuging the solution, there will be a small amount of solution (50-100 μ L) left in the top and just under 4ml in the bottom of the tube. Place the bottom solution into a sterile conical tube
 16. Add remaining extract solution into the top of the same 10k centrifuge tube using a different 25 mm syringe filter with 0.45 μ m polypropylene membrane
 17. Centrifuge the remaining solution for 10 minutes at 7,500g
 18. Combine filtrates in the labeled conical tube
 19. Place concentrate in new conical tube
 20. Add approximately 850 μ L 1xPBS (to dilute to 1 mL) into top of centrifuge tube to remove as much protein as possible and transfer to concentrate tube
 21. Extraction is ready for UV-Vis, fluorescence, BCA, HPLC and ELISA

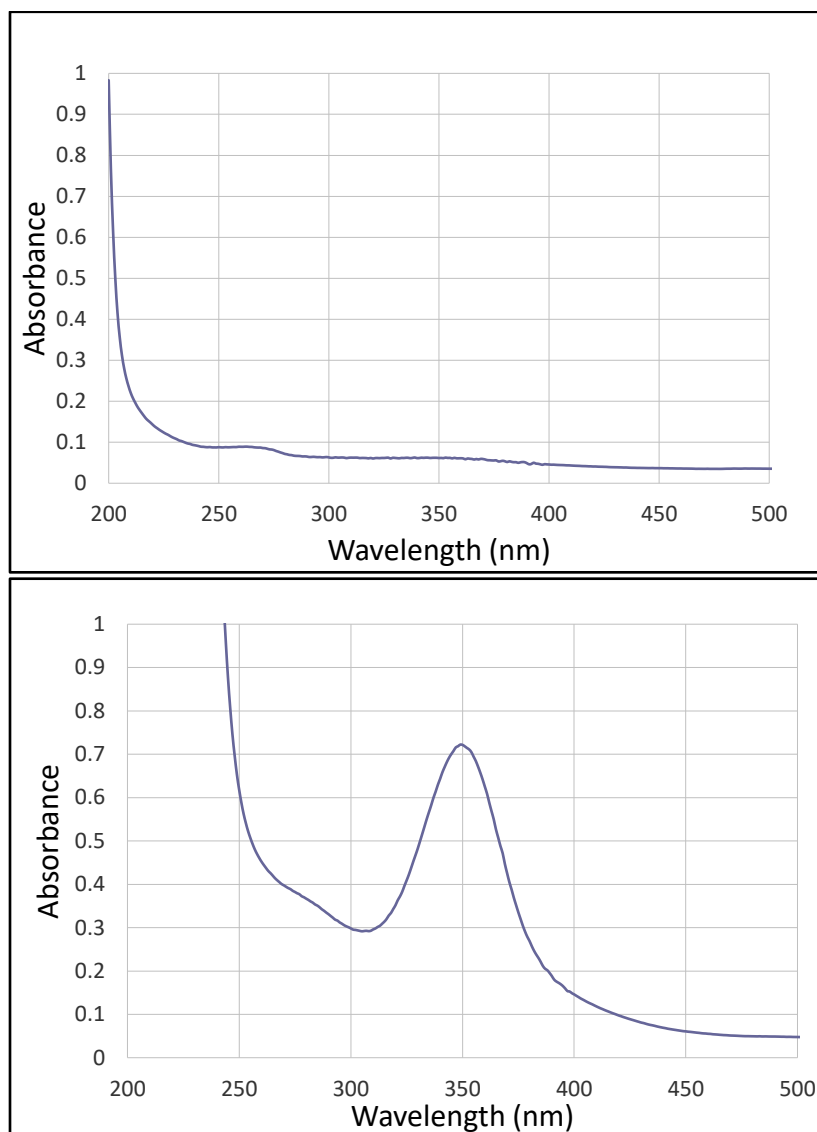


Figure H1. Absorbance spectra of unmodified pollen extract (top) and nitrated pollen extract (bottom) Concentration determined by BCA to be 0.03 mg/mL.

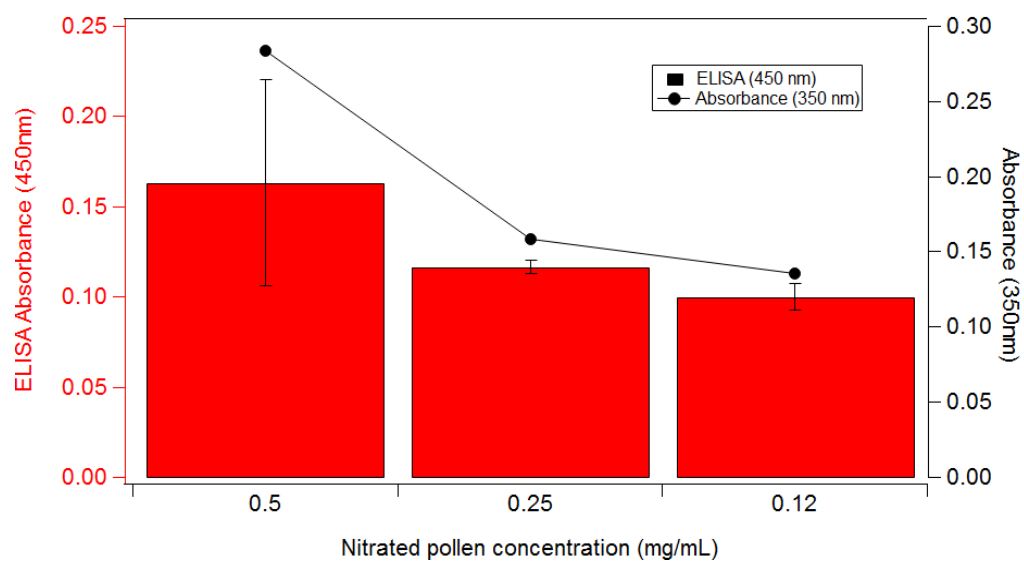


Figure H2. NTyr ELISA quantification of nitrated pollen extract.

Appendix I: Amb a 1 and Amb a 11 preliminary results

This work was conducted at the Max Plank Institute for Chemistry in Mainz, Germany.

For preliminary results of the nitration of ragweed pollen allergens, various protein samples were nitrated and analyzed. Amb a 1 and Amb a 11, the major ragweed pollen allergens, were obtained from collaborators (Roxana Buzan). Amb a 1 was also purchased from Indoor Biotech. Each sample was digested with trypsin and analyzed via LC-QTOF-MS/MS following the methodology outlined in Chapter 6. Each protein was able to be detected, including several of the Tyr-containing peptides of interest. However, samples were too diluted to see entire amino acid sequence.

Purchased Amb a 1 from Indoor Biotech was nitrated with ONOO^- using the protocol outlined in Chapter 6 at molar ratios of 5/1 and 20/1 to serve as preliminary results to test the nitration of Amb a 1 with ONOO^- . Figure I1 shows the results, showing that Amb a 1 is nitrated by ONOO^- and a similar trend of ND increasing and then decreasing is seen (as in Chapters 5 and 6).

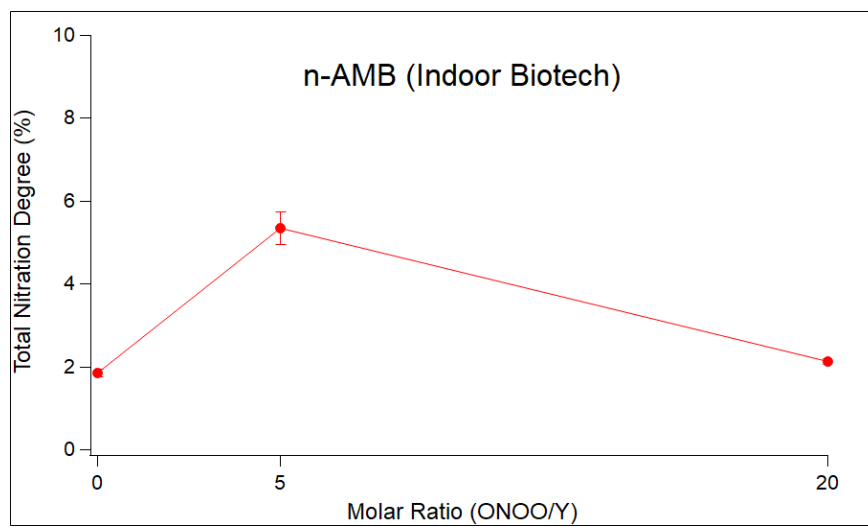


Figure I1. Preliminary results of n-AMB reacted with ONOO⁻.

Appendix J: NTyr ELISA protocol

This is an updated direct NTyr ELISA protocol for use in semi-quantifying the NTyr concentration in protein and pollen samples. The protocol followed by *Alhalwani et al.* was modified for use with pollen samples (Alhalwani et al., 2023).

Protocol:

A. Coating:

1. Make carbonate buffer ahead of time
2. Make serial dilutions in snapcaps with vortexing
3. Place 100uL of each dilution in respective wells
4. Put sealing tape and foil on plate
5. Place in fridge overnight

B. Blocking:

1. Set plate out at RT
2. Get PBS and SuperBlock out and set to RT
3. Make diluent solutions: 1/3 superblock, 2/3 PBS (one detection antibody, one HRP)
4. 1:300 dilution ratio used for detection antibody (anti NTyr), place antibody in detection antibody solution
5. Make PBSt (50mL PBS, 25uL Tween, shake)
6. Wash plate (dump plate into trash, pat on Kimwipe, wash with 2xPBSt 250uL per well)
7. Place 290uL Superblock in each well, dump, pat, do twice

8. wash 2x with 250uL PBS

C. Detection antibody:

1. Pour detection antibody solution in trough, get all out with pipette
2. Place 100uL solution in each well
3. Wrap in cling wrap and foil, make sure plate is flat
4. Let sit at RT for 2-3 hours

D. Enzyme – HRP Streptavidin:

1. 1:20,000 ratio used; place amount of HRP in diluent solution made earlier
2. Wash plate 2x with 250uL PBSt
3. Add 100uL HRP solution to each well
4. Cover with cling wrap and foil, let sit for 45 min
5. Warm up plate reader

E. TMB:

1. Place TMB in falcon tube and cover in foil, place in drawer to get to RT
2. Wash plate 2x with 250uL PBSt, dump, pat
3. Place 100uL TMB in each well, wait until turns blue (around 4 min)
4. To stop, place 100uL 2M H₂SO₄
5. Read immediately at 450 nm

Appendix K: TNM nitration protocol

This is an updated protocol for nitrating protein or pollen samples with TNM. The protocol followed by *Alhalwani et al.* was modified for use with protein and pollen samples (Alhalwani et al., 2018, 2023). Nitrate according to a TNM/Tyr (nitrating agent to tyrosine) molar ratio (i.e. a 10/1 TNM/Tyr ratio means we put in 10 mol TNM for every tyrosine residue). BSA has 21 Tyr residues. Place 4% of the total reaction volume MeOH (i.e. 1,000 μ L total volume uses 40 μ L MeOH) into the reaction vessel before adding TNM. This helps the TNM suspend and react more efficiently, as TNM is not soluble in aqueous solutions. PBS (1x) is used to maintain the pH at 7.4.

Protocol:

1. Place MeOH, BSA stock, and PBS in snapcap, falcon tube, cuvette, etc.
2. Take UV-Vis spectrum of reaction mixture pre-nitration
3. Add TNM using “TNM-only” micro syringe (add in fume hood)
 - Make sure syringe is cleaned with PBS first
4. Wait 90 minutes (record exact time)
5. Take UV-Vis spectrum post-nitration
6. Clean samples with Amicon centrifuge tube (4 mL, 10 kDa cutoff)
7. Dilute sample back to 1 mL using PBS
8. Take UV-Vis spectrum post-cleaning

Appendix L: Theoretical pH calculations

As discussed in Chapter 5, the pH of the reaction mixture upon addition of ONOO⁻ increases depending on the buffer capacity. The theoretical final pH values of various experimental reactions of proteins with ONOO⁻ were calculated. Table L1 shows the results for the addition of the 0.5/1 ONOO⁻ volume to phosphate buffer (PB) and Table L2 shows the results for 5/1. PB was used as opposed to PBS to decrease the complexity of the calculation. Final pH represents the calculated theoretical final pH upon addition of the ONOO⁻ to the reaction with each corresponding starting pH.

Table L1. Theoretical pH calculations for the addition of 0.5/1 ONOO⁻/Tyr to PB.

Starting pH	starting volume (uL)	Final pH	ONOO added (uL)	final volume (uL)
7	400	7.014296002	0.316	400.316
7.4	400	7.414253425	0.316	400.316
8	400	8.028884431	0.316	400.316
8.4	400	8.463345272	0.316	400.316
9	400	9.294590597	0.316	400.316
9.05	400	9.397482877	0.316	400.316
9.25	400	10.11554521	0.316	400.316
9.3	400	10.78419519	0.316	400.316
9.4	400	11.29459515	0.316	400.316
11.4	400	11.44948537	0.316	400.316
12	400	12.02012237	0.316	400.316

Table L2. Theoretical pH calculations for the addition of 5/1 ONOO⁻/Tyr to PB.

Starting pH	starting volume (uL)	Final pH	ONOO added (uL)	final volume (uL)
7	400	7.13927755	3.16	403.16
7.3	400	7.440368196	3.16	403.16
7.8	400	8.04910414	3.16	403.16
8	400	8.392911707	3.16	403.16
8.2	400	9.031261782	3.16	403.16
8.25	400	9.458135764	3.16	403.16
8.3	400	9.885597431	3.16	403.16
8.4	400	10.67837676	3.16	403.16
8.6	400	11.02904806	3.16	403.16
10.8	400	11.54909525	3.16	403.16
12	400	12.18612744	3.16	403.16

Appendix M: Average ambient data Igor code

This Igor code is used to average the ambient data collected (O₃, NO₂, RH, temperature) automatically when applying filter start and end date and times.

```
Function AverageAmbientData (XWvInput, YWvInput, RefPtsWv, AvgWindowVar)
    Wave XWvInput, YWvInput
    Wave RefPtsWv
    Variable n, startpt, endpt

    Make/o/n=(numpts(RefPtsWv)) AvgPtsWv, StDevPtsWv
    AvgPtsWv = nan
    StDevPtsWv = nan

    For (n = 0 ; n < numpts(RefPtsWv) ; n += 1)
        startpt = RefPtsWv[n]
        endpt = RefPtsWv[n]
        WaveStats/q/r=(startpt, endpt) YWvInput
        AvgPtsWv[n] = V_avg
        StDevPtsWv[n] = V_sdev

    Endfor

End Function
```

Appendix N: UV-Vis calibration

To ensure accurate calculations when using the UV-Vis spectrometer, the UV-Vis was calibrated using potassium dichromate and sulfuric acid (H₂SO₄).

Table N1. UV-Vis spectrometer calibration using potassium dichromate.

<i>Wavelength (nm)</i>	<i>A (1% 1cm)</i>	<i>Accepted Values</i>
235	114.6	122.9-126.2
257	136.5	142.8-145.7
313	45.37	47.0-50.3
350	103.3	105.6-108.2
430	13.98	15.7-16.1

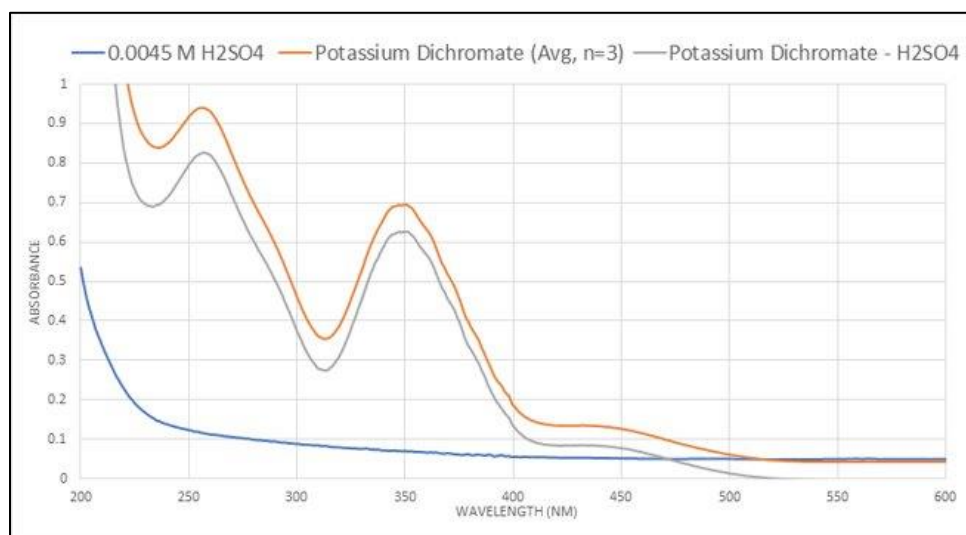


Figure N1. UV-Vis calibration using potassium dichromate.

Appendix O: A poem to my PhD.

The overall topic of my PhD is nitration; its role in the body, mechanisms, and ambient concentration.

Countless hours searching through web of science, sifting through methods comparing their reliance.

Collecting ambient samples and monitoring their air flow, checking the weather and praying for no more snow.

UV-Vis readings, waiting for that 357 peak, 106 HPLC samples down, damn what a week.

Studying tyrosine and its ROS modification, finding the best way for its quantification.

Long science talks with my fav twin, discussing my new bud, a QTOF named Quinn.

On hour eight of the immunoassay, fingers crossed it turns blue in its 96 well tray.

Analyzing the concentrations of Denver's NO_x and ozone, it's scary all their effects are still unknown.

So much time spent analyzing data, all to find out what's happening in Amb's beta (sheets).

A biochemist on one end, looking at inflammation and proteins' interconnection, but analytical on the other because I also wonder about its limit of detection.

My PhD is near done so I give you this ode, to commemorate all the time spent looking at Igor code.

Yes, it was stressful and at times I wanted to flee, but I can say now it was all worth it for this Doctor of Philosophy.